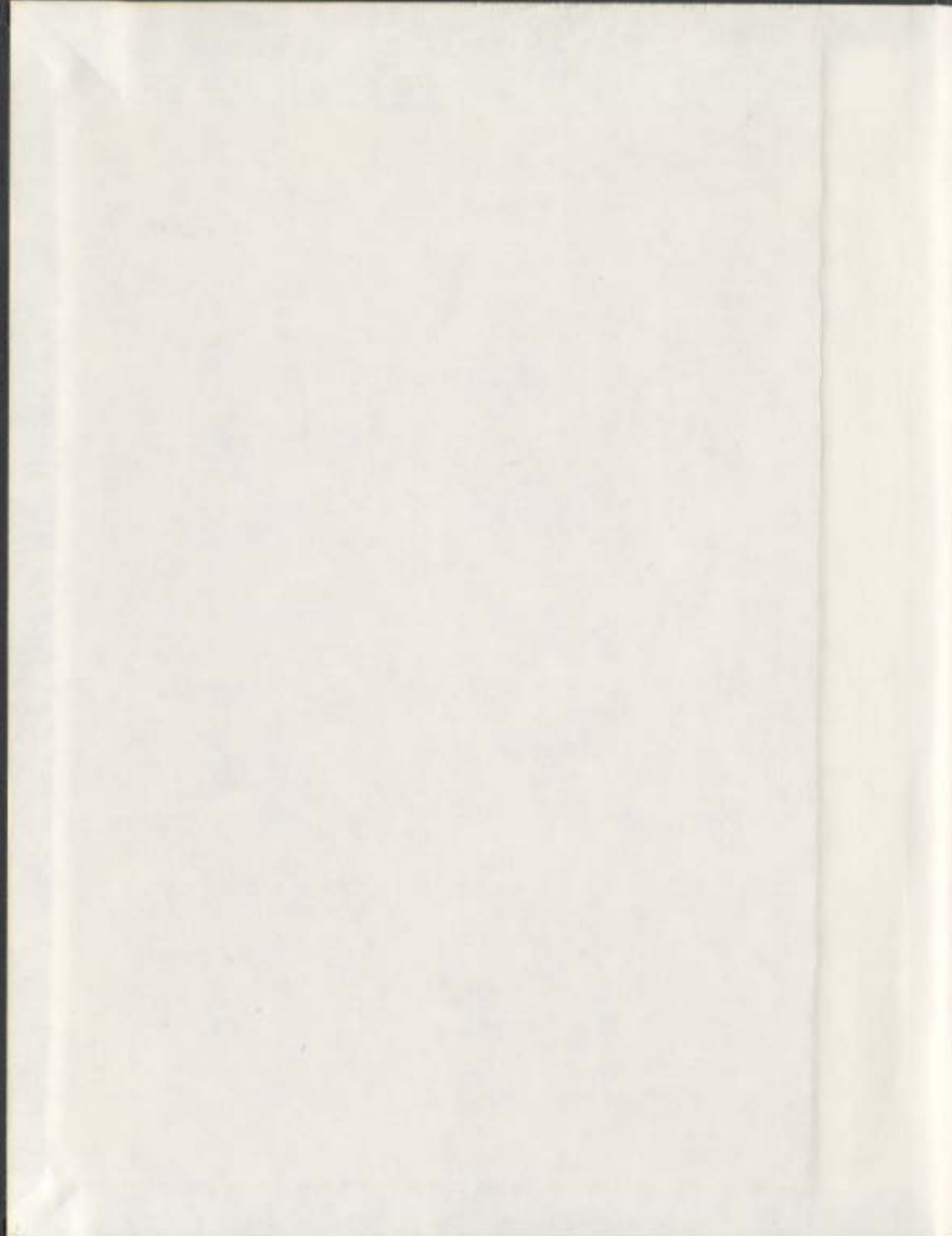


HUMIC SUBSTANCES STUDIES AND NEW APPROACHES
TO ANALYSIS OF SMALL MOLECULES BY MALDI-TOFMS

SAMUEL MUTUURA MUGO





Library and
Archives Canada

Published Heritage
Branch

395 Wellington Street
Ottawa ON K1A 0N4
Canada

Bibliothèque et
Archives Canada

Direction du
Patrimoine de l'édition

395, rue Wellington
Ottawa ON K1A 0N4
Canada

Your file *Votre référence*
ISBN: 978-0-494-42112-3
Our file *Notre référence*
ISBN: 978-0-494-42112-3

NOTICE:

The author has granted a non-exclusive license allowing Library and Archives Canada to reproduce, publish, archive, preserve, conserve, communicate to the public by telecommunication or on the Internet, loan, distribute and sell theses worldwide, for commercial or non-commercial purposes, in microform, paper, electronic and/or any other formats.

The author retains copyright ownership and moral rights in this thesis. Neither the thesis nor substantial extracts from it may be printed or otherwise reproduced without the author's permission.

AVIS:

L'auteur a accordé une licence non exclusive permettant à la Bibliothèque et Archives Canada de reproduire, publier, archiver, sauvegarder, conserver, transmettre au public par télécommunication ou par l'Internet, prêter, distribuer et vendre des thèses partout dans le monde, à des fins commerciales ou autres, sur support microforme, papier, électronique et/ou autres formats.

L'auteur conserve la propriété du droit d'auteur et des droits moraux qui protègent cette thèse. Ni la thèse ni des extraits substantiels de celle-ci ne doivent être imprimés ou autrement reproduits sans son autorisation.

In compliance with the Canadian Privacy Act some supporting forms may have been removed from this thesis.

While these forms may be included in the document page count, their removal does not represent any loss of content from the thesis.

Conformément à la loi canadienne sur la protection de la vie privée, quelques formulaires secondaires ont été enlevés de cette thèse.

Bien que ces formulaires aient inclus dans la pagination, il n'y aura aucun contenu manquant.


Canada

**HUMIC SUBSTANCES STUDIES AND NEW APPROACHES TO
ANALYSIS OF SMALL MOLECULES BY MALDI-TOFMS**

By

Samuel Mutuura Mugo

B.Sc. (Hons), Jomo Kenyatta University of Agriculture and Technology

Nairobi, Kenya 2001

A dissertation submitted to the School of Graduate Studies in partial fulfillment of the requirements for the degree of Doctor of Philosophy (Ph.D.)

Department of Chemistry
Memorial University of Newfoundland
St. John's, Newfoundland, Canada
5 April 2007

Copyright © Samuel M. Mugo 2007

Abstract

Humic substances (HS) are complex natural materials that are thought to be produced by decomposition of biogenic matter. HS are known to be involved in various processes such as amending soil fertility, metal chelation and sequestration of organic contaminants; they also are precursors of harmful water disinfection byproducts (DBPs). To understand the role of HS in all these processes it is imperative to understand their structural features. A MALDI-TOF MS method has been developed to characterize these materials and the results showed clear evidence of the oligomeric nature of HS. However, the inherent complexity of HS demands a multipronged approach, thus thermally assisted hydrolysis-methylation-GC-MS was employed to aid in elucidating possible structural constituents of HS. Thermochemolysis results demonstrated a strong similarity between natural organic matter standard and humic acid model synthesized from polymerization of 4-oxo-2-butenoic acid, derived from oxidation of furfural, a well known product of dehydration of polysaccharides. These results suggest the concept that polysaccharides are important precursors in HS formation.

Studies of DBPs resulting from chlorination and chloramination of HS were also carried out. Based on our understanding of key structural features of HS and rigorous mass spectral analysis, haloketones were found to be one of the major classes of DBPs formed and numerous other potentially new DBPs were also identified. Their formation was replicated using selected plant flavanoids as model compounds for HS. Most of the resulting DBPs were polar, thermally labile and of high molecular weight and hence not amenable to analysis by the standard technique, GC-MS. To circumvent these problems, we have developed a new, rapid, selective, quantitative and very sensitive (detection

limits in the sub parts per billion range) “reactive matrix”-LDI MS method for the analysis of carbonyl and α -dicarbonyl compounds. These techniques can be extended to the analysis of carbonyl compounds of importance in other fields: *e.g.*, metabolomics, clinical diagnostics, food science, *etc.* Finally with good understanding of the structural properties of HS obtained from our studies, aquatic fulvic acid has been demonstrated as a novel universal MALDI matrix.

This dissertation has been dedicated to my parents, Stanley Mugo and Mary Wanjiru, for their prayers, love and rich heritage they have passed on to me.

Acknowledgements

A number of people are worth heart felt acknowledgements for their help during my four year romantic affair with humic substances, reactive matrices and MALDI-TOFMS. Dr. Christina Bottaro my supervisor deserves first mention for her support, guidance and encouragement during the course of my research program. Her exceptional work ethics that involves creating a non-threatening environment where student ideas are valued fosters analytical thinking and research abilities. The fact that she believed in me and gave me a position in her research group has certainly been monumental in my personal and career development.

I wish to acknowledge, my supervisory committee: Chris Flinn, Dave Thompson and Yuming Zhao, for their guiding comments during the course of my studies. I recognize, Dr. Robert Helleur for gladly providing us with his GC-MS equipped with the pyrolysis unit, supplying us with Armadale soil fulvic acid sample, his help during preparation of several manuscripts and for generous contribution of his research ideas over the duration of my studies. Others who deserve honourable mention include: C-CART staff for instrumentation training, Susan Avery for her role in the development of an isolation protocol for aquatic fulvic acid and Memorial University analytical group members for the ideas we have shared over the years.

Heartfelt appreciation to my wife, Anne Njambi, for her unwavering support, understanding and patience during the course of bringing this dissertation to fruition. My principle gratitude is to God, who is my anchor, strength and focal point.

Table of Contents

Title.....	i
Abstract.....	ii
Dedication.....	iv
Acknowledgements.....	v
Table of Contents.....	vi
List of Tables.....	xi
List of Figures.....	xii
List of Abbreviations.....	xviii

Chapter 1 – Introduction and Overview

1.1 Introduction.....	1
1.2 Thesis Objectives Summary.....	7
1.3 Literature Review.....	8
1.3.1 Humic Substances Composition and Structure.....	8
1.3.2 Humic Substances Characterization by Degradation Techniques.....	12
1.3.3 Soft Ionization Methods and HS Characterization.....	15
1.3.3.1 ESI and Basic Instrumentation	16
1.3.3.2 ESI-MS Application to HS Analysis.....	18
1.3.3.3 MALDI Basic Operational Theory.....	23
1.3.3.4 MALDI-MS Applications to HS Characterization.....	29
1.3.4 Disinfection By-products Formation.....	31

1.3.5 Analysis of Small Molecules by MALDI-MS.....	41
1.4 Bibliography.....	47

**Chapter 2 – Characterization of Humic Substances by Matrix Assisted Laser
Desorption Ionization Time of Flight Mass Spectrometry (MALDI-TOF-MS)**

2.1 Introduction.....	57
2.2 Experimental and Methods.....	60
2.2.1 Samples and Chemicals.....	60
2.2.2 MALDI Instrumentation.....	61
2.3 Results and Discussions.....	62
2.3.1 Analysis by LDI.....	62
2.3.2 Analysis by MALDI-TOFMS.....	69
2.4 Conclusions.....	77
2.5 References.....	77

**Chapter 3 – Comparative Study of Suwannee River Natural Organic Matter and
Humic Like Substances (HULIS) Synthesized from Acid Polymerization of 4-Oxo-2-
Butenoic Acid by Online Thermochemolysis Techniques**

3.1 Introduction.....	81
3.2 Materials and Methods.....	87
3.2.1 Procedure for Synthesis of HS Model from furfural oxidation.....	87
3.2.2 Analytical Thermochemolysis.....	89
3.2.3 GC-MS Instrumentation.....	89

3.3 Results and Discussion.....	89
3.4 Conclusion.....	100
3.5 References.....	101

Chapter 4 – Application of Aquatic Fulvic Acid as a Matrix Assisted Laser

Desorption Ionization (MALDI) Matrix

4.1 Introduction.....	104
4.2 Materials and Methods.....	108
4.2.1 Extraction of Aquatic Long Pond (Newfoundland) Fulvic acid.....	108
4.2.2 SEM Imaging of Fulvic Acid.....	109
4.2.3 UV-Vis Spectrophotometry.....	109
4.2.4 Sample Preparation.....	109
4.2.5 MALDI-TOFMS Instrument Conditions.....	110
4.3 Results and Discussion.....	110
4.3.1 Analysis of Carbohydrates.....	113
4.3.2 Analysis of Peptides.....	120
4.3.3 Analysis of polyethylene glycol.....	121
4.3.4 Application to Real World Samples.....	123
4.4 Conclusion.....	124
4.5 References.....	125

Chapter 5 – Characterization and Comparative Study of Disinfection by-Products from Suwannee River Natural Organic Matter, Fulvic, Humic Acid and Model Compounds

5.1 Introduction.....	129
5.2 Materials and Methods.....	135
5.2.1 Procedure for Chlorination.....	135
5.2.2 Preparation of Monochloramine.....	137
5.2.3 GC-MS Instrumentation.....	138
5.2.4 ESI MS Instrumentation.....	139
5.3 Results and Discussion.....	139
5.3.1 Results from the Model compounds.....	148
5.3.2 UV-Vis Spectrophotometric Studies.....	150
5.4 Conclusion.....	152
5.5 References.....	153

Chapter 6 – Rapid On-Plate Derivatization of Carbonyl Compounds for Enhanced Detection by MALDI MS Using a Tailor-Made Reactive Matrix (Derivatizing Agent), 4-Dimethylamino-6-(4-Methoxy-1-Naphthyl)-1,3,5-Triazine-2-Hydrazine (DMNTH)

6.1 Introduction.....	157
6.2 Material and Methods.....	163
6.2.1 Preparation of the DMNTH and Analyte Solutions.....	164
6.2.2 Derivatization Procedure.....	164

6.2.3 Synthesis of the Internal Standard.....	166
6.2.4 MALDI-MS Instrumentation.....	166
6.3 Results and Discussion.....	168
6.4 Conclusion.....	182
6.5 References.....	183

Chapter 7 – Method Development for the Analysis of Dicarbonyl Compounds by MALDI MS Using 9-(3,4-Diaminophenyl)Acridine (DAA) as a Reactive Matrix

7.1 Introduction.....	187
7.2 Materials and Methods.....	189
7.2.1 Synthesis of 9-(3,4-diaminophenyl)acridine.....	190
7.2.2 UV-Vis Spectrophotometry.....	190
7.2.3 Sample Preparation.....	191
7.2.4 MALDI Mass Spectrometry.....	192
7.3 Results and Discussion.....	192
7.4 Conclusion.....	204
7.5 References.....	204

Chapter 8 – Summary.....

8.1 References.....	213
---------------------	-----

List of Tables

Table 1.1	Classification of common known DBPs.....	34
Table 1.2	Contaminants carcinogenicity rankings categories.....	34
Table 2.1	Matrices used and their concentrations.....	66
Table 2.2	Frequently occurring peaks obtained for aquatic FA, aquatic HA and soil FA by LDI and MALDI.....	67
Table 3.1	HA model-thermochemolysis.....	93
Table 3.2	NOM-thermochemolysis.....	94
Table 4.1	Ion intensities and S/N values (sodiated peaks) for carbohydrates using 1S101F and LFA as matrices.....	120
Table 5.1	Some DBPs observed in the chlorination studies of HS.....	145
Table 6.1	Detection limits for DMNThydrazones by RM-LDI-TOFMS.....	174
Table 7.1	Summary of limit of detection for quinoxalines of dicarbonyls tested by RM-LDI-TOFMS.....	203
Table 7.2	Figures of merit with hydrophobic MALDI target.....	203

List of Figures

Chapter 1

Figure 1.1	Classification of NOM.....	9
Figure 1.2	Thermochemolysis mechanism.....	14
Figure 1.3	Schematic of a typical electrospray system in negative mode.....	17
Figure 1.4	Structures of common MALDI organic matrices employed.....	24
Figure 1.5	MALDI TOFMS principle.....	28
Figure 1.6	Disinfection byproducts formation process.....	32
Figure 1.7	Health risk tradeoffs of drinking water disinfection.....	33
Figure 1.8	Model pathway of halogenated DBPs formation.....	37
Figure 1.9	Derivatization schemes for polar compounds: a) PFBHA and carbonyls b) DNPH and carbonyls c) alkyl chloroformates with carboxylic acids, alcohols and amides.....	39
Figure 1.10	Model of tailor made reactive matrix.....	47

Chapter 2

Figure 2.1	LDI spectra of Fulvic acids in 0.1%TFA/ACN 7:3: a) 1S101F 5 mg mL ⁻¹ ; b) IR101F 5 mg mL ⁻¹ ; c) ASFA 5 mg mL ⁻¹	64
Figure 2.2	Mass spectra of some of the matrices used: a) CHCA; b) HABA; c) DHBA.....	72
Figure 2.3	Mass spectra of fulvic acids obtained using CHCA, HABA and DHBA matrices prepared using the dried-droplet method: a) IR101F and CHCA (1:100); b) IR101F and HABA (1:25); c) IR101F and	

	DHBA (1:1000).....	73
Figure 2.4	Mass spectra of humic substances acquired using DHBA and matrix suppression with increase in matrix a) 1S101H, DHBA, 1:10000; b) ASFA, DHBA, 1:10000.....	75
Chapter 3		
Figure 3.1	Schematic of synthesis of HULIS.....	88
Figure 3.2	Total ion chromatogram of TMAH-GC-MS of humic acid model.....	91
Figure 3.3	Total ion chromatogram of TMAH-GC-MS of NOM from IHSS.....	92
Figure 3.4	Some structures which possibly originate from 4-oxo-2-butenoic acid...	97
Figure 3.5	Possible hypothetical structure from thermochemolysates.....	98
Figure 3.6	¹ H NMR of 10 mg mL ⁻¹ HULIS in DMSO.....	99
Figure 3.7	¹ H NMR of 11 mg mL ⁻¹ 1R101N in DMSO.....	100
Chapter 4		
Figure 4.1	SEM of fulvic acid as a matrix, a) 2 μL of 2 mg mL ⁻¹ LFA, b) 2 μL of 2 mg mL ⁻¹ 1S101F c) 2 μL of 2 mg mL ⁻¹ LFA doped with 2 μL of 1 mg mL ⁻¹ trialanine, d) higher magnification of c).....	111
Figure 4.2	Test compounds employed with AFA matrices.....	113
Figure 4.3	MALDI-TOFMS spectra using 2 mg mL ⁻¹ 1S101F as a matrix: a) 1 mg mL ⁻¹ glucose b) 1 mg mL ⁻¹ maltotriose, and using 2 mg mL ⁻¹ LFA as a matrix, c) 1 mg mL ⁻¹ maltotriose, d) 1 mg mL ⁻¹ 2,3,4,6-methyl glucose.....	115

Figure 4.4	MALDI-TOFMS spectra of: a) LDI of 2 mg mL ⁻¹ 1S101F, b) 10 µg mL ⁻¹ 1S101F and 1 mg mL ⁻¹ 6 methyl-D-galactose, c) 100 µg mL ⁻¹ chlorogenic acid and 10 µg mL ⁻¹ 1S101F.....	117
Figure 4.5	MALDI-TOFMS spectra of: a) 1 mg mL ⁻¹ α-cyclodextrin and 2 mg mL ⁻¹ LFA, b) 1 mg mL ⁻¹ α-cyclodextrin and 2 mg mL ⁻¹ 1S101F, c) 1 mg mL ⁻¹ β-cyclodextrin and 2 mg mL ⁻¹ LFA.....	119
Figure 4.6	MALDI-TOFMS spectra of peptides using 2 mg mL ⁻¹ 1S101F as matrix: a) Calibration Mixture 1, (angiotensin 1, ~1.3 M and dcs-Arg ¹ -Bradykinin, 1.0 M), b) trialanine 1.0 mg mL ⁻¹	121
Figure 4.7	a) Matrix-less LDI of polyethylene glycol b) 1 mg mL ⁻¹ PEG with 2 mg mL ⁻¹ 1S101F as matrix.....	122
Figure 4.8	MALDI-TOFMS spectra acquired using 2 mg mL ⁻¹ LFA as matrix on: a) cantaloupe juice, b) 1 mg mL ⁻¹ acetaminophen.....	124

Chapter 5

Figure 5.1	Schematic of the chlorination procedure employed.....	136
Figure 5.2	FIA-ESI-MS mass spectrum of DBPs extraction from chlorinated NOM.....	140
Figure 5.3	Chromatograms of chlorinated Suwannee River a) HA b) FA c) NOM.....	142
Figure 5.4	Structures of some DBPs observed in the HS chlorination studies.....	146

Figure 5.5	Mass spectra of a) 1,1,1,3,3-pentachloro-2-propanone, b) 2,3-dichloro-2-propenoic acid, c) 2-chloro-3-methylmaleic anhydride d) methyl cis-3-chloropropenoate.....	147
Figure 5.6	Structures of model compounds tested.....	149
Figure 5.7	UV-Vis spectra of chlorine reaction with a) NOM, b) chrysin, and c) chlorogenic acid, ϵ is the molar (mass for NOM) absorptivity coefficient.....	152
 Chapter 6		
Figure 6.1	Synthesis of DMNTH.....	163
Figure 6.2	General scheme for reaction of DMNTH with carbonyl compounds to produce DMNThydrazones.....	165
Figure 6.3	RM-LDI-TOFMS spectra of; a) synthesized internal standard, furfural DMNThydrazone, b) Furfural labelled <i>in-situ</i> , c) LDI-TOFMS spectrum of 0.161mM DMNTH.....	167
Figure 6.4	Time dependent study of reactions of 8.05 mM DMNTH and 20 $\mu\text{g mL}^{-1}$ carbonyl compounds. Aromatic carbonyls were reacted separately from aliphatic carbonyls.....	169
Figure 6.5	RM-LDI-TOFMS spectra of a) 10 $\mu\text{g mL}^{-1}$ aliphatic carbonyls, b) 10 $\mu\text{g mL}^{-1}$ aromatic carbonyls, c) calibration curve for 4-methoxybenzaldehyde with <i>in-situ</i> labelled furfural as an internal standard.....	172
Figure 6.6	Sample RM-LDI-TOFMS spectra for carbonyl compounds that were analyzed by on-plate derivatization with 0.5 μL of 0.161 mM DMNTH.	

	For all carbonyls, 0.5 μL was spotted on-plate at a concentration of 100 $\mu\text{g mL}^{-1}$	176
Figure 6.7	RM-LDI-TOFMS spectra of 0.5 ng mL^{-1} of 4-methoxybenzaldehyde with 0.161mM DMNTH, a) one-pot derivatization, b) on-plate derivatization.....	178
Figure 6.8	RM-LDI-TOFMS spectra of unfiltered beer spiked with 10 $\mu\text{g mL}^{-1}$ furfural.....	179
Figure 6.9	a) Spot-spot reproducibility of 5 $\mu\text{g mL}^{-1}$ 4-methoxybenzaldehyde derivatized with 1.61mM DMNTH and 5 $\mu\text{g mL}^{-1}$ furfural internal standard (IS) using one-pot derivatization method, b) Representative RM-LDI-TOFMS spectrum from which data was drawn in construction of the control chart.....	181
Chapter 7		
Figure 7.1	Synthetic scheme for derivation of 9-(3,4-Diaminophenyl)acridine.....	191
Figure 7.2	UV-Vis absorption spectra of 10 $\mu\text{g mL}^{-1}$ DAA in 10mM acetic acid in 8:2, water and acetonitrile.....	193
Figure 7.3	LDI-TOFMS spectrum of 10 μM DAA.....	194
Figure 7.4	Derivatization chemistry. The schematic shows acid catalyzed condensation reaction of DAA and α -dicarbonyl compounds namely; methyl glyoxal, diacetal and diphenylglyoxal to form their respective quinoxalines.....	195
Figure 7.5	A time dependent study of DAA reaction with α -dicarbonyls.....	196

Figure 7.6	RM-LDI TOFMS spectra of alpha-dicarbonyls quinoxalines obtained by one-pot derivatization (1hr reaction time); a) 5 $\mu\text{g mL}^{-1}$ methyl glyoxal b) 50 $\mu\text{g mL}^{-1}$ 2,3-butanedione c) 50 $\mu\text{g mL}^{-1}$ diphenylglyoxal.....	197
Figure 7.7	a) Representative RM-LDI-TOFMS spectrum obtained by on-plate derivatization of a mixture of 30 $\mu\text{g mL}^{-1}$ methyl glyoxal, diphenylglyoxal and diacetal, b) RM-LDI-TOFMS spectrum of beer spiked with 5 $\mu\text{g mL}^{-1}$ methyl glyoxal.....	198
Figure 7.8	a) Representative mass spectra of a mixture of 10 $\mu\text{g mL}^{-1}$ methyl glyoxal and diacetal and 20 $\mu\text{g mL}^{-1}$ diphenylglyoxal as an <i>in situ</i> labelled internal standard, b) Calibration curves for methyl glyoxal and (c) dimethylglyoxal, using 20 $\mu\text{g mL}^{-1}$ <i>in situ</i> labelled diphenylglyoxal as an internal standard.....	201

List of Abbreviations

ACN – acetonitrile

AFA – aquatic fulvic acid

APCI – atmospheric-pressure chemical ionization

ASFA– Armadale soil fulvic acid

CHCA – α -cyano hydroxycinnamic acid

CID – collisional induced dissociation

CNT– carbon nanotubes

CTAB– cetyltrimethylammoniumbromide

DAA – 9-(3,4-diaminophenyl)acridine

DMNTH – 4-dimethylamino-6-(4-methoxy-1-naphthyl)-1,3,5-triazine-2-hydrazine

DMSO – dimethyl sulfoxide

DBP – disinfection by-product

DIOS – desorption ionization on silicon

DHBA – 2,5-dihydroxybenzoic acid

DL- detection limit

DMG– dimethylglyoxal

DNPH – 2, 4-dinitrophenylhydrazine

DPD– N, N-diethyl-p-phenylenediamine

DPG– diphenylglyoxal

EI– electron ionization

ESI-MS – electrospray ionization mass spectrometry

ESI-FAIMS-MS – electrospray ionization high field asymmetric waveform ion mobility spectrometry mass spectrometry

FA – fulvic acid

FT-ICRMS – Fourier transform ion cyclotron resonance

GC-MS – gas chromatography mass spectrometry

HABA – 2 (4-hydroxyphenylazo) benzoic acid

HA – humic acid

HKs – haloketones

HAAs – haloacetic acids

HULIS- humic like substances

HPLC – high performance liquid chromatography

HS – humic substances

IHSS – International Humic Substances Society

IR – infra red

KMD – Kendrick mass defect

LFA – Long Pond fulvic acid

LDI-TOFMS – laser desorption ionization time of flight mass spectrometry

LC-MS – liquid chromatography mass spectrometry

MALDI-TOFMS – matrix-assisted laser desorption/ionization time of flight mass spectrometry

MCL – maximum contaminant level

MG– methylglyoxal

MS – mass spectrometry

MSE – matrix suppression effect

MS-MS – tandem mass spectrometry

MW– molecular weight

MX– 3-chloro-4-(dichloromethyl)-5-hydroxy-2(5H)-furanone

m/z – mass-to-charge ratio

NDMA – N-nitrosodimethylamine

NIST– National Institute of Standard Testing

NOM – natural organic matter

PEG – polyethylene glycol

PFBHA- pentafluorobenzylhydroxylamine

PSD – post source decay

ppb – parts per billion

QIT – quadrupole ion trap

QqQ – triple quadrupole

QqTOF – quadrupole time-of-flight

RM-LDI-TOFMS – reactive matrix laser desorption ionization time of flight mass spectrometry

RSD – relative standard deviation

SALDI – surface-assisted laser desorption/ionization

SEC – size exclusion chromatography

SEM– scanning electron microscopy

SEND – surface-enhanced neat desorption

S/N – signal to noise ratio

SRM – selected reaction monitoring

THF – tetrahydrofuran

THM – Thermally assisted hydrolysis and methylation

TFA –trifluoroacetic acid

TMAH – Tetramethyl ammonium hydroxide

Trihalomethanes – THMs

U.S. EPA – U.S. Environmental Protection Agency

UV – ultraviolet

XAD-4 – non-ionic macroporous sorbents composed of styrene divinyl benzene

XAD-8 – non-ionic macroporous sorbents composed of acrylic esters

CHAPTER 1

Introduction and Overview

1.1 Introduction

Despite many years (> 200 years ago) of sustained research, humic substances (HS) remain a structurally enigmatic and virtually indefinable organic mixture of compounds that are only operationally classified based on their aqueous solubility. The solubility properties are normally exploited in the isolation of HS into their individual classes: fulvic acid, humic acid and humin.¹ Fulvic acid (FA) is soluble in all pH ranges, humic acid (HA) is soluble in alkali and insoluble in acidic (pH < 1) solution, whilst humin is the insoluble fraction.¹⁻⁶ The variations in their solubility behavior could be associated with probable differences in their chemical composition, acidity, molecular weight, degree of hydrophobicity and self association of the constituent molecules. Arguably, HS are formed from the decomposition and degradation of biogenic materials over time (humification), resulting in heterogeneous multifunctional materials with both aromatic and aliphatic constituents linked by chemical (hydrogen bond interactions) as well as physical interactions.^{7,8} Nevertheless, the understanding of the sources and mechanisms behind their formation is still inexact, probably due to the numerous and variable forces of nature (biogeochemical transformations) that are normally in play in the natural environment. The generality of the above definition clearly reveals the complexity of the problem in the scientific community on the identity of these substances. For instance, biogenic materials literally encompass a staggering number of living things and their waste products. The process of decomposition and degradation on the other hand, could involve both chemical and microbial processes, which varies geographically. All

these issues have resulted in the labeling of these substances by Ghabbour *et al.*⁷ as “nature’s most versatile materials”.

The enormous utility of HS in the environment is in agreement among HS researchers and this has probably been the major impetus for the research effort that has been invested in HS characterization. The earliest recognition of the significance of humic substances was in its potential to enhance soil fertility by soil pH buffering and water retention. They were also recognized as possible precursors of fossil fuels. In addition, HS are probably the strongest naturally-occurring chelating agents known and their interaction (either by: sequestration, mobilization or oxidative and reductive transformation) with numerous environmental pollutants (*e.g.* pesticides, heavy metals, poly aromatic hydrocarbons, *etc.*) has been widely investigated. Such studies represent a concerted effort to understand the impact on bioavailability and efficiency of pollutants detoxification mechanisms on interaction with HS, which is critical in remediation and toxicological studies.^{9,10} Moreover, due to their chelating nature, HS have also been used extensively as medicinal products.¹¹ HS are known also to influence drinking water quality since they are the principal precursors of a large number of potentially harmful disinfection byproducts (DBPs) resulting from HS reaction with disinfectants such as chlorine.^{9,10,12} HS also could have a significant effect on climate influence since they are a major fraction (50-70 %) of atmospheric aerosol particles, which act as cloud condensation nuclei by affecting cloud and fog formation.^{13,14}

It is believed the vastness of possible applications of HS is far from being exhausted and hence they remain an attractive research undertaking. However, to be able to tap the wealth therein, rigorous analytical studies to unravel this enigma must continue,

albeit to build on sustained and often productive work that has been done over the years to understand their structure, origin and reactivity.

The initial primary research goal was to characterize polar and high molecular weight disinfection byproducts (DBPs) ensuing when drinking water containing HS is chlorinated. As a prelude for studying DBPs chemistry, it was imperative to first understand the structural properties of the DBPs precursors, humic substances. Hitherto, an enormous amount of data has been obtained by degradation (*e.g.* pyrolysis/thermochemolysis with gas chromatography mass spectrometry (GC-MS)),²⁰⁻²⁸ and electrospray ionization mass spectrometry (ESI-MS) techniques.³⁰⁻⁴⁷ However, the ultra sensitive and the versatile matrix assisted laser desorption ionization time-of-flight mass spectrometry (MALDI-TOFMS) has not been used to any significant extent in the analysis of HS, as evident in the sparsely available literature,⁵⁰⁻⁶⁸ making it a worthy research endeavor. MALDI-TOFMS could be particularly useful in determining the molecular weight of HS and general structural similarities between different classes of HS and should complement the data already generated by other methods. Application of MALDI-TOFMS for analysis of HS has been limited by difficulties encountered especially in choosing the right matrix and optimizing sample preparation, which are the crucial steps that determine the success of MALDI. The complexity of sample preparation and matrix selection is exacerbated by the complexity of the HS and their poorly understood structural conformations. Optimization of sample preparation and the testing of different matrices to find the most appropriate one were thoroughly investigated. Since, humic substances are highly UV absorbing, LDI-MS was also employed and the results were compared with the MALDI variant. The efficiency of various matrix materials

investigated was based on their ability to enhance ionization and shield the analyte from fragmentation.

To further understand HS, different techniques have to be employed for no single analytical tool is sufficient to fully characterize HS. The use of different techniques (multiple method approach) has been proposed to be the only panacea for the analysis of HS.⁹ The use of the commonly employed pyrolysis techniques has been very important since significant structural information has been derived. The use of thermally assisted hydrolysis methylation using the alkylating agent, tetramethylammonium hydroxide (TMAH), which is known to preserve the structural authenticity of the analyte was especially useful. This technique was used to compare the structural similarities of HS from different sources, essential in possibly understanding the similarities in their formation.

In complex scientific problems, modeling plays a very useful role. A humic acid model was synthesized, based on acid polymerization of furfural; identified widely as a common pyrolysate/ chemolysate of HS. In our study, the synthesized humic acid model was very similar to the isolated HA when characterized with THM methods and was deemed humic like substances (HULIS), which augmented previous studies by Susic.²⁷ With the structural revelation unearthed from these studies and augmented by the literature, especially regarding the functionalities present in fulvic acid, *e.g.* carboxylic acid groups, which undoubtedly have labile protons, it was envisioned it would be possible to utilize fulvic acid as a matrix for MALDI. Application of fulvic acid as a matrix for MALDI was impressive. It is believed that FA as a matrix, our original concept, could radically influence the formation of new MALDI targets. For example, we

think fulvic acid could be employed in making surface-modified MALDI plates by immobilizing a fulvic acid-metal complex (since FA are very strong chelating agents) on a plate that could be used as affinity probes for different compounds such as phosphoproteins. This is the so called affinity mass spectrometry.

Equipped with a better understanding of HS, chlorination experiments were done by mimicking water disinfection treatment systems and the resulting byproducts extracted and analyzed both by GC-MS and liquid chromatography mass spectrometry (LC-MS). Since different disinfection processes are being used in effort to reduce DBPs occurrence, the study also encompassed the use of the now common chloramination process, and similarly, the DBPs formed were evaluated. This was very insightful and diversified the research objectives. A plethora of byproducts formed contained a carbonyl and/or dicarbonyl moieties, certainly alluding to the presence of large numbers of such moieties in the HS backbone. Most of these compounds are difficult to analyze due to their characteristic high polarity making them difficult to extract and separate by typical non-polar solid phase extraction methods. They also suffer from poor detectability with mass spectrometry due to poor ionization efficiency and suppression from sample matrices due to their low molecular weights. Their analysis therefore required some sort of derivatization methodology.

With our major interest in widening the scope of MALDI-TOFMS applicability for small molecules, strategies were developed to analyze small molecules containing carbonyl and dicarbonyl moieties by derivatization and analysis by MALDI-TOFMS. The quantitative limitations of MALDI were also addressed and ways to improve the reproducibility of this technique were sought. Two novel tailor-made derivatizing agents,

otherwise christened “reactive matrices”, were synthesized and successfully employed with remarkable sensitivity for the reactive matrix LDI-MS analysis of carbonyl and alpha-dicarbonyl target compounds. The tailor-made derivatizing agents were, out of necessity, bulky and consisted of ionization-enhancing pendant groups in the backbone. With our key interest in improving sample preparation techniques by minimizing sample handling, we developed what we referred to as on-plate derivatization and one-pot derivatization. The former is particularly ideal for high throughput screening in areas such as toxicology and environmental monitoring.

1.2 SUMMARY OF THESIS OBJECTIVES

- 1) To develop a method for characterization of humic acids and fulvic acids from different sources using MALDI-TOFMS.
- 2) To model the formation of humic substances and to compare the synthesized model with humic substances standards from IHSS using established THM-GC-MS characterization.
- 3) To investigate new and non-conventional applications of fulvic acid; *e.g.* use of aquatic fulvic acid as a MALDI matrix.
- 4) To analyze previously unidentified disinfection byproducts resulting from chlorination and chloramination of humic water and to establish possible mechanistic pathways using selected model compounds.
- 5) To develop methodologies for analysis of small molecules (*e.g.* polar DBPs) using novel reactive matrices with LDI-MS.

1.3 LITERATURE REVIEW

1.3.1 Humic Substances Composition and Structure

Humic substances were first reported by German chemist Karl Achard in 1786. Since then, over two centuries of research effort have been expended in an effort to determine the fundamental aspects of structure and composition of HS with little success. As a result, resignation seems to have set in with some scientists believing that it is impossible to structurally define these materials due to their inherent heterogeneity—comprising a mixture of hydrophobic, polar and hydrophilic components— and hence are not amenable to standard analytical tools.⁷⁻¹⁰ Different equivocal terms have been used to describe HS such as natural polymers, polyelectrolytes, macromolecules, supermixtures, and supramolecules. In general, it is agreed that HS are brown to black colored substances formed by chemical and biological transformations of residues from plants, animals and exudates from microorganisms.²⁻¹⁴ These definitions are sometimes contradictory and infamously fall short in conveying the essential features of HS. They are often characterized by an empirical definition based on solubility properties, categorizing HS as fulvic acid (FA), humic acid (HA) and humin.⁹

Humic substances can either be terrestrial or aquatic. The sources of organic matter in water have been classified as either autochthonous sources or allochthonous. The former refers to carbon resulting from leachate from dead organisms, phytoplankton, organisms exudates and other in-stream processes. The later on the other hand includes leachate from neighboring terrestrial elements (soils, flora *etc.*).² A schematic summarizing the NOM classification is shown in Figure 1.1.

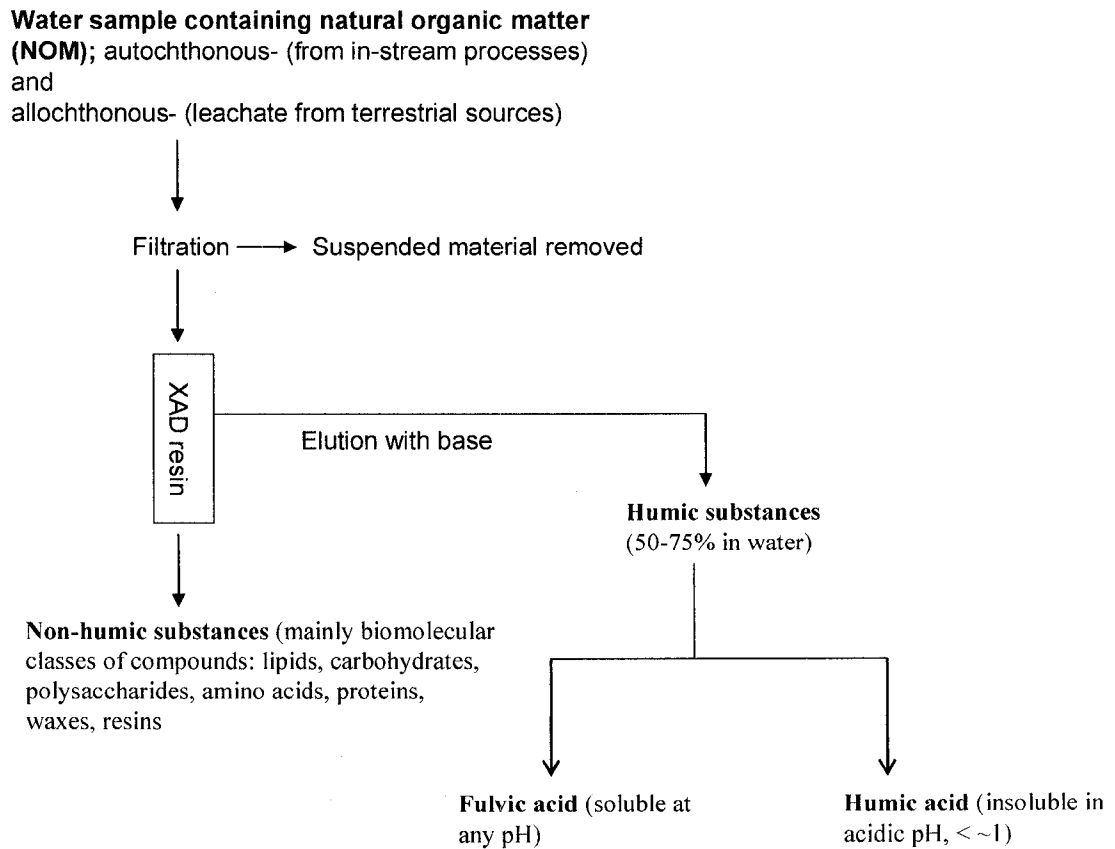


Figure 1.1. Classification and fractionation of NOM.

While there has been an agreement about the color, elemental composition and inherent complexity of HS, differences in opinion still exist regarding the exact genesis of these materials, but molecular weight (MW) and the possible polymeric nature of HS are probably the parameters that have been most controversial and an ongoing debate has ensued in the scientific community. Most of the early humic chemists, *e.g.* McCarthy,² Swift,⁴ Anderson,¹⁶ *etc.*, believed in the polymeric model of HS. This was essentially based on experimental results from older techniques such as vapor pressure osmometry (VPO), ultracentrifugation and size exclusion chromatography (SEC), which estimated HS sizes to range from several hundreds to thousands of Daltons.² It is intriguing that different techniques result in different molecular weight distribution values, attesting to the dynamic nature of HS in solution environment.

Traditionally, SEC with UV detection has been the premier tool for molecular mass analysis. SEC works on the principle of a molecular sieve (consisting of pores of different sizes) mechanism that resolves the macromolecule based on its relative size (hydrodynamic volume) compared to the pore sizes present in a polymer packed column. Molecules that are too big compared to any pore size are eluted through the column without any separation, whilst those that are small penetrate further into and spend more time in the pores and elute last. Those that are moderately sized are eluted, where bigger ones precede the small ones. SEC results suggest that HS are thousands of Daltons in molecular weight, but the results obtained are highly suspicious due to the inherent pitfalls of SEC for molecular weight determination. The most common drawback is charge interactions between the packing and HS that can overestimate or underestimate the MW as well as sorption effects that result in increased elution volumes.¹⁵ Further, the fact that the standards used to generate calibration plots are of narrow polydispersity (*e.g.* polyethylene oxide, polyethylene glycol, *etc.*) and possess different structures and chemistry from HS, makes the results obtained from SEC-UV very questionable. This prompted the use of SEC-mass spectrometry, which can determine molecular mass very accurately.^{7,15}

As previously stated, there are two main views of HS structural identity, polymeric and supramolecular view. The polymeric view was mainly given credence because of the historical hypothesis that associated HS formation with condensation of biological materials derived from degradation of lignin, polyphenols, cellulose and amino acids.⁴⁻⁶ The fact that HS are recalcitrant also gave acceptance to the polymer model since one would expect polymers to be very stable. Furthermore, it was believed that HS are

largely aromatic (consisting of benzene carboxylic and phenolics) due to the belief they are formed from lignin. Recent studies, however, have shown that humic substances contain a lot of aliphatic components, and thus lignin may not necessarily be their primary precursor.³ A composite group of compounds with sources from plant refuse such as cellulose, hemicellulose, lignin, tannins, sugars, amino acids, proteins, lipids, fats, oils, waxes, resins *etc.*, could all be potential precursors of humic substances.

Increasingly the polymer model is being replaced by the supramolecular model, initiated by Piccolo *et al.*,¹⁷ which indicates that HS may consist of collections of diverse, relatively low MW compounds (100-2000 Da). These low MW compounds are held together by hydrogen bonding, hydrophobic intermolecular aggregation and polyvalent cation interactions, leading to a cluster of molecules easily confused with polymers on analysis. This new concept has mainly been supported with the results from soft ionization techniques.¹⁸ The aforementioned HS associations have been hypothesized to form into micellar structures strongly binding other components, *e.g.* biomolecules, making it impossible to purify HS without cleaving the covalent bonds of the humic substances fraction. As such, it has been argued that any component intimately associated with HS should be labeled as HS.^{8,17} This vague boundary between humic substances and non-humic substances (biomolecules such as carbohydrates, proteins, lipids, lignin's, cellulose *etc.*), otherwise referred to as "the humic acid problem", has resulted in diverse and often contradictory interpretations of analytical results.

Considerable information on bulk properties of HS has been achieved by the use of solid and liquid-state nuclear magnetic resonance spectroscopy (NMR), infrared spectroscopy (IR) and VPO. On the other hand, degradation methods (*e.g.* chlorination,

ozonation, hydrolysis, pyrolysis, oxidation and reduction) coupled with GC-MS reveal more specific molecular-level details on existing chemical components, although with limitations because these techniques sometimes severely alter the HS structure. Furthermore, the widespread presence of polar functionalities (alcohols and carboxylic acids) in HS limit volatility and detection of some products and hence molecular characterization is not representative.^{2, 8,13} With the evolution of more powerful analytical instruments, especially those with soft ionization methods, more molecular weight profile information has been revealed about compositional aspects of HS.¹⁷⁻²⁴ Nevertheless, even with such state-of-the-art analytical tools, the results can be contradictory due to the indefinable nature of HS (*cf.* humic acid problem). The HA problem has been minimized by the establishment of the International Humic Substances Society (IHSS), founded at the United States Geological Survey (USGS) Water Research Laboratories in Denver, Colorado, in September 1981. The IHSS mission is to isolate relatively uniform humic substances and provide them to the scientific community for analysis.²⁹ This has greatly reduced the disparity of the results obtained.

1.3.2 Humic Substances Characterization by Thermal Degradation Techniques

Most structural elucidation of HS has been accomplished by pyrolysis-GC-MS with electron ionization, effectively developed for analysis of intractable and non-volatile macromolecules such as coal, kerogen, asphaltene, plastics and recently humic substances. At the high temperature, > 550° C used, thermally mediated chemical bond cleavage occur yielding lower molecular weight molecules (called pyrolysates). The pyrolysates are usually separated by GC on the basis of fragment's volatilities and

interactions with stationary phase of the column (typically the nonpolar DB-5) with ion detection by MS. Classically, the pyrolysis-GC-MS system consist of an integrated pyrolyzer unit (vertical-furnace pyrolyzer is very common) interfaced directly with a GC-MS, thereby reducing analyte losses.²⁰ Although pyrolysis-GC-MS has assisted considerably in the analysis of HS, as manifested by numerous hypothetical structural concepts (often called pseudostructures) produced as a result of its use, it has several limitations.^{2,10,19} The high pyrolysis temperatures employed result in uncontrolled sample degradation and concomitant recombination of pyrolysates, leading to severe adulteration of the original structure of the sample, making the products difficult to relate to the precursors. Many analytical artifacts are also formed from minerals catalyzed cyclization, aromatization, and often decarboxylation (loss of carboxyl group as carbon dioxide) processes.^{24,25,26}

In the 1990s, the softer (sub-pyrolysis temperatures $\sim 250^{\circ}\text{C}$ employed) pyrolysis variant, thermally-assisted hydrolysis and methylation (THM) was described by Challinor.²⁴ The process uses quaternary alkylammonium hydroxides to mediate thermally-assisted chemolysis (hydrolysis), leading to *in-situ* alkylation (methylation being the most common) with the generated products sufficiently volatile to be analyzed by GC-MS. Tetra-methyl ammonium hydroxide (TMAH) is the principal reagent used, providing efficient esterification of carboxylic acids, etherification of alcohols and *N*-alkylation of amino acids *etc.*, with the products (otherwise called chemolysates) bearing a direct relationship to the parent molecule(s). Other reagents such as trimethyl sulfonium hydroxide and trimethyl anilium hydroxide have also been employed, although to a lesser extent than TMAH.^{22,28} The THM mechanism (Figure 1.2) involves formation of

tetramethylammonium salts of phenols or carboxylic acids followed by high temperature base-prompted pyrolysis to the respective alkyl derivatives. In addition, under the reaction conditions, the excess TMAH breaks down to produce tertiary amine and methanol.

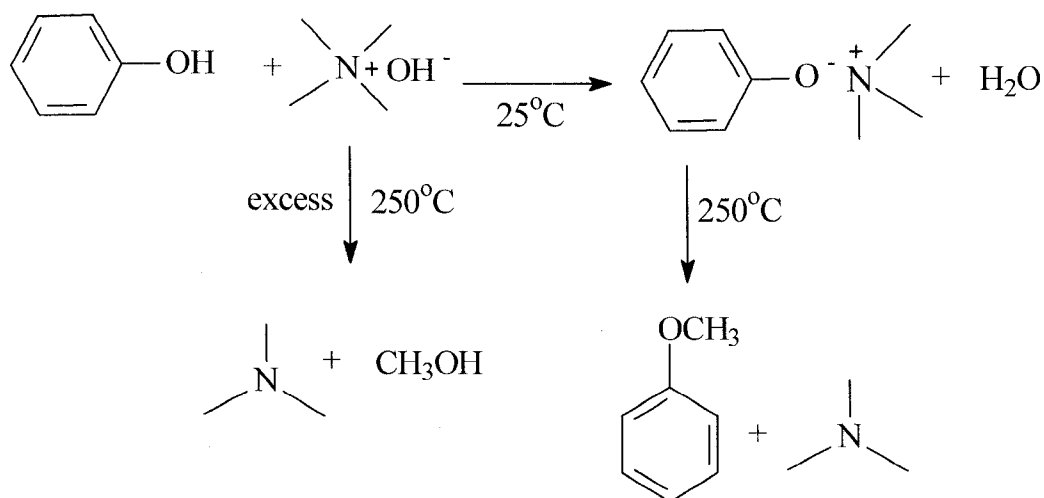


Figure 1.2. Thermochemolysis mechanism.²⁴

THM circumvents some of the limitations of pyrolysis-GC technique. For the most part, THM assists in the methylation of polar aromatic carboxylic acids and phenols, which otherwise undergo decarboxylation and are poorly resolved in chromatography. Carboxylic acids are methylated to methyl esters and alcohols and phenols to methyl ethers. There are a number of disadvantages of using TMAH: One is that methylated components cannot be distinguished from the methyl esters and ethers originally present in the sample (unless isotopically labelled TMAH reagent is used), thus making structural identification uncertain. The solution has been to use ethyl or butyl analogues of the base

as the butylated forms occur less frequently naturally.²⁸ Also, TMAH is a strong base and apart from methylation the highly basic conditions are likely to induce a variety of peripheral reactions (*e.g.* Cannizzaro reaction), which can make interpretation complex, especially when the substrate is also complex, *e.g.* HS. In addition, it has been recently reported that decarboxylation may occur with TMAH thermochemolysis depending on the position of hydroxyl substitution relative to the carboxylic group, with ortho and para substituted aromatic carboxylic acids, being more susceptible.²⁵ The use of model compounds is therefore essential for better understanding of the underlying mechanism, although it must be stated that, the literature is deficient in this kind of studies.

1.3.3 Soft Ionization Methods and HS Characterization

The advent of the landmark, new soft ionization methods, as well as growth in the capabilities of mass spectrometers is revolutionizing and spurring new interest in the characterization of HS. The new ionization methods of note are electrospray ionization (ESI), an atmospheric pressure form of ionization and matrix assisted laser desorption ionization (MALDI).

ESI is a low fragmentation (soft) technique that preferentially ionizes hydrophilic analytes that are polar (*e.g.* carboxylic acids and other heteroatom functionalities) and/or thermally labile. As such, it has evolved to be one of the core methods in protein analysis, environmental, pharmaceutical and pharmacokinetic applications.^{30,31} ESI has numerous advantages including little fragmentation of protonated molecules, wide applicability, and high sensitivity. It is also readily coupled to LC and affords analysis of macromolecules. When many protonatable moieties are present, ESI can produce multiply charged species,

reducing the m/z ratio accordingly so that the ion of a high mass molecule can be analyzed using low mass range mass analyzers, such as quadrupole. ESI is also ideal for both qualitative and quantitative (especially with MS-MS and selected reaction monitoring) work. With these many benefits, ESI has seen a proliferation of research papers and reviews on many aspects and applications, including humic substances research.³⁰⁻⁴⁷ Before discussing ESI applications in HS, it is pertinent to briefly discuss its theory.

1.3.3.1 ESI Basic Instrumentation

Electrospray had been used as a painting technique before Dole and co-workers (1960s and early 1970s) and later Fenn *et al.* (1980s) developed it into an ionization method for mass spectrometry.^{30, 31} Without labouring intensively on the fundamentals of ESI; succinctly, an analyte solution, either from LC or directly infused, is pushed at flow rates (~ 0.1 - $40 \mu\text{L}/\text{min}$) through a thin metal capillary (normally, 0.1 mm internal diameter and 0.2 mm outer diameter). The capillary is held at high potential (± 2 - 5 kV) and is located at about 1 - 3 cm from the counter electrode; consequently forming a mist of highly charged droplets. The high electric field at the tip of the capillary results in partial charge separation, such that for negative ion mode, negative ions are enriched at the surface of the capillary tip, while positive ions are pushed inside the capillary. The synergy of the repulsive forces between the ions and the pull of the electric field on the ions overcomes the surface tension making the liquid expand into what is called a Taylor cone. The tip of the cone is unstable and as solvent is nebulized and evaporated with the help of a neutral drying gas *e.g.* nitrogen, the charged droplet shrinks considerably, thereby increasing the

electrostatic repulsion within the droplet ultimately reaching a critical value called the Rayleigh limit (Coulombic repulsion \gg surface tension). At this limit, coulombic explosion occurs; producing a fine spray of charged droplets and eventually releasing charged molecules. Positive or negatively charged ions can be formed depending on the functional groups present in the analyte. For example, acidic functional groups (*e.g.* carboxylic acids) preferentially form negative charged ions usually by deprotonation, while basic (*e.g.* amines) ones would form positively charged ions generally by protonation. For analytes without sufficient basic moieties to enable protonation, cationization is observed. Notably, ESI favours production of multiply charged ions especially with macromolecules containing multiple charged centres.³¹ A figure delineating the mechanism is shown in Figure 1.3.

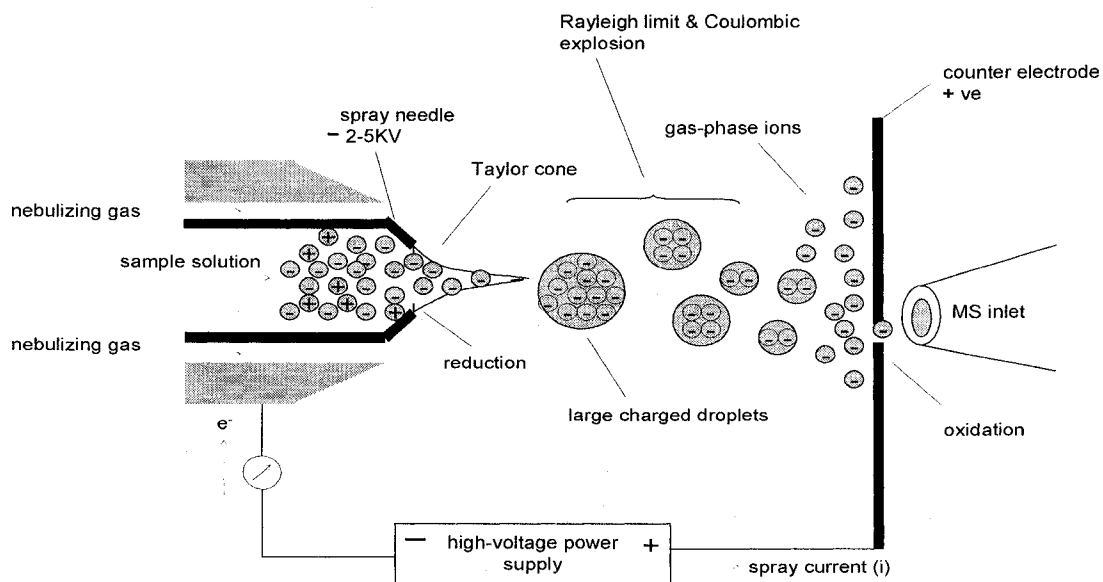


Figure 1.3. Schematic of a typical ESI system in the negative mode.³¹

1.3.3.2 ESI-MS Application to HS Analysis

ESI coupled to different powerful analyzers with tandem MS capabilities: (triple quadrupole (QqQ), Fourier Transform ion cyclotron resonance (FT-ICR), quadrupole time-of-flight (QqTOF) and quadrupole ion-trap (QIT)) have been employed for the characterization of HS. These studies have led to insights into the structure of HS components. The earliest report on the use of ESI-MS for HS characterization was by Fievre *et al.*³² in 1997, using a FT-ICRMS. To improve desorption probability and detection efficiency for HS, HPLC was incorporated and fractions separated prior to analysis, thus reducing the polydispersity index of the HS. In their work, they used positive mode of ionization and compared the results from laser desorption ionization ($200 \leq m/z \leq 800$) with those of ESI, with the latter generating mass spectra with only few prominent ions and higher mass ions (up to m/z 3000), attesting to less selective ionization and minimal fragmentation. From their work, they proposed the possibility of determining unique molecular formulas for individual exact ion masses for detailed structure elucidation. However to achieve this, several tandem MS experiments are necessary especially with the use of collisional induced dissociation (CID) or sustained off-resonance irradiation (SORI) in FT ICRMS. In mass spectrometry, CID otherwise referred as collisional activated dissociation (CAD) refers to a mechanism of fragmentation of molecular ions typically in a vacuum of a mass spectrometer by collision with neutral gas molecules (often helium, nitrogen or argon). McIntyre *et al.*³³ used negative mode ESI and a QqQ mass analyzer to analyze groundwater HS. Complex mass spectra were reported with ions at virtually every mass unit with a large mass

distribution between m/z 100-1200 with a maximum around m/z 350. The possibility of the presence of multiply charged ions as well as spectral dependence on solvent made the obtained molecular weight distribution questionable. However, very useful information was obtained with CID experiments, where consistent loss of CO_2 and mass series of peaks separated by 14 and 2 Da, characteristic of CH_2 group and olefinic and/or ring structures were observed, all pointing to a mix of aliphatic and unsaturated polycarboxylic acid compounds in HS.

As discussed previously, carboxylic acids and phenolic moieties ionize best in the negative mode, whereas amines ($-\text{NH}_2$) are preferentially ionized in positive mode. McIntyre *et al.*³³ observed a higher (at least one order of magnitude) total ion current in the negative mode, which indicates a predominance of acidic molecules in ground water HS and so spectra acquired in negative ion mode could be more representative. However, in general, the negative ionization conditions can be used for the characterization of the acidic HS fraction, believed to constitute mono/dicarboxylic acids and polycarboxylic acid components, whilst the positive mode elucidates the basic fraction. Even with the use of the two modes, it is critical to mention that the resultant mass spectra may not accurately reflect the composition of the sample, since part of the neutral fraction (*e.g.* polyols, polyethers, *etc.*) may be difficult to ionize and also due to the preferential ionization of the hydrophilic components containing functional groups such as carboxylic acids, alcohols, and especially amines.³⁵

McIntyre *et al.*³⁴ confirmed the presence of individual classes of carboxylic acids in soil and peat fulvic acid standards from IHSS, using ESI tandem mass spectrometry (MS-MS). In their work, the fulvic acids were fractionated based on their solubility in

methanol and the precursor and product ion studies produced mass spectra indicating the presence of benzene, phenol, dihydrobenzene, furan and thiophene carboxylic acids. Aromatic carboxylic acid standards were used to verify the fragmentation patterns observed in the product ion spectra of FAs. Their results give credibility to the findings of degradation techniques (pyrolysis and thermochemolysis), where most of these are reported as pyrolysates.

Kujawinski *et al.*³⁶ and Plancque *et al.*³⁷ employed ESI with a QqTOF mass analyzer, while Leenheer *et al.*³⁸ using a multistage MS-MS (ion trap) have proposed hypothetical structures of lower molecular weight HS, as well as plausible fragmentation pathways. The use of sample infusion with QqTOF and QqQ mass spectrometers was, however, unable to fully resolve the individual HS ions. The remedy to this was proposed by Reemtsa *et al.*³⁹ and others,⁴⁰⁻⁴³ who demonstrated that on-line coupling of SEC (using 80/20 (v/v) water/methanol with 10mM NH₄HCO₃) to MS-MS could significantly add a new dimension to the mass spectral information obtainable. Coupling SEC to MS/MS reduces the polydispersity of the HS entering the mass spectrometer at a given time thus minimizing ionization competition and increasing ionization efficiency, leading to more representative mass spectra. Moreover, by separating the inorganic impurities from the analytes, there is a reduction in adduct formation, which simplifies spectral interpretation. Using SEC-QqTOFMS, sufficient mass resolution was possible to allow identification of low MW FA (consisted of high carboxylate content). The obtained data can be extrapolated for identification of high MW components, especially for the polymeric model of HS. Nonetheless, even with these advantages, the use of SEC is limited due to non-specific ionic interactions, adsorption phenomena, hydrophobic (high at high ionic

strength) and electrostatic (high at low ionic strength) interactions. Judicious selection of the mobile phase is also critical because only a few solvents and buffers can solubilize the HS and are amenable to ESI-MS.

Numerous studies have been conducted with the ultra-high resolution ($R = m/\Delta m$) FT-ICRMS (theoretically $R > 100,000$), which was found to afford detection of individual fulvic acid molecules.⁴⁴⁻⁴⁶ This is due to its immense capability for resolving species that are nominally isobaric (*e.g.* species with a mass difference of up to 0.0034 Da) without chromatographic separation. Stenson *et al.*,⁴⁵ using ESI-FT-ICRMS, was able to detect individual molecules in Suwannee River HS assigning them elemental compositions and exact molecular formulas for low mass ions. Reemtsa *et al.*⁴⁶ has further demonstrated the utility of coupling SEC to ESI-FT-ICRMS, applying this technique to the analysis of fulvic acids from different origins (Suwannee River FA, Waskish peat elutriate and Nordic aquatic fulvic acid). From their study, up to 700-1900 molecular formulas of FAs components were derived. From these results, they concluded that the different fulvic acids had very similar molecular pattern and that (poly-) carboxylic acids with only few hydroxyl groups are the dominant class in the fulvic acids tested. The use of FT-ICRMS technique is still a very active research area in humic substances studies and other related fields such as petroleomics due to the untapped potential therein.⁴⁷ The major disadvantages of FT-ICRMS are that it is extremely expensive, and thus not available to many academic institutions, and is not suited for coupling with LC.

Some disadvantages with ESI have also been noted, such as mass dependent ionization and possible in source fragmentation, which may explain the radical variations of HS molecular mass distribution obtained with ESI compared to those obtained by SEC

and other techniques.^{7,15} Although there are still divergent views as to the cause of this discrepancy, suggested explanations include preferential ionization of relatively low MW components of HS, formation of multiple charges (confirmed by Pfeifer⁴⁰) with ESI, or that the HS are supramolecules consisting of small molecules that tend to behave as macromolecules under strong ionic conditions employed with SEC. Leenheer *et al.*,³⁸ using polyacrylic acid as a proxy for aquatic fulvic acids, has intimated that ESI generates fragments and multiply charged ions of HS, especially in the case of those fractions with high carboxylic content, although given the softness of ESI and the fact that HS may not easily accommodate multiple charges, the extent of the fragmentation and multiple charges have not been ascertained. The propensity of ESI for formation of multiply charged ions, although an advantage especially in proteomics, can be a drawback in analyzing very complex mixtures like HS because of the complexity of the resulting mass spectra. This necessitates use of complicated data visualization protocols such as the Kendrick mass defect (KMD). KMD has been used for HS data analysis by Kujawinski *et al.*⁴⁴, but was initially developed to identify compounds found in petroleum, which are related to each other by addition or subtraction of a methylene group. In addition, HS analysis by ESI-MS may require use of complex deconvolution software to interpret the mass spectra, such as GRAMS/32® reported by Plancque *et al.*³⁷ Additionally, Kuwajinski *et al.*⁴⁸ has recently demonstrated use of an automated compound identification algorithm for analysis of mass spectra of NOM acquired by ESI-MS.

Conversely, MALDI is known to form mainly singly charged ions and hence the resulting mass spectra are considerably easier to interpret. Surprisingly, there is only

scant literature in the use of MALDI to characterize HS, making it an attractive research endeavor.

1.3.3.3 MALDI Basic Operational Theory

The use of MALDI was first demonstrated simultaneously in two laboratories, by Koichi Tanaka (Shimadzu Corporation, Kyoto, Japan), and by Michael Karas and Franz Hillenkamp (both of University of Muenster, Germany) in 1987.^{50,51} Tanaka used a pulsed N₂ laser (337 nm emission wavelength) and a slurry of glycerol and colloidal cobalt as a matrix and reported a mass spectrum of lysozyme (MW 14,307).⁵⁰ On the other hand, Karas and Hillenkamp used a frequency-quadrupled pulsed neodymium YAG laser (266 nm emission wavelength) with nicotinic acid as a matrix and a mass spectrum of bovine serum albumin (MW 66,750) was reported.⁵¹ Since then, MALDI has been used widely, especially for qualitative analysis of non-volatile macromolecular analytes such as proteins, oligonucleotides, oligosaccharides and synthetic polymers. The ability of MALDI to analyze various classes of analytes (especially macromolecules) by converting them to ions in the gas phase, and its utility as a surface analytical method, attests to its versatility and wide applicability and hence frenetic activity in its use has resulted, as manifested by a large volume of publications.⁵²⁻⁵⁶

MALDI is a classical example of a technique whose commercialization and wide-range of applications preceded a thorough understanding of elementary mechanistic principles governing ion generation processes and desorption; the multifaceted MALDI mechanism is still an active research area. In essence, MALDI involves co-crystallization of the analyte with a molar excess of matrix (100:1 to 10,000:1) on a stainless steel

sample stage. MALDI matrices are typically UV absorbing small molecular weight organic acids, (structures of common matrices are shown in Figure 1.4).

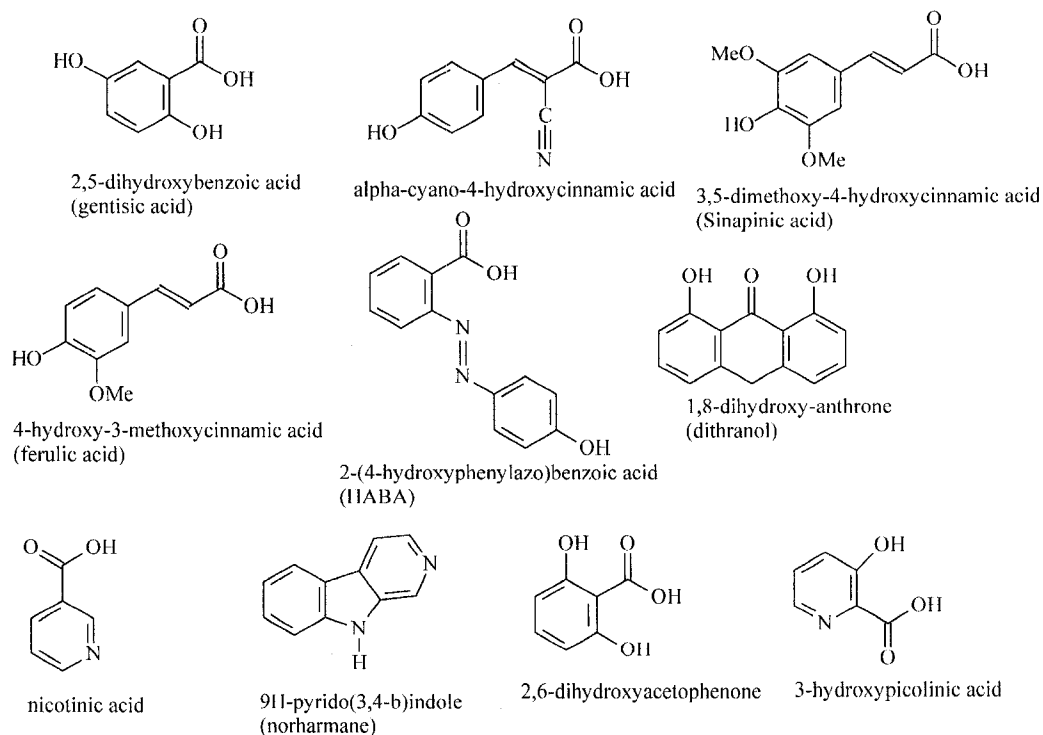


Figure 1.4. Structures of common MALDI organic matrices employed.

Energy from a focused UV (or IR) laser beam is directed to the cocrystallite (condensed phase of analyte-matrix) and a couple of processes occur. The matrix absorbs the energy from the laser and transfers the thermal energy softly to the analyte; with sufficient laser energy density (threshold irradiance), an explosive formation of a dense plume expanding at supersonic velocities results. The plume consists of protonated molecules, deprotonated molecules, electrons, hydrogen atoms, matrix radicals and neutral matrix fragments and analytes. There has been an ongoing debate, however, on the necessity of

cocrystallization for the success of MALDI. As a result of the success of other non-matrix surface-based techniques, a number of researchers are casting doubt on this long held notion.⁵⁷⁻⁵⁹

Ionization is a very complex phenomenon that is much less understood than desorption. This is especially so because of the many possible ions that result including protonated, deprotonated, cationized and radical species, with only very remote dependence on matrix, solvent composition, solution pH and analyte acid-base properties. Whether ions are preformed in the solid solution or are formed in the expanding plume remains a debate, although, in general, the secondary reactions dictate the ions that are eventually detected. One proposed ionization mechanism that has been propagated extensively is donation of a proton from the matrix to the analyte (eqn 1.1) analogous to chemical ionization.



where M^* is the excited matrix and A, is the analyte.

Cationization (mainly K^+ and Na^+ adducts are observed) can also be prevalent depending on the nature of the analyte, particularly those with low proton affinity such as carbohydrates and synthetic polymers.^{59,60} Odd-electron ion formation (either by electron transfer or electron capture, eqn 1.2) has also been observed especially for non-polar matrices (*e.g.* C_{60} , anthracene, terthiophene *etc.*) and analytes such as ferrocene and its derivatives. It has been postulated that charge transfer is possible if the ionization energy of the matrix slightly exceeds that of analyte.⁵⁹



The role of the matrix is multifold:

- Dilute and isolate analyte molecules to avoid analyte cluster formation.
- Absorb the laser energy via electronic (UV-MALDI) or vibrational (IR-MALDI) excitation resulting in disintegration, while shielding the analyte from the energy deposited by the laser. This reduces analyte fragmentation by soft and uniform energy transfer from the matrix to the analyte.
- Assist in desorbing the analyte from the sample surface and in analyte ionization.

Most of the known matrices have stood the test of time and have been used since MALDI inception, but there is ongoing research on the exploration of new matrices, because none of the known matrices is ideal and able to meet all the above functions. Selection of a good matrix thus remains one of those challenges in MALDI applications, particularly because MALDI is a complex physico-chemical process happening in nanosecond timescale, and there are no rational guidelines or criteria for matrix selection. As such, the matrices are only operationally-defined as either “hot” or “cool” depending on their phase transfer temperatures, with the former causing more analyte fragmentation than the latter.⁵⁸⁻⁶¹

The analyte interaction with the matrix has also been a very contentious issue, with two schools of thought being dominant: possibility of analyte incorporation into the matrix solid, forming the so called ‘solid solution’, which refers to analyte solvation in the matrix crystal. The other possibility is where the matrix acts as support for the

analyte. To study these two phenomenon, high resolution scanning electron microscopy (SEM), a well developed microscopic technique, has been widely employed.^{61,62}

MALDI is generally coupled to a time-of-flight (TOF) mass analyzer, particularly suited due to the pulsed nature of the laser (commonly N₂), which results in pulsed ion generation. In the TOF mass analyzer, ions originating from same position at the same time are accelerated by a constant electric field, to a constant kinetic energy equal to zV (eqn 1.3b), where z is the charge of the ion, v is the velocity of the ions and V is the accelerating pulse potential. The measured mass-to-charge ratio (m/z) relationship is shown in eqn 1.4. The lighter ions travel faster than the heavier ones and reach the detector earlier, (typically a microchannel plate detector) placed at the end of the flight tube (of length L).^{63,64} Figure 1.5 shows a schematic of MALDI-TOFMS.

Equation governing TOF separation:

$$v = (2qV/m)^{1/2} \dots\dots\dots \text{Eqn 1.3a}$$

Where: $q = z \times e$, and z is the number of elementary charges and e is 1.6×10^{-19} C

Therefore,

$$v = (2zeV/m)^{1/2} \dots\dots\dots \text{Eqn 1.3b}$$

and

$$m/z = 2Ve (t/d)^2 \dots\dots\dots \text{Eqn 1.4}$$

d - length of field free drift region

t - measured time of flight of the ion

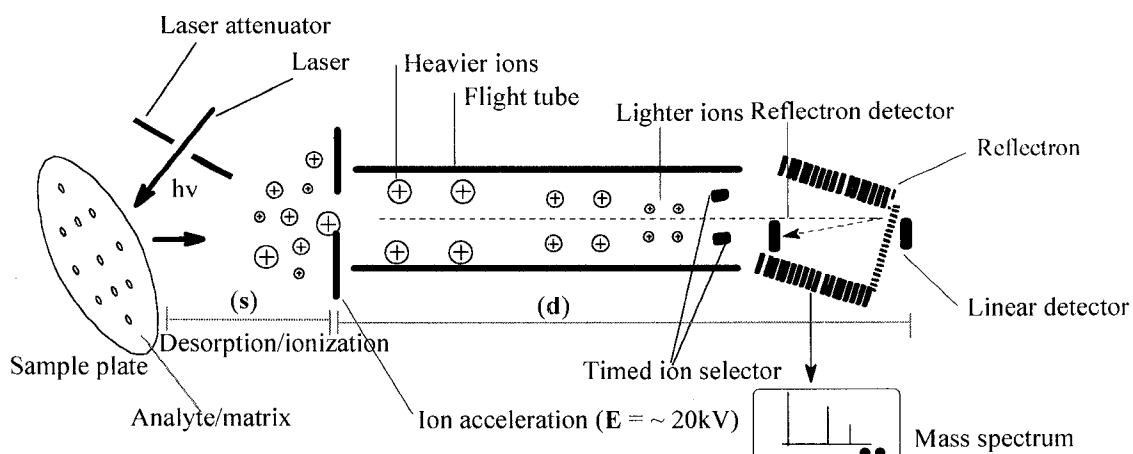


Figure 1.5. MALDI TOFMS principle (adapted from reference ⁶³)

Some of the noteworthy advantages of TOF include: high ion transmission, high sensitivity, theoretically unlimited mass range, very high spectrum acquisition rate, multiplex detection capability for each ionization pulse, low cost and relatively simple instrumentation to conceptualize. The common limitations of TOF analyzers comprise of relatively poor resolution compared to FT-ICRMS (although high resolution hybrid TOF now available *e.g.* QqTOF and TOF-TOF) and incompatibility with continuous ion sources. Coupling MALDI to TOF, especially using the conventional axial geometry, requires the synchronization of mass analysis to the ionization and desorption steps, and which are highly variable, and can adversely affect the instrument performance. Nonetheless, with the development of time-lag focusing, the performance and robustness of MALDI have been greatly improved. Furthermore, the decoupling of the mass analysis from laser timing using orthogonal MALDI (analyzer perpendicular relative to the ion source) has not only improved the MALDI performance but also made MALDI amenable to coupling with other continuous beam mass analyzers (QqTOF, QqQ, IT *etc.*).⁶⁴

1.3.3.4 MALDI-MS Application to HS Characterization

Laser desorption ionization (LDI), the matrixless variant of MALDI, has been employed for the determination of molecular weight distributions of humic substances by a number of researchers. Novotny *et al.*⁶⁵ characterized five IHSS fulvic acids of different origins (from soil, peat, Nordic, and Suwannee River) using LDI-FTMS revealing broad molecular weight distributions of m/z 100-1100 with number average molecular weights of m/z 400-600 and intensity maxima at 370 and 530 Da. Brown *et al.*⁶⁶ reported molecular weight distribution in the positive mode for FA to be about m/z 1000 with most abundant ions in the m/z 500-600, which complemented the results achieved previously by Novotny *et al.*⁶⁵. In the negative mode, the molecular weight distribution ($\sim m/z$ 700, most intense ions m/z 400-500) was lower and more reproducible mass spectra were obtained. Very similar results were obtained by Fievre *et al.*³² and Srzić *et al.*⁶⁷ In all cases, the featureless and poorly resolved mass spectra obtained were frustrating but confirmed the sheer complexity of these substances. Hence, interpretation was limited to MS fingerprinting of different FA classes and approximation of molecular weight distribution. Their results, however, provided some proof that lower MW substances dominate the mixture comprising FA, since the molecular weight distribution was significantly lower (centered \sim 500-700 Da) than those determined by other traditional methods (*e.g.* ultra filtration, SEC, VPO *etc.*), further casting doubt on the notion that HS are macromolecules spanning hundreds of thousand Daltons.^{2,7,15} One major limitation of LDI, however, is that analytes are not shielded from the laser energy leading to analyte fragmentation, and this was suspected to be one of the possible reasons for lower mass

distribution. This therefore necessitated the use of the much softer ionization method, MALDI.

The oldest reported attempt for characterization of HS by MALDI-TOFMS was by Reemler *et al.*⁶⁸ in his seminal paper in 1995. They confirmed the presence of basic groups in humic acid (isolated from lake water and from a bog) due to the amenability of HS to protonation. However, they reported that the technique was limited because of cluster formation, fragmentation phenomena and probable preferential desorption and ionization of lower molecular weight compounds.

Haberhauer *et al.*⁶⁹ among others,⁷⁰⁻⁷³ additionally confirmed, using MALDI-TOFMS, that HS (samples used of terrestrial origin) may not consist of high molecular weight compounds as once thought, but could be composed of smaller building blocks not bound together by covalent bonds. Similar conclusions had been arrived at from ESI results.⁴²⁻⁴⁶ Major obstacles encountered in the use of MALDI-MS technique include: detection problems due to the inherent complexity of HS, which could contain a highly varied mixture of low concentration constituents and selection of an ideal matrix. MALDI is also prone to the formation of cluster ions, which are indistinguishable from molecular ions, fragment ions and isobaric matrix interferences, thus complicating spectra interpretation. Moreover, impure samples such as HS are likely to contain impurities that could adversely affect the ion yield. It is likely that only a small fraction of the entire mixture is desorbable and ionizable, thus the spectrum may not be representative of the whole sample, leaving a proportion of HS constituents unidentified. Nevertheless, MALDI-MS was found to afford characterization and differentiation of HS from terrestrial and aquatic origins.⁶⁹ The similarity of MALDI mass spectra of FAs from

different origins (*e.g.* derived from coal, leornadite, soil, peat *etc.*) was noted by Gajdošová *et al.*⁷⁰⁻⁷² suggesting similarities in their genesis. The commonalities in the molecular composition of FAs have also been noted by Reemtsa *et al.*⁴² in their comparative investigation of FA from surface water, ground water and peat. The fact that similar *m/z* ions have been reported for different HS of different origins, including those from Antarctica where very limited vegetation is present, further attests to HS similarity, hinting at common precursors and a common genesis of these substances. In spite of the limitations, the potential of MALDI has not been fully exploited. With careful sample preparation, matrix selection and optimization of parameters such as matrix/analyte ratio, more information on HS can be obtained, which can bring deeper insight into their chemical nature. It is practical to envision that since there has been tremendous progress in the innovation of new analytical tools, the knowledge on the structural properties of HS will continue to be revealed. For example, the success in coupling of LC to MALDI integrated with FT-ICRMS has created a very powerful platform for proteomics, but could also have applications for materials like HS.⁷⁶

1.3.4 Disinfection Byproducts Formation

According to estimates by the United Nations, up to 1.1 billion people lack access to safe drinking water. It is further estimated that 6000 children in developing countries die of waterborne diseases every day. Water contaminants *e.g.* metals, pesticides *etc.* further exacerbate an already dire situation. With the water shortage that is already being felt around the globe, water reuse by disinfection is one feasible solution; however, this approach is not without potential pitfalls. Ultimately, the onus for providing safe drinking water rests on the water chemists who must consider all aspects of water quality.^{77,78}

Although disinfection especially by chlorination has nearly eradicated the morbidity and mortality of water borne diseases caused by pathogens (*e.g. Salmonella typhi, vibrio cholerae, E.coli, Cryptosporidium, Giardia etc.*), it is counterproductive since chlorine reacts with aquatic NOM (HS being the major component) and inorganic materials present in water to form numerous potentially harmful disinfection byproducts (DBPs), some of which are suspected carcinogens.^{12,79} The reaction pathways for NOM and chlorine are not well understood due to the structural ambiguity regarding NOM, but could include electrophilic substitution, radical reactions, oxidation, addition *etc.* These reactions produce a mixture of DBPs, widely differing in polarity, molecular weight and physical and chemical properties.⁸⁰⁻⁸² Figure 1.6 shows a simple schematic of the DBPs formation process.

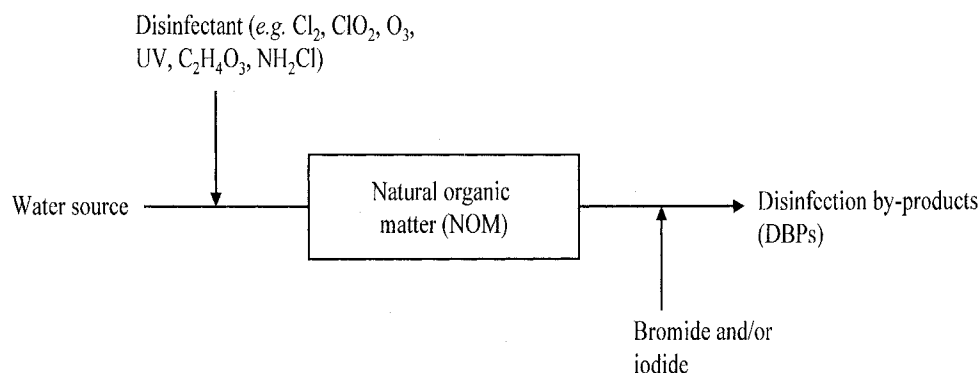


Figure 1.6. Formation of disinfection byproducts.

A delicate balance must be maintained between complete disinfection to kill pathogens and minimization of DBPs formation. This is a big challenge because the parameters leading to improved disinfection efficiency similarly increase DBPs formation.⁸¹ Figure 1.7 delineates in graphical form this relationship.⁸¹

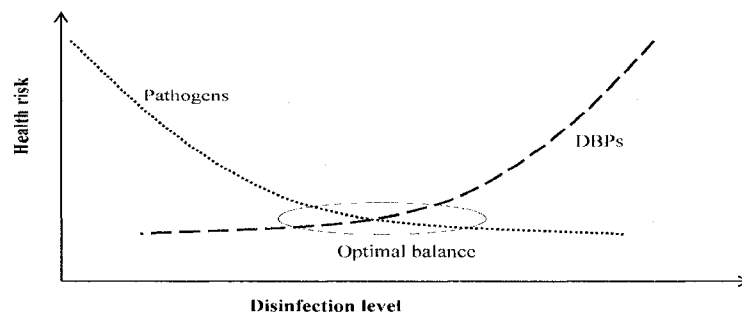


Figure 1.7. Health risk tradeoffs of drinking water disinfection.

The first case of DBPs occurrence was reported by Rook¹² in the 1970s when he discovered chloroform in drinking water. Since then, a lot of research time and resources have been expended in the characterization of DBPs and over 600 DBPs have been identified. As a result, there is a substantial accumulation of literature on DBPs over the last decade, which would be too large to comment on in its entirety. However, authoritative reviews on emerging contaminants including a detailed list of specific priority DBPs are produced annually by Richardson.⁸²⁻⁸⁴ Tables summarizing the categories of DBPs and the semi-quantitative carcinogenicity rankings and rating scale categories are provided in **Table 1.1** and **Table 1.2** respectively.

It is in general agreed among DBPs specialists that the known compounds only represent a small component (< 40%) of the existing DBPs in the water systems and thus their characterization remains a grueling task. By studying as many DBPs as possible, the resulting knowledge could be used to generate databases that could be useful and time saving for researchers in the future. Other issues, such as the formation of DBPs *in vitro* resulting from reactions of organic matter (foods) and other compounds such as pharmaceutical products with residual disinfectant in drinking water, have so far received little research effort and yet merits serious investigation.⁸⁴

Table 1.1. Classification of common known DBPs.⁸²⁻⁸⁴

DBPs class	Example	Toxicology rating	Disinfectant source
Halomethanes (THM)	chloromethane	B2	Cl ₂ , NH ₂ Cl
Haloacetic acids	dichloroacetic acid	B2	Cl ₂ , NH ₂ Cl
Haloketones	1,1,1,3-tetrachloropropanone	C	Cl ₂ , O ₃ , ClO ₂
	chloropropanone	C	
Haloaldehydes	dichloroacetaldehyde	C	Cl ₂ , NH ₂ Cl
	chloroacetaldehyde	C	
Haloacetonitriles	chloroacetonitrile		Cl ₂ , O ₃ ,
Haloamides	dichloroacetamide		Cl ₂ , NH ₂ Cl
MX and MX analogues	3-chloro-4-(dichloromethyl)-5-hydroxy-2(5H)-furanone	B1	Cl ₂ , ClO ₂ , NH ₂ Cl
Inorganic compounds	chlorite	D	O ₃ , ClO ₂
Nonhalogenated carbonyls	methylglyoxal	C	O ₃
Other priority DBPs	nitroso compounds, <i>e.g.</i> nitrosodimethylamine	B1	Cl ₂ , NH ₂ Cl, ClO ₃
	iodo acids, <i>e.g.</i> iodoacetic acid, iodobromoacetic acid <i>etc.</i>		NH ₂ Cl

Some of the ratings were approximated from the structure activity analysis rankings proposed by Woo *et al.*⁸⁷ (see Table 1.2 below)

Table 1.2. Contaminants carcinogenicity rankings categories.

Class^{80,81}	Description	Woo <i>et al.</i>⁸⁷ carcinogen rankings	Approximate Carcinogenicity scale*
A	Human carcinogen	Highly likely	A
B1, B2	Probable human carcinogen	High moderate	B1
C	Possible human carcinogen	Moderate	B2
D	Not classified	Low moderate	C
E	Non-carcinogen	Marginal	D
		Low	E

*Classifications presented are estimated for comparison with the rating system in general use.

Briefly, traditional classes of DBPs such as trihalomethanes (THM) and five of the nine haloacetic acids (HAA) have already been regulated and maximum contaminant levels fixed by organizations such as the United States Environmental Protection Agency (US EPA) and the World Health Organization. For example, in 1998, the US EPA set the maximum contaminant levels (MCLs) of total THMs and HAA5 (the sum of five main HAAs) to 80 and 60 μgL^{-1} respectively.^{83,84} Other identified DBPs, such as the strong mutagen, 3 chloro-4-(dichloro-methyl)-5-hydroxyl-2(5H)-furanone (MX), initially identified as a DBP in bleached pulp water in Finland, have generated tremendous scientific interest and numerous studies have been published detailing their formation and occurrence.^{79, 85} The main reason for the large number of studies is that MX reportedly accounts for 15-57% of the total mutagenic activity in chlorinated drinking water and 50-100% in chlorinated humic-rich water. However, other MX analogues especially brominated forms of MX (BMXs) or DBPs similar in structure to MX have also been reported.^{79, 84,85} Many more emerging DBPs, some of which have been categorized as high-priority DBPs, have been recognized to be more important in their effect to human health.^{79,85} For example, nitrosodimethylamine (NDMA) recently discovered in drinking water in Ontario has been recognized as a probable human carcinogen and is now a byproduct of great concern. Ontario has set its maximum allowable limit to 9 ng L^{-1} . NDMA is normally produced when chloramines and, to a lesser extent, chlorine and chlorine dioxide are used as a disinfectant.⁸⁶ Other high-priority DBPs include chlorinated, brominated and iodinated forms of halomethanes, haloacetonitriles, haloketones, haloaldehydes, haloacids, halonitromethanes, halofuranones, haloamides *etc.* Iodinated DBPs have been found to be the most toxic followed by brominated and then

chlorinated analogues. For instance, dibromonitromethane has been reported to be at least one order of magnitude more genotoxic to mammalian cells than MX. The occurrence of both iodinated and brominated byproducts is common when surface waters are contaminated with coastal waters containing iodide and bromide, which react with chlorine (HOCl/OCl^-) to form hypiodous acid (HOI/OI^-) and hypobromous acid (HOBr/OBr^-), respectively. Most of these compounds have been classified as possible human carcinogens and, though inconclusive, epidemiology studies have identified them as potentially teratogenic and cytotoxic. Studies on human exposure have shown that ingestion is only one of the exposure routes; inhalation and dermal absorption through bathing could be even more significant.⁸²⁻⁸⁴

However, it is virtually impossible to regulate every single DBP and therefore it has been suggested that bulk measurements (*e.g.* total dissolved organic halides) as well as predictive models would be the most practical way of occurrence prediction and decision making regarding regulatory measures.⁸¹ Use of mechanism based structure activity relationship analysis has also been exploited by Woo *et al.*⁸⁷ to rank carcinogenicity of various DBPs. Nevertheless, the study of individual formation of newly discovered DBPs outside the realm of traditional DBPs such as THM and HAA remains a legitimate research area. This could be essential in understanding DBPs formation mechanisms— since to date only hypothetical pathways have been proposed (Figure 1.8) — especially if suitable model compounds are employed. Model compounds such as flavanoids (hesperetin), aromatic acids (syringaldehyde) and phenolic compounds

(e.g. resorcinol, have been employed to model the reaction pathways leading to the formation of DBPs.⁸⁸⁻⁹⁰

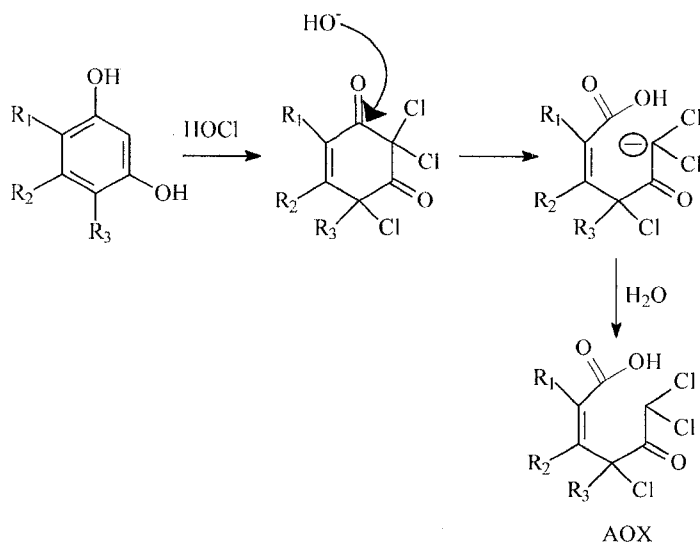


Figure 1.8. Model pathway of adsorbable halogenated DBPs (AOX) formation.^{10, 12}

Most of the uncharacterized DBPs are of relatively high molecular weight (> 500 Da), polar and/or thermally labile compounds, and are not easily amenable to analysis by the gold standard technique GC-MS (used for thermally stable analytes with adequate vapor pressure). Minear *et al.*⁹¹⁻⁹³ have published several papers describing attempts to characterize high molecular weight DBPs using SEC-ESI-MS and ESI-MS-MS. The identification of specific high molecular weight DBPs has been largely unsuccessful due to the complexity of the mass spectra, with peaks present at every mass unit. By using FT-ICRMS, it might be feasible to produce better resolved mass spectra and definitive structural assignments may be possible. The analysis of the polar DBPs is also very challenging especially because of their characteristic low octanol-water partition coefficient, hence their extraction is difficult. Derivatization using reagents such as *O*-

(2,3,4,5,6-pentafluorobenzyl)hydroxylamine (PFBHA) and 2,4-dinitrophenylhydrazine (DNPH) for carbonyl compounds (Figure 1.9a,b), in conjunction with GC-MS and LC-MS, respectively, have been used successfully. PFBHA has mainly been used to derivatize aldehyde DBPs, leading to formation of oximes that are amenable to analysis by GC.^{85,94} DNPH on the other hand, reacts with both aldehydes and ketones to form hydrazones, which are sufficiently acidic and thus amenable for detection in negative mode ESI-MS.⁹⁴ It is possible to distinguish hydrazones resulting from aldehydes and ketones either by their difference in chromatographic behavior (syn and anti isomers coelute for aldehydes, but are resolvable for ketones) or by collision induced dissociation, where a fragment ion m/z 163 is present in aldehydes but not in ketones. Vincenti *et al.*⁹⁵ recently synthesized water-soluble, stable highly fluorinated alkyl and aryl chloroformates (Figure 1.9c) and demonstrated their use for rapid (< 10 min) derivatization of highly hydrophilic DBPs (*e.g.* carboxylic acids, alcohol, phenols, *etc.*) with subsequent detection by electron capture negative ionization mode GC-MS. They reported detection limits ranging from 0.1-10 $\mu\text{g L}^{-1}$ for a number of classes of compounds (*e.g.* hydroxycarboxylic acids, hydroxylamine, di/trihydrobenzenes, *etc.*). Although the derivatives had a relatively high molecular weight, the multiple highly-fluorinated functionalities, made them sufficiently volatile. Using this technique, malic acid, tricarballic acid and 1,2,3-benzenetricarboxylic acid could be identified as DBPs from ozonation. These techniques are limited because GC-MS can only be used for the relatively volatile compounds and derivatization may also result in compounds that are too bulky for GC-MS.^{83,94,95} Additionally, the derivatives normally undergo extensive

fragmentation in the high temperature injection port of the GC, and hence, the molecular ion is almost always absent in the spectra making interpretation difficult. On the other hand, when the derivatives are analyzed by LC-MS, resolution using the LC column into discrete peaks is difficult and thus identification is seldom achievable. Since DBPs are typically present in water at ultra low levels (*e.g.* sub ng L⁻¹ levels), sensitivity can be a problem; as a result, most of the derivatizing reagents employed require long reaction times and rigorous sample preparation followed by extraction. The use of LC-MS in DBPs analysis is a hot research area with tremendous potential for growth.⁸⁴

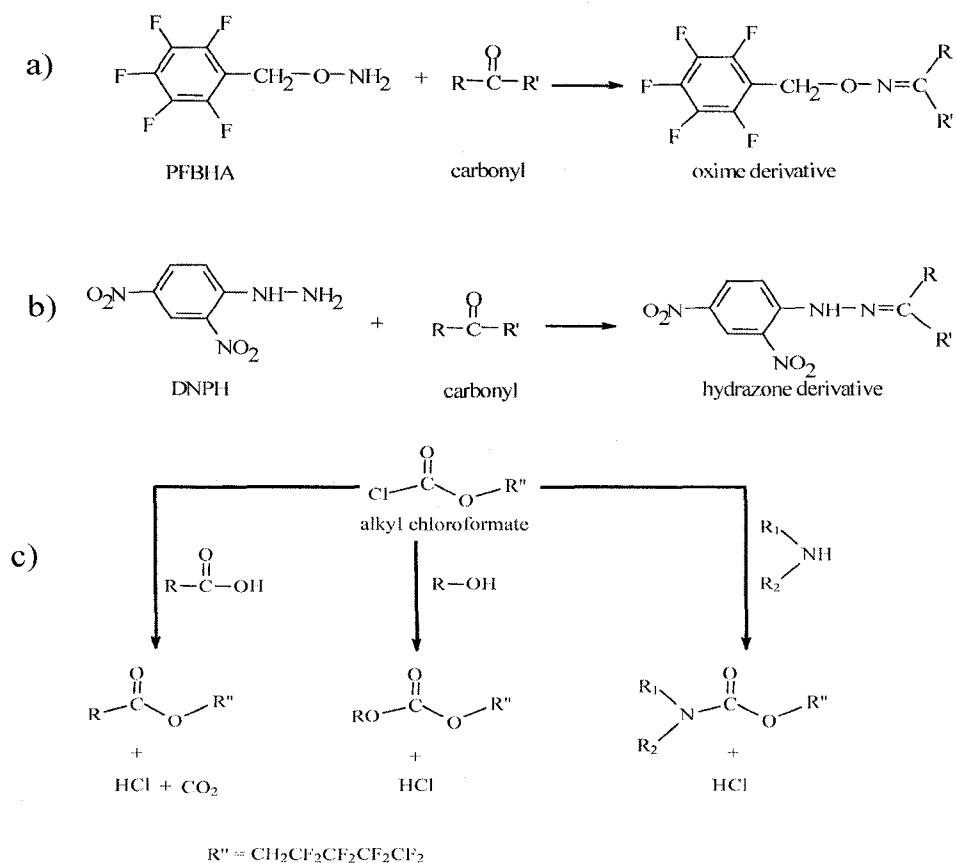


Figure 1.9. Derivatization schemes for polar compounds: a) PFBHA and carbonyls b) DNPH and carbonyls c) alkyl chloroformates with carboxylic acids, alcohols and amides.^{94,95}

Understanding the parameters that influence DBPs formation is critical to reducing their formation. Such parameters include pH, temperature, NOM properties, bromide and iodide levels and chlorine dose. In brief, THM and in general total organic halide (TOX) formation increases with increasing pH and temperature, although mixed effects have been reported for HAA species with pH variation. Higher chlorine dose has been found to favor HAA formation over THM. On the other hand, halogenated DBP formation increases with the activated aromatic content of NOM and UV 254 has been found as a good surrogate for DBPs.⁹⁶

Due to the magnitude of the DBPs problem, different approaches have been investigated for minimizing them. For example, alternative disinfectants *e.g.*, chloramines, ozone, UV and peracetic acid have been investigated resulting in reduction in the use of chlorine as a disinfectant. Many plants (*e.g.* the local Bay Bulls water treatment in St. John's, Newfoundland, supplying water to more than 100,000 residents) are mainly using ozonation in tandem with chloramination, which has been found to reduce the DBPs occurrence. Nevertheless, chlorine still remains the most widely used disinfectant due to its superior disinfection efficiency.^{97,98} The search for more benign disinfectants is ongoing with the very recent promising discovery of TAML[®]-activated hydrogen peroxide, which is being explored by the Institute for Green Oxidation Chemistry (based in Carnegie Mellon University and directed by Dr. Terry Collins),⁹⁹ as a means to destroy chemical pollutants in water, as well as an inexpensive water disinfection technology. Such technologies are still, however, in the research stage and it might take decades before their use becomes common in large scale water treatment.

Nevertheless, it has been argued that changing the means of disinfection would only result in the formation of different DBPs. For example, it was found that ozonation resulted in formation of bromonitromethanes, while iodo-THMs, nitrosodimethylamine and dihaloaldehydes are prominent when chloramine is used as the disinfectant.^{82,83} Ultra-filtration (membranes can remove particles of 0.001 – 0.1 μm) of the natural organic matter has been suggested as a more pragmatic approach, but the fulvic acid component of NOM, which is largely the known precursor of DBPs, is highly soluble in water and hence complete removal is a very challenging endeavor. Catalytically-induced oxidative coupling reactions when combined with ultrafiltration to remove most of the HS have been suggested by Weber *et al.*¹⁰⁰

1.3.8 Analysis of Small Molecules by MALDI

The analysis of small molecules by MALDI has become an active research area especially over the past decade, catapulted by the desirable properties of MALDI especially its sensitivity, relative ease of sample preparation, small sample size requirement, and amenability to automation, which is desired for high throughput analysis in pharmaceutical applications. In addition, MALDI is also more tolerant of salts and buffers compared to ESI, and is also environmentally friendly since large amounts of organic solvents can be avoided. Despite MALDI being a mature technique for the analysis of biomolecules, most of the hurdles limiting its full application in small molecule analysis are yet to be fully surmounted and therefore its application to small molecules is still in its infancy. Cohen *et al.*¹⁰¹ published an excellent treatise on small molecule analysis by MALDI.

Some of the common hurdles for application of MALDI in small molecule analysis include matrix interference in the low mass region, excessive volatility of small analytes especially in the vacuum chamber and poor ionizability of most small molecules. The inherent irreproducibility associated with random analyte deposition in the matrix crystal also greatly affects the possibility of using the technique for quantitative analysis of small molecules. Different approaches have been attempted to alleviate these obstacles with varying degrees of success. Use of more innovative sample preparation strategies other than the conventional dried droplet method, such as fast evaporation,¹⁰² vacuum crystallization,¹⁰³ electrospray matrix deposition,¹⁰⁴ multicomponent matrices,¹⁰⁵ *etc.* have been shown to yield more homogeneous analyte-matrix cocrystallization and thus better signal reproducibility. A matrix suppression effect (MSE) obtained by optimizing the ratio of analyte to matrix was proposed by Knochenmuss *et al.*¹⁰⁶ Although this technique worked for some classes of analytes, the rationale is cumbersome and a tedium since it is based on trial and error and thus too time-consuming. Matrix suppression has also been achieved using surfactants such as cetyltrimethylammoniumbromide (CTAB), Triton X100, sodium dodecyl sulphate (SDS), among others.¹⁰⁸ The use of such surfactants, however, can be counterproductive since the suppression is not specific to matrix ions but also suppresses the analyte, thereby compromising the signal to noise ratio, significantly eroding detection limits. Reproducibility has been improved by use of suitable internal standards as reported by Volmer *et al.*^{108,109} and other authors.^{110,111} Additionally, the use of selected reaction monitoring (SRM) scan mode (only diagnostic product ion is monitored), especially with triple quadrupole (has highest duty cycle scan available) and

equipped with high repetition rate laser has been demonstrated to improve S/N ratio, reduce matrix interference and to be effective for small molecule quantitation.¹⁰⁹⁻¹¹¹

Another approach has been to use high molecular weight matrices, which have limited matrix peaks in the low mass region. Such high MW matrices reported include porphyrin based matrices, *e.g.* meso-trakis(pentafluorophenyl)porphyrin (MW, 974.6 Da).¹¹² Recently, there has been an emergence in the use of carbon nanotubes (CNTs), originally discovered by Iijima,¹¹³ as matrices.¹¹⁴⁻¹²¹ This is an off-shoot of the use of inorganic matrices as laser energy absorbing materials, which were the materials used at the inception of MALDI.⁵⁰ Black *et al.*¹²² has also proposed the use of pencil lead, which is essentially graphite, as a matrix which has also shown considerable promise for use as a matrix. The major problem with these carbon based substrates is their susceptibility to contain impurities, which contaminate the ion source. For example, CNTs are rich in metallic impurities, suspected to be the main reason for ion source contamination, sometimes leading to instrument damage and costly repairs. The contamination of the ion source is exacerbated by the fact that CNTs do not adsorb firmly on the stainless steel MALDI stage and thus fly off upon irradiation with a laser. To solve this problem, Ren *et al.*¹¹⁸ immobilized CNTs on the target using a polyurethane adhesive. Another challenge with CNTs is that they are insoluble and thus result in inhomogeneous sample spots. To increase solubility, Pan *et al.*^{119,120} found it imperative to introduce carboxylate groups to enhance protonation of analytes, and to further increase CNTs surface polarity. Oxidation of CNTs is laborious and time consuming, requiring up to 20 hours of refluxing with nitric acid. Further functionalization has been attempted by bathing CNT in a citric acid solution resulting in an anionic surface.¹²⁰ Introduction of phenolic hydroxyl to the

surface of the CNT has been attempted by amidation of oxidized CNTs and the resulting (CNT 2,5-dihydroxybenzoyl hydrazine) derivative was found to possess a high surface area, labile protons available for chemical ionization and strong UV absorption at the laser wavelength. This reagent was originally used by Ren *et al.*¹²¹ for enrichment and identification of peptides.

There has been sustained attempts to use matrix free substrates for laser desorption, while trying not to compromise the efficiency of the technique by seeking ways to shield the analyte from the fragmentation by the laser pulses. A good example is the development by Wei *et al.*,¹²³ in 1999, of the matrix-free method desorption ionization on silicon (DIOS), which is categorized as “surface MALDI”. DIOS was primarily developed to alleviate the matrix interference problem, common with MALDI, thus making it applicable for small molecule analysis. The sample stage is typically generated by electrochemical anodization and deposition or by chemical etching of crystalline silicon substrate to produce arrays (either photopatterned spots or grids). The resulting porous silicon has high optical absorption in the ultraviolet, thus meeting the criterion of an ideal matrix and is capable of trapping analyte molecules, enabling their desorption and ionization. DIOS has been demonstrated to offer low detection limits in the femtomole range for various analytes such as peptides, glycolipids, antiviral drug molecule *etc.*) and is compatible with silicon-based microfluidics and microchip technologies. However, DIOS suffers from difficulties in manufacture, due to chip to chip irreproducibility, non uniformity and contaminants (*e.g.* etchants) trapped in the porous surface, limited mass range and poor applicability to differing classes of compounds.^{123,124} Research on how to solve these problems and increase the applicability

of this technique is on going. There are other interesting attempts developed to eliminate the matrix addition step from MALDI-MS technology, including use of resorcinol-formaldehyde aerogels as LDI substrate, use of deposited nanostructured silicon films, sol-gel derived 2,5-dihydroxybenzoic acid assisted LDI and use of a surface bound-polymer containing a UV-absorbing molecule, a technique christened, Surface Enhanced Neat Desorption (SEND).¹²⁵⁻¹²⁷ Recently Kitagawa¹²⁸ reported the successful use synthetic polyelectrolyte (poly- α -cyano-4-methacryloyloxycinnamic acid) as an LDI platform for peptides analysis. In his work, he indicated that a suitable polyelectrolyte for LDI should have laser-energy absorbing molecules on the polymeric backbone. The polymer must also bear moieties with labile protons such as carboxyl that could easily form a “proton cloud” that is available for donation to analyte, on excitation by the laser. With the loss of protons and subsequent formation of negative charges, the polyelectrolyte matrix, should be in a configuration that allows increased inductive repulsive effect, which eventually contributes to desorption.

Increasingly, the application of derivatization is becoming a practical approach to circumventing most of the aforementioned problems with MALDI small molecule analysis. While chemical derivatization is a routine part of GC and HPLC analysis with UV and fluorescence detection,¹³⁰ it is only recently that it has been attempted for ESI and MALDI, and thus the application of derivatization enhanced LDI is still in its germinal stage.¹³¹⁻¹³⁹

Site-specific chemical derivatization (often referred to as tagging or labelling) in MALDI has become more common, especially for the analysis of peptides and

carbohydrates, probably due to very well known, rapid and high yield chemical reactions, but applications to small molecule analysis is only in its preliminary stages. Examples of common chemical modification with these analytes include Schiff base reactions, guanidation, dehydration of carbonyls with arylhydrazines and reductive amination with aromatic amine.¹³²⁻¹³⁹ For example, Volmer *et al.*¹³¹ has also applied 2,4-dinitrophenylhydrazine (DNPH) as a reactive matrix for corticosteroids. Formation of imines, for example, is a common biological reaction in enzyme-substrate binding, where the carbonyl group acts as a “handle”. The use of charge bearing derivatization reagents for ESI-MS, such as precharged phosphonium based derivatizing agents (to analyze alcohols and carbonyls) and addition of a quaternary amine tag (peptide labelling) have also been attempted by Waterhouse *et al.*¹³³ and Mirzaei *et al.*,¹³⁵ respectively. Karst and co-workers,¹⁴⁰⁻¹⁴² pioneered the concept of “purpose-designed derivatizing agents” where a compound is tailor-made to incorporate the most ideal attributes of good derivatizing agents such as: a reactive moiety that is analyte selective, sufficient stability, polarity and good detectability. However, it is not trivial to integrate all these properties in one molecule. Karst *et al.*¹⁴⁰ synthesized a novel compound, 4-dimethylamino-6-(4-methoxy-1-naphthyl)-1,3,5-triazine-2-hydrazine (DMNTH), which they used to analyze for carbonyl compounds using fluorescence and UV detection. The concept of modularly designed derivatizing agents is summarized schematically in Figure 1.10, adapted from the work of Werlich *et al.*¹⁴³ on selective analysis of isocyanates and diisocyanates in air. This concept has not been utilized to our knowledge in synthesizing custom- reagents for use as reactive matrices with MALDI, and was envisioned to have great potential for the analysis of various analytes such as DBPs.

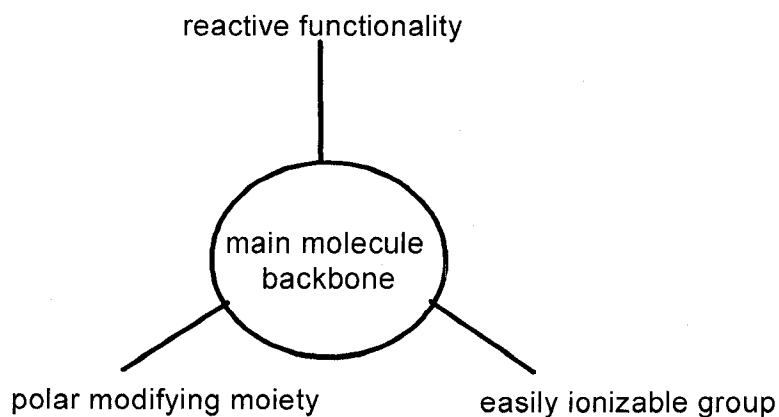


Figure 1.10. Model of tailor made reactive matrix.

1.4 References

1. Thurman EM, Malcolm RL. *Environ. Sci. Technol.* 1981; **15**:463-466.
2. MacCarthy P. *Soil Sci.* 2001; **166**: 738-751.
3. Stevenson FJ. *Humus chemistry: genesis, composition, reactions* (2nd Ed). John Wiley & Sons: New York, 1994:10.
4. Swift RS. *Soil Sci.* 1999; **164**: 790-802.
5. Shevchenko SM, Bailey GW. *Crit. Rev. Environ. Sci. Technol.* 1996; **26**: 1-57.
6. Derenne S, Largeau C. *Soil Sci.* 2001; **166**: 833-847.
7. Ghabbour E A, Davis G. *Humic substances: Nature's most versatile materials*. Taylor and Francis, Inc: New York, 2004: 9-15
8. Hayes M HB, Clapp CE. *Soil Sci.* 2001; **166**: 723-737.
9. Abbt-Braun G, Lankes U, Frimmel FH. *Aquat. Sci.* 2004; **66**: 151-170.
10. Frimmel FH. *Agronomie*, 2000; **20**: 451-463.
11. Peña-Méndez EM, Havel J, Patočka J. *J. Appl. Biomedicine*, 2005; **3**: 13-24.
12. Rook Johannes J. *Environ. Sci. Technol.* 1977; **11**: 478-482.

13. Cappiello A, De Simoni E, Fiorucci C, Mangani F, Palma P, Trufelli H, Decesari S, Facchini M C, Fuzzi S. *Environ. Sci. Technol.* 2003; **37**: 1229-1240.
14. Samburova V, Zenobi R, Kalberer M. *Atmos. Chem. Phys.* 2005; **5**: 2163-2170.
15. De Nobili M, Chen Y. *Soil Sci.* 1999; **164**: 825-833.
16. Anderson, Russell J D. *Nature* 1976; **260**: 597.
17. Piccolo A. *Soil Sci.* 2001; **166**: 810-832.
18. Sutton R, Sposito G. *Environ. Sci. Technol.* 2005; **39**: 9009-9015.
19. Burdon J. *Soil Sci.* 2001; **166**: 752-769.
20. McDonald S, Bishop AG, Prenzler PD, Robards K. *Anal. Chim. Acta* 2004; **527**: 105-124.
21. Hatcher PG, Dria KJ, Kim S, Frazier SW. *Soil Sci.* 2001; **166**: 770-794.
22. Janos P. *J. Chromatogr. A*, 2003; **983**: 1-18.
23. Irwin WJ. *Analytical pyrolysis: A comprehensive guide*. Marcel Dekker, Inc: New York, 1982: 8-30.
24. Challinor JM. *J. Anal. Appl. Pyrolysis* 1989; **16**: 323-333.
25. Joll CA, Huynh T, Heitz A. *J. Anal. Appl. Pyrolysis* 2003; **70**: 151-167.
26. Faure P, Schlepp L, Mansuy-Huault L, Elie M, Jardé E, Pelletier M. *J. Anal. Appl. Pyrolysis* 2006; **75**: 1-10.
27. Susic M. <http://www.fortunecity.com/skyscraper/solomon/1735/>. [on-line reference, accessed 26 October 2006].
28. Lehtonen T, Peuravuori J, Pihlaja K. *J. Anal. Appl. Pyrolysis* 2003; **68-69**: 315-329.
29. International Humic Substances Society homepage. <http://www.ihss.gatech.edu/> [on-line reference, accessed 26 July 2006].

30. Fenn JB. *Journal of molecular techniques*, 2002; **13**: 101-118.
31. Gaskell SJ. *J. Mass Spectrom.* 1997; **32**: 677-688.
32. Fievre A, Solouki T, Marshall AG, Cooper WT. *Energy Fuels*, 1997; **11**: 554-560.
33. McIntyre C, Jardine DR, Batts BD. *J. Mass Spectrom.* 1997; **32**: 328.
34. McIntyre C, McRae C, Jardine DR, Batts BD. *Rapid Commun. Mass Spectrom.* 2002; **16**: 1604-1609.
35. Rostad CE, Leenheer JA. *Anal. Chim. Acta* 2004; **523**: 269-278.
36. Kujawinski E B, Hatcher PG, Freitas MA, Zang X, Green-Church KB, Jones RB. *Org. Geochem.* 2002; **33**: 171-180.
37. Plancque G, Amekraz B, Moulin V, Toulhoat P, Moulin C. *Rapid Commun. Mass spectrom.* 2001; **15**: 827-835.
38. Leenheer JA, Rostad CE, Gates PM, Furlong ET, Ferrer I. *Anal. Chem.* 2001; **73**: 1461-1471.
39. Reemtsma T, These A. *Anal. Chem.* 2003; **75**: 1500-1507.
40. Pfeifer T, Klaus U, Hoffmann R, Spiteller M. *J. Chromatogr. A*, 2001; **926**: 151-159.
41. Piccolo A, Spiteller M. *Anal. Bioanal. Chem.* 2003; **377**: 1047-1059.
42. Reemtsma T, These A. *Environ. Sci. Technol.* 2005; **39**: 3507-3512.
43. These A, Reemtsma T. *Anal. Chem.* 2003; **75**: 6275-6281.
44. Kujawinski EB, Hatcher PG, Freitas MA. *Anal. Chem.* 2002; **74**: 413-419.
45. Stenson AC, Marshall AG, Cooper WT. *Anal. Chem.* 2003; **75**: 1275-1284.
46. Reemtsma T, These A, Springer A, Linscheid M. *Environ. Sci. Technol.* 2006; **40**: 5839-5845.
47. Marshall AG, Rodgers RP. *Acc. Chem. Res.* 2004; **37**: 53-59.

48. Kujawinski E B, Behn MD. *Anal. Chem.* 2006; **78**: 4363-4373.
49. Kim S, Kramer RW, Hatcher PG. *Anal. Chem.* 2003; **75**: 5336-5344.
50. Tanaka K, Waki H, Ido Y, Akita S, Yoshida T. *Rapid Commun. Mass Spectrom.* 1988; **2**: 151-158.
51. Karas M, Bachmann D, Bahr U, Hillenkamp F. *Int. J. Mass Spectrom. Ion Processes* 1987; **78**: 53-68.
52. Harvey DJ. *Int. J. Mass Spectrom.* 2003; **226**: 1-35.
53. Nielen MW. *Mass Spectrom. Rev.* 1999; **18**: 309-344.
54. Murgasova R, Hercules DM. *Int. J. Mass Spectrom.* 2003; **226**: 151-162.
55. Fenselau C, Demirev PA. *Mass Spectrom. Rev.* 2001; **20**: 157-171.
56. Griesser HJ, Kingshott P, McArthur SL, McLean KM, Kinsel GR, Timmons RB. *Biomaterials*, 2004; **25**: 4861-4875.
57. Dreisewerd K. *Chem. Rev.* 2003; **103**: 395-425.
58. Karas M, Kruger R. *Chem. Rev.* 2003, **103**: 427-439.
59. Knochenmuss R. *Analyst* 2006; **131**: 966-986.
60. Erb WJ, Hanton SD, Owens KG. *Rapid Commun. Mass Spectrom.* 2006; **20**: 2165-2169.
61. Gluckmann M, Pfenninger A, Krüger R, Thierolf M, Karas M, Horneffer V, Hillenkamp F, Strupat K. *Int. J. Mass Spectrom.* 2001; **210/211**: 121-132.
62. Horneffer V, Reichelt R, Strupat K. *Int. J. Mass Spectrom.* 2003; **226**: 117-131.
63. Guilhaus M. *J. Mass Spectrom.* 1995; **30**: 1519-1532.
64. Krutchinsky AN, Loboda AV, Spicer VL, Dworchak R, Ens W, Standing KG. *Rapid Commun. Mass Spectrom.* 1998; **12**: 508-518.

65. Novotny FJ, Rice JA, Weil DA. *Environ. Sci. Technol.* 1995; **29**: 2464-2466.
66. Brown TL, Rice JA. *Org. Geochem.* 2000; **31**: 627-634.
67. Srzić D, Kazazić S, Martinović S, Paša-Tolić L, Kezele N, Vikić-Topić D, Pečur S, Vrančić A, Klasinc L. *Croat. Chem. Acta* 2000; **73**: 69-80.
68. Remmler M, Georgi A, Kopinke FD. *Eur. J. Mass Spectrom.* 1995; **1**: 403-407.
69. Haberhauer G, Bednar W, Gerzabek MH, Rosenberg E. *Special Publications of the Royal Society of Chemistry*, 2000; **259**: 143-152.
70. Gajdošová D, Porkona L, Kotz A, Havel J. *Special Publication Royal Society of Chemistry* 1999; **247**: 289-298.
71. Porkona L, Gajdošová D, Havel J. *Special Publication Royal Society of Chemistry* 1999; **247**: 107-119.
72. Gajdošová D, Novotná K, Prosek P, Havel J. *J. Chromatogr. A*, 2003; **1014**: 117-127.
73. Shonozuka T, Shibata M, Yamaguchi T. *J. Mass Spectrom. Soc. Jpn.* 2004; **52**: 29-32.
74. Pacheco ML, Havel J. *Electrophoresis* 2002; **23**: 268-277.
75. Pacheco ML, Peña-Méndez EM, Havel J. *Chemosphere* 2003; **51**: 95-108.
76. Peters EC, Brock A, Horn DM, Phung QT, Ericson C, Salomon AR, Ficarro SB, Briall LM. http://www.cellpathway.com/papers/LCGC_MALDI_FTICR.pdf .2002.
77. Illman DL. *Anal. Chem.* 2006; **78**: 5266-5272.
78. <http://www.unesco.org/water/wwap/wwdr2/>: 2006.
79. Kronberg L, Holmbom B, Reunanen M, Tikkanen L. *Environ. Sci. Technol.* 1988; **22**: 1097.
80. Ashbolt JN. *Toxicology* 2004; **198**: 255-262.
81. Sadiq R, Rodriguez MJ. *Sci. Total Environ.* 2004; **321**: 21-46.

82. Richardson SD, Ternes TA. *Anal. Chem.* 2005; **77**: 3807-3838
83. Richardson SD. *Anal. Chem.* 2006; **78**: 4021-4046.
84. Krasner SW, Weinberg HS, Richardson SD, Pastor SJ, Chinn R, Scilimenti MJ, Onstad GD, Thruston AD. *Environ. Sci. Technol.* 2006; **40**: 7175-7185.
85. Cancho B, Ventura F. *Global Nest: The International Journal*, 2005; **7**: 16-36.
86. Choi J, Valentine RL. *Water Res.* 2002; **36**: 817-824.
87. Woo YT, McLain JL, Manibusan MK, Dellarco V. *Environ. Health Perspect.* 2002; **110**: 75-87.
88. Lu J, Benjamin MM, Korshin GV, Gallard H. *Environ. Sci. Technol.* 2004; **38**: 4603-4611.
89. Huixian Z, Zirui Y, Junhe L, Xu X, Jinqi Z. *Water Res.* 2002; **36**: 4535-4542.
90. Yang X, Shang C. *Environ. Sci. Technol.* 2004; **38**: 4995-5001.
91. Zhang X, Minear RA. *Environ. Sci. Technol.* 2002; **36**: 4033-4038.
92. Zhang X, Minear RA, Barrett SE. *Environ. Sci. Technol.* 2005; **39**: 963-972.
93. Zhang X, Minear RA. *Water Res.* 2006; **40**: 221-230.
94. Richardson SD. *J. Environ. Monit.* 2002; **4**:1-9
95. Vincenti M, Biazzi S, Ghiglione N, Valsania MC, Richardson SD. *J. Am. Soc. Mass Spectrom.* 2005; **16**: 803-813.
96. Suktan J, Gabryelski W. *Anal. Chem.* 2006; **78**: 2905-2917.
97. Nikolaou AD, Kostopoulou MN, Lekkas TD. *Global Nest: The International Journal*, 1999; **1**: 143-156.
98. Mohamed YZ, Eish A, Wells MJM. *J. Chromatogr. A* 2006; **1116**: 272-276.

99. Gupta SS, Stadler M, Noser CA, Ghosh A, Steinhoff BA, Lenoir, D, Horwitz CP, Schramm KW, Collins TJ. *Science* 2002; **296**: 326-328.
100. Weber WJ, Huang Q, Pinto RA. *Environ. Sci. Technol.* 2005; **39**: 5446-6452.
101. Cohen LH, Gusev AI. *Anal. Bioanal. Chem.* 2002; **373**: 571-586.
102. Nicola AJ, Gusev AI, Proctor A, Jackson EK, Hercules DM. *Rapid Commun. Mass Spectrom.* 1995; **9**: 1164-1171.
103. Ling YC, Lin L, Chen YT. *Rapid Commun. Mass Spectrom.* 1998; **12**: 317-327.
104. Hensel RR, King RC, Owens KG. *Rapid Commun. Mass Spectrom.* 1997; **11**: 1785-1793.
105. Gusev AI, Wilkinson WR, Proctor A, Hercules DM. *Anal. Chem.* 1995; **67**: 1034-1041.
106. McCombie G, Knochenmuss R. *Anal. Chem.* 2004; **76**: 4990-4997.
107. Guo Z, Zhang Q, Zou H, Guo B, Ni J. *Anal. Chem.* 2002; **74**: 1637-1641.
108. Hatsis P, Brombacher S, Corr J, Kovarik P, Volmer DA. *Rapid Commun. Mass Spectrom.* 2003; **17**: 2303-2309.
109. Sleno L, Volmer DA. *Rapid Commun. Mass Spectrom.* 2006; **20**: 1517-1524.
110. Gobey J, Cole M, Janiszewski J, Covey T, Chau T, Kovarik P, Corr J. *Anal. Chem.* 2005; **77**: 5643-5654.
111. Kampen JJA, Burgers PC, Groot R, Luider TM. *Anal. Chem. A* 2006; **78**: 5403-5411.
112. Ayorinde FO, Hambright P, Porter TN, Keith QL. *Rapid Commun. Mass Spectrom.* 1999; **30**: 2474-2479.
113. Iijima S. *Nature*, 1991; **354**: 56.

114. Xu S, Li Y, Zou H, Qiu J, Guo Z, Guo B. *Anal. Chem.* 2003; **75**: 6191-6195.
115. Chen WY, Wang LS, Chiu HT, Chen YC, Lee CY. *J. Am. Soc. Mass Spectrom.* 2004; **15**:1629-35.
116. Zhang J, Wang HY, Guo YL. *Chin. J. Chem.* 2005; **23**:185-189.
117. Ren SF, Zhang L, Cheng ZH, Guo YL. *J. Am. Soc. Mass Spectrom.* 2005; **16**: 333-339.
118. Hu L, Xu S, Pan C, Yuan C, Zou H, Jiang G. *Environ. Sci. Technol.* 2005; **39**: 8442-8447.
119. Pan C, Xu S, Hu L, Su X, Ou J, Zou H, Guo Z, Zhang Y, Guo B. *J. Am. Soc. Mass Spectrom.* 2005; **16**: 883-892.
120. Pan C, Xu S, Zou H, Guo Z, Zhang Y, Guo B. *J. Am. Soc. Mass Spectrom.* 2005; **16**: 263-270.
121. Ren S, Guo Y. *J. Am. Soc. Mass Spectrom.* 2006; **17**: 1023-1027.
122. Black C, Poile C, Langley J, Herniman J. *Rapid Commun. Mass Spectrom.* 2006; **20**: 1053-1060.
123. Wei J, Buriak JM, Siudak G. *Nature* 1999; **399**: 243-246.
124. Shen Z, Thomas JJ, Averbuj C, Broo KM, Engelhard M, Crowell JE, Finn MG, Siuzdak G. *Anal. Chem.* 2001; **73**: 612-619.
125. Voivodov KJ, Ching J, Hutchens TW. *Tetrahedron Lett.* 1996; **37**: 5669-5672.
126. Cuiffi JD, Hayes DT, Fonash SJ, Brown KN, Jones AD. *Anal. Chem.* 2001; **73**:1292-1295.
127. Lin YS, Chen YC. *Anal. Chem.* 2002; **74**:5793-5798.
128. Kitagawa N. *Anal. Chem.* 2006; **78**: 459-469.

129. Okuno S, Arakawa R, Okamoto K, Matsui Y, Seki S, Kozawa T, Tagawa S, Wada Y. *Anal. Chem.* 2005; **77**: 5364-5369.
130. Halket JM, Waterman D, Pyzyborowska AM, Patel RK, Fraser PD, Bramley PM. *J. Exp. Bot.* 2004; **56**: 219-244.
131. Brombacher S, Owen SJ, Volmer DA. *Anal. Bioanal. Chem.* 2003; **376**: 773-779.
132. Tholey A, Wittmann C, Kang MJ, Bungert D, Hollemeyer K, Heinzle E. *J. Mass Spectrom.* 2002; **37**: 963-973.
133. Barry SJ, Carr RM, Lane SJ, Leavens WJ, Manning CO, Monte S, Waterhouse I. *Rapid Commun. Mass Spectrom.* 2003; **17**: 484-497.
134. Lee PJ, Chen W, Gebler JC. *Anal. Chem.* 2004; **76**: 4888-4893.
135. Mirzaei H, Regnier F. *Anal. Chem.* 2006; **78**: 4175-4183.
136. Saraiva MA, Borger CM, Florencio MH. *J. Mass Spectrom.* 2006; **41**: 216-228.
137. Fenaille F, Tabet JC, Guy PA. *Anal. Chem.* 2004; **76**: 867-873.
138. Lattova E, Perreault H. *J. Chromatogr. B* 2003; **793**: 167-179.
139. Sekiya S, Wada Y, Tanaka K. *Anal. Chem.* 2005; **77**: 4962-4968.
140. Kempter C, Potter W, Binding N, Klaning H, Witting U, Karst U. *Anal. Chim. Acta* 2000; **410**: 47-64.
141. Kempter C, Berkhoudt TW, Tolbol GC, Egmosse KN, Karst U. *Anal. Bioanal. Chem.* 2002; **372**: 639-643.
142. Kempter C, Zurek G, Karst U. *J. Environ. Monit.* 1999; **1**: 307-311.
143. Werlich S, Stockhorst H, Witting U, Binding N. *Analyst*, 2004; **129**: 364-370.

CHAPTER 2

Characterization of Humic Substances by Matrix Assisted Laser

Desorption Ionization Time of Flight Mass Spectrometry

A version of this chapter has been published. Mugo SM, Bottaro CS. Characterization of Humic Substances by Matrix Assisted Laser Desorption Ionization Time of Flight Mass Spectrometry. *Rapid Commun. Mass Spectrom* 2004; **18**: 2375-2382.

2.1 Introduction

Humic substances (HS) are brown to black colored compounds, which comprise a highly complex mixture of heterogeneous substances, believed to result from stochastic decomposition of diverse biogenic materials. This definition is equivocal and limited in explaining the structural properties of humic materials and so traditionally humics are operationally subdivided in terms of solubility aspects in aqueous media as a function of pH into three fractions: humins are non-soluble, humic acids (HA) are insoluble at acidic conditions, $\text{pH} < 1$ and fulvic acids (FA) are soluble at all pH values. Humics are an important class of organic ligand that play a major role in the mobility and bioavailability of hydrophobic organic pollutants, trace metals and radionuclides in the environment. HS have also been implicated as the principal precursors of halogenated disinfection by-products (DBPs) which are a concern to public health because of their suspected carcinogenicity, reproductive effects and hepatic toxicity. These critical issues, among others explain the continued interest in the characterization of HS compounds.¹⁻⁴

In spite of so many years of extensive research, much remains unknown about their genesis, molecular weight (MW), and absolute structure. However, during the past few decades, applications of a host of different analytical techniques have led to significant advances in the study of HS particularly with regard to their chemical composition. Gel filtration chromatography (GFC), vapor phase osmometry (VPO), field flow fractionation (FFF), and ultrafiltration (UF) have been used to probe the molecular weight distribution of HS.²⁻⁵ GFC, which employs soft gels such as Sephadex and Bio-Gel, has been hampered by poor resolution and long analysis time, and so increasingly has been replaced with high performance size exclusion chromatography (HPSEC). Using HPSEC,

Piccolo and co-workers⁴ reported that contrary to the long-standing assumption that HS are high MW polymeric compounds (10 000-200 000 Da), HS are supramolecular compounds consisting of relatively small heterogeneous molecules (masses ~500 Da) held together by hydrogen bonds, and other weaker forces such as van der Waals among other interactions. HPSEC results are questionable due to lack of suitable calibration standards. Furthermore, the elution of polyelectrolytes such as HS is highly dependent on parameters such as ionic strength, pH, and stationary phase of the column and in general the nature of the buffer system. Optimization of these parameters to enhance fractionation to truly reflect size can be a formidable challenge and therefore SEC can only be used in determining apparent molecular weight distributions. Mass spectrometry, on the other hand, has become an important tool over the past decade for the analysis of these natural macromolecules. Most previous mass spectrometric studies of HS used conventional electron impact ionization, giving important information about constituent moieties but resulting in extensive fragmentation of HS ($m/z \sim 200$ Da) and yielding little insight into the actual overall structure. Nevertheless, most of the models describing HS structure have been deduced using this method in conjunction with nuclear magnetic resonance (NMR) data.^{2,4,6} With fundamental evolution in soft ionization techniques, such as fast atomic bombardment, laser desorption, electrospray and MALDI, intact high molecular gas-phase ions can be obtained and analyzed by mass spectrometry. LDI has been employed by Novotny *et al.*⁵ and other authors⁶⁻¹¹ for the determination of FA molecular weight distribution; the values reported were consistently lower than those from GFC and VPO. The function of LDI-MS is dependent on a number of variables such as laser wavelength, laser power, analyte nature, polarity of acquisition of the spectra, among

other factors, and hence spectra can differ significantly with varying conditions.⁷

However, LDI is a relatively energetic ionization method that might produce excessive fragmentation of HS, and so other softer approaches like MALDI and electrospray ionization (ESI) are more likely to lead to formation of intact molecular ions. ESI is finding more widespread application because it is considered to be the softest ionization method. When coupled with ultrahigh resolution Fourier transform ion cyclotron resonance mass spectrometry (FT-ICRMS) at 9.4 Tesla, full resolution of individual peaks separated by less than 1 Da has been achieved for HS mixtures.¹² Using ESI-FTICRMS Stenson *et al.*^{12,13}, as well as others,¹⁴⁻¹⁷ have tried to determine the exact masses and chemical formulae of HS constituents, but getting the exact structure is still a formidable challenge due to the many constitutional isomers that may be represented by one chemical formula.

Analysis of HS by MALDI, another relatively soft ionization technique, was first attempted by Reemler *et al.*¹⁸ and later by Haberhauer *et al.*¹⁹ among other researchers.⁹⁻¹¹ They reported the method had only limited utility due to cluster formation and fragmentation phenomena and thus has not found widespread acceptance. However, it is believed with properly optimized sample preparation, the potential of MALDI has been unexploited in the analysis of HS. It has the advantage of forming singly charged ions (which simplifies the spectra), unlike ESI, which has the propensity of forming multiple charges. MALDI in combination with TOFMS has the added benefit of high mass range of detection, whereas ESI has been reported to show bias in favor of low molecular weight compounds.^{5,6} It would be naive to claim that only one of these methods will ultimately resolve the humic materials entirely, however it is feasible that through the

proper application of these soft ionization techniques a significant contribution can be made to the study of HS.

2.2 Experimental

2.2.1 Samples and chemicals

Suwannee River fulvic (1R101F, 1S101F) and humic acids (1S101H) were purchased from International Humic Substances Society (IHSS), St. Paul, Minnesota. Extensive elemental analysis of these compounds has been done by the IHSS. The Armadale soil fulvic acid (ASFA) from Prince Edward Island, Canada was donated by Dr. Robert Helleur of Memorial University. Acetonitrile, methanol, tetrahydrofuran (THF) and water, all of HPLC grade, and trifluoroacetic acid (TFA) were purchased from Sigma Chemical Co. (St. Louis, MO., USA). A number of MALDI matrices were tested: 2,5-dihydroxybenzoic acid (DHBA or gentisic acid), α -cyano-4-hydroxycinnamic acid (CHCA), 3,5-dimethoxy-4-hydroxycinnamic acid also known as sinapinic acid (SA), dithranol (1,8,9-anthracenetriol), 9H-pyrido(3,4-b) indole (norharmane) and 2-(4-hydroxyphenyl-azo)-benzoic acid (HABA) all from Sigma Chemical Co.

A number of solvents were used to dissolve samples of HS including acetonitrile/water, acetonitrile/0.1% aqueous TFA, water, methanol, 5 M urea, aqueous solutions of 20 mg mL⁻¹ NaOH and KOH. The respective matrices concentrations investigated are shown in Table 2.1. The sample/matrix ratios investigated were; 1:10, 1:100, 1:1000, 1:10000 (w/w). Each of these were combined with different matrices and 1 μ L spotted and co-crystallized on the sample plate. The significance of the sample preparation method was also examined. The usual methods include the dried droplet

method (originally described by Karas and Hillenkamp²⁰), fast evaporation, and the overlayer method. In the dried droplet method, a drop of aqueous matrix compound is mixed with analyte solution and dried leaving a deposit of analyte-doped matrix crystal. On the other hand, with fast evaporation, the matrix and sample are deposited separately. The matrix solution is first spotted on the sample stage and once crystallized, a drop of the analyte solution is applied on top of the matrix deposit. In overlayer method, fast evaporation is used to form the first layer of crystals and over this, a mixture of matrix and analyte solution is deposited.²¹

HS spectra were also acquired in the laser desorption ionization mode (LDI), that is, without use of matrix.

2.2.2 MALDI Instrumentation

MALDI mass spectra were acquired using a Voyager-DE Biospectrometry MALDI-TOFMS instrument (Applied Biosystems) with the following features: a 3 nanosecond pulsed nitrogen laser (337 nm) with a maximum intensity of 4600 (arbitrary units), positive and negative ion detection, linear or reflectron mode operation; ion path length of 2.0 meters in linear mode and 3.0 meters in reflectron mode. It was also equipped with a post-source decay (PSD) analysis capability, automated single-plate sample-loading system, m/z range in excess of 300 kDa, timed-ion selection, low mass gate matrix suppression, video camera and monitor for sample viewing, among other features. In the linear mode, the upper mass range is 350 kDa with a resolution of 1,000 (for m/z 17,000) while in the reflectron mode, the upper mass range is 6,000 Da with a

resolution of 10,000 (for m/z 5,700), making it the preferred mode. In the work reported here, the reflectron mode was mainly used.

The analyte/matrix samples were ablated and ionized from the sample holder with the nitrogen laser and ions accelerated into the flight tube with 20kV. Fifty laser shots were acquired then signal averaged. Other optimized instrumental settings were grid voltage, 73.4%; mirror voltage ratio, 1.12; guide wire, 0: 0.002%; extraction delay time, 200 ns; acquisition mass range, 100-2000 Da. Both positive and negative modes were investigated; only the former is reported in this paper.

2.3 Results and Discussion

2.3.1 Analysis by LDI

Humic substances are known to absorb at wavelengths in the UV region, which includes the wavelength of the laser used in this work (337 nm). This provides an opportunity to make use of LDI (no matrix). Representative spectra obtained by LDI-TOFMS (positive mode) are shown in Figure 2.1, noting that the samples were prepared in acetonitrile/0.1% aqueous TFA (7:3), and that the spectra reported were acquired in positive mode. Various solvents (water, methanol, dimethylsulfoxide, acetone, acetonitrile) and sample concentrations were investigated to determine their effect on the quality of the spectra, with the acetonitrile/0.1% aqueous TFA performing best, in part because it was effective in dissolving the sample and resulted in less spreading of spots on the plate.

In LDI, the tendency for humic substances to form either positive or negative ions has been shown to depend on the laser wavelength. For example, Brown *et al.*⁷ reported

that with IR laser wavelengths of both 10.6 nm and 1.06 μm , humic substances appeared to more readily form negative ions. However, with the laser wavelength used in this work (337 nm), HS produces predominantly positive ions, a feature that was previously reported by Srzić *et al.*⁸ and Gajdošová, *et al.*⁸⁻¹¹ Additionally, Srzić *et al.*⁸ used an adjustable wavelength pulsed ND:YAG laser emitting at 1064 nm, 532 nm and 355 nm, with Fourier transform ion cyclotron MS and found that HS spectra acquired using different laser wavelengths yielded different characteristic peaks.

It should be noted here, that laser power was carefully controlled as laser flux higher than the threshold value for desorption/ionization causes metastable decay and reduces resolution in TOFMS. An increase in the laser power from 2532 (arbitrary units) to the highest laser intensity possible (4600) caused significant fragmentation and only m/z 242 persisted.

The spectra shown in Figure 2.1 are also less complex and better resolved than the featureless spectra (highly complex) obtained using negative mode reported by Brown *et al.*⁶ The simplicity of the spectrum acquired in positive mode is not surprising as there are fewer sites (probably amines and phenols) available in HS for positive ionization. However, the greater the abundance of moieties present that can be easily ionized in the negative mode, such as phenolic and carboxylic groups, the more complex the spectra. It is also possible that there may be a process of selective ionization occurring so that ions measured in the positive ion mode may actually be structurally different from the species observed in the negative mode.²² Furthermore, it is also possible that positive ions can form clusters through interactions with neutral HS molecules, a feature reported by Brown *et al.*⁶ and Klaus *et al.*²², which may further complicate analysis of the spectra.

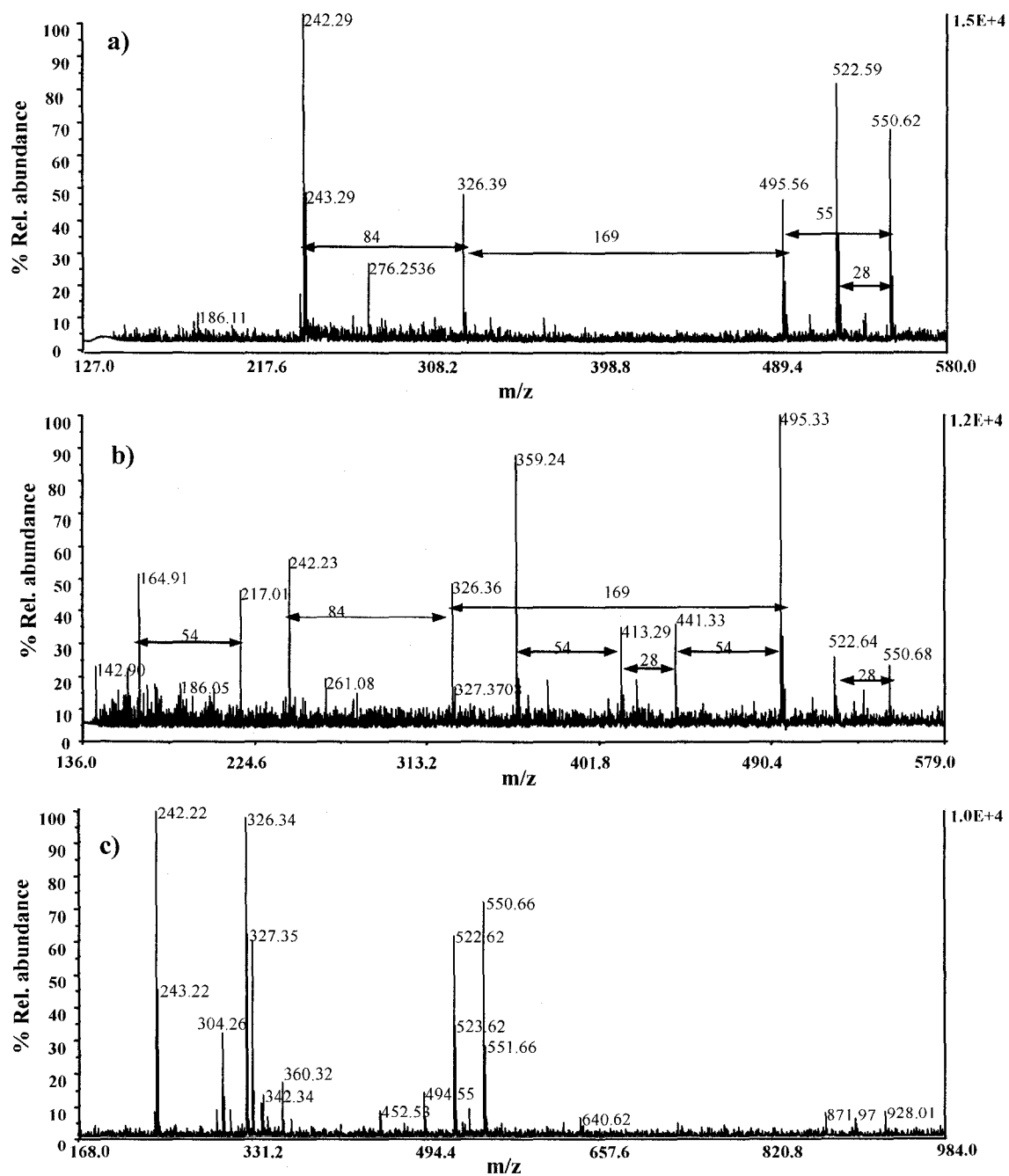


Figure 2.1. Positive LDI spectra of Fulvic acids in 0.1%TFA/ACN 7:3: a) 1S101F 5 mg mL⁻¹; b) IR101F 5 mg mL⁻¹; c) ASFA 5 mg mL⁻¹.

The LDI spectra of soil and aquatic fulvic acids were consistently found to contain a number of common peaks, indicating that humic substances are comprised of some common structural components, irrespective of their origin. Table 2.2 summarizes conspicuous peaks, which were shared by aquatic and soil FA, as well as aquatic HA. The relative abundance of these individual peaks was not always reproducible (a limitation of mass spectrometry and MALDI), hence this value is not reported in the table. However, a few labeled peaks (♦) were always observed in relatively high abundance (>40%). In addition to the consistency seen within the results obtained in this work, the peaks at m/z 495, 522, 550, have been reported by other authors⁵⁻¹¹ using LDI-MS under other experimental conditions and with humic material from sources unrelated to those used in the work reported here. Using a CO₂ (10.6 μm) laser, Novotny *et al.*⁵ reported relatively high intensity peaks for FA in the 370-530 Da region. These results are in agreement with our work. Similar results were reported for humic acid from Croatia by Srzić *et al.*⁸ using Fourier transform ion cyclotron resonance MS with an adjustable wavelength pulsed laser. They found some prominent peaks that were also obtained in our work including m/z 550, 523, 495, 257 and 163. Other conspicuous peaks like m/z 164, 283, 359, and 495 were also obtained by Gajdošová *et al.*^{9,10} using LDI-TOFMS analysis on humic acids from Antarctica and coal derived HA. Similarities between our work and the work of others who used different samples confirm that humification processes result in humic substances containing similar chemical structures. The presence of humic substances in Antarctica, despite the absence of plants containing lignin, further casts doubts on the theory that HS are by-products of lignin degradation. Although it may be

difficult to firmly assign specific structures to these masses, it is noteworthy to point out that in his study of dissolved organic matter by a Py-GC-MS technique, Huang *et al.*²³ found that peaks at m/z 256, 282, 359, 495, 523, 550 (all seen in our work) were associated with n-fatty acids. Most of the peaks obtained by LDI, such as 164, 177, 241, 283, 326, 359, *etc.*, agree with those reported in previous work by Planque, *et al.*¹⁵ and Reemtsma, *et al.*¹⁶, who made use of ESI-TOFMS and SEC/ESI-MS-MS, respectively. It is notable, that the peak at m/z 177 was detected as a common molecular substructure of FA by Planque *et al.*¹⁵ and has been associated with lignin derivatives, specifically ferulic acid²³.

Table 2.1. Matrices used and their concentrations.

Matrix	Concentration	Solvent
α -cyano-4-hydroxycinnamic acid (CHCA)	10 mg mL ⁻¹	acetonitrile/ 0.1%TFA (1:1)
HABA	1.3 mg mL ⁻¹	acetonitrile/ 0.1%TFA (1:1)
Gentisic acid (DHBA)	10 mg mL ⁻¹	acetonitrile/water (3:7)
Sinapinic acid	10 mg mL ⁻¹	acetonitrile/ 0.1%TFA (1:1)
Dithranol	10 mg mL ⁻¹	THF
Norharmaline	10 mg mL ⁻¹	acetonitrile/water (3:7)

Table 2.2. Frequently occurring peaks obtained for aquatic FA, aquatic HA and soil FA by LDI and MALDI.

LDI-MS		MALDI-MS	
m/z [M+H] ⁺	Mass	m/z [M+H] ⁺	Mass
815	814	1848 [♦]	1847
642 [♦]	641	1734 [♦]	1733
615	614	1619 [♦]	1618
551 [♦]	550	1565 [♦]	1564
522 [♦]	521	1451 [♦]	1450
508	507	1336	1335
495 [♦]	494	1450 [♦]	1449
494	493	1280 [♦]	1279
452	451	1166 [♦]	1165
391	390	1052	1051
360 [♦]	359	997 [♦]	996
368	367	883 [♦]	882
332	331	769 [♦]	768
327 [♦]	326	758	757
326	325	714	713
312	311	686	685
284	283	669	668
258	257	660 [♦]	659
243 [♦]	242	600	599
242 [♦]	241		
178	177		
165	164		

[♦]Peaks consistently observed as highly abundant, others present in low abundance and not obvious in spectra.

Note: There is also a possibility that some of the observed ions could be [M+Na]⁺.

Repeating patterns were observed in the spectra obtained in our work, the most important being differences of multiples of 14 Da associated with $-(CH_2)_n$. Though, differences of 28 Da might also be due to loss of one $-CO-$ unit. Studies of fulvic acids by ESI-MS-MS by Leenheer *et al.*¹⁷, using standards of carboxylic acids thought to be associated with FA, demonstrated that losses of 28 Da were associated with lactone esters, such as those in coumarin-3-carboxylic acid. Stenson *et al.*¹³ attempted MS-MS experiments to try identify some of the structural components of individual FA ions and found that while negative ions lose CO_2 (MS-MS data), positive ions lose CO together with water, which authenticates our work. The difference of 14 and 28 Da between adjacent peaks been associated with the presence of aliphatic carboxylic groups in HS which is consistent with the functional groups expected to be present in HS (i.e. carboxylic, alkyl, carbonyl, and aromatic groups). It is also common to find peaks separated by 1-2 Da spacings, typically associated with ring structures and varying degrees of saturation. It was further noted that, peaks observed in the mass spectra are at well defined spacings, $\Delta m \approx 169$ (Figure 1), a feature that is more clear in MALDI spectra reported further in this study.

Only ions up to m/z 642 could consistently be observed using LDI, with peaks around m/z 800-900 only sporadically detected. These results are in agreement with the work of Gajdošová *et al.*^{9,11}, who reported the disappearance of ions around m/z 800 on switching from linear positive mode to reflectron positive mode, which attests to the low stability of the higher mass ions produced by LDI. As such, analysis of humic substances using LDI is limited by rapid heating of the analyte during laser irradiation, resulting in extensive fragmentation. Matrix assisted LDI can be used to facilitate energy dispersion

and enhance sample ionization, this tends to produce intact molecular ions with minimal or no fragmentation, making this method more suitable for the analysis of HS than simple LDI.

2.3.2 Analysis by MALDI-TOFMS

Reemler *et al.*¹⁸ and Haberhauer *et al.*¹⁹, pioneers in the application of MALDI TOFMS to the analysis of HS, reported complicated and featureless spectra. However, we found that through careful optimization of the critical parameters governing efficacy of ionization, *i.e.*, sample preparation, analyte/matrix ratio, matrix selection, laser intensity, delayed extraction together with other instrumental settings, well-resolved spectra could be obtained.

Aside from the choice of matrix, which will be discussed in depth below, the success of MALDI is in part governed by the sample preparation step (co-crystallization of analyte and matrix). In this step, it was critical to produce well-formed, homogeneous crystals to ensure good shot to shot reproducibility. To achieve this aim, the analyte and matrix needed to be miscible in a range of concentrations, and also be capable of co-crystallization. A number of factors were found to influence the quality of the crystals and the rate of matrix/analyte co-crystallization, such as sample purity, proportion of solvent, quality and type of substrate surface, and environmental conditions such as temperature and humidity. In addition, a host of related sample preparation options exist, with the conventional dried droplet method being the most common. Fast evaporation method has been acclaimed to produce very homogeneous spots,²⁰ but failed in this work. Both the dried droplet method and the overlayer method performed satisfactorily, although

overlayer slightly improved the homogeneity of the crystals, improving the chances of forming the “sweet spots”. Sweet spots, refers to certain position on the analyte-matrix cocrystallite that shows better mass signals than other positions.

It was also found that suppression of potentially interfering matrix ions was greatly enhanced by ensuring good mixing of the matrix and analyte in the solid phase, proper optimization of the matrix/analyte ratio and tuning the time interval of the delayed extraction to ensure complete matrix-analyte reaction in the plume before ions are moved to the flight tube as demonstrated by Knochenmuss *et al.*²⁴

The choice of matrix is a critical aspect of MALDI analysis. A good matrix is defined as one that preferentially absorbs the laser energy and gently transfers the energy to the analyte, forming gas phase ions with significantly less internal energy than those produced with LDI, hence reducing fragmentation phenomena. A good matrix should also produce spectra with reasonable signal-to-noise ratios (>3) with minimum laser power, produce few interfering ions at the mass range of interest, enhance ionization of analyte, and the analyte should be soluble in the matrix.²⁵

Dithranol, known to be a good matrix for non-polar polymers, did not yield acceptable results for HS. The major problem encountered here was analyte-matrix miscibility; precipitation occurred when the solution of HS in acetonitrile, water, or methanol with TFA, was mixed with dithranol in THF. It should be noted that all of the solvents used were miscible, so the insolubility can only be attributed to solute/matrix immiscibility. Norharmane, on the other hand, formed very nice crystals but ionization was inefficient even at very high laser intensity.

Spectra of the CHCA, HABA and DHBA, the matrices that produced the best results for humic substances, can be seen in Figure 2.2. The spectra are shown over the mass range of interest, that is, up to 2000 Da. Prominent peaks that could be attributed to the matrices are identified (with an asterisk, '*') in the analyte spectra shown in Figures 2.3 and 2.4. Among the matrices used, DHBA emerged to be the most suitable matrix for HS elucidation (Figure 2.3c and Figure 2.4). The sample spectra produced with DHBA have low spectral noise that can be attributed to the matrix, in fact, the matrix peaks are nearly completely suppressed and have no interference with identified analyte peaks.

Comparing the spectra for the Suwannee River fulvic acid sample, 1R101F, obtained using the three matrices CHCA, HABA, and DHBA (Figures 2.3 a, b, c respectively), the highest ion current was produced using DHBA. Although HABA yields good ionization at much lower laser intensity (~2140), the spectra produced (Figure 2.2b) are much more noisy within the mass range of interest than that produced with DHBA. CHCA, like DHBA, gave good ion current at a similar laser intensity, but was not as effective as DHBA in enhancing ionization of HS. Furthermore, the ionization efficiency for the high mass components of this fulvic acid sample was superior using DHBA (Figure 2.3c), with many more prominent peaks in the region from m/z 1281 to m/z 1848. In the spectra for the fulvic acid using CHCA, the base peak at m/z 825 is likely a matrix peak. With HABA, relatively good spectra were obtained, but the most abundant peak at m/z 547 can also be attributed to a matrix ion. Using DHBA the base peak occurs at m/z 1166 or 1450. These peaks are also present in the other spectra for the same fulvic acid though at much lower abundance, supporting both the supposition that

they are truly analyte peaks and that DHBA is the best matrix of those evaluated here for the study fulvic acids.

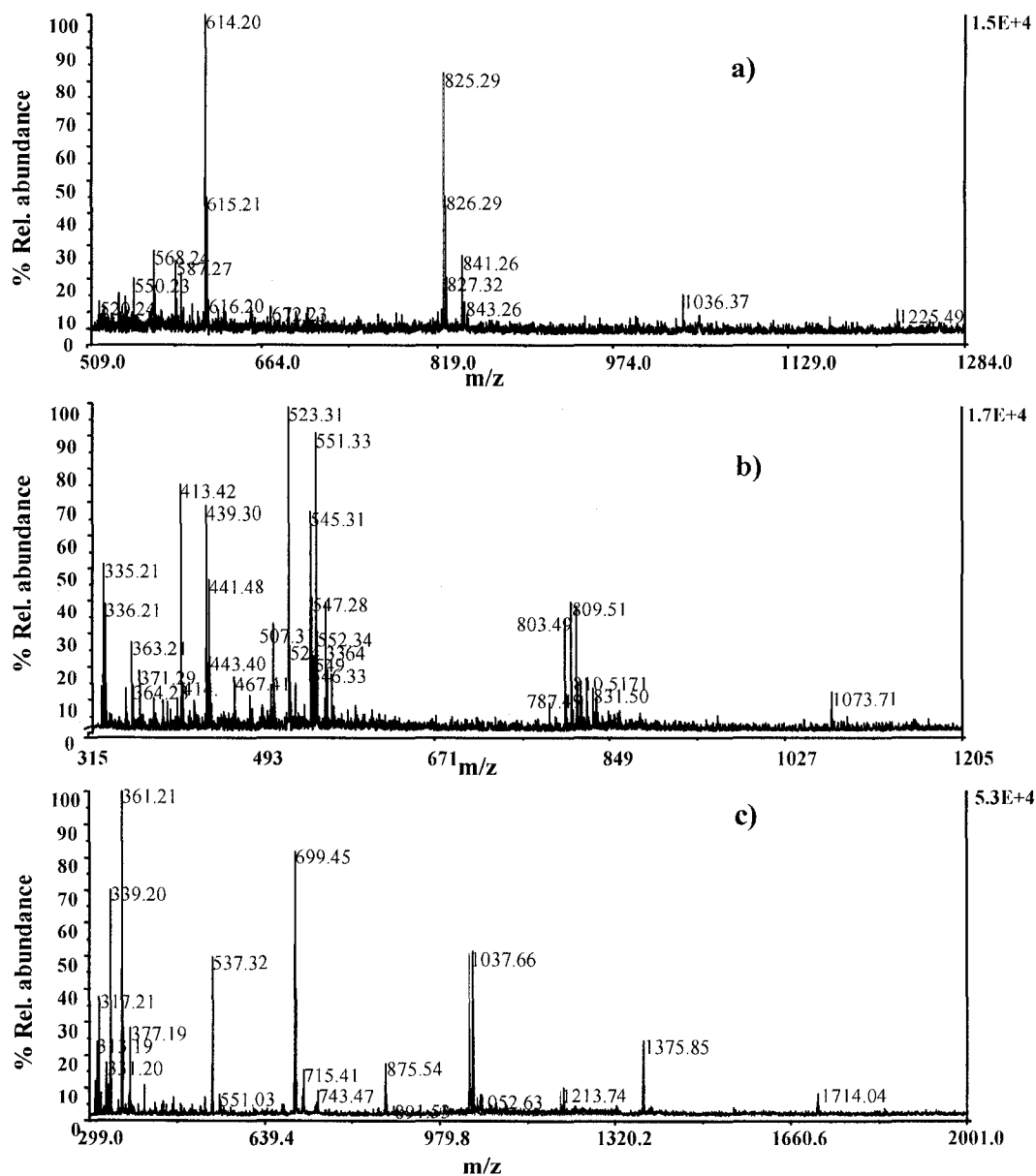


Figure 2.2. Mass spectra of some of the matrices used: a) CHCA; b) HABA; c) DHBA.

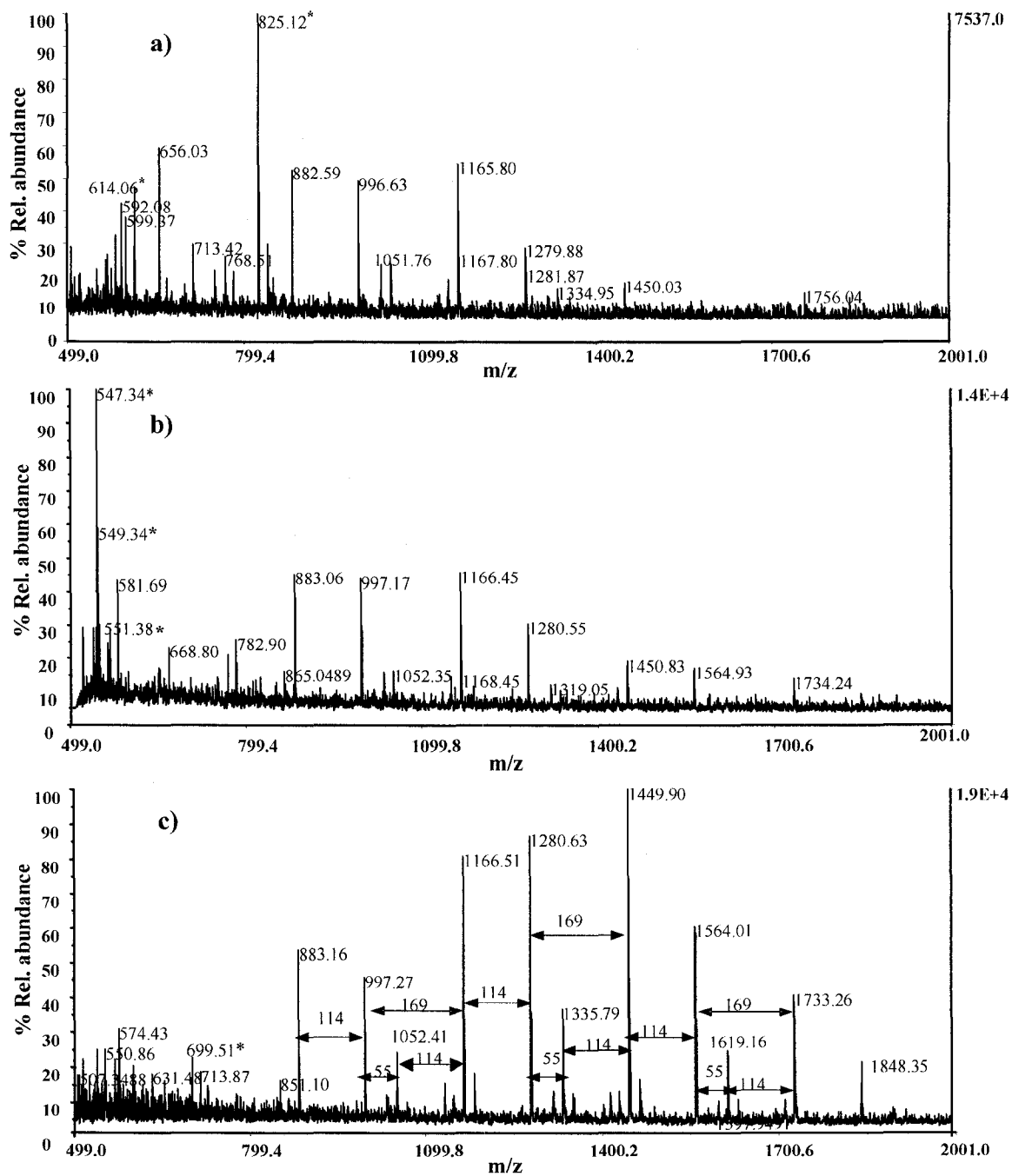


Figure 2.3. Mass spectra of aquatic fulvic acids obtained using CHCA, HABA and DHBA matrices prepared using the dried-droplet method: a) 1R101F and CHCA (1:100); b) 1R101F and HABA (1:25); c) 1R101F and DHBA (1:1000). *Matrix peaks.

Though it was clear that river fulvic acid samples could be ionized efficiently using DHBA, it was important to also determine the performance of this matrix with fulvic acid from other sources and humic acid. DHBA was found to perform similarly with the alternate samples. Some of the results are presented in Figure 4, where again very good enhancement of ionization at relatively high mass is seen and no interfering peaks from the matrix can be found.

The molar ratio of analyte/matrix is also a critical parameter which must be optimized (no presumptive basis for prediction) to produce the most effective ratio. Because of the important role of the matrix in isolating analyte molecules from one another, shielding the analyte from the laser energy and enhancing matrix suppression, it was expected that lower analyte to matrix ratios would, within limitations, provide better results; which was confirmed in the results. From the wide-range of analyte to matrix ratios (w/w) tested, on average 5 mg mL⁻¹ HS with 1.3 mg mL⁻¹ HABA, 0.1 mg mL⁻¹ HS with 10 mg mL⁻¹ CHCA and 0.01 and even 0.001 mg mL⁻¹ HS with 10 mg mL⁻¹ DHBA gave the best results. Increasing the ratio to 1:10000 HS to DHBA (Figure 2.4) was found to greatly suppress the matrix peaks in the lower mass region. There may be some questions as to why the relative concentration of humic substance to matrix for the HABA experiments is high in comparison to the ratios for the other matrices. Results using a lower concentration of HS for this matrix were poorer than those using the concentration cited above; therefore experiments using ratios that approach those used with the other matrices were never attempted. Degradation of high molecular weight ions is normally minimal when using MALDI; nonetheless, like LDI, increasing the laser power beyond

the threshold (sufficient power for ionization and desorption, which differs depending on the matrix) systematically degraded the high molecular weight ions.

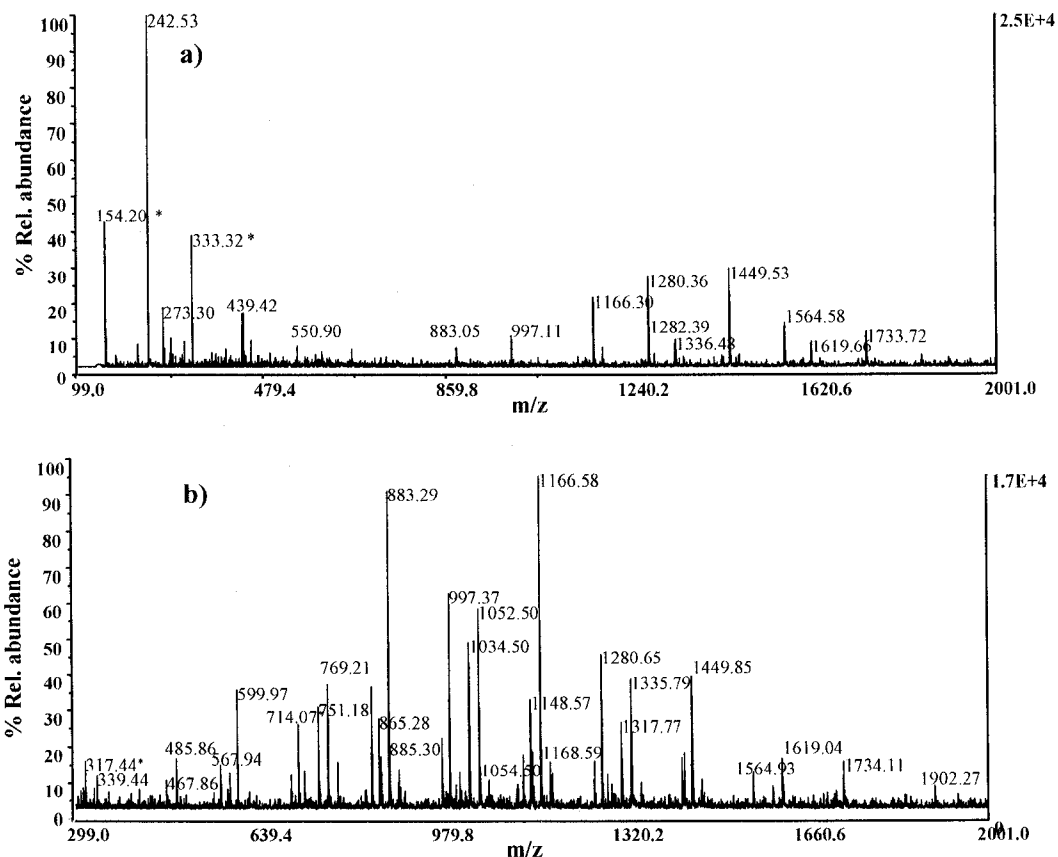


Figure 2.4. Mass spectra of humic substances acquired using DHBA and matrix suppression with increase in matrix a) 1S101H, DHBA, 1:10000; b) ASFA, DHBA, 1:10000.

As noted earlier, the use of a matrix, especially DHBA, significantly enhanced ionization (*i.e.* higher ion currents obtained) of HS, particularly in the higher mass ranges. For example, without the matrix the highest mass detectable was at m/z 928, whereas peaks as high as m/z 1848 could be observed only when a matrix was employed. This suggests that, as is expected with MALDI, much of the laser energy was absorbed by the

matrix and only partially transferred to the sample during ionization resulting in significantly less fragmentation. There is evidence in the MALDI spectra (Figures 2.3 and 2.4) to support the idea that fragmentation is occurring in LDI, for example, the ion detected at m/z 883, could be the parent of fragments detected at m/z 523 and m/z 360, both apparent in the LDI spectra (Figure 2.1). This theory can be confirmed by further MS-MS studies.

There were a number of notable features consistently observed in the MALDI spectra of nearly all the humic substances studied. Most obvious, was a Gaussian-shaped distribution of peaks, a feature reminiscent of distributions usually seen in the analysis of synthetic and natural polymers. Additionally, when the number of mass units separating prominent peaks was investigated, consistent values became apparent. The most prominent values were 55, 114 and 169 Da, occurring repeatedly (see pattern in Figures 2.3c, also evident in Figure 2.3a, b and 2.4). It is possible that 114 and 169 could be fragments of m/z 283, a prominent peak observed in our work using LDI-TOFMS and also very conspicuous in the work of Gajdošová *et al.*^{10,11} (LDI-TOFMS). It is also a prevalent peak in other spectra acquired by ESI.^{15,17} The peak at m/z 114 has been associated with 4-hydroxy-5,6-dihydro-(2H)-pyran-2-one, widely reported as a polysaccharide marker from py-GC MS.^{23,26,27} This is reasonable in light of the evidence that HS are formed from polysaccharides and sugars, a theory that has been described in detail by Susic.²⁸ Finally, there were a number of peaks that aquatic FA, HA and soil FA were found to share consistently, *e.g.* m/z 883, 1166, 997, 1280, 1450, 1563, 1733, 1848, indicating common structural elements, not surprising given the related origin (*i.e.*

humification of plant material) of these macromolecules. Peaks at m/z 883, 997 and 1280 were also reported by Gajdošová, *et al.*^{9,10,11}

Although at the moment, we can only speculate on the possible structures of these repeating units, it gives more evidence that humic substances, although complex, are not on the whole stochastic, but may be highly-ordered systems with polymeric characteristics. MS-MS experiments performed by post-source decay (PSD) and triple quadrupole should be carried out to investigate these patterns, which are proposed to be building blocks of HS.

2.4 Conclusions

MALDI-TOFMS has been found to be a very versatile tool and adds a new dimension to the analysis of humic substances. This method can potentially be used in the determination of molecular weight and may also be utilized to determine structural elements, particularly if post source decay (PSD) can be employed on the observed sample peaks. PSD was however not attempted because of equipment failure. Proper selection of the matrix and careful optimization of sample preparation procedures has been found to greatly improve the results that are obtained using TOFMS on humic substances. It is however, acknowledged that HS are very complex substances consisting of a large number of macromolecules with a wide mass range distribution, and so detection and characterization is not a trivial undertaking. Nonetheless, this work has also shown that MALDI-TOFMS can be used to obtain important information about HS, yielding a spectral fingerprint and providing additional structural information beneficial for future work on characterization. One striking feature of this work was that a number

of peaks were consistently found in the spectra of the soil FA, aquatic HA, and aquatic FA, indicative of shared structural elements. Although MALDI and LDI are not as soft ionization techniques as ESI, they produce single charged ions making the interpretation of the spectra more straightforward. Thus MALDI-TOFMS and LDI-TOFMS produce complementary information to ESI-TOFMS and ESI-FTICRMS and will be useful tools in unraveling the mystery of HS.

2.5 References

- 1) MacCarthy P. *Soil Sci.* 2001; **166**: 738-751.
- 2) Piccolo A. *Soil Sci.* 2001; **166**: 810-832.
- 3) Hatcher P G, Dria K J, Kim S, Frazier S W. *Soil Sci.* 2001; **166**: 770-794.
- 4) Janos P. *J. Chromatogr. A* 2003; **983**: 1-18.
- 5) Novotny F J, Rice J A. *Environ. Sci. Technol.* 1995; **25**: 2464-2466.
- 6) Fievre A, Solouki T, Marshall AG, Cooper WT. *Energy Fuels* 1997; **11**: 554-560.
- 7) Brown TL, Rice JA. *Organic Geochemistry* 2000, **31** (7-8), 627-634.
- 8) Srzić D, Kazazić S, Martinović S, Paša-Tolić L, Kezele N, Vikić-Topić D, Pečur S, Vrančić A, Klasinc L. *Croatica Chemica Acta* 2000; **73**: 69-80.
- 9) Gajdošová D, Novotná K, Prošek P, Havel J. *J. Chromatogr. A* 2003; **1014**: 117-127.
- 10) Gajdošová D, Porkona L, Kotz A, Havel J. *Special publication royal society of chemistry* 1999; **247**: 289-298.
- 11) Porkona L, Gajdošová D, Havel J. *Special publication royal society of chemistry* 1999; **247**: 107-119.
- 12) Stenson AC, Marshall AG, Cooper WT. *Anal. Chem.* 2003; **75**: 1275-1284.

- 13) Stenson A C, Landing W M, Marshall AG, Cooper WT. *Anal. Chem.* 2002; **74**: 4397-4409.
- 14) Kujawinski EB, Hatcher PG, Freitas MA. *Anal. Chem.* 2002; **74**: 413-419.
- 15) Plancque, G, Amekraz B, Moulin V, Toulhoat P, Moulin C. *Rapid Commun. Mass Spectrom.* 2001; **15**: 827-835.
- 16) Reemtsma T, These A. *Anal. Chem.* 2003; **75**: 1500-1507.
- 17) Leenheer JA, Rostad CE, Gates PM, Furlong ET, Ferrer I. *Anal. Chem.* 2001; **73**: 1461-1471.
- 18) Remmler M, Georgi A, Kopinke F D. *Eur. Mass Spectrom.* 1995; **1**: 403-407.
- 19) Haberhauer, G., Bednar, W., Gerzabek, M. H., Rosenberg, E. *Special publications of the royal society of chemistry* 2000; **259** 143-152.
- 20) Karas M, Hillenkamp F. *Anal. Chem.* 1988; **60**:2299-2301.
- 21) Sigma-Aldrich. MALDI-Mass spectrometry. www.sigma-aldrich.com/analytical. *Analytix.* 2001; **6**.
- 22) Klaus U, Pfeifer T, Spiteller M. *Environ. Sci. Technol.* 2000; **34**: 3514-3520.
- 23) Huang Y, Eglinton G, Van derhage E R E, Boon J J, Bol R, Ineson P. *Eur. J. Soil Science* 1998, **49**, 1-15.
- 24) Knochenmuss R, Karbach V, Wiesli U, Breuker K, Zenobi R. *Rapid Commun. Mass Spectrom* 1998; **12** (9): 529-534.
- 25) Karas M, Kruger R. *Chemical Reviews.* 2003; **103**: 427-439.
- 26) Schulten H R. *Fresenius J. Anal. Chem.* 1995; **351**: 62.
- 27) Kelly J, Mackey M, Helleur R J. *J.Anal.Appl Pyrolysis.* 1991, **19**, 105-117.
- 28) Susic M. <http://www.fortunecity.com/skyscraper/solomon/1735/structurems/humicms.htm>. 2003.

CHAPTER 3

Comparative Study of Suwannee River Natural Organic Matter and Humic Like Substances (HULIS) Synthesized from Acid Polymerization of 4-Oxo-2-Butenoic Acid by Online Thermochemolysis Techniques.

3.1 Introduction

Humic substances (HS) are naturally occurring, environmentally ubiquitous (in soils, sediment, waters), refractory, and heterogenous complex mixtures, which are believed to be formed by death and decay of wide-varied biogenic materials.¹⁻⁶ Although these compounds have been studied for an inordinately long time, complete structural elucidation and understanding remains elusive and hence, as a group, they remain a puzzle yet to be solved by the scientific community.^{1,7} Apart from their inherent complexity, which has certainly been the greatest impediment to their full characterization, delay in the development of analytical techniques that are amenable to their analysis contributed to the slow pace in their characterization. The frustration in their analysis resulted in fatigue and resignation, with some researchers indicating that, HS cannot be characterized at the molecular level.^{1,2} Hitherto, HS continue to be operationally-defined based on their aqueous solubility at different pH, a definition that is often unsatisfactory when trying to understand and predict their behaviour in real systems, such as when HS is acting toward the enrichment of soils or as precursors to production of disinfection by-products.⁵⁻⁷ Nonetheless, using conventional analytical tools such as FT-IR, titrimetric methods, nuclear magnetic resonance (NMR), size exclusion chromatography (SEC), pyrolysis-GC-MS *etc.*, a significant understanding of the predominant chemical features of HS are known with a fairly high degree of confidence.¹⁻⁶ Most commonly reported moieties include a staggering variety of aromatic and aliphatic hydrocarbon structures functionalized with amide, carboxyl, and hydroxyl groups, among others. These many functionalities make the chemistry of HS very complex, dynamic and extremely fascinating, making it a dominant player in numerous

global processes such as in carbon and nitrogen cycling. In addition, HS not only influence ecosystems through their role in soils, but also through sequestration, chelating ability, transport enhancement, toxicity attenuation and bioremediation of hazardous organic chemicals and metals.³⁻⁶ Their well documented, strong complexing abilities have also lead to research into their ability to act as free radical scavengers, antiviral agents and other important therapeutic properties.⁷

Originally, HS have always been described as macromolecules with molecular weight of up to thousands of Daltons, partially from data obtained from SEC, but primarily from anecdotal evidence that HS are precursors of lignins (high molecular weight naturally occurring polymers).¹⁻³ However, recent studies especially using the recently developed soft ionization techniques such as ESI and MALDI have revealed that HS consists of relatively small molecular weight compounds (100-1000 Da).⁸⁻¹¹ Picollo¹² has suggested that the large apparent molecular weights may in fact be due to characteristic aggregation (self-assembly) of relatively small molecules at higher concentrations, which results in a supramolecular structure for HS. This insight adds further to the confusion in the structural characterization of HS. The application of imaging techniques like small angle scattering and X-ray microscopy has also helped explain the aggregation properties of humic substances.¹³

The debate on the exact source of HS has also been raging since their discovery, with HS experts divided on whether they are mainly formed from lignins, cellulose, polysaccharides or amino acid compounds. Fingerprinting of HS from different sources (mainly by FT-IR and degradative techniques) to determine their differences based on origin has been an important field of research.^{2,14} For instance, Leeheer *et al.*³ has

described that the composition of HS is to some extent dependent on the origin, with aquatic HS (believed to be synthesized from macrophytes, algae and bacteria) having more aliphatic character than terrestrial derived HS. These aliphatic and aromatic groups with their pendant functional groups were conventionally believed to be intricately linked to form highly heterogeneous supramolecular assembly of materials.¹ However, research using non degradative ionization methods (*viz.* ESI and MALDI) coupled to high resolution mass spectrometric tools such as FT-ICRMS, TOFMS, QTOFMS has revealed that HS are composed of relatively fewer major building blocks (oligomeric nature) with some structural similarities irrespective of their origin.⁸⁻¹¹ The future of the ultra-high resolution ESI-FT-ICRMS (resolving power > 80, 000 and mass accuracy, <1 ppm) is particularly bright for the analysis of HS because of its ability to resolve individual molecules in complex humic substances mixtures, making it possible to assign exact molecular formulae.¹¹ However, the cost of FT-ICRMS is too high to be affordable to most academic institutions and regardless of its high resolution capability, it cannot single-handedly solve the HS puzzle, since it has limitations as well. Some of the general FT-ICRMS limitations include subjectivity to space charge effects and ion molecule reactions, limited dynamic range, and mass spectra quality dependence on many experimental parameters (excitation, trapping, collision energy, detection conditions *etc.*). The use of other more common and powerful approaches have a pivotal role to play in uncovering some of the complexities of HS materials. Given the array of methodologies that could be employed in this work, it must be emphasized that the multi-pronged approach of studying these compounds by different techniques and gleaning as

much information as possible from data obtained from each technique is the most astute strategy, since every method is substantially limited on its own.¹⁶

It is believed the use of the now mature chemical and/or thermal degradative approaches and subsequent analysis of the fragments by GC-MS still has potential in generating new HS structural insights. In particular, conventional pyrolysis-GC-MS has already been most heavily applied in efforts to elucidate HS structure.^{1,4,6,14,15} While crucial cues have been gleaned from such work, pyrolysis-GC-MS does have some limitations. In particular, only a small fraction of any sample is actually pyrolyzed to GC-amenable products and so results may not be representative of the overall structure of HS and, more importantly, at the high-temperatures employed (> 550 °C) possible secondary reactions such as rearrangement, decarboxylation, cyclization and aromatization can occur. Hence the possibility of artefacts formation is a significant pitfall, which must be acknowledged and utmost care should be taken in the interpretation of the resulting data.¹⁴⁻¹⁶ The present HS hypothetical structures (often used for modelling purposes), most of which have been derived from pyrolysis-GC-MS data, should therefore be questioned since they may not reflect the true picture of HS. For example, most of the hypothetical structures are mainly polyphenolic, and ESI techniques have shown HS contain a substantial amount of aliphatic components.^{12,14}

Contrary to thermal degradation, chemical degradation is more selective to only particular linkages and the fragments can be easily extrapolated to map the parent molecule. Chemical degradation has found wide acceptance in various disciplines. In proteomics for example, an enzyme is used to cleave proteins and the resulting peptides fingerprinted, leading to information on the parent protein. Similarly, HS can be

degraded, for example by acid hydrolysis (H_2SO_4), basic oxidative hydrolysis (CuO), saponification (KOH), use of other oxidants such as ozone and hypochlorite have been accomplished.⁴⁻⁶ A much more useful chemical degradation approach is the application of thermally assisted hydrolysis and methylation (THM), developed by Challinor^{17,18} in the 1980s, which uses tetra-alkyl ammonium hydroxide reagents, typically tetramethylammonium hydroxide (TMAH). This method has gained widespread acceptance as a powerful tool for structural analysis with principal applications in synthetic and natural resins, lipids, waxes, polysaccharides, proteins, kerogen, biotreat agents, soil and HS, *etc.* The primary reason for the widespread applicability of THM is because it helps to overcome some of the analytical limitations of direct pyrolysis by improving the detection of polar compounds (*e.g.* dicarboxylic acids), while evading decarboxylation of acidic groups, dehydration of alcohol moieties and cyclization reactions. This is because THM requires use of sub-pyrolysis temperatures (250-300 °C), thereby preventing the loss of important structural information. It also renders more of the degradation products to be amenable to GC-MS analysis by concomitant hydrolysis of ester and ether linkages and *in situ* methylation of the resulting OH- and COOH groups.^{19,20} Additionally, the mechanism through which TMAH cleaves and subsequently methylates structural linkages is relatively well understood and hence the relationship between the degradation products and the original composition of humic substances can be ascertained.¹⁸ Though some of the chemolysates produced and detected, using this technique are still categorized to be of unknown origin (not known whether they are lignin, polysaccharide derived *etc.*); THM-GC-MS has been used to a great extent in defining the possible origin of humic material. Most aromatic moieties that

have been detected, *e.g.*, syringic and *p*-coumaric units, have mainly been associated with lignin, while other fragments have been associated with polysaccharides and fatty acid methyl esters.²¹⁻²³ However, one major limitation of TMAH is that it does not differentiate between naturally occurring methyl ethers or methyl esters from those formed during thermochemolysis. Nevertheless, the use of tetrabutylammonium hydroxide and isotopically-labelled TMAH could be used to make differentiation possible.²⁴ In addition, the results of THM are highly dependent on experimental conditions, as recently reported by Cynthia *et al.*²⁵ who found an increase in decarboxylation reaction with increase in the mole ratio of TMAH to model compounds, hence the interpretation of the results shouldn't be without caution. Furthermore, as compellingly noted by McIntyre *et al.*⁹ and other authors,^{25,26} the most logically valid and sound strategy in the study of HS must involve study of known compounds as surrogate for HS for prior optimization and interpretation; this approach remains, by all measures, a major research challenge.

The idea of synthesizing humic acid models from known starting materials by attempting to mimic nature has been propagated by Susic²⁷, and it gives solid evidence as to the possible origin and nature of these molecules. Susic has also noted that some of the complexity of these compounds is possibly due to their dynamic supramolecular structures, which results from intermolecular interactions involving carboxylic, phenolic and hydroxyl moieties. In this communication, we have taken up the challenge of synthesizing a humic acid model (HULIS) as described by Susic, and characterized it in concert with the intensively studied, naturally occurring NOM Suwannee River standards obtained from the International Humic Substances Society (IHSS). It should be noted that

the humic substances content in NOM is approximated to be between 50-90%. Because of their widespread use and their abilities to provide clues as to chemical structure, we have focused on the use of thermochemolysis GC-MS and ^1H NMR for the analysis of these compounds.

From this work, very telling information was obtained regarding the origin of humic substances and possible indicators of polysaccharide biomarkers in HS have been clearly identified. The origin of pyrolysates that were previously described as of unknown origin has been identified, and possible error of associating all phenolics and aromatic moieties with lignins has been soundly questioned.

3.2 Materials and Methods

The 1R101N sample (Suwanee River natural organic matter) was bought from IHSS, St. Paul, MN, USA. Chemicals for synthesis of humic acid model such as furfural, hydrogen peroxide, dichloromethane and other solvents we bought from Sigma Aldrich Chemical Co. (Oakville Ontario) and used without further purification. TMAH was purchased from Aldrich chemical company, Milwaukee, WI, USA. All chemicals and solvents were of analytical grade and were used without purification.

3.2.1 Synthesis of HS Model from Furfural Oxidation

The procedure employed was modified from one described by Susic.²⁷; in particular, reactant ratios have been optimized to ensure complete reaction. Furfural (0.12 mols) was oxidized by shaking with 30% (v/v) aqueous hydrogen peroxide at 25°C for 3 days until the two phases combined. The residual furfural was extracted from the

mixture by liquid-liquid extraction with dichloromethane and discarded. The resulting product which consisted of 4-oxo-2-butenoic acid as the major product and maleic acid as minor component was acid polymerized *in-situ* by addition of a few drops of concentrated hydrochloric acid. The precipitate formed was washed with distilled water to remove the unreacted hydrogen peroxide and dried. The dark brown product obtained bore the same operational definition as humic acid, *i.e.* it was insoluble in acidic media, but soluble at basic pH. As is usually done for the purification of HA, the product was adsorbed on XAD-8 and eluted with 0.012 M ammonia, pH 10.45.^{1,2} A schematic of the synthesis is shown in Figure 3.1. The product was analyzed by ¹H NMR and thermochemolysis GC-MS and the results were compared to similar analyses of IHSS NOM standard.

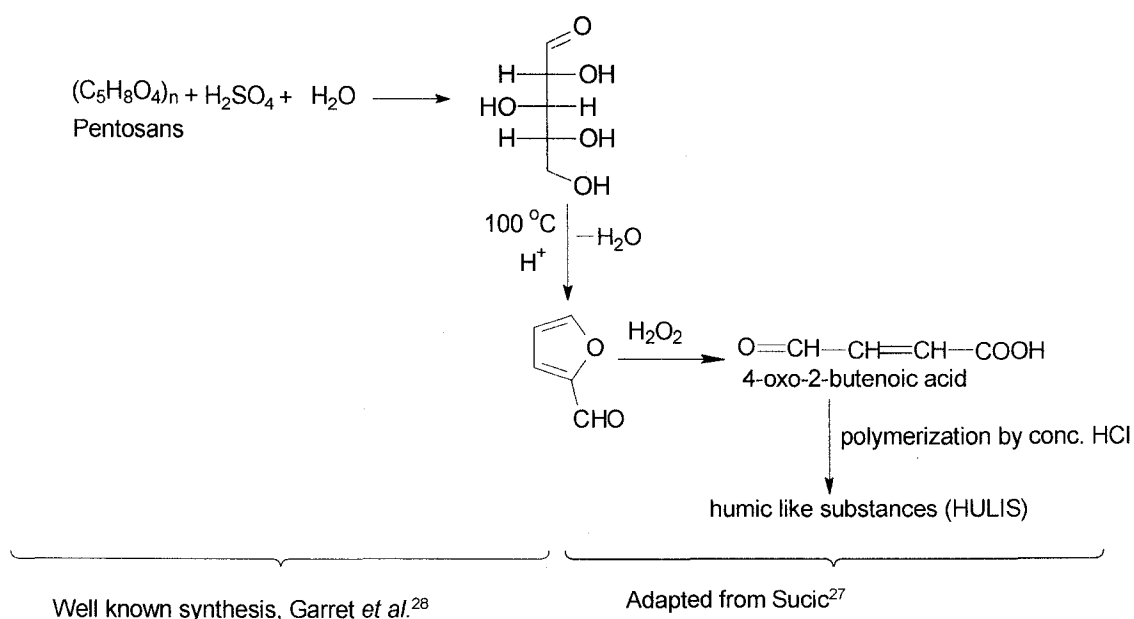


Figure 3.1. Schematic of synthesis of HULIS.

3.2.2 Analytical Thermochemolysis

IR101N or synthesized humic acid model (~ 500 µg) were weighed and deposited in the pyrolysis cup and 40 µL of 10% TMAH in methanol added. The mixture was then dried in a gentle stream of nitrogen and then introduced in the pyrolyzer unit for analysis by THM-GC-MS.

3.2.3 GC-MS Instrumentation

A Varian Star 5890 series GC with a Hewlett Packard 5971 series MS (equipped with an online Frontier lab pyrolyzer unit) was employed for the analysis. The GC column was a DB-5 (0.25 mm i.d. x 30 m, 0.25 µm film thickness). The carrier gas (He) head pressure was set at 10 psi, split flow 30 mL min⁻¹. The THM furnace temperature was kept at 280 °C and the transfer line was heated to 290 °C. The GC oven temperature program was as follows; initially the temperature was set at 40 °C and held for 2 minutes, then ramped at a rate of 4 °C min⁻¹ to a final temperature of 280 °C and held for 10 min. The ionization mode for the MS was electron ionization (EI) at 70 eV, and the scan range was 35-550 *m/z*.

Thermochemolysis conditions were chosen based on the work done by Lehenon *et al.*²⁰ who reported that relatively high temperature (> 300 °C conditions were necessary for optimal TMAH degradation of HS matter, but a delicate balance had to be maintained to avoid aromatization of aliphatic chemolysates that is possible at elevated temperatures.

3.3 Results and Discussion

The formation of furfural (common industrial solvent) from xylose and other pentosans derived from corn cobs, and sugarcane bagasse has been well-documented

over the decades and the reactions mechanism leading to its formation have been well understood.^{28,29} As such it was logical to start with furfural as the starting material for the HULIS synthesis. The resulting precipitate (HS model) synthesized from 4-oxo-2-butenic acid (HULIS) had the same solubility characteristics and brown color as HS, which is quite telling in that it provides evidence of a link between HS and simple sugars. However, information about molecular structure is essential to confirm this relationship, since many organic materials could have similar physical and solubility characteristics to HS and still not fit the complete definition of HS. The mature thermochemolysis GC-MS can afford the necessary structural information and was thus carried out with dilute TMAH (10%) and at sub-pyrolysis temperatures (280 °C), which ensures minimum breakdown and adulteration of the sample, thereby maintaining maximal structural integrity and providing a better picture of the original structure of these compounds. The results obtained demonstrate a very interesting trend and important similarities between standard NOM (major fraction humic substances) and the synthesized model. The total ion pyrogram of the humic acid model is shown in Figure 3.2 and that of the 1R101N standard is shown on Figure 3.3. As the pyrograms were very complex, as expected, through careful examination and comparison of the results for the standard NOM and the humic acid model, some very subtle but useful information was obtained. In this approach, compounds were identified based on their EI mass spectral matches with National Institute of Standards and Technology (NIST) Mass Spectral Library Version 1.6, as well as through mass spectral elucidation. Though many similarities were found, only the most informative peaks are cited, those whose compounds could be identified with a high degree of confidence by obtaining high

agreement matches from the NIST library as well as through THM-GC-MS data from literature. The identified pyrolysates of the HULIS are shown in **Table 3.1** while those of the 1R101N are shown in **Table 3.2**.

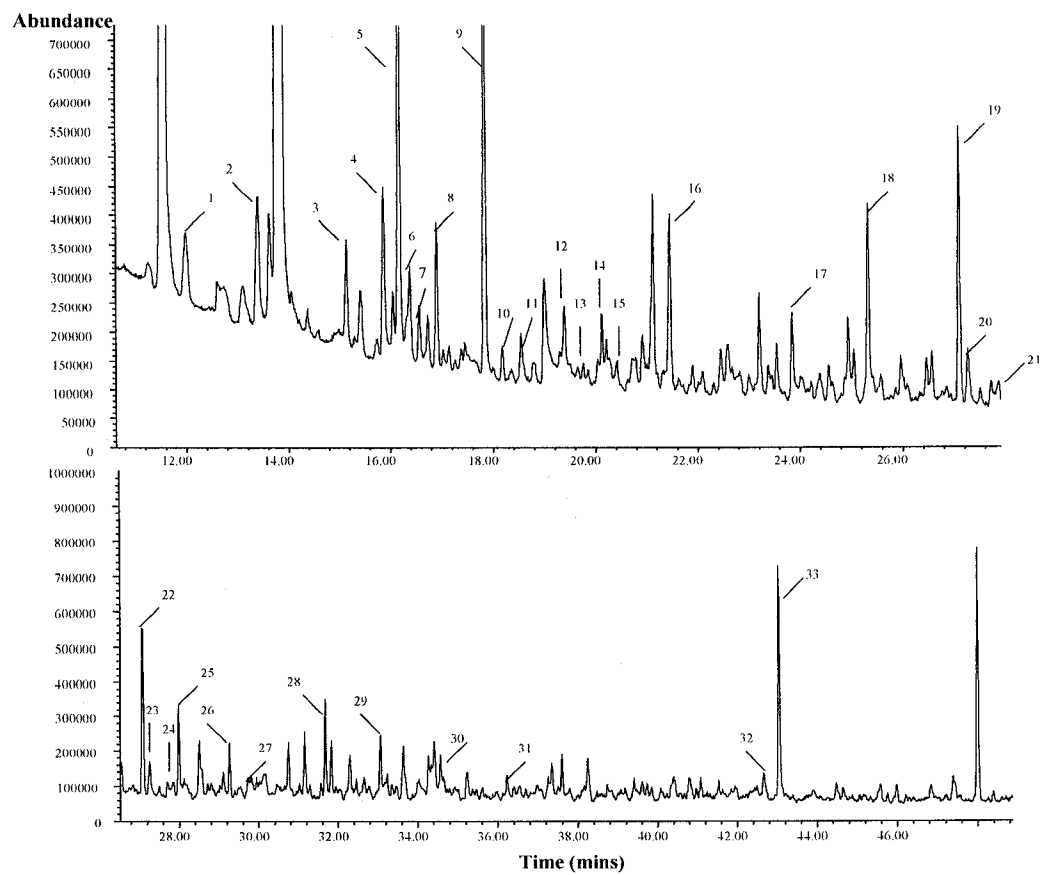


Figure 3.2. Total ion chromatogram of THM-GC-MS of Humic acid model. (The peak at 48.00 min is a bleed from the column)

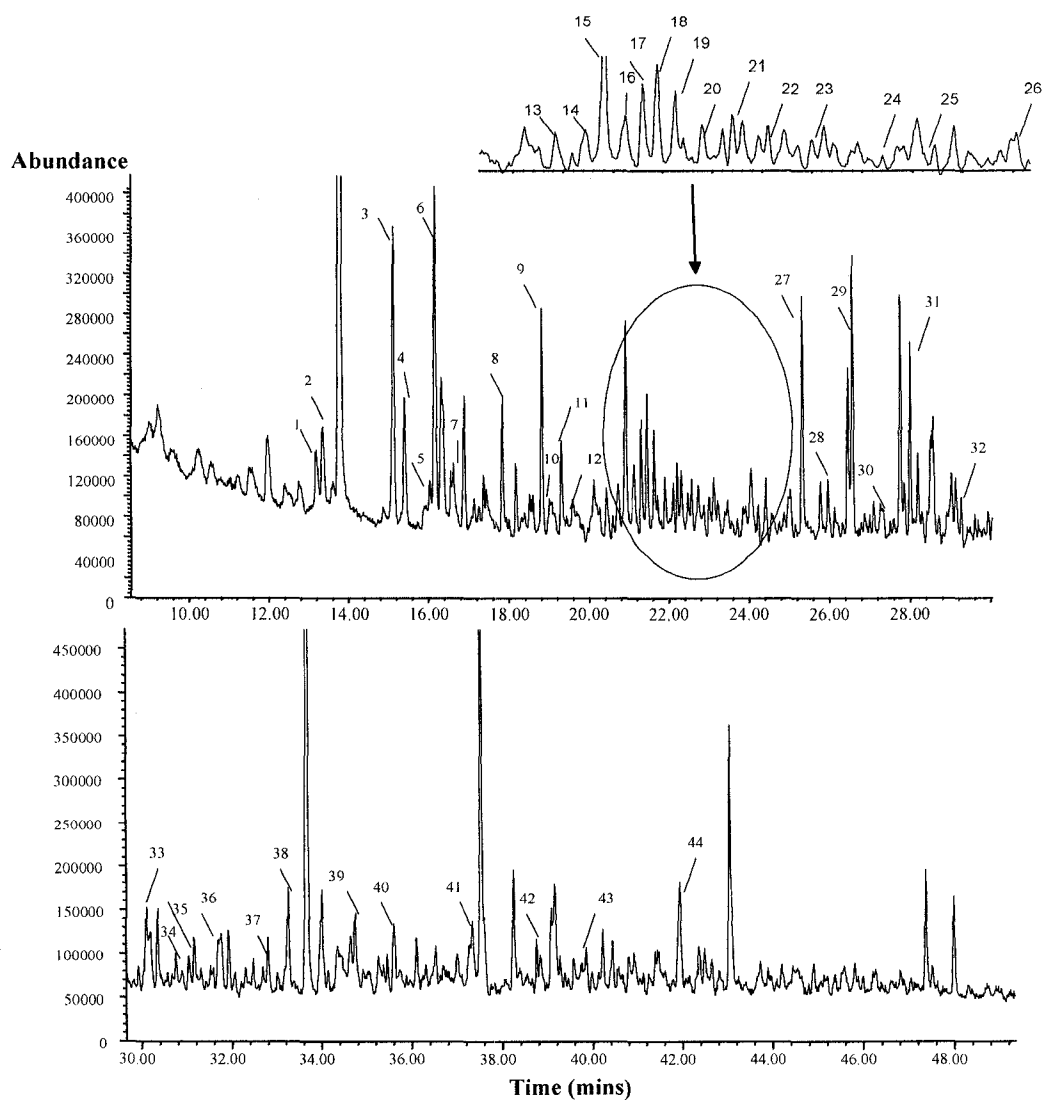


Figure 3.3. Total ion chromatogram of THM-GC-MS of Suwannee River NOM.

Table 3.1. HA model-thermochemolysis products

Peak Number*	Compound
1.	Methoxymethylbenzene
2.	2-Ethyl-2,3,3-trimethylbutanoic acid
3.	Hexanoic acid, 3-oxo-, methyl ester
4.	2,5-Pyrrolidinedione, 1-methyl-
5.	Benzoic acid, methyl ester
6.	1,4-Benzenediol, 2-methoxy-
7.	2-Cyclohexenylacetic acid, methyl ester
8.	Dimethyl ethylidenemalonate
9.	Pentanedioic acid, dimethyl ester
10.	Ethanol, 2,2'-oxybis-, diacetate
11.	2-Furancarboxylic acid, 3-methyl-, methyl ester
12.	Dimethyl 2-ethyl succinate
13.	Pentanedioic acid, 2-methylene-, dimethyl ester
14.	Butanedioic acid, ethylidene-, dimethyl ester
15.	2-Furancarboxylic acid, anhydride
16.	Pentanedioic acid, 2-oxo-, dimethyl
17.	2-Furancarboxylic acid, 3-methyl-, methyl ester
18.	Propanedioic acid, (2-methyl-2-propenyl)-, dimethyl
19.	2,5-Furandicarboxylic acid, dimethyl ester
20.	1-Cyclopentene-1,2-dicarboxylic acid, dimethyl ester
21.	Phenol, 5-methoxy-2-(methoxymethyl)-
22.	2,5-Furandicarboxylic acid, dimethyl ester
23.	1-Cyclopentene-1,2-dicarboxylic acid, dimethyl ester
24.	Ethanedione, di-2-furanyl-
25.	Trimethyl 1,2,3-propanetricarboxylate
26.	Octanedioic acid, dimethyl ester
27.	Methyl 4-methoxysalicylate
28.	1,2,4-Butanetricarboxylic acid, trimethyl
29.	1,2-Benzenedicarboxylic acid, 4-methyl-, dimethyl
30.	1,2-Benzenedicarboxylic acid, 4-hydroxy-, dimethyl ester
31.	1,2,4-Benzenetricarboxylic acid, trimethyl ester
32.	Benzenebutyric acid, 2,3-dimethoxy-
33.	3-Ethyl-5,7-dihydroxy-4H-chromen-4-one

* As assigned in Figure 3.2

Table 3.2. NOM-thermochemolysis products

Peak Number*	Compound
1.	2-Butenedioic acid (E)-, dimethyl ester
2.	Ethanol, 2-(2-methoxyethoxy)-
3.	Butane, 1,2,4-trimethoxy-
4.	2,5-Pyrrolidinedione, 1-methyl-
5.	Pentanedioic acid, 2-methyl-, dimethyl ester
6.	1,4-Benzenediol, 2-methoxy-
7.	Butanedioic acid, 2,3-dimethyl-, dimethyl ester
8.	Dimethyl ethylidenemalonate
9.	Pentanedioic acid, dimethyl ester
10.	Ethanol, 2,2'-oxybis-, diacetate
11.	Benzene, 1,2-dimethoxy-
12.	Dimethyl 2-ethyl succinate
13.	Benzene, 1,4-dimethoxy-
14.	3,4-Methylpropylsuccinimide
15.	Piperazine, 1-(2-furanylcarbonyl)-
16.	1-Cyclohexene-1-carboxylic acid, 3-oxo-, methyl
17.	N-Nitrosodimethylamine
18.	Pentanedioic acid, 2-oxo-, dimethyl ester
19.	2,5-furandicarboxylic dimethyl ester
20.	1,2,6-Trimethoxy-hexane
21.	5-Hydroxy-4,5-dimethyl-2,5-dihydrofuran-2-one
22.	4-Methoxycarbonyl-4-butanolide
23.	3,4-Bis(Methoxycarbonyl)furan
24.	2,4-Hexadienedioic acid, dimethyl ester, (E,E)-
25.	1,2,3-Trimethoxybenzene
26.	L-Proline, 1-methyl-5-oxo-, methyl ester
27.	Benzene, 4-ethenyl-1,2-dimethoxy-
28.	Benzoic acid, 4-methoxy-, methyl ester,
29.	2-Furancarboxylic acid, tetrahydro-3-methyl-5-oxo-, methyl
30.	d-Xylopyranoside, methyl 5-C-methoxy-2,3,4-tri-O-methyl-
31.	1,2,4-Butanetricarboxylic acid, trimethyl ester
32.	Benzoic acid, 3,4,5-trimethoxy-,
33.	1,3-Benzodioxole-5-carboxylic acid, methyl ester
34.	1,4-Benzenedicarboxylic acid, dimethyl
35.	1,3-Benzenedicarboxylic acid, dimethyl
36.	1,2,3,4-Tetramethoxybenzene
37.	1,2-Benzenedicarboxylic acid, 4-methyl-, dimethyl
38.	2,4'-Dihydroxy-3'-methoxyacetophenone,
39.	Benzoic acid, 3,5-dimethoxy-, methyl ester
40.	Acetic acid, 2-(3,5-dimethoxyphenyl)-, methyl ester
41.	Benzeneacetic acid, 3,4-dimethoxy-, methyl ester,
42.	Benzoic acid, 3,4,5-trimethoxy-, methyl ester
43.	2-Propenoic acid, 3-(3,4-dimethoxyphenyl)-, methyl ester,
44.	Pentadecanoic acid, 14-methyl-, methyl ester

* as assigned in Figure 3.3

Upon comparison, it was found that the major thermochemolysis products of NOM were very similar to those of the prepared humic acid model, which clearly points to similarities in their structure, and in all probability their origins. Further, the HA model, which by nature of its synthesis should be devoid of aromatic structures (precursor primarily aliphatic), showed evidence of some benzenoid compounds such as benzene tricarboxylic acids, benzene butyric acids, methoxy substituted benzene, *etc.*, all of which have been attributed to lignins in the literature. For example, Leenheer *et al.*³ have associated methoxyphenols with lignins. However, as strongly demonstrated by Frazier *et al.*²⁴ (found methoxybenzene compounds *e.g.*, 1,2- and 1,4-dimethoxybenzenes to be TMAH products from carbohydrates) as well as in our work, these aromatic products are not always specific to lignins. Other previously reported potential lignin-derived TMAH products such as 1,2-dimethoxybenzene, 3,4-dimethoxybenzoic acid methyl ester, and methyl benzoate were also formed from thermochemolysis of this polymerized 4-oxo-2-butenic acid. Given the ambiguity as to the origin of the aromatic structures detected by thermochemolysis GC-MS, it seems that it would be difficult to use this technique to ascertain the degree to which each possible source (*i.e.* lignin, carbohydrate, *etc.*) may contribute to the formation of HS as attempted for NOM by Frazier *et al.*²⁴ who associated 21-35% of NOM with lignin-derived compounds. As such, we believe that this work demonstrates that, in spite of the fact that these aromatic compounds are usually ascribed to lignin derivatives in NOM, their presence is not necessarily indicative of lignin content or intrinsic aromaticity.

In addition to the aromatic compounds detected, some of the methyl esters of fatty acids like octanedioic acid and hexanoic acid usually detected in the thermochemolysis of

HS, were also found from the synthetic humic acid model. However, evidence of higher molecular weight fatty acids (C9-C18) was not found. It has been reported by others,^{6,16} including Lehtonen *et al.*²⁰, that the most abundant identifiable chemolysate products of HS include dimethyl diesters of 2-butenedioic acid and butanedioic acid, which is in agreement with a 4-oxo-2-butenic acid polymerization model reported herein. It is interesting to note that benzenediols detected in the HULIS have been noted as important markers of anthropogenic NOM by Poerschmann *et al.*¹⁵

The difficulties in understanding the thermochemolysis GC-MS signature of NOM is further exacerbated by the numerous chemolysates whose structures have been identified but whose origins have not yet been determined.^{19,24-26} In the analysis of our synthesized HULIS, we have identified a number of these TMAH degradation products in abundance including butanedioic acid dimethyl ester, pentanedioic acid dimethyl ester, and other substituted analogues of diacid methyl esters, as well as hydroxy and methoxy substituted butyric acid methyl esters. These results seem to reinforce the fact that the majority of humic acid composition is carbohydrate derived and further augments the work by Susic who advanced the idea that 4-oxo-2-butenic plays a key role in the formation of humic substances.

The similarities of the aforementioned compounds, which are present in both the THM products of HULIS and the NOM with 4-oxo-2-butenic acid, proposed to be a major building block of humic substances can be seen in Figure 3.4, which shows some structurally remarkable chemolysates, which heavily support this evidence. A very notable one is 3,4-bis(methoxycarbonyl)furan, present in NOM, and which looks like a dimer of 4-oxo-2-butenic acid. Others, like dimethyl ethylidenemalonate, fumaric acid,

oxalic acid and malic acid, which are known to be oxidation products of NOM obtained by GC-MS, seem to be derived from the proposed monomer 4-oxo-2-butenoic acid. The well-documented presence of 4-oxo-2-butenoic acid as one of the major components of atmospheric aerosols, which is estimated to contain more than 60% humic substances, further gives credence to our proposal that 4-oxo-2-butenoic acid may be a major building block of HS.³⁷

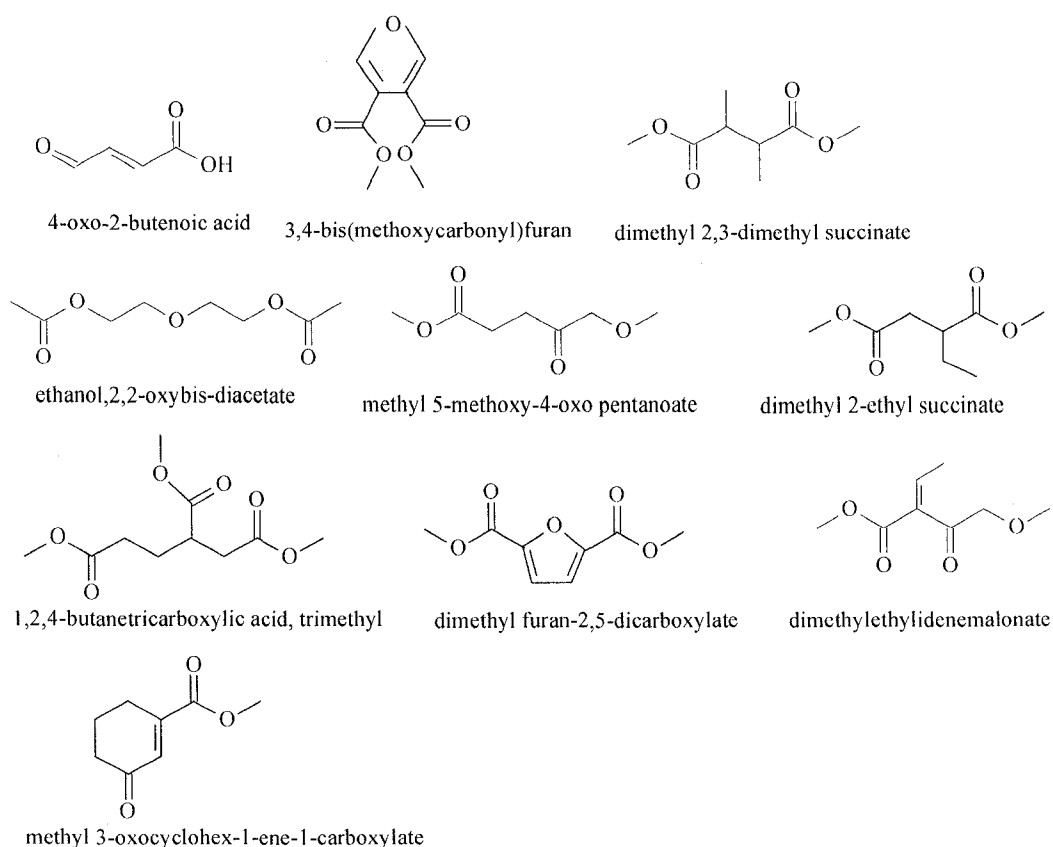


Figure 3.4. Some structures of THM products (also shown in Table 3.1 and Table 3.2) which possibly originate from the acid polymerization of 4-oxo-2-butenoic acid.

The chemolysates obtained from THM-GC-MS could be used to develop credible hypothetical structures of HS and thus eventually help in understanding these materials.

This is particularly so because hydrolysis and methylation are selective and hence the chemolysates bear a strong relationship with the NOM. We have in a rudimentary way attempted to construct a HS component as shown in Figure 3.5. However, we should clearly state that developing credible hypothetical structures is not a trivial undertaking due to the numerous chemolysates that are generated.

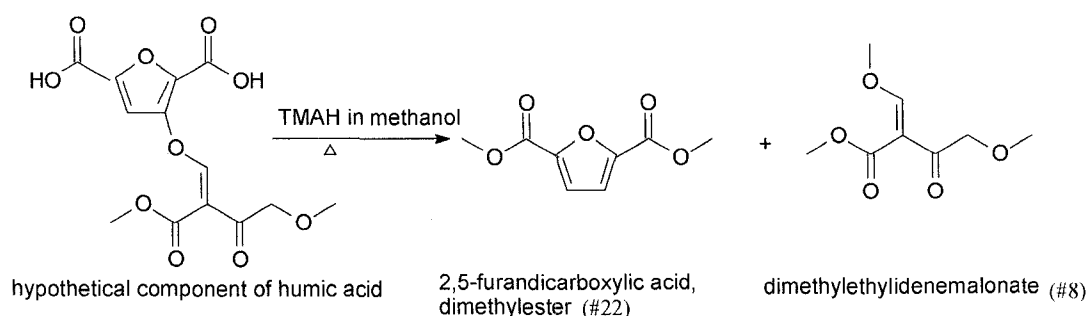


Figure 3.5. Possible hypothetical structure of aquatic FA from thermochemolysate data.

In order to further the multiple approach strategy, ¹H NMR studies were conducted on both the synthetic model and the NOM standard, both of which gave very similar spectra (Figures 3.6 and 3.7) and from which some useful information could be extrapolated. The most telling feature is the absence of peaks in region where aromatic protons, which normally occur at ~ 7 ppm, would usually absorb, even though aromatic moieties are observed in the GC-MS data. The peaks with chemical shift ~3.7 ppm, shows an evidence of presence of functionalities such as -OCH₂- linkages, which further authenticates the thermochemolysis data, suggesting a similarity between the HULIS and the natural NOM. It should be noted that while discrete peaks appear in this region for the HULIS, only an envelope of peaks, likely due to a complex mixture of protons at closely

related environments, is seen for the NOM; this observation is consistent with the expected complexity of NOM. Therefore, it can be concluded that humic substances may be primarily aliphatic, and it is probable that the genesis of humic acid may not be from the condensation of polyphenols as often believed, but, as reported by Susic, the dynamic structural nature of these materials allow them to be converted to aromatic structures that may not be necessarily related to lignin-derived compounds such as vanillic and syringic acids.^{3, 27} The fact that Gajdosova *et al.*¹⁰ reported there are plentiful humic substances in Antarctica, which have very similar structural properties to other HS and yet there exists no plants with lignin is further compelling evidence that the primary building block of HS are polysaccharides rather than lignins.

NMR is however designed for analysis of pure or less complex mixtures and hence only minimal information (spectra not representative) could be obtained when used to analyze HS, which may consist of many components in low concentrations. The fact that HS conformation is so dependent on its solution environment further casts a limitation on solution NMR data shown in our study. It is probably for this reason that HS has mainly been characterized by solid NMR recently.^{31,32}

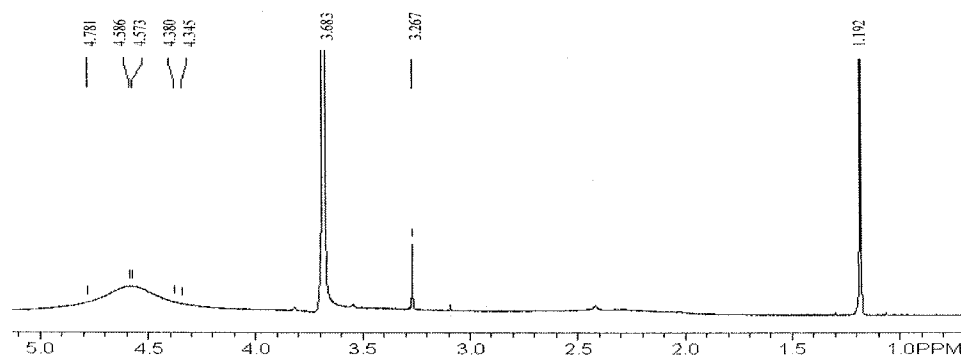


Figure 3.6. ¹H NMR of 10 mg mL⁻¹ HULIS in DMSO.

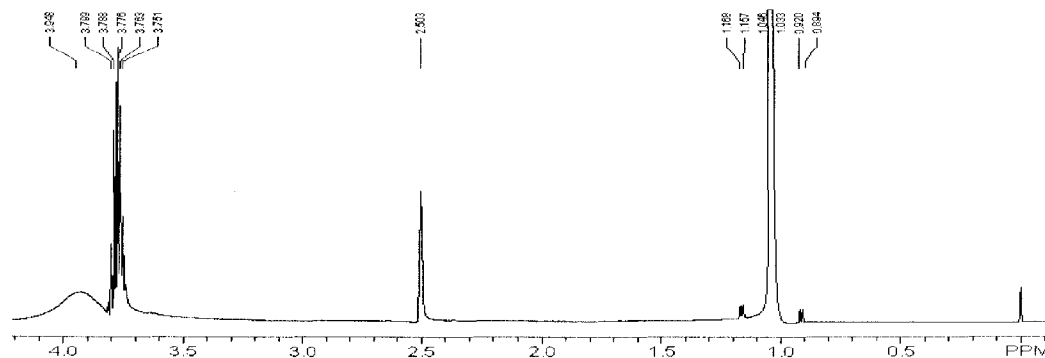


Figure 3.7 ^1H NMR of 11 mg mL^{-1} 1R101N in DMSO (peak at 2.5 ppm is from DMSO).

3.4 Conclusion

The results of this work have demonstrated that caution should be taken when associating some TMAH byproducts with lignins, as these aromatic structures are not specific to lignins and are possibly polysaccharide-derived. Some of the hitherto pyrolysates reported to be of unknown origin have been determined to arise from carbohydrates. The knowledge of the origin of these pyrolysates is crucial, since it can help provide bulk characterization of the composition of NOM, and may help to end the uncertainty as to the origin of humic substances. Evidence has also been presented that the most probable route for the formation of humic substances is from polysaccharides, which has been proposed previously, though it is not widely accepted. Continued application of this strategy; combining the application of multiple analytical techniques to studies of both synthetic NOM models and extracted NOM should lead to a more exact picture of the chemistry of humic substances. For example, it would be desirable to

compare fingerprint spectra of NOM and humic acid models using LDI, MALDI and even ESI.

3.5 References

1. Swift R S. *Soil Sci.* 1999; 164: 790-802.
2. MacCarthy P. *Soil Sci.* 2001; **166**: 738-751.
3. Leenheer JA, Croue JP. Aquatic organic matter. *Environ. Sci. Technol.* 2003: 19A.
4. Janos P. *J. Chromatogr. A* 2003; **983**; 1-18.
5. Hatcher PG, Dria KJ, Kim S, Frazier SW. *Soil Sci.* 2001; **166**: 770-794.
6. Peña-Méndez E M, Havel J, Patočka J. *J. Appl. Biomedicine* 2005; **3**: 13-24.
7. Chefetz B, Salloum MJ, Deshmukh AP, Hatcher PG. *J. Soil Sci. Soc. Am.* 2002; **66**:1159-1171.
8. McIntyre C, Jardine D, McRae C. *Rapid Commun. Mass Spectrom.* 2001, **15**; 1974-1975.
9. Kalberer M. *Anal. Bioanal. Chem.* 2006; **385**: 22-25.
10. Gajdošová D, Novotná K, Prošek P, Havel J. *J. Chromatogr. A*, 2003; **1014**: 117-127.
11. Stenson AC, Marshall AG, Cooper WT. *Anal. Chem.* 2003, **75**: 1275-1284.
12. Piccolo A. *Soil Sci.* 2001; **166**: 810-832.
13. Pranzas P K, Willumeit R, Gehrke R, Thieme J, Knochel A. *Anal. Bioanal. Chem.* 2003; **376**; 618-625.
14. Schulten HR, Gleixner G. *Water Res.* 1999; **33**: 2489-2499.
15. Poerschmann J, Kopinke FD, Balcke G, Mothes S. *J. Microcolumn Sep.* 1998; **10**: 401-411.

16. Abbt-Braun G, Lankes U, Frimmel FH. *Aquat. Sci.* 2004; **66**: 151-170.
17. Challinor JM. *J. Anal. Appl. Pyrolysis* 1989; **16**: 323-330.
18. Challinor JM. *J. Anal. Appl. Pyrolysis* 2001; **61**: 3-34.
19. Hatcher PG, Gary EM, Larry WD. *Organic Geochem.* 1994; **21**: 1081-1092.
20. Lehtonen T, Peuravuori J, Pihlaja K. *J. Anal. Appl. Pyrolysis* 2000; **55**: 151-160.
21. Guignard C, Lemee L, Ambles A. *Agronomie*, 2000; **20**: 465-475.
22. Martin F, Almendros G, Gonzalez-Vila FJ, Verdejo T. *J. Anal. Appl. Pyrolysis* 2001; **61**: 133-145.
23. Grasset L, Guignard C, Ambles A. *Org. Geochem.* 2002; **33**: 181-188.
24. Frazier S W, Nowack KO, Goins KM, Cannon FS, Kaplan LA, Hatcher PG. *J. Anal. Appl. Pyrolysis* 2003; **70**: 99-128.
25. Cynthia A, Huynh T, Heitz A. *J. Anal. Appl. Pyrolysis* 2003; **70**: 151-167 .
26. Tanczos I, Rendl K, Schmidt H. *J. Anal. Appl. Pyrolysis* 1999; **49**: 319-327.
27. Susic M. <http://www.fortunecity.com/skyscraper/solomon/1735/>.
28. Garrett ER, Dvorchik BH. *J. Pharm. Sci.* 1969; **58**: 813-820.
29. Vedernikov N. *Proc. 10th Intern. Symp. Wood and Pulping Chemistry*. Yokohama, Japan, June 7-10, 1999; 3: 468-470.
30. Jang M, Czoschke NM, Northcross AL. *ChemPhysChem*, 2004; **5**:1646-1661.
31. Amir S, Hafidi M, Merlina G, Hamdi H, Revel JC. *Agronomie* 2004; 24: 13-18.
32. Lu XQ, Hanna JV, Johnson WD. *Applied Geochemistry* 2000; 15: 1019-1033.

CHAPTER 4

Aquatic fulvic acid as a matrix for MALDI-TOFMS analysis.

A version of this chapter has been published. Mugo SM, Bottaro CS. Aquatic fulvic acid as a matrix for matrix assisted laser desorption/ionization time of flight spectrometric analysis. *Rapid Commun. Mass Spectrom.* 2006; **21**: 219-228

4.1 Introduction

Matrix-assisted laser desorption ionization time of flight mass spectrometry (MALDI-TOFMS), first reported by Hillenkamp and Karas in 1987, has evolved to become the gold standard in the qualitative analysis of high molecular weight molecules in a suite of scientific disciplines, especially proteomics and polymer research.^{1,2} The surge in the acceptability of the MALDI technique is due to its unmatched sensitivity, high throughput, softness in ionization, relatively uncomplicated spectra (with formation of mainly singly-charged ions), and essentially unlimited mass range when coupled to TOF analyzer.³⁻⁸ Furthermore, unlike other ionization techniques (*e.g.* electrospray), MALDI is somewhat more tolerant of impurities, salts and buffers, attributed to what Cohen *et al.*³ called “chromatographic on-target cleanup effect”, where impurities are excluded from incorporation in the analyte/matrix crystal.⁴

The success of MALDI analysis relies on appropriate sample preparation and the nature of matrix employed. A MALDI matrix must meet a litany of requirements such as: reasonable absorption at the wavelength of the laser (N₂ operating at 337 nm wavelength and frequency-tripled Nd:YAG at 335 nm lasers are most common), stability at high vacuum (around 10⁻⁶ torr), compatible solubility with analyte, ability to isolate analytes while hindering their aggregation, and ability to promote analyte ionization. However, no one known matrix or even handful of matrices meets all these archetypical features for analytes with widely varying masses and structures, in other words, most matrices are analyte specific.⁵⁻⁷

The traditional matrices are typically low molecular weight (< 500 Da) organic acids *e.g.* 2,5-dihydroxybenzoic acid (DHB), α -cyano-4-hydroxycinnamic acid (α -

CHCA), and 3,5-dimethoxy-4-hydroxycinnamic acid (sinapinic acid), *etc.*^{1,3,4,5,6} Their carboxylic moieties play a key role in enhancing protonation of the analyte, though the suitability of a compound as a MALDI matrix is not exclusively determined by presence of a labile proton. In general, MALDI ionization occurs through proton transfer, cation adduction (forming potassium and sodium adducts), electron transfer or electron capture.^{6,7} It should be emphasized that since the mechanisms governing desorption and ionization processes are complex and still only vaguely understood, there are no absolute criteria that must be met in matrix selection and the field remains open for exploration. Moreover, investigation of as many compounds as possible as MALDI matrices will eventually be helpful in better understanding these fundamental processes.

The use of prototypical matrices is problematic for small molecule analysis due to spectral noise (resulting from matrix, matrix fragments, and cluster ions) in the low mass region (< 1000 Da), making it difficult to distinguish the analyte ion peaks from matrix peaks. As such, there has been intense research to adapt these matrices to the analysis of small molecules by using various approaches to decrease matrix interference. These approaches include: matrix suppression effect based on optimization of the analyte to matrix ratio,⁸ surfactant-based matrix ion suppression,⁸⁻¹⁰ and use of matrix co-additives (*e.g.* nitrocellulose).⁹ To circumvent the problem of matrix interference in the mass region of interest altogether, high molecular mass matrices^{11,12} (*e.g.* porphyrinic molecules), matrix-less techniques (*e.g.*, desorption ionization on silicon (DIOS)^{13,14}) and ionization enhancing films (UV energy absorbing polymers,¹⁵ sol-gel,¹⁶ and nanostructured silicon¹⁷) have been employed.

Recently, there has been tremendous interest in experimentation with carbon nanotubes (CNT) and related materials, (*e.g.* graphite from a pencil lead) as MALDI matrices.¹⁸⁻²⁷ CNT have been found quite promising in enhancing ionization – especially through cationization (sodiation and potassiation) – of a wide range of small molecules, such as carbohydrates, amino acids, peptides and proteins, environmental samples, *etc.* Nevertheless, there are still many limitations that are yet to be overcome, for example, low solubility of CNT, matrix interference at high laser power, poor adsorption on MALDI target surfaces and problems with metallic impurities, which are suspected to be the main reason for ion source contamination and can potentially lead to instrument downtime and costly repairs. These limitations necessitate chemical modification of CNTs by functionalization and immobilization strategies, which are laborious.^{21, 23, 24} On the other hand, aquatic fulvic acid (AFA), a heterogeneous mixture of compounds with aromatic and aliphatic character, exhibits many of the desirable properties associated with CNT matrices but without many of their limitations. AFA is inherently highly functionalized, very soluble in water and needs no demanding functional modifications, making MALDI sample preparation straightforward. Also the supramolecular morphology of AFA provides a large surface area, which could be useful in sufficiently dispersing analyte molecules and preventing sample aggregation.

The idea of using fulvic acid as a MALDI matrix was borne from recognition of its key unique structural features that should lend it to use in this capacity. Fulvic acid is a component of a class of materials called humic substances that are thought to be formed from degradation of biogenic materials. Although the complex structure of AFA is not fully understood, ¹³C-NMR, IR, UV, titrimetric characterizations, pyrolysis and

thermochemolysis techniques and electrospray ionization-MS have provided convincing evidence for the presence of a number of representative functionalities.²⁸⁻³³ These include numerous keto acids, aromatic and aliphatic carboxyl groups and polycarboxylic α -ether and α -ester structures, which endow AFA with considerable acidic character (pK_a of Suwannee River FA estimated to be $< 2-3.0$).²⁸⁻³⁰ As such, fulvic acid is undoubtedly rich in labile protons, which could be utilized for protonation of embedded analyte, making it, in principle, a good candidate for use as a MALDI matrix.

During the preparation of this manuscript the use of a synthetic polyelectrolyte (poly- α -cyano-4-methacryloyloxycinnamic acid) as a polymer surface platform for LDI-MS was reported by Kitagawa.³⁴ In his work, he indicated a suitable polyelectrolyte for LDI should bear laser-energy absorbing structures on the polymeric backbone and moieties with labile protons, such as carboxyl groups, that could easily form a “proton cloud” that is available for donation to the analyte on excitation by the laser. With the loss of protons and subsequent formation of negative charges, the polyelectrolyte matrix should be in a configuration that allows increased inductive repulsive effects, which contribute to desorption. These features are shared by AFA, and thus it may be defined as a natural polyelectrolyte. This work using the synthetic polyelectrolyte assisted LDI-MS, further gives credence to the possible utility of fulvic acids in MALDI matrix applications.

4.2 Materials and Methods

Poly(ethyleneglycol) 1000 (PEG 1000), 2,3,4,6-tetramethylglucose, xylose, chlorogenic acid, allose, α - and β -cyclodextrins (CD), (D)-glucose, trialanine, maltose, maltotriose and 6-methyl-D-galactose were bought from Sigma-Aldrich Canada Ltd; Oakville, Ontario and used without purification. MALDI Calibration Mixture 1 containing angiotensin-1, des-Arg¹-Bradykinin, Glu-fibrinopeptide B and neurotensin was obtained from PerSeptive Biosystems; Foster City, California. Suwannee River FA standard 1S101F was bought from the International Humic Substances Society (IHSS), St. Paul, Minnesota, USA. All solutions used in this work were made up in distilled deionized water unless otherwise indicated. The AFA matrices were made up at concentrations of 2.0 mg mL⁻¹ and all analytes at 1.0 mg mL⁻¹, other than the proteins in Calibration Mixture 1, which were present at 1.0 M, except for angiotensin-1 at 1.3 M. Cantaloupe and generic pharmaceutical grade acetaminophen (500 mg tabs) manufactured for Loblaws Inc. Montreal, were obtained locally.

4.2.1 Extraction of Aquatic Long Pond (Newfoundland) Fulvic Acid

Fulvic acid from Long Pond (LFA), St. John's, Newfoundland, was isolated using the method described by Thurman and Malcolm,³⁵ with some modifications. Concisely, one hundred litres of water from Long Pond (St. John's, Newfoundland) were filtered using 0.45 μ m hydrophilic polypropylene membrane filters and the pH adjusted to \sim 1.95 using 6M HCl. The water was then pumped (flow rate, 6-7 mL min⁻¹) through a pre-cleaned XAD-8 column (bed volume, \sim 81 mL) and eluted in the reverse direction with

one molar NH_3 . The eluent was acidified to $\sim\text{pH}=1.95$ using 6M HCl, reconcentrated on a smaller XAD-8 column (bed volume, ~ 38 mL) and eluted with one molar NH_3 , resulting in a concentrate of fulvic and humic acid (HA). HA was isolated by acid precipitation, the pH of the concentrate was adjusted to 0.90 with HCl, followed by centrifugation. The fulvic acid fraction was reconcentrated on XAD-8, washed with two bed volumes of water to remove salts, eluted with one molar NH_3 , and then dried under vacuum.

4.2.2 SEM Imaging of Fulvic Acid

Two μL s of 2 mg mL^{-1} Long Pond fulvic acid and 2 μL s 1S101F (2 mg mL^{-1}) were spotted on a stainless steel sample stage and imaged using a scanning electron microscope (Hitachi 5570 SEM with Tracor Northern 5500 EDX and backscattered electron detector). A 2- μL aliquot of 1 mg mL^{-1} trialanine was spotted separately on the LFA spot and imaged as well.

4.2.3 UV-Vis Spectrophotometry

Ten $\mu\text{g L}^{-1}$ solutions of LFA and 1S101F were prepared in distilled deionized water and characterized spectrophotometrically using a Hewlett Packard 8452A diode array spectrophotometer. UV-vis spectra were obtained over a wavelength range of 190-440 nm.

4.2.4 Sample Preparation

The very convenient *fast evaporation method* was employed as a sample preparation protocol. One μL of 2 mg mL^{-1} (determined experimentally to be a suitable

concentration) AFA dissolved in water/acetonitrile (1:1, v/v) was spotted on a MALDI 100-sample capacity stainless steel sample stage and allowed to dry under ambient conditions. This formed a homogeneous film of the matrix. One- μL aliquots of the analyte solutions were then spotted onto the dried matrix spots and allowed to dry. The sample stage was then loaded in to a MALDI-TOFMS instrument for analysis.

4.2.5 MALDI-TOFMS Instrument Conditions

The MALDI-TOF mass spectra reported herein were acquired in positive ion mode using an Applied Biosystems DE-RP equipped with a reflectron, delayed ion extraction and a pulsed nitrogen laser beam (337 nm). The accelerating voltage was 20kV, extraction delay time was 200 nsec and the grid voltage was 74.4%. The mass acquisition range was chosen based on the molecular weight of analyte, with the upper limit ranging between m/z 1000-2000. Low mass ions were rejected by gating ions below m/z 100 to avoid detector saturation. The laser intensity was varied depending on the analyte analyzed, but for the purpose of obtaining good signal-to-noise ratio (S/N) was adjusted to slightly above the experimentally determined ionization threshold. Spectra reported are the average of 30 laser shots.

4.3 Results and Discussion

Topographical images from SEM of the IHSS Suwannee River fulvic acid standard 1S101F and the locally-extracted Long Pond fulvic acid (LFA) are presented in Figure 4.1. A comparison of images of the two fulvic acids (Figure 4.1a and b) shows

differences in the gross morphology.

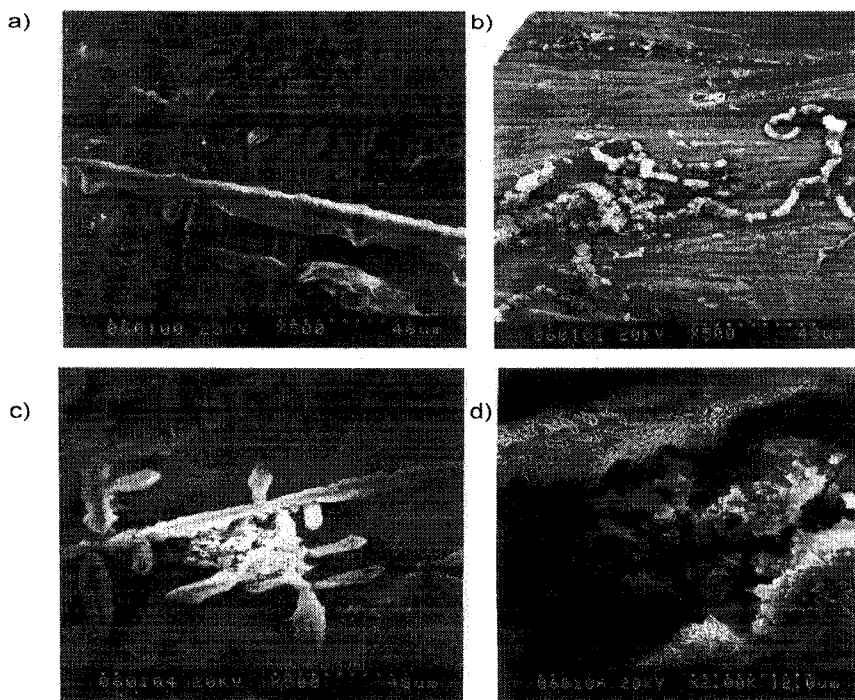


Figure 4.1. SEM of fulvic acid as a matrix, a) 2 μL of 2 mg mL^{-1} LFA, b) 2 μL of 2 mg mL^{-1} 1S101F c) 2 μL of 2 mg mL^{-1} LFA doped with 2 μL of 1 mg mL^{-1} trialanine, d) higher magnification of c).

Supramolecular morphology is borne from molecular structure, where even subtle differences can have significant effects on supramolecular assembly. The observed disparities can be attributed to the source of AFA, isolation techniques, and physico-chemical properties, noting that it is well accepted that the actual differences in functionality between humic substances from different places are marginal.³¹ Nonetheless, LFA seems to form a more homogenous and porous surface than its 1S101F counterpart. There is also evidence that LFA performs better as a matrix, as will be illustrated later with examples of the mass spectra. The differences in their performance

as MALDI matrices could, in part, be explained by the disparity in their surface morphology (porosity and roughness), which has been noted to be an important parameter in enhancing desorption/ionization.³⁶ As can be seen from the SEM images, LFA seems to form a crystalline morphology, which is now known to be an ideal condition for successful MALDI desorption/ionization.³⁴

Even though there is no obvious relationship between the morphology of a matrix and its utility as a MALDI matrix, the study of morphology is important in understanding, albeit only partially, analyte-matrix interactions. Based on the two known schools of thought on analyte-matrix interaction required for a successful analysis, the analyte should either be included into the matrix crystal lattice through cocrystallization or interact with matrix by adsorption or chemisorption.^{5,6} It is critical to mention that our attempts to use the dried droplet sample preparation method (mixture of matrix/analyte solution spotted and dried) never worked well for these matrices, but the fast evaporation method (drop of matrix allowed to dry on sample stage to which a drop of analyte solution is then added) was found to be quite efficient, which might suggest that surface interaction (AFA acting as a support) is the dominant process and plays a critical role in the success of fulvic acid as a matrix. This is contrary to what is considered to happen with conventional matrices, where cocrystallization with the analyte is a prerequisite for success in MALDI. Spotting trialanine on the fulvic acid matrix spot did not seem to change the general morphology of the AFA, suggesting the analyte is trapped in the sub-micrometre cavities (evident at high magnification, Figure 4.2d) of the matrix from which they are desorbed and ionized, a mechanism that is analogous to DIOS, which is a form of surface assisted laser desorption/ionization (SALDI).^{13,31} Further surface morphology

matrices cannot be employed because of interferences, various ways of introducing charged moieties have been employed, such as use of quaternary ammonium centers, which Gouw *et al.*³⁷ reported to significantly enhance ionization. On the other hand, we have found that AFA facilitates ionization through cation adduct formation (a similar function is seen with CNTs) with small carbohydrates like xylose, glucose, 2,3,4,6-tetramethylglucose, maltotriose, xylose, allose, glucose, and galactose; mass spectra for a selection of these analytes are shown in Figure 4.3. Sodiated analyte peaks were most intense, potassium ion adducts were also observed though at lower intensity and with less prevalence, but $[M+H]^+$ peaks were observed only infrequently.

Matrixless LDI was also used in assessing the efficiency of fulvic acid in enhancing ionization of the carbohydrates. It was found that most of the analytes, such as maltotriose, xylose and galactose, could not be analyzed by matrix-free-LDI and spectra produced showed no identifiable peaks, only noise. With AFA as the matrix (Figure 4.3), analyte peaks were easily recognized on a background with only a few fragment or matrix peaks present, at relatively low intensity. For comparison, a spectrum of the 1S101F AFA matrix alone can be seen in Figure 4.4a; a number of prominent peaks are apparent, which are absent in the spectra found in Figure 4.3. A comparable spectrum was observed for the LFA AFA matrix.

Serial dilutions of these carbohydrates were carried out to test for detection limits using fulvic acid as a matrix. The detection limits were found to be relatively high and no analyte peaks could be identified below concentrations of $10 \mu\text{g mL}^{-1}$. This may be due to the sequestration of analyte in the fulvic acid matrix cavities. Studies on models of fulvic

acid have attributed its ability to strongly bind organic compounds to its numerous polycarboxylic acid groups.^{28,29} This might explain why, in general, higher laser intensities than those used with conventional matrices had to be employed for these analyses.

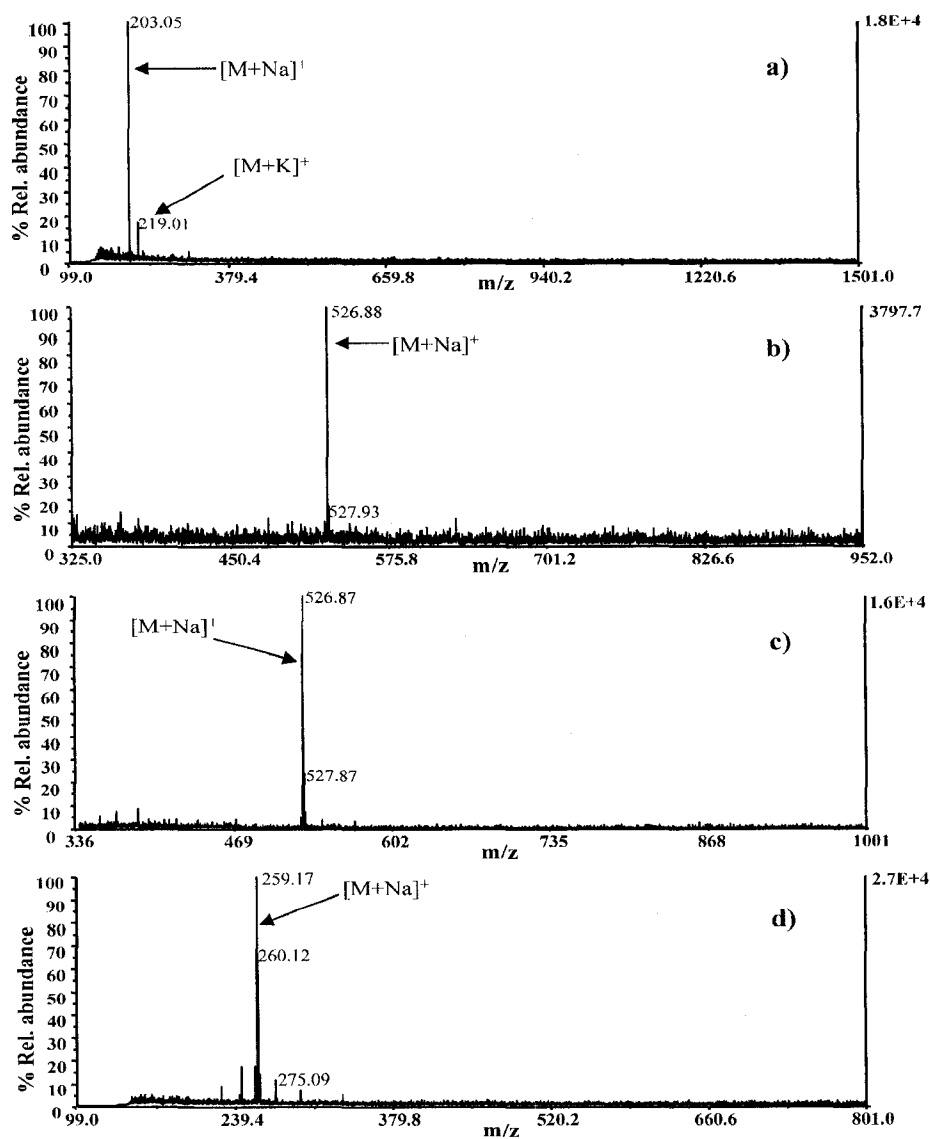


Figure 4.3. MALDI-TOFMS spectra using 2 mg mL⁻¹ 1S101F as a matrix: a) 1 mg mL⁻¹ glucose b) 1 mg mL⁻¹ maltotriose, and using 2 mg mL⁻¹ LFA as a matrix c) 1 mg mL⁻¹ maltotriose d) 1 mg mL⁻¹ 2,3,4,6-methyl glucose.

It is well known that optimization of the ratio of matrix to sample is important for MALDI applications, and thus, the most appropriate concentration of matrix to use was sought. Aquatic fulvic acid concentrations ranging from 1 mg mL⁻¹ to 5 mg mL⁻¹ were evaluated and minimal differences in the results were observed. Since there was no advantage in using higher loadings of AFA, an intermediate concentration of 2 mg mL⁻¹ was selected. Interestingly, at a low fulvic acid concentration (10 µg mL⁻¹) simple sugars (concentration, 1 mg mL⁻¹) such as galactose, allose and chlorogenic acid (has a carbohydrate chain) were found to enhance ionization of AFA components (Figure 4.4b). This role reversal could be attributed to the fact that at low AFA concentrations, the sugar (now in molar excess) is not shielded from laser irradiation, experiences an increase in internal energy, degrades, and undergoes collisional cooling that enhances ionization of fulvic acid components, making their ions prominent.³⁸ Enhancement of ionization by sugar additives is not a new phenomenon and has been reported and employed previously in the analysis of oligonucleotides.^{38,39} Related to these results, the use of the phenolic compound, chlorogenic acid (molar absorptivity at 337 nm, 920 M⁻¹ cm⁻¹), also substantially improved the signal strength of AFA peaks and could indeed be used as a matrix or matrix additive for analysis of fulvic acids (Figure 4.4c). These improvements in ionization could be employed in the further characterization of AFA, as the signal intensities of the fulvic acid peaks (*e.g.* *m/z*, 360, 388, 494, 522, 550, *etc.*) are made strong enough to allow the possibility of fragmentation experiments with post source

decay (PSD). It is essential to underscore that the resulting peaks are not necessarily representative of fulvic acid as a whole, but only the components that are most amenable to ionization in MALDI in positive mode.

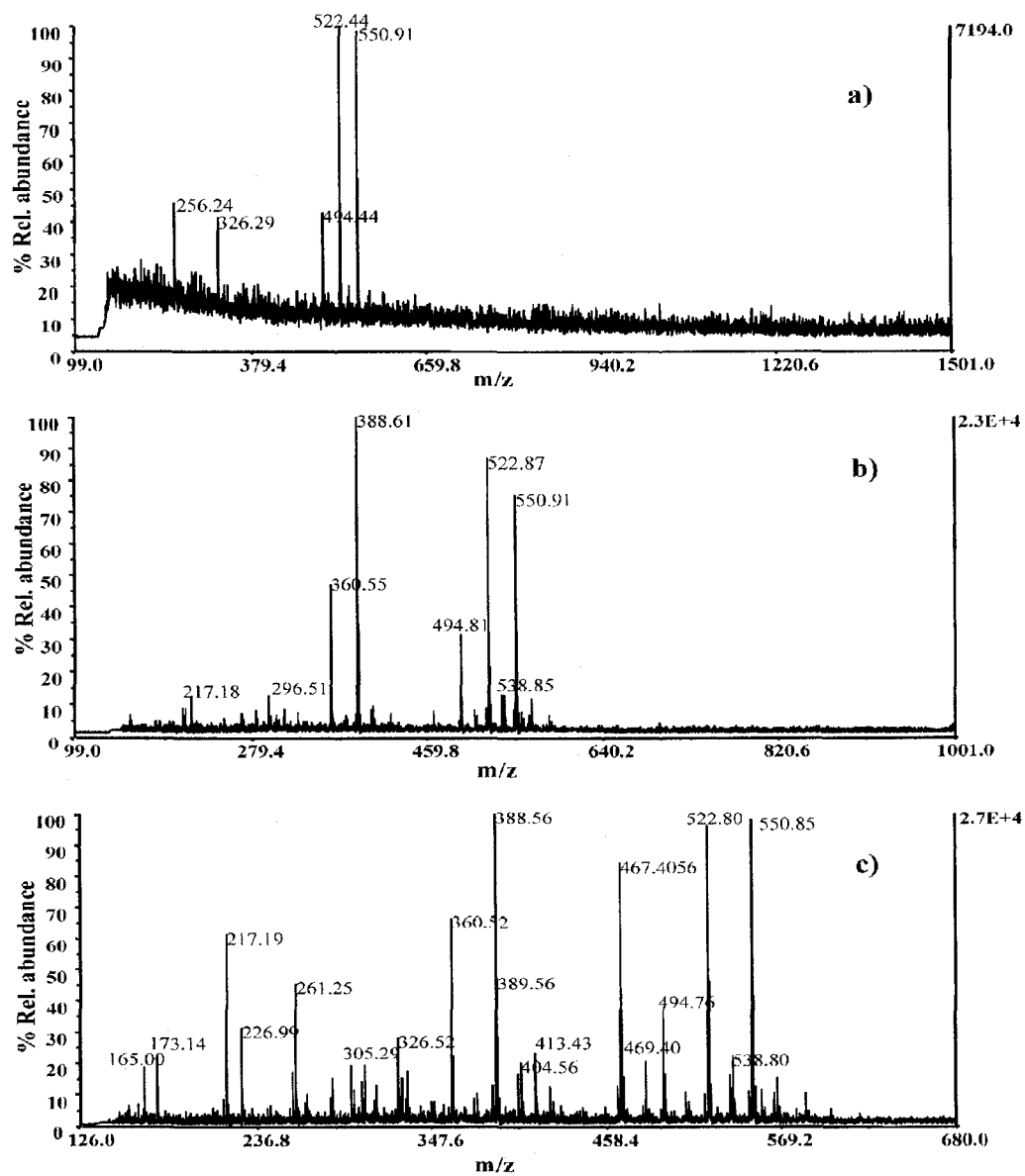


Figure 4.4. MALDI-TOFMS spectra of: a) LDI of 2 mg mL⁻¹ 1S101F, b) 10 µg mL⁻¹ 1S101F and 1mg mL⁻¹ 6 methyl-D-galactose, c) 100 µg mL⁻¹ chlorogenic acid and 10 µg mL⁻¹ 1S101F.

Excellent performance of AFA as a matrix was further demonstrated for CDs, specifically β -CD (7-glucopyranoside units) and α -CD (6-glucopyranoside units). This class of compounds are bucket shaped oligosaccharides used in a number of applications, including pharmaceutical formulations. Although CDs could be ionized using LDI, ionization is greatly enhanced using AFA matrices. The α - and β -cyclodextrin ions (m/z , 995 and 1157 respectively) detected were predominantly sodium adducts (Figure 4.5), formed through gas phase scavenging of Na^+ from the matrix, not unexpected since protonated carbohydrates are inherently unstable and thus cationization is the predominant ionization process.

It was also found that the locally extracted LFA performed better than 1S101F as a matrix for the carbohydrates, exemplified by the marked increase in intensity using LFA in the analysis of maltotriose (Figure 3b and c) and α -cyclodextrin (Figure 4.5). The differences in the efficiency of the two AFA matrices can be seen in Table 4.1, which gives peak intensities and S/N associated with the sodiated molecules of a number of carbohydrates. Again, LFA is shown to be a more effective matrix than the 1S101F AFA standard. It is not completely apparent why this is the case, since the spectrophotometric data showed that the mass extinction coefficient at the laser wavelength (337 nm) was approximately ten times higher for 1S101F than for LFA. So 1S101F should be able to better absorb the laser energy and thus lead to more efficient ionization. Although in general, mass spectral quality increases with increase in the absorption coefficient of the matrix, it has been reported that above a certain threshold the effect of the UV absorbance coefficient on the quality on the mass spectrum is minimal.⁵ Therefore, the difference in

performance between the two AFA matrices could be attributed to a more significant role of other factors, for instance, structure, functionality and amenability to form crystalline solid support.

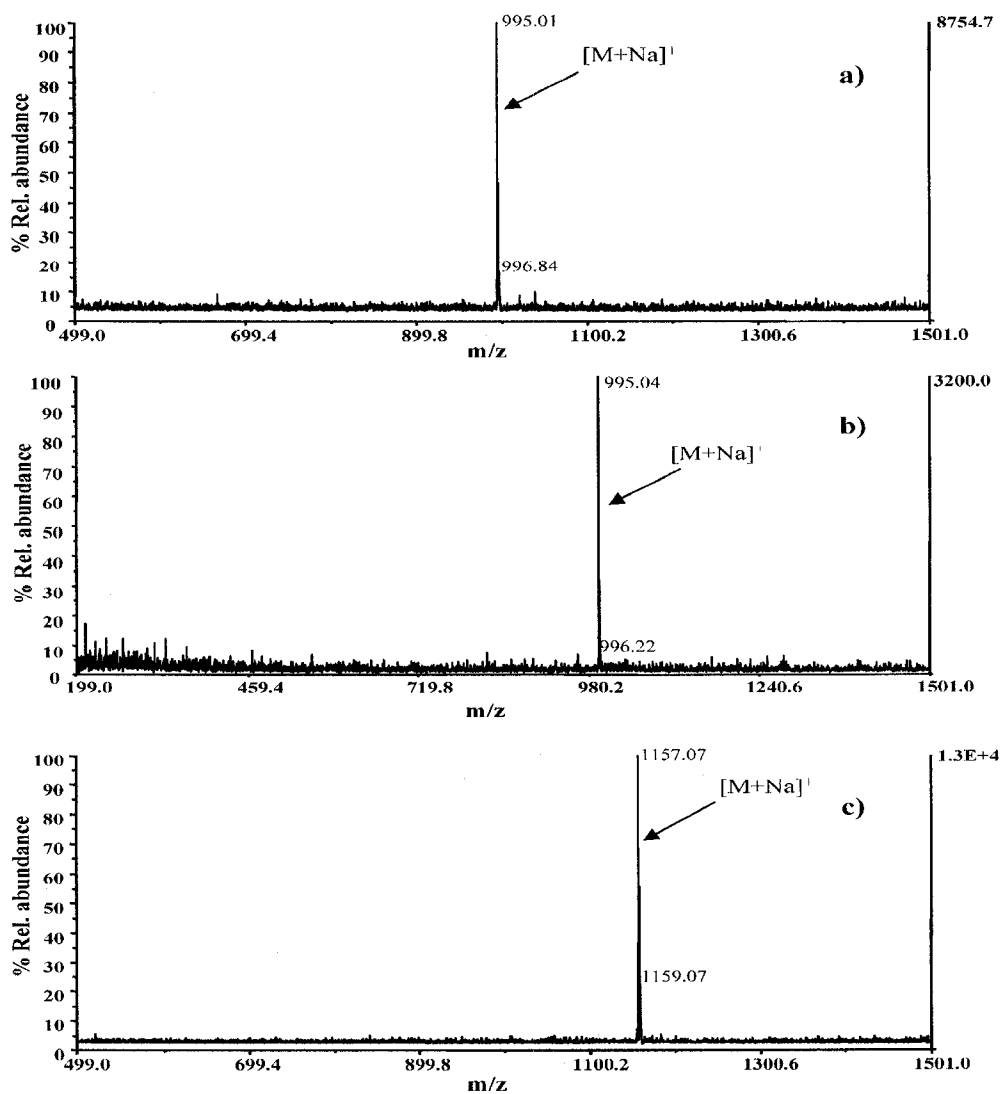


Figure 4.5. MALDI-TOFMS spectra of: a) 1 mg mL⁻¹ α -cyclodextrin and 2 mg mL⁻¹ LFA, b) 1 mg mL⁻¹ α -cyclodextrin and 2 mg mL⁻¹ 1S101F, c) 1 mg mL⁻¹ β -cyclodextrin and 2 mg mL⁻¹ LFA.

Table 4.1. Ion intensities and S/N values (sodiated peaks) for carbohydrates using 1S101F and LFA as matrices.

Analyte	1S101F		LFA	
	Intensity	(S/N)	Intensity	(S/N)
α -cyclodextrin	6.6×10^3	(124.1)	1.0×10^4	(275.8)
β -cyclodextrin	6.4×10^3	(108.1)	1.3×10^4	(439.6)
glucose	6.1×10^3	(105.8)	2.0×10^4	(338.6)
maltotriose	4.1×10^3	(94.0)	1.6×10^4	(468.0)
xylose	1.1×10^4	(202.4)	2.5×10^4	(333.7)

4.3.2 Analysis of Peptides

As can be seen in Figure 4.6, AFA was found to be effective for the analysis of peptides of a range of masses. Trialanine (MW, 231.30), angiotensin 1 (MW, 1296.68) and des-Arg¹-Bradykinin (MW, 904.47) ionized well using either 1S101F or LFA. The workable mass range of AFA, however, seems to be limited to < 1500 Da since Glu-fibrinopeptide B (MW, 1570.67) and neurotensin (1672.91) couldn't be detected. We speculate this could be associated with the ability of AFA to only accommodate the lower molecular weight analytes in its pores, where efficient transfer of the laser energy to analyte results in ionization and desorption, while the higher molecular weight compounds may be excluded from the fulvic acid cavities, reducing their chance of ionization/desorption. However, further studies should be carried out to assess the utility of fulvic acid for high molecular weight peptides. Proteins have sufficient basic sites for

facile protonation, so as anticipated $[M+H]^+$ was the dominant peak for the peptides tested and sodiated adducts were only rarely present.

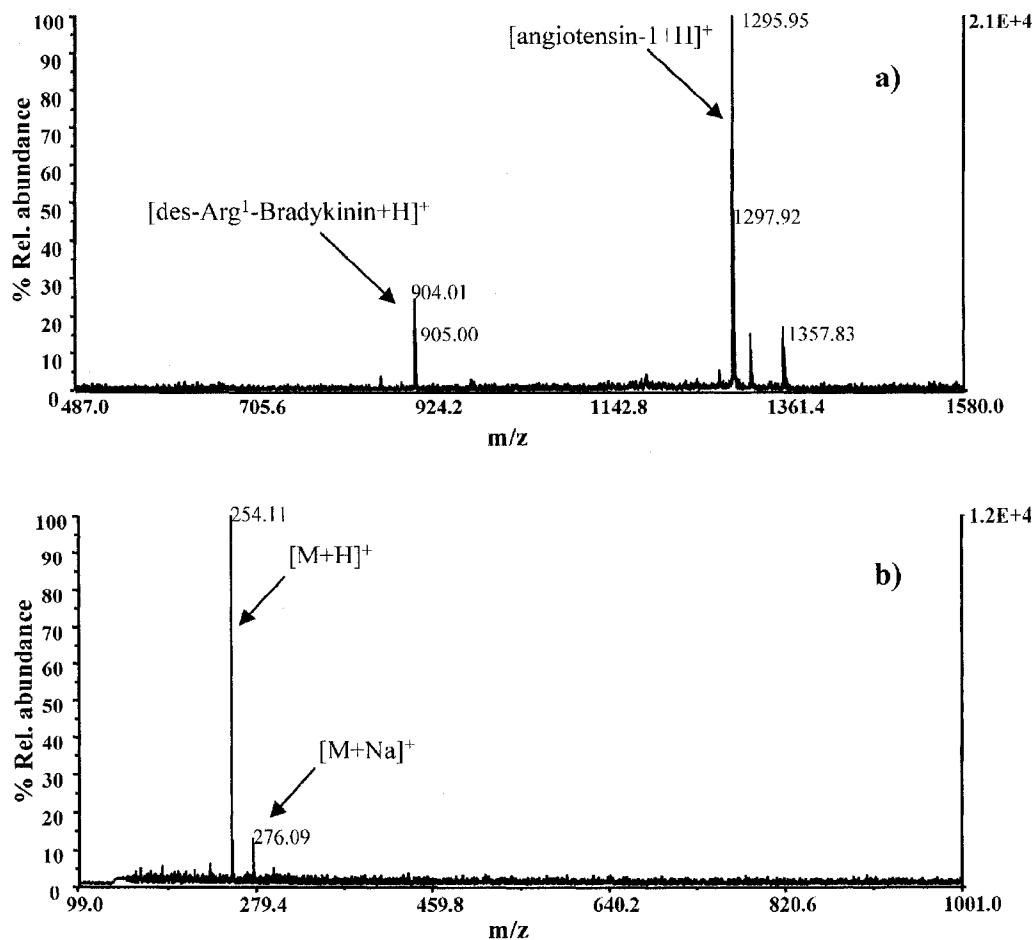


Figure 4.6. MALDI-TOFMS spectra of peptides using 2 mg mL^{-1} 1S101F as matrix: a) Calibration Mixture 1, (angiotensin 1, $\sim 1.3\text{ M}$ and des-Arg¹-Bradykinin, 1.0 M), b) trialanine 1.0 mg mL^{-1} .

4.3.3 Analysis of PEG

The use of AFA matrices was also successful for the analysis of the commercially important non-polar polyethylene glycol, PEG 1000, which ordinarily requires addition of a metal cation to obtain a charged oligomer that can be detected in MALDI-TOFMS. LDI

can also be used in its analysis; the result is a distribution of peaks typical for polymers. When AFA is used as a matrix for this class of analytes, the overall pattern of peak distribution does not change, *i.e.* the typical repeating pattern of peaks separated by 44 Da was clearly evident and consistent with the $-\text{CH}_2\text{CH}_2\text{O}-$ monomer of PEG (Figure 4.7). However, more peaks at higher mass are observed and the peak intensities increase by an impressive $\sim 300\%$. Both 1S101F and LFA were comparable in their efficiency to ionize PEG, with most of resulting ion peaks deduced to be sodiated.

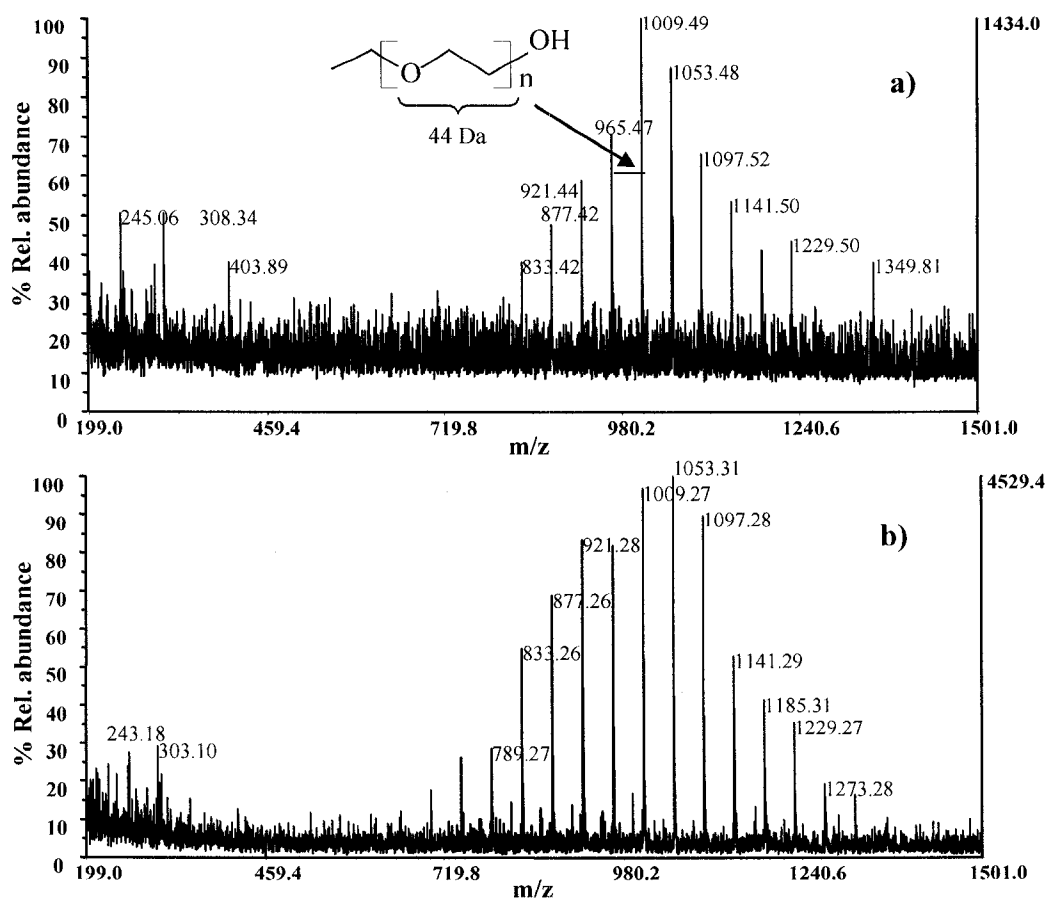


Figure 4.7. a) Matrix-less LDI of polyethylene glycol b) 1 mg mL^{-1} PEG with 2 mg mL^{-1} 1S101F as matrix.

4.3.4 Application to Real World Samples

The utility of LFA for the application of real samples was tested in the analyses of the juice from a small piece (2 g) of macerated cantaloupe, and a solution made from a 500 mg acetaminophen tablet dissolved and diluted it to $\sim 1 \text{ mg mL}^{-1}$ acetaminophen. All solutions were filtered resulting in clear colorless solutions. No extraction or separation was necessary. One- μL aliquots of the solutions were spotted onto dried spots of $1 \mu\text{L}$ of 2 mg mL^{-1} LFA. For cantaloupe, the peak at m/z 203 (Figure 4.8a) was tentatively identified as either glucose or fructose with its potassium adduct at m/z 219. Other peaks, such as m/z 313, 419 and 717 were also present, but they couldn't be readily identified. It is envisioned that identification may be possible through the use of PSD, however, the PSD in our TOFMS equipment was not functioning at that time. For the acetaminophen tablet (Figure 4.8b), the active ingredient was unambiguously identified in its easily protonated form (m/z 152), resulting from protonation of the available basic site in the structure, and its sodiated form (m/z 174); the other peaks present (the polymer cluster) could result from the corn starch, which is normally added to acetaminophen tablets as a binder.

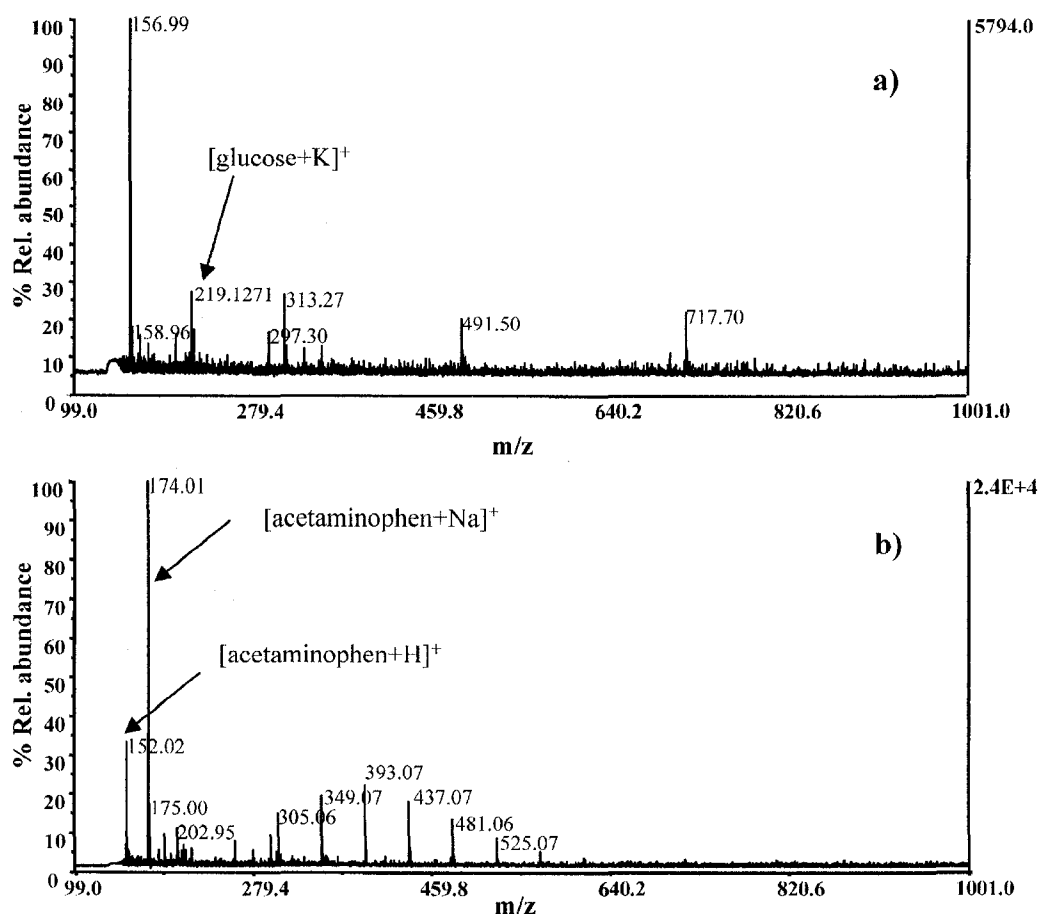


Figure 4.8. MALDI-TOFMS spectra acquired using 2 mg mL⁻¹ LFA as matrix on: a) cantaloupe juice, b) 1 mg mL⁻¹ acetaminophen.

4.4 Conclusion

The potential of aquatic fulvic acid for use as a MALDI matrix has been successfully shown. Particularly interesting is the remarkable performance of locally-isolated fulvic acid as a MALDI substrate material, which was significantly better than that of the IHSS AFA standard. To our knowledge this is the first time that AFA has been investigated and reported as a MALDI matrix. With this breakthrough, the use of both MALDI and fulvic acid could be widened. It is envisioned that with proper optimization, these benign aquatic fulvic acids could have potential for use as universal MALDI

matrices. Of special note is the matrix/analyte role reversal observed at low concentration of fulvic acid with sugars in excess, this behaviour is intriguing and it is undoubtedly worth further investigation as it may be useful in the characterization of fulvic acid by MALDI-TOFMS.

4.5 References

1. Karas M, Hillenkamp F. *Anal. Chem.* 1988; **60**: 2299-2301.
2. Karas M, Bachmann D, Hillenkamp F. *Anal. Chem.* 1985; **57**: 2935-2939.
3. Cohen SL, Chait BT. *Anal. Chem.* 1996; **68**: 31-37.
4. Cohen LH, Gusev AI. *Anal. Bioanal. Chem.* 2002; **373**: 571-586.
5. Dreisewerd K. *Chem. Rev.* 2003; **103**: 395-425.
6. Karas M, Kruger R. *Chem. Rev.* 2003; **103**: 427-439.
7. Schurenberg M, Dreisewerd K, Hillenkamp F. *Anal. Chem.* 1999; **71**: 221-229.
8. Knochenmuss R, Dubois F, Dale JM, Zenobi R. *Rapid Commun. Mass Spectrom.* 1996; **10**: 871-877.
9. Donegan M, Tomlinson AJ, Nair H, Juhasz P. *Rapid Commun. Mass Spectrom.* 2004; **18**: 1885-1888.
10. Guo Z, Zhang Q, Zou H, Guo B, Ni J. *Anal. Chem.* 2002; **74**: 1637-1641.
11. Chen YT, Ling YC. *J. Mass Spectrom.* 2002; **37**: 716-730.
12. Ayorinde F, Garvin K, Saeed K. *Rapid Commun. Mass Spectrom.* 2000; **14**: 608-615.
13. Wei J, Buriak JM, Siudak G. *Nature* 1999; **399**: 243-246.
14. Finkel NH, Prevo BG, Velev OD, He L. *Anal. Chem.* 2005; **77**: 1088-1095.

15. Voivodov KJ, Ching J, Hutchens TW. *Tetrahedron Letters*, 1996; **37**: 5669-5672.
16. Cuiffi JD, Hayes DT, Fonash SJ, Brown KN, Jones AD. *Anal. Chem.* 2001; **73**:1292-1295.
17. Lin YS, Chen YC. *Anal. Chem.* 2002; **74**: 5793-5798.
18. Xu S, Li Y, Zou H, Qiu J, Guo Z, Guo B. *Anal. Chem.* 2003; **75**: 6191-6195.
19. Chen WY, Wang LS, Chiu HT, Chen YC, Lee CY. *J. Am. Soc. Mass Spectrom.* 2004; **15**:1629-1635.
20. Zhang, J, Wang H-Y, Guo Y-L. *Chin. J. Chem.* 2005; **23**:185-189.
21. Ren S, Guo Y. *Rapid Commun. Mass Spectrom.* 2005; **19**: 255-260.
22. Hu L, Xu S, Pan C, Yuan C, Zou H, Jiang G. *Environ. Sci. Technol.* 2005; **39**: 8442-8447.
23. Ren SF, Zhang L, Cheng ZH, Guo YL. *J. Am. Soc. Mass Spectrom.* 2005; **16**: 333-339.
24. Pan C, Xu S, Hu L, Su X, Ou J, Zou H, Guo Z, Zhang Y, Guo B. *J. Am. Soc. Mass Spectrom.* 2005; **16**: 883-893.
25. Pan C, Xu S, Zou H, Guo Z, Zhang Y, Guo B. *J. Am. Soc. Mass Spectrom.* 2005; **16**: 263-270.
26. Ugarov MV, Egan T, Khabashesku DV, Schultz JA, Peng H, Khabashesku VN, Furutani H, Prather KS, Wang HW, Jackson SN, Woods AS. *Anal. Chem.* 2004; **76**: 6734-6742.
27. Black C, Poile C, Langley J, Herniman J. *Rapid Commun. Mass Spectrom.* 2006; **20**: 1053-1060.
28. Leenheer JA, Wershaw RL, Reddy MM. *Environ. Sci. Technol.* 1995; **29**: 393-398.

29. Anderson, Russell JD. *Nature* 1976; **260**: 597.
30. McDonald S, Bishop AG, Prenzler PD, Robards K. *Anal. Chim. Acta.* 2004; **527**: 105-124.
31. Reemtsma T, These A. *Environ. Sci. Technol.* 2005; **39**: 3507-3512.
32. Kujawinski EB, Hatcher PG, Freitas MA. *Anal. Chem.* 2002; **74**: 413-419.
33. Plancque G, Amekraz B, Moulin V, Toulhoat P, Moulin C. *Rapid Commun. Mass Spectrom.* 2001; **15**, 827-835.
34. Kitagawa N. *Anal. Chem.* 2006; **78**: 459-469.
35. Thurman, EM, Malcolm RL. *Environ. Sci. Technol.* 1981; **15**: 463-466.
36. Alimpiev S, Nikiforov S, Karavanskii V, Minton T, Sunner J. *J. Chem. Phys.* 2001; **115**: 1891.
37. Gouw JW, Burgers PC, Trikoupis MA, Terlouw JK. *Rapid Commun. Mass Spectrom.* 2002; **16**: 905-912.
38. Shahgholi M, Garcia BA, Chiu NHL, Heaney PJ, Tang K. *Nucl. Acids Res.* 2001; **29**: 1-10.
39. Distler AM, Allison J. *Anal. Chem.* 2001; **73**: 5000-5003.

CHAPTER 5

Characterization and Comparative Study of Disinfection By-Products

from Suwannee River Natural Organic Matter, Fulvic, Humic Acid and

Selected Model Compounds.

5.1 Introduction

Though other forms of disinfectants, such as ozone, chlorine dioxide, inorganic chloramines and, recently, peracetic acid, are becoming increasingly common, chlorination remains the most widely used form for disinfection of drinking water worldwide.¹⁻⁵ The main advantage of chlorination is its low cost, well-established practices, broad spectrum germicidal potency ($\sim 40 \text{ mg L}^{-1}$ enough to kill enteric disease causing pathogens such as *E. coli*, *Salmonella Typhimurium*, etc.), and ability to provide a stable disinfectant residual (typically $0.2\text{-}1.0 \text{ mg L}^{-1}$).¹ Although the effectiveness of chlorination as a disinfectant is undisputed, its use results in the formation of unintended potentially harmful chemical disinfection by-products (DBPs) generated from reactions with ubiquitous natural or xenobiotic organic compounds and bromide or iodide ions (mainly present in coastal waters).⁴⁻⁸ Some DBPs have been associated with bladder and colorectal cancer, and teratogenic effects, and are therefore of serious concern.^{9,10}

DBPs formation (*i.e.* reaction pathways and end products) remain poorly understood even though three decades now have been dedicated to their study since the discovery of chloroform in drinking water by Rook.² Balancing health risks associated with drinking water disinfection with the risk of pathogen exposure, therefore, remains a significant challenge for the modern drinking water professional. Complicating this picture is the fact that an inordinate number (> 600) of DBPs have been identified to date and many more remain unidentified, moreover, their analysis is not analytically trivial.⁸ Only a few of the known DBPs are routinely quantified and regulated; the primary focus has been on the two most abundant DBPs classes, namely trihalomethanes (THMs) and

haloacetic acids (HAAs).⁴⁻⁸ Other classes of DBPs identified in treated drinking water include: haloacetonitriles, halonitromethanes, haloacetones, haloacids, haloaldehydes, haloacetates, haloamides and other non-halogenated organic compounds. Most of these are considered emerging high priority DBPs by the US EPA, with iodinated and brominated analogs of particular concern as they have been found to exhibit higher toxicity compared to their chlorinated counterparts.^{6,8}

Because of the large number of DBPs that have been identified in drinking water and/or predicted by occurrence predictive models, it is not practical to do epidemiological and toxicological studies for each, thus toxicity and carcinogenicity rankings are normally done using structure-activity relationship models.^{11,12} However, even for relatively well studied DBPs such as MX, which has been known to be a highly potent mutagen for more than a decade, regulations are yet to be in place in most countries.¹³ For instance, occurrence of MX concentrations of as high as 67 ng L⁻¹ and up to 80 ng L⁻¹ have been reported in Finland and Massachusetts water supplies, respectively.^{14,15} A recent study on DBPs in a small Alberta community showed drinking water often exceeded the maximum contaminant level for THMs.¹⁶ Therefore, it must be emphasized that most water treatment plants are yet to comfortably minimize the most abundant, simple and well-understood DBPs, *i.e.*, the THMs and HAAs.

Many other issues complicate the study of DBPs, for example, contrary to the conventional belief that ingestion is the only significant exposure route, research has demonstrated that other exposure routes such as inhalation, dermal adsorption (from bathing, swimming, and other activities) could have varying degrees of importance,

depending on type of DBP in question.^{4,5,8} Furthermore, most of the research on DBPs occurrence has been conducted by sampling treated water from the treatment plant before distribution and yet it is obvious that the nature of DBPs could change with time, for example, by reduction of DBPs by iron oxides in the distribution pipes or by boiling water in homes.^{17,18}

In addition to the aforementioned issues, the DBPs problem cannot be ignored in light of the knowledge that a huge portion of relatively polar, thermally labile and high molecular weight products defy analysis by the gold standard technique, GC-MS and therefore have yet to be characterized. Most of the genotoxicity in water is attributed to this uncharacterized fraction.¹⁹⁻²² Attempts to analyze the often complex mixture by LC-MS is not trivial since resolution into discrete peaks by HPLC has not been possible and continues to be a hot topic of research. A number of other approaches have been used in attempts to characterize this intractable fraction. Of note, electrospray ionization high field asymmetric waveform ion mobility spectrometry mass spectrometry (ESI-FAIMS-MS) has been exploited due to its characteristic high selectivity, sensitivity and gas-phase ion separation capability at atmospheric pressure (760 Torr) and room temperature. ESI-FAIMS-MS is proving useful for trace analysis of highly polar non-target DBPs.²³

DBPs formation is influenced by a variety of water quality parameters including total organic carbon, pH, temperature, contact time, disinfectant dose and residual disinfectant, all of which must be optimized to ensure maximum disinfection and minimal byproduct formation. In effort to comply with stringent regulations of THMs and HAAs, water facilities in North America are increasingly being redesigned to incorporate the use

of nanofiltration in order to remove dissolved organic matter prior to disinfection and to use alternative disinfectants such as ozone, chlorine dioxide, UV and chloramine.^{1,24} Chloramines (monochloramine is highest in germicidal potency), though weaker disinfectants than chlorine and with low persistence in the distribution system, have been shown to produce considerably less chlorinated DBPs than chlorine, probably due to their lower oxidation potentials. Thus chloramines are considered less hazardous in this regard and are a preferred choice, especially as a secondary disinfectant (ozone a common primary disinfectant). However, it is obvious that use of alternative disinfectants such as chloramines is not a panacea to the DBPs problem, since DBPs classes could also be formed when chloramines react with the natural organic matter (NOM).²⁵ The DBPs that would result from chloramination of water containing NOM are not well characterized and thus their study is a critical research gap that warrants increased scrutiny. Nevertheless, it is well accepted that two competing reaction pathways exist with the use of chloramines, auto-decomposition of monochloramine and direct reaction of monochloramine with NOM.^{1,26} Monochloramine has been reported to form dichloroacetaldehydes, though HAA are the primary DBPs formed with dichloroacetic acid being dominant. In the presence of bromide, brominated and mixed halogenation acetic acids have also been reported as other possible DBPs that could be formed. Apart from the DBPs formation, chloramination has been associated with the release of lead into drinking water from distribution system pipes, which could further toxify drinking water.²⁵

Studies by Choi *et al.*²⁷ among others,²⁸ also suggest that *N*-nitrosodimethylamine (NDMA), a non-halogenated and probable human carcinogen – previously a known contaminant in foods and consumer products such as meats, beer, tobacco smoke and rubber products such as baby bottle nipples – could result from the reaction of monochloramine and NOM during drinking water disinfection. A maximum allowed limit for NDMA of 9 ng L⁻¹ has been suggested in Ontario and 10 ng L⁻¹ in California.²⁸ Analysis of NDMA and other related compounds are analytically challenging due to lack of standard analytical methods, difficulty of extraction due to their high polarity, thermal instability, low-molecular weight and occurrence at very low concentrations; thus could require derivatization strategies. Sensitive (nanogram-level) methods of analysis of NDMA have been reported, such as GC-MS-MS with chemical ionization and, recently, HPLC with fluorescence detection of a dansyl amine derivative.²⁹

The complexity of DBPs characterization stems especially from the poorly defined structural nature of their precursors, NOM of which the major components are humic substances (HS). The puzzle is further complicated by the intricate reaction pathways between NOM and disinfectants, such as chlorine. Wu *et al.*,³⁰ as well as other researchers,³¹⁻³³ have postulated that, since chlorine is an electrophile, most DBPs would result from its reaction with the electron-rich moieties such as aromatic structures in NOM. The reaction pathways that have been suggested involve oxidation, radical reactions, electrophilic substitution, *etc.*, ensuing into an abundance of both oxidative and chlorination products, as well as metastable products, all at very low concentrations.³⁰⁻³³ Unravelling the formation mechanisms as well as characterizing all these by-products is

arduous and thus many scientists have begun using hydroxyl and methoxy substituted aromatic compounds as surrogate compounds for HS to study DBPs formation.³⁴⁻⁴⁰ For example, Huixian *et al.*³⁴ has attributed MX formation to the reaction of substituted aromatic aldehydes and amino acids with chlorine. Apart from using model compounds to model formation mechanisms of known DBPs, new DBPs have also been documented from the chlorination of model compounds by quite a number of authors. For example, in the process of searching for MX precursors, Gong *et al.*³⁵ identified 2,2,4-trichloro-5-methoxycyclopent-4-ene-1,3-dione from chlorinated syringaldehyde, which was later detected by GC-MS in chlorinated drinking water. Studies by Rook² showed that flavanoids such as rutin, hesperetin and hesperidin and polyhydroaromatic compounds, especially orcinol and resorcinol, are potential precursors in chloroform formation. It is crucial to note that model compounds must be carefully chosen, and should bear significant functional similarity to known HS structures. Compounds constituting highly substituted aromatic rings, which are inherently prone to electrophilic attack by chlorine, have been found to mimic HS very well in the formation of certain DBPs.³⁴⁻⁴⁰

In our study, Suwannee River fulvic acid (FA), humic acid (HA) and NOM were chlorinated separately and the products were screened using GC-MS. Several DBPs were identified using the National Institute of Standard Testing (NIST) mass spectral library and by interpretation of spectra. Studies on DBPs that result from use of monochloramine are relatively few and so our work also compares the products that are generated from the use of chlorine to those produced using monochloramine in water containing HS. To better understand the formation of haloketones, which were prevalent from both

chlorination and chloramination of NOM, chrysin, quercetin, quercitrin and chlorogenic acid were used as model compounds.

5.2 Materials and Methods

Fulvic acid (1S101F), humic acid (1S101H) and NOM (1R101N) were bought from the International Humic Substances Society (IHSS), St. Paul, MN. Sodium hypochlorite (10-13% free chlorine), ferrous ammonium sulphate, sodium sulphate, sodium sulphite were purchased from Sigma Chemicals Co. (Oakville, ON). *N, N*-diethyl-*p*-phenylenediamine (DPD No. 1) was bought from Palintest House, Kingsway (Team Valley, UK). Amberlites XAD-4 and XAD-8 were purchased from Supelco Ltd, (Bellefonte, PA). Quercetin, quercitrin, chrysin and chlorogenic acid were purchased from Sigma Aldrich (St. Louis, MO). All chemicals were at least of reagent grade and were used without further purification.

5.2.1 Procedure for Chlorination

The procedure used for the chlorination has been shown schematically in Figure 5.1. Briefly, 150-mL of 100 $\mu\text{g mL}^{-1}$ of NOM (1R101N), HA (1S101H) and FA (1S101F) prepared in distilled deionized water were each added separately to 150-mL portions of freshly prepared aqueous sodium hypochlorite containing 100 $\mu\text{g mL}^{-1}$ of free available chlorine; concentration was approximated by titration with ferrous ammonium sulphate with *N, N*-diethyl-*p*-phenylenediamine as an indicator.¹

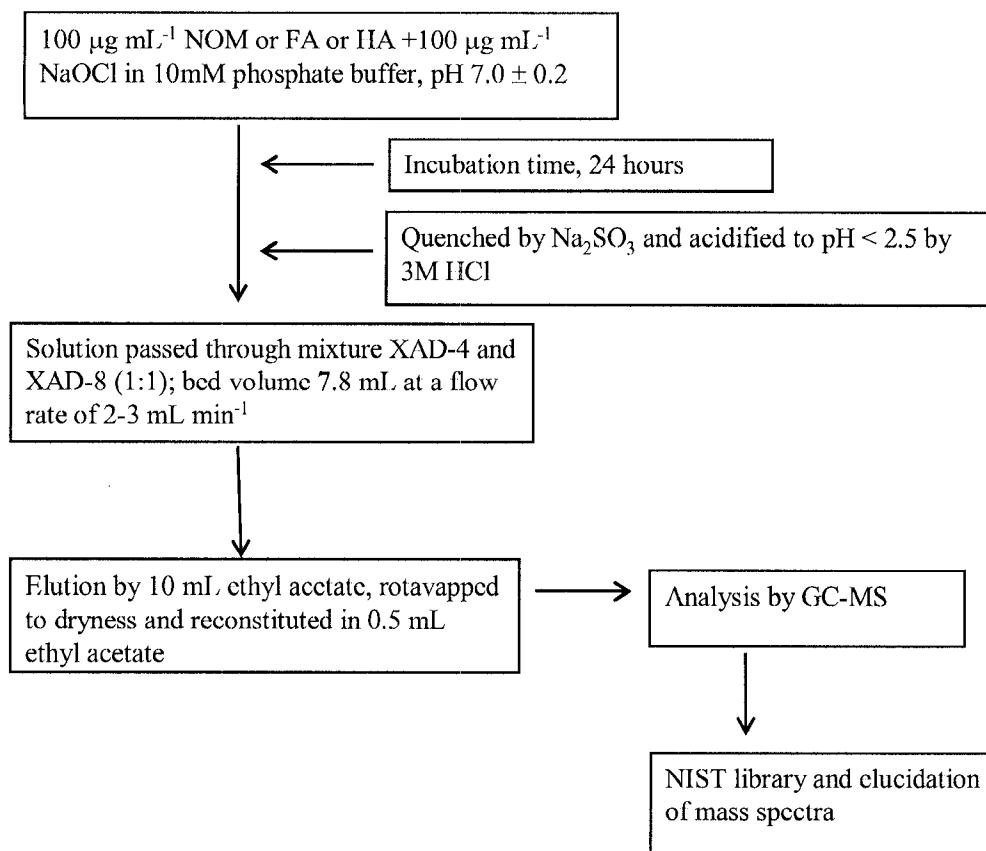


Figure 5.1. Schematic of the chlorination procedure employed.

Chlorination was conducted in 300-mL capacity borosilicate glass bottle equipped with Teflon lined caps. The high NOM and chlorine concentrations and a relatively long contact time (24 hours) used were similar to those employed by Zhang *et al.*¹⁹, which is in effort to maximize the formation of DBPs, making their detection more straightforward. For model compounds, 10 µg mL⁻¹ of quercetin, chlorogenic acid, chrysin, quercitrin were chlorinated for 2 hours and 24 hours. Since chrysin is relatively insoluble in water, 5% acetonitrile was added to assist in solubility. A method blank, prepared by incubating 150-mL of distilled deionized water with 150-mL hypochlorite solution was also run

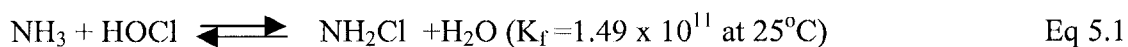
using the aforementioned procedure. All solutions were buffered with phosphate buffer at pH 7.0 (pH at which chlorine is freely available) and incubated at room temperature in the dark to avoid photochemical oxidation of chlorine to ClO_2 . The residual chlorine in solution was reduced to chloride by quenching with an equimolar quantity of sodium sulphite and acidification to pH 2.5 using 3 M HCl. To isolate DBPs, the solution is passed through a column packed with pre-cleaned XAD-4 (macroreticular styrene-divinylbenzene copolymer resins) /XAD-8 (methyl acrylate and trimethylolpropane trimethacrylate copolymer resins) in a 1:1 ratio. The combination of XAD-8 with XAD-4 has been shown to be effective in adsorbing a wide range of organic compounds, including MX.¹³⁻¹⁵

DBPs of interest were eluted using ethyl acetate, and the eluate was dried over anhydrous sodium sulphate, concentrated to 0.5 mL and analyzed by GC-MS and FIA-ESI-MS. Based on the polarity of ethyl acetate, the DBP fraction targeted was moderately polar and so undoubtedly, the higher polar compounds may be retained on the column (in XAD-8 resin). This fraction could be eluted using a more polar and aggressive eluent, perhaps DMF, DMSO, or derivatization prior to isolation on the column might be used. However, the overly hydrophilic compounds might not be retained at all in the column.

5.2.2 Preparation of Monochloramine

A stock solution was prepared by mixing 8.3 g L^{-1} of aqueous ammonia with 5% (v/v) NaOCl, forming a solution with a pH of ~9.0. The formation of monochloramine, dichloramine or trichloramine is pH dependent. The concentration of the prepared monochloramine stock solution was approximated by the DPD titrimetric method.¹ Using

this reliable method, it was ascertained that no detectable residual free chlorine was available in the freshly prepared chloramine solution. The working solution was prepared by diluting the stock solution to 100 mg L⁻¹ monochloramine, which was used to treat 100 µg mL⁻¹ of FA or NOM. The incubation time was 24 hours, which was carried out at room temperature under darkness to reduce the autodecomposition of monochloramine which is inherently unstable. After the 24 hours contact time the monochloramine residue was found to be ~11 mg L⁻¹. Without dechloraminating, the treated solution was extracted as shown in Figure 1. The series of bimolecular reactions that result when chlorine reacts with ammonia are shown below. The formation constant (K_f) for monochloramine attests to its stability and high rate of monochloramine formation is known.^{15, 16}



5.2.3 GC-MS Instrumentation

An Agilent Technologies 5890N Network GC system equipped with 7683 series automatic injector coupled to an Agilent 5973 mass selective detector in EI mode (70 eV) was employed for the analysis. The GC column used was Agilent 19091S-433 HP-5MS (0.25-mm i.d. x 30 m, 0.25-µm film thickness). The carrier gas (He) head pressure was set at 11.99 psi, splitless mode used, injection volume was 2 µL, solvent delay set to 4 min, MSD transfer line was heated at 280 °C, injector temperature was 280 °C. The mass range (35-550 Da) was scanned at 2.76 scans/sec. The oven temperature program was as

follows: initial temperature was set at 40 °C and held for 2 minutes, then ramped at a rate of 4 °C/min to a final temperature of 270 °C, which was held for 10 min.

Changes in the absorption spectra of the precursors were monitored during the chlorination process using a Hewlett Packard 8452A diode array spectrophotometer. . Equal volumes of 10 µg mL⁻¹ of HS, model compounds and chlorine solutions were mixed in a 1 cm quartz cuvette and UV spectra acquired at different times including: 30 s, 10 min, 20 min, 30 min, 40 min and 24 hours.

5.2.4 ESI MS Instrumentation

A Hewlett Packard (HP) 1100 series LC system equipped with a HP 1100 series MSD single quadrupole was employed for the analysis of the chlorinated extract. The mobile phase used consisted of acetonitrile/ water (50:50) and the flow rate was 0.8 mL/min. The acquisition mass range in negative ion mode was 35-1000 Da.

5.3 Results and Discussion

It has been well-documented that most of the DBPs formed that are yet to be characterized are highly polar and/or high molecular weight and thus not amenable to analysis by GC-MS due to their limited volatility and likely lack of thermal stability.¹⁹⁻²² However, attempts to analyze the extracts of chlorinated HS by LC-MS was found to be a challenge because the sample consisted of a complex mixture of compounds. Moreover, even though the extraction procedure used only affords extraction of a fraction of the moderately polar DBPs, the mass spectra obtained consisted of peaks at every mass unit. With the low resolution of quadrupole mass analyzer used, identification of the components was not possible. Figure 5.2 shows the complex mass spectrum obtained by

flow injection (FIA) analysis with ESI detection in the negative mode. Negative ESI is preferred to the positive mode, since it was expected that most of the compounds would be anionic (carboxylic acid groups are the dominant functionalities in HS) and hence are either pre-ionized in solution or are easily ionized in the spray. From the mass spectrum obtained, peaks associated with DBPs were found from m/z 100- ~1000, with most concentrated around m/z 300-500. An attempt to separate the compounds to individual components chromatographically was not effective and only poor separations resulted. Difficulties associated with the characterization of the high-molecular weight DBPs have also been noted by Mincar *et al.*,¹⁹⁻²² who have attempted to use size exclusion chromatography (SEC) with ESI-MS-MS, without much success in unequivocal identification of specific DBPs.

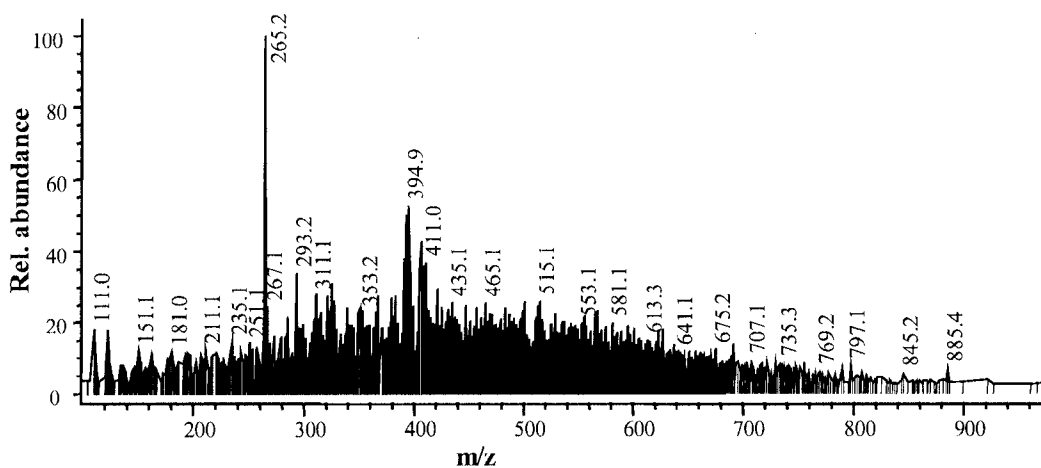


Figure 5.2. FIA-ESI-MS mass spectrum of DBPs extraction from chlorinated NOM.

It is envisioned that by employing MALDI-TOFMS, MALDI-QqTOFMS and nano capillary LC/LC-MS-MS to the characterization of these high MW DBPs, much more could be learnt and further studies in our laboratory are being conducted in these areas. In

addition, the use of FT-ICRMS, which characteristically has high resolving power and has become more common in the analysis of complex mixtures such as humic materials and petroleum, might be the best technique to resolve and identify complex mixtures of DBPs.⁴¹ However, a lack of availability of such expensive instruments is a major obstacle and thus reliance on the widely available GC-MS continues.

The results shown in this chapter are from GC-MS and thus account for only a small portion (mainly semi-volatile and volatile components) of this complex mixture. Nonetheless, the use of GC-MS with electron ionization is favourable because it offers unique advantages that are unmatched by other analytical methods. These include very high sensitivity, availability of the now mature mass spectral libraries, and also well understood fragmentation mechanisms, making it feasible to carry out structure elucidation. The resulting total ion chromatograms (Figure 5.3) were, as expected, so complicated that identifying individual compound has proven to be difficult. From a superficial look at the profiles depicted in the chromatograms, it seems valid that more numerous DBPs result from fulvic acid (chromatogram with more detectable peaks) compared to humic acid, a principle that is well accepted.² A possible explanation for this is that FA is the predominant fraction of HS present in water. Since FA may be more highly functionalized than HA, it may be more prone to attack by chlorine leading to a lot of small DBPs, detectable by GC-MS. Each chromatogram was background corrected and the NIST (> 100,000 spectra) mass spectral library databases (Version 2.0) and elucidation of spectra were used in identification.

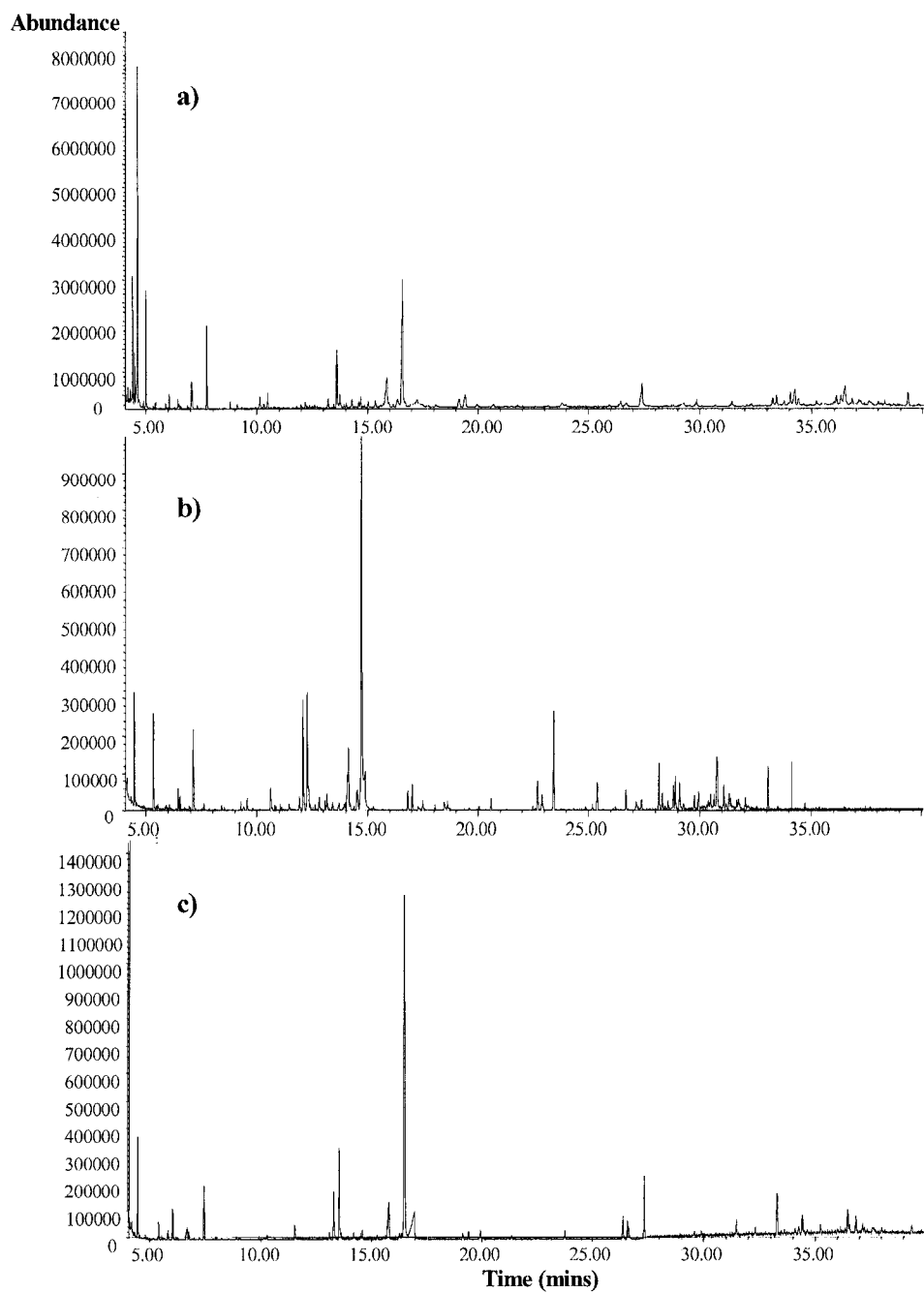


Figure 5.3. Chromatograms of chlorinated Suwannee River a) HA b) FA c) NOM.

Several interesting DBPs that have previously been reported were quickly identified (> 80% match), and are delineated in Table 5.1. Some of their structures and a few selected mass spectra are shown in Figure 5.4 and Figure 5.5, respectively. Most of the DBPs resulting from chlorination of the different classes of NOM (*i.e.*, HA, FA and NOM) were quite similar, which further supports the idea that humic and fulvic acids are structurally similar.

Haloketones (HKs) were the predominant class of DBPs in the fractions studied for all the organic materials chlorinated. Although this class of compounds has been previously reported, it is yet to be regulated, despite the fact that there is compelling evidence that these compounds could be mutagenic. For instance, Curicux *et al.* found that dichloropropanone and trichloropropanone induce primary DNA damage in *E. Coli* and in the *Salmonella Typhimurian* strain TA100.⁴² Haloketones have also been reported by Woo *et al.*¹² as likely to be weakly carcinogenic or carcinogenic toward a single species/target at relatively high doses. It is for this reason that Richardson *et al.*⁴⁻⁸ of the US EPA have recently classified HKs as priority DBPs.

Preliminary results also show that some of the DBPs identified were found to be specific to definite classes of NOM. For example, chloroacetamides (*e.g.*, 2,2,2-trichloroacetamide) and dichloronitromethane were only produced from the chlorination of NOM suggesting that they result from components of NOM other than FA and HA, such as aminoacids. Halogenated furanones like 2-chloro-3-methyl maleic anhydride and 3-chloro-2,5-furandione, as well as non-halogenated furanones (*e.g.*, 3-(1,1-dimethylethyl)- 5-furandione) were mainly detected from NOM and FA, but were not

pronounced in fractions from chlorination of HA. It appears that these furanones mainly result from chlorination of the fulvic acid precursor; however, further studies are underway to ascertain this. The study of furanones is very important because mechanism-based structure activity relationships indicate that they are toxicologically-significant compounds, attributable to structural similarity to the highly potent mutagen MX.¹²

Other DBPs observed with a high degree of confidence that have not been previously emphasized as DBPs included 2,2-dichloro-1,3-cyclopentanedione, 5,5-dichloro-2,2-dimethyl-(1,3)-dioxane-4,6-dione, 2,3-dichloro-2-propenoic acid, chloroacrylic acid, and methyl 3-chloropropenoate. Arguably, the reactions between chlorine and the DBPs precursors proceed via a number of routes, including degradation of HS through oxidation reactions to produce reactive sites followed by substitution reactions to produce the halogenated DBPs.³⁰⁻³³ Evidence for this oxidative pathway is demonstrated by the presence of oxidation products found along with their chlorinated analogues. Some of the oxidative products identified are summarized in Table 5.1. Most of these products are similar to those that result from pyrolysis or thermochemolysis of humic substances; a number of these experiments that have been done in our lab. These products add a new dimension to the understanding of the structural components that make-up HS. For example, butenedioic acid, one of the oxidative products obtained on chlorination (Figure 5.4) was observed as a major chemolysate of HS, and since it was demonstrated (Chapter 3) to be present in humic acid model derived from polysaccharides; this work gives further credence to the hypothesis that HS are

predominantly polysaccharides derived. Furthermore, the consistent presence of furanone derivatives formed on chlorinating HS attests to a polysaccharide origin.

Table 5.1. Some DBPs observed in the chlorination studies of HS

DBPs	Retention time (min)
Haloketones	
1) 1,1,1-trichloro 2-propanone	5.55
2) 1,1,3-trichloro 2-propanone	9.12
3) 1,1,3,3-tetrachloro 2-propanone	11.64
4) 1,1,1,3,3-pentachloro 2-propanone	11.62
Haloacids ♦	
5) 2,3-dichloro-2-propenoic acid	13.40
6) chloroacrylic acid	9.20
Chlorinated furanones ♦	
7) 3-chloro-2,5 furandione	9.33
8) 2-chloro-3-methyl malcic anhydride	10.96
Haloamides	
9) 2,2,2-trichloroacetamide*	16.32
Halonitromethanes	
10) dichloronitromethane*	12.99
Haloester	
11) methyl 3- chloropropenoate	8.04
Other halogenated compounds	
12) pentachloro-cyclopropane ♦	13.09
13) 4,5-dichloro-1,3-dioxolan-2-one ♦	7.56
Oxidative products	
14) 3-methyl-2,5-furandione ♦	8.82
15) 3-(1,1-dimethylethyl)- 5-furandione ♦	8.85
16) propanoic acid	7.60
17) 3-methyl butanoic acid	6.04
18) 4-methyl, 3-penten-2-one	6.37
19) 2-butenedioc acid	6.38
20) 2-methyl-, 2-methylpropyl ester, 2-propanol	11.43
21) 4-hydroxy-4-methyl, 2-pentanone	6.24

* Observed only in chlorinated NOM, ♦ observed in NOM and FA and not in HA

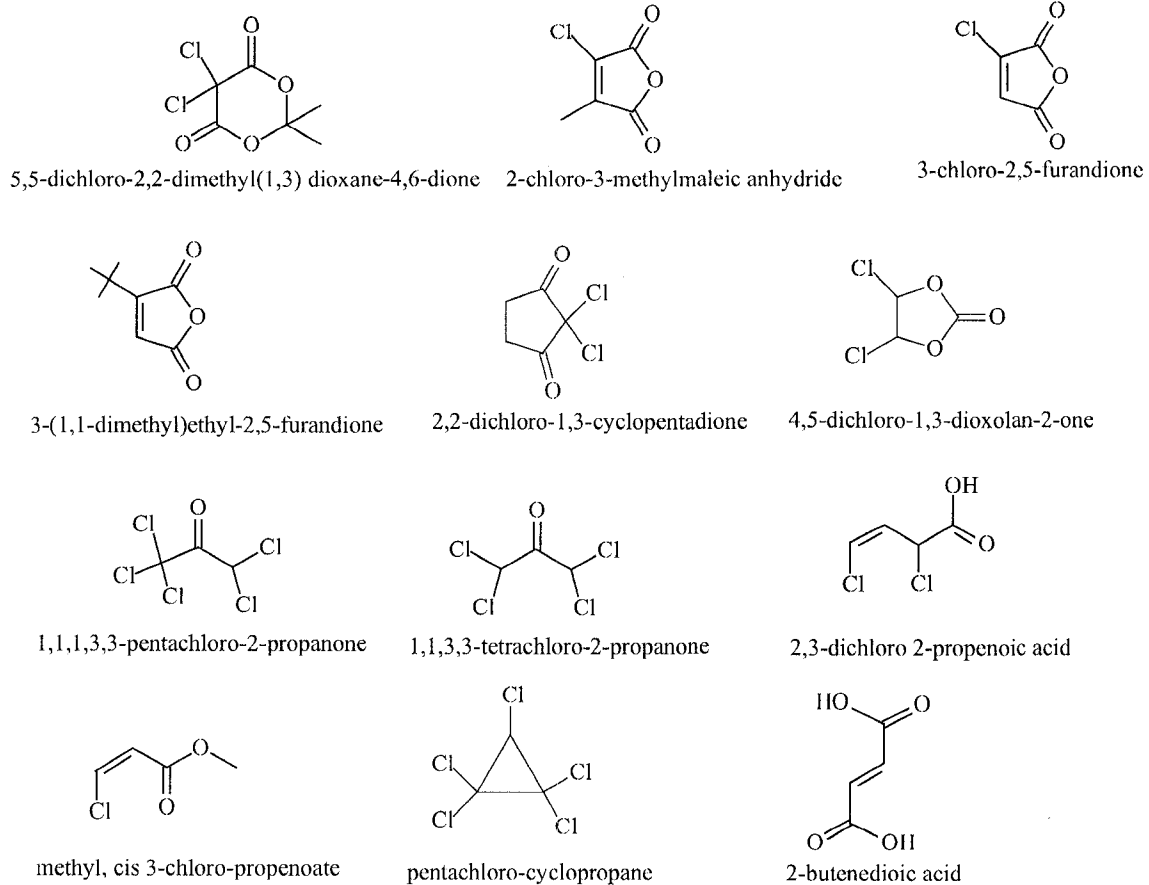


Figure 5.4. Structures of some DBPs observed in the HS chlorination studies.

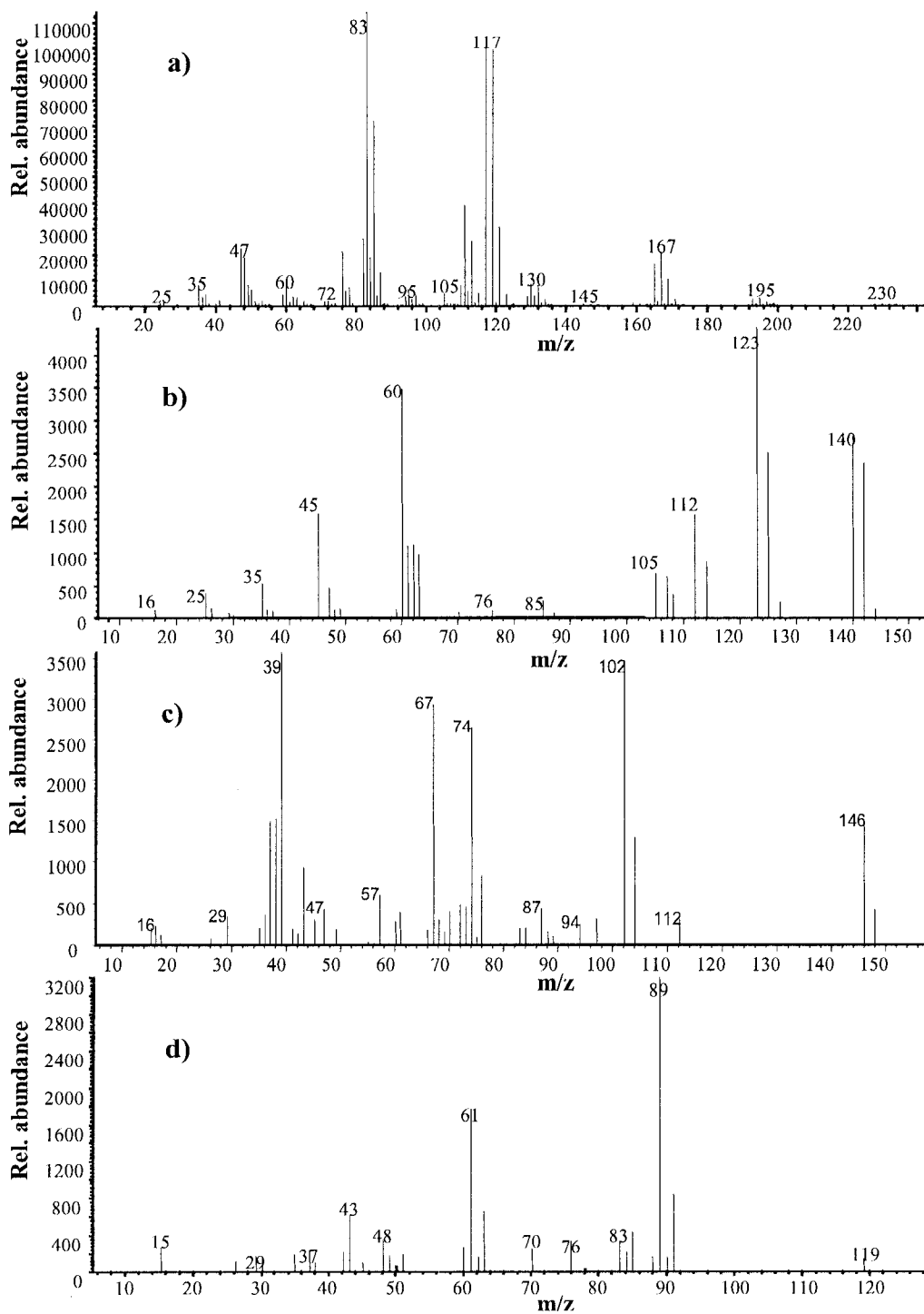


Figure 5.5. Mass spectra of a) 1,1,1,3,3-pentachloro-2-propanone, b) 2,3-dichloro-2-propenoic acid, c) 2-chloro-3-methylmaleic anhydride d) methyl cis-3-chloropropenoate

Similar to chlorination, chloramination of FA and NOM also resulted predominantly in formation of HKs and a few HAAs, which is in agreement with previous research by Wu *et al.*³⁰, who have indicated HAAs are the major monochloramine DBPs.³⁰ However, for chloramination of NOM, the chlorinated DBPs detected were fewer compared to those obtained by chlorination, which is consistent with why increasingly chloramine is replacing chlorine as a disinfectant.

5.3.1 Results from the model compounds

Since HKs were found to be the most prominent DBPs formed by both chlorination and chloramination of the different NOM classes studied, it was imperative to determine their exact precursors. Because the detailed structure of NOM is uncertain, the most practical approach to the study of HKs formation is to use carefully selected model compounds. The model compounds used were quercetin, quercitrin, chrysin, (all flavanoids) and chlorogenic acid, which is a major phenolic compound in coffee and a known anti-oxidant. The rationale used for the model compounds selection is the fact that they are known plant materials and thus expected to be part of the raw materials that lead to the formation of HS. Chlorogenic acid and quercitrin structures also have a unique combination of aromatic and sugar moiety, and similar structural association has been suspected for HS, making them suitable surrogate compounds.² Chlorination of quercetin, quercitrin and chrysin (structures shown in Figure 5.6) resulted in the formation of some of the HKs, which had previously been obtained with chlorinated NOM including 1,1,3,3-tetrachloro-2-propanone and 1,1,1,3,3-pentachloro-2-propanone and 1,1,1,3,3,3-hexachloro-2-Propanone. However, for chlorogenic acid, none of the HKs or any other

chlorinated species were identified. From these results, we speculate the precursor site responsible for the HKs formation is the *meta*-dihydroxy substituted ring present in the

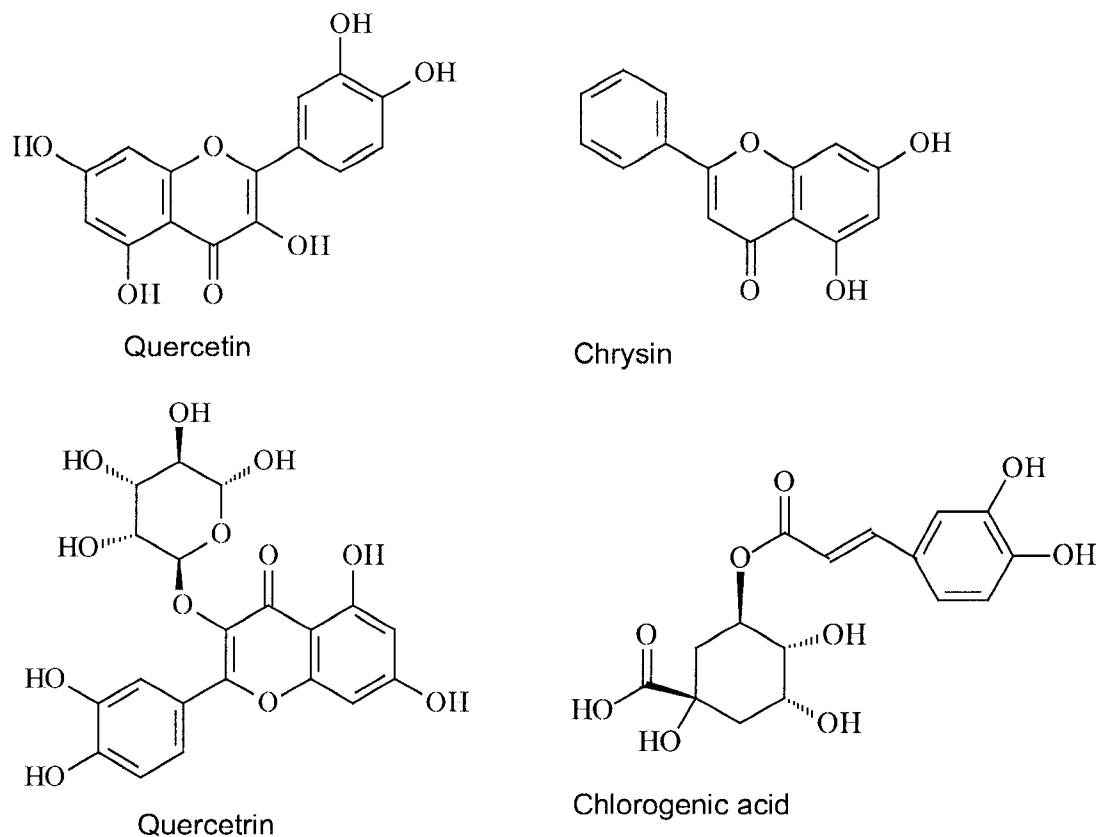


Figure 5.6. Structures of model compounds tested.

flavanoids and absent in chlorogenic acid, which contains the *ortho*-dihydroxy substituents instead. These results are in agreement with previous studies on chlorination and chloramination of various aromatic phenols such as resorcinol, phoroglucinol, orcinol, *etc.*, which were found to produce large amounts of chloroform and chloroacetic acid, attributed to chlorine attack at the *meta*-dihydroxy substituted ring.^{2,36,39,40} The formation of chlorinated compounds from hydrogen substitution of the activated carbon

in β -diketone, is also evident from the formation of 2,2-dichloro-1,3-cyclopentadione and 5,5-dichloro-2,2-dimethyl (1,3) dioxane-4,6-dione detected in chlorinated NOM (Figure 5.3).

5.3.2 UV-Vis Spectrophotometric Studies

Correlating the changes in UV absorption of NOM or model compounds being chlorinated and DBPs formation has been found to be a practical and reliable approach and has further been used to probe the mechanisms of the underlying reactions.³²

Although the intent of our research was to screen for new DBPs on chlorination of NOM and its component classes rather than to undertake an in depth mechanistic study of the chlorination process, preliminary studies on monitoring the reaction of NOM and model compounds with chlorine using UV-vis spectrophotometry was attempted. This was done by mixing NOM and model compounds solutions with hypochlorite solution in a 1-cm glass cuvette as described earlier and acquiring UV-vis spectra at different times in the reaction process. Figure 5.7 shows representative UV spectra of NOM, chlorogenic acid and chrysin before chlorination and at 30 seconds and 30 minutes after chlorination. With longer reaction times (>30 min), only very minimal changes in the spectra were observed and no significant information could be deduced and thus are not shown in the spectra. As shown in the UV spectra on chlorination of chrysin (spectra shown in Figure 5.7a, which was very similar to quercetin), there was a dramatic bathochromic (shift to longer wavelength) and hyperchromic shift (increased intensity) of the peak at ~270 nm to ~300 nm immediately on chlorination. The above mentioned spectral shift may be as a result of

the α -substitution sensitive $n \rightarrow \pi^*$ transition (associated with ketones), which occurs in the range of 270-300 nm and thus has been exploited as a diagnostic band for monitoring chlorination incorporation reactions.^{31,32,44} This observed spectral shift can be attributed to chlorine (auxochrome) incorporation by substitution at a carbon atom at the *ortho* position with respect to both phenolic hydroxyl substituents in the chrysin (believed to be the site most prone to an electrophilic attack). Based on the mechanism proposed by Rook,² (mechanism shown in Figure 1.8) chlorine substitution subsequently leads to the formation of a β -diketone as an intermediate. The peak (~ 300 nm) gradually reduced in intensity (hypochromic shift), which could be associated with the breakdown of the aromatic ring as a result of oxidation and/or hydrolysis reactions with possible substitution reactions as well. Similarly, with NOM, although the spectrum (Figure 5.7b) has no discrete minima or maxima, due to the large number of double bonds that are conjugated with carbonyl moieties as well as numerous alkyl substituents— the $\pi \rightarrow \pi^*$ transitions almost completely obscure the diagnostically valuable $n \rightarrow \pi^*$ band— there is weak evidence on initial chlorination that similar spectral shifts described for chrysin may occur.³⁰⁻³³ The bathochromic and hyperchromic spectral shifts discussed were not clearly evident for chlorogenic acid (Figure 5.7c), which could mean oxidation rather than substitution is the dominant reaction pathway, and could further explain why no chlorinated byproducts were detected. It was also apparent that the reaction between chlorogenic acid with chlorine was extremely rapid as attested by the immediate disappearance of the brown color of chlorogenic acid and the large hypochromic shifts shown in the UV Spectra in comparison to other compounds evaluated.

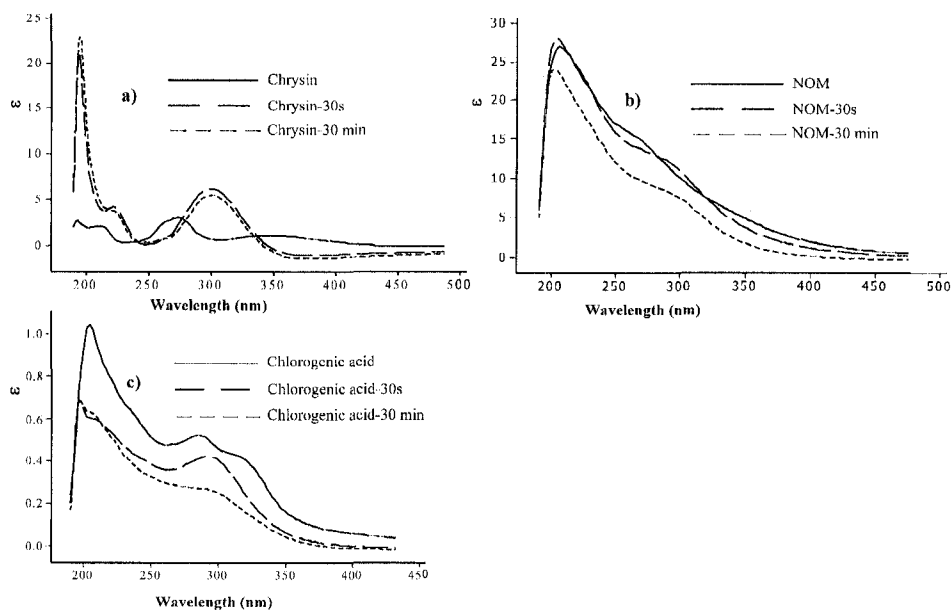


Figure 5.7 UV-Vis spectra of chlorine reaction with a) NOM, b) chrysin, and c) chlorogenic acid, ϵ is the molar (mass for NOM) absorptivity coefficient.

5.4 Conclusion

After three decades, the DBPs are an old DBPs problem but remain a legitimate research area with so much information regarding their formation, occurrence and effects on human health still nebulous. In this study, several rarely reported DBPs, including a number of furanone derivatives and haloketones were identified from chlorination and chloramination of Suwannee River NOM, HA and FA. From the chlorination studies using chrysin, quercetrin and quercetin as model compounds, a strong candidate for a structural precursor site for the formation of HKs was identified in the aromatic *meta*-dihydroxy ring component. The selected model compounds were also confirmed to be

suitable surrogates for NOM because of their remarkable similarity to the byproducts formed on chlorination. Although preliminary UV spectroscopy results show some similarity in response to chlorination of NOM and model compounds, further spectroscopic study of the reaction pathway would be essential in effort to establish the exact mechanism of action for the formation of haloketones. On-going studies in our lab also include analysis of other polar and high molecular weight byproducts formed from the reaction of model compounds and NOM with chlorine using ESI-MS-MS, which could help identify the thermally labile components.

In our mass spectral elucidation of the ethyl acetate extract of the chlorinated NOM, numerous peaks were observed with fragmentation patterns characteristic of carbonyls, m/z : 43, 57, 71, 85, suggesting dominance of the presence of carbonyl groups and hence the need to carry out carbonyl derivatization to enhance their detection. In addition, most water treatment plants use ozone as a primary disinfectant, which is known to form a plethora of carbonyl containing byproducts on reaction with organic matter.⁴⁵ Therefore subsequent studies in our laboratory have been tailored towards developing methodologies for analyzing carbonyls and dicarbonyl compounds by derivatization and analysis by MALDI-TOFMS.

5.5 References

1. Clifford WG. *The handbook of chlorination and alternative disinfectant* (4th Ed). J. Wiley publishing: New York, Toronto, 1999: 212-250.
2. Rook JJ. *Environ. Sci. Technol.* 1977; **11**: 478-482.

3. Monarca S, Richardson SD, Feretti D, Grottolo M, Thruston AD Jr, Zani C, Navazio G, Ragazzo P, Zerbini I, Alberti A. *Environ. Toxicol. Chem.* 2002; **21**: 309–318
4. Richardson SD, Ternes TA. *Anal. Chem.* 2004; **76**: 3346-3350.
5. Richardson SD, Ternes TA. *Anal. Chem.* 2006; **78**: 4021-4046.
6. Richardson SD, Thruston AD, Rav-Acha C, Groisman L, Popilevsky I, Juracv O, Glezer V, Mckague AB, Plcwa MJ, Wagner ED. *Environ. Sci. Technol.* 2003; **37**: 3782-3793.
7. Richardson SD, Thruston AD.
http://www.epa.gov/athens/publications/EPA_600_R02_068.pdf. 2002: 11
8. Krasner SW, Weinberg HS, Richardson SD, Pastor SJ, Chinn R, Scimienti MJ, Onstad GD, Thruston AD. *Environ. Sci. Technol.* 2006; **40**:7175-7185.
9. Cordier S, Jaakkola JJK, King WD, Lynch CF, Porru S, Kogevinas M. *Epidemiology*, 2004; **15**:357-367.
10. King WD, Dodds L, Armson BA, Allen AC, Fell DB, Nimrod C. *J. Exposure Anal. Environ. Epidemiol.* 2004; **14**:466-472.
11. Sadiq R, Rodriguez MJ. *Sci. Total Environ.* 2004; **321**: 21-46.
12. Woo YT, McLain JL, Manibusan MK, Dellarco V. *Environ. Health Perspect.* 2002; **110**: 75-87.
13. Kronberg L, Holmbom B, Reunanen M, Tikkanen L. *Environ. Technol.* 1988; **22**: 1097.
14. Suzuki N, Nakanishi J. *Chemosphere*, 1995; **30**: 1557-1564.
15. Wright JM, Schwartz J, vartiainen T, Maki-Paakkanen J, Altshul L, Harrington JJ, Dockery DW. *Environ. Health Perspect.* 2002; **110**: 157-164.

16. Charrois J W A, Graham D, Hrucey SE, Froese K L. *J. Toxicol. Environ. Health., Part A*, 2004; **67**: 1797-1803.
17. Krasner SW, Wright JM. *Water res.* 2005; **39**: 855-864.
18. Chun CL, Hozalski RM, Arnold WA. *Environ. Sci. Technol.* 2005; **39**: 8525-8532.
19. Zhang X, Mincar RA. *Environ. Sci. Technol.* 2002; **36**: 4033-4038.
20. Zhang X, Mincar RA, Guo Y, Hwang CJ, Barret SE, Ikeda K, Shimizu Y, Matsui S. *Water Res.* 2004; **38**: 3920-3930.
21. Zhang X, Mincar RA, Barrett SE. *Environ. Sci. Technol.* 2005; **39**: 963-972.
22. Zhang X, Mincar RA. *Water Res.* 2006; **40**: 221-230.
23. Suktan J, Gabryclski W. *Anal. Chem.* 2006; **78**: 2905-2917.
24. Chellam S, Krasner SW. *Environ. Sci. Technol.* 2001; **35**: 3988-3999.
25. Renner R. *Environ. Sci. Technol.* A-pages, 2004; **38**: 342A-343A.
26. Kanniganti RJD, Johnson LM, Ball MJ. *Environ. Sci. Technol.* 1992; **26**:1998.
27. Choi J, Valentine RL. *Water Res.* 2002; **36**: 817-824.
28. Mitch WA, Sharp JO, Trussell RR, Valentine RL, Cohen LA, Sedlak DL. *Environ. Eng. Sci.* 2003; **20**: 389-404.
29. Cha W, Fox P, Nalinakumari B. *Anal. Chim. Acta* 2006; **566**: 109-116.
30. Wu WW, Chadik PA, Delfino JJ. *Environ. Toxicol. Chem.* 2003; **22**: 2845-2852.
31. Korshin GV, Kumke MU, Li CW, Frimmel FH. *Environ. Sci. Technol.* 1999; **33**: 1207-1212.
32. Li CW, Benjamin MM, Korshin GV. *Environ. Sci. Technol.* 2000; **34**: 2570-2575.
33. White DM, Garland D S, Narr J, Woolard CR. *Water Res.* 2003; **37**: 939-947.
34. Huixian Z, Zirui Y, Junhe L, Xu X, Jinqi Z. *Water Res.* 2002; **36**: 4535-4542.

35. Gong H, You Z, Xian Q, Shen X, Zou H, Huan F, Xu X. *Environ. Sci. Technol.* 2005; **39**: 7499-7508.
36. Lu J, Benjamin M M, Korshin G V, Gallard H. *Environ. Sci. Technol.* 2004; **38**: 4603-4611.
37. Boyce SD, Hornig JF. *Environ. Sci. Technol.* 1983; **17**: 202-211.
38. Yang X, Shang C. *Environ. Sci. Technol.* 2004; **38**: 4995-5001.
39. Heasley VL, Alexander MB, DeBoard RH, Hanley JC, MacKee TC, Wadley BD, Shellhamer DF. *Environ. Toxicol. Chem.* 1999; **18**: 2406-2409.
40. Chang EE, Chiang PC, Chao SH, Lin YL. *Chemosphere*, 2006; **64**: 1196-1203.
41. Marshall AG, Rodgers RP. *Acc. Chem. Res.* 2004; **37**: 53 -59.
42. Curieux F, Marzin D, Erb F. *Mut. Res.* 1994;341:1
43. Matsuda H, Ose Y, Nagase H, Sato T, Kito H, Sumida K. *Sci. Total Environ.* 1991; **103**: 141-149.
44. Lambert JB, Shurvell HF, Lightner DA, Cooks RG. *Organic Structural Spectroscopy*. Prentice-Hall, Inc: New Jersey, 1998: 274-289.
45. Richardson SD, Thruston AD, Coughran TV, Chen PH, Collette TW, Floyd TL. *Environ. Sci. Technol.* 1999; **33**: 3368-3377.

CHAPTER 6

Rapid On-Plate and One-Pot Derivatization of Carbonyl Compounds for Enhanced Detection by Reactive Matrix LDI-TOFMS Using the Tailor-Made Reactive Matrix, 4-Dimethylamino-6-(4-Methoxy-1-Naphthyl)-1,3,5-Triazine-2-Hydrazine (DMNTH).

A version of this chapter has been published. Mugo SM, Bottaro CS. Rapid On-Plate and One-Pot Derivatization of Carbonyl Compounds for Enhanced Detection by Reactive Matrix LDI-TOFMS Using the Tailor-Made Reactive Matrix, 4-Dimethylamino-6-(4-Methoxy-1-Naphthyl)-1,3,5-Triazine-2-Hydrazine (DMNTH).

J. Mass Spectrom. On-line Dec. 2006.

6.1 Introduction

Many of the pollutants that compromise the quality of air and drinking water are compounds with carbonyl moieties. Consequently, carbonyl compounds have attracted the interest of environmental chemists, toxicologists, pharmaceutical researchers, and biotechnologists, among others.¹⁻⁹ Though a number of techniques have been developed for the determination of these compounds, the polar nature of carbonyls complicates the analysis by making isolation from water difficult and analysis by methods that use gas chromatography (GC) challenging.^{1,2} Further, direct application of the available ionization methods (*e.g.* atmospheric pressure ionization) for mass spectrometry can be hampered by the fact that these compounds are not easily protonated or deprotonated to form charged species.⁴ The most common technique that has been applied to circumvent these problems entails derivatization of carbonyl groups with pentafluorobenzylhydroxylamine (PFBHA) to form oximes, thereby imparting nonpolar character to carbonyl containing molecules, aiding extraction from aqueous substrates and facilitating subsequent analysis by GC-MS. Nonetheless, this method has only led to the identification of a few polar disinfection by-products (DBPs), which are amenable to GC-MS.^{1,2,5} Another complementary technique, though typically less sensitive than the aforementioned method, involves the formation of hydrazones through derivatization of carbonyls with 2, 4-dinitrophenylhydrazine (DNPH) followed by analysis using liquid chromatography mass spectrometry (LC-MS).¹⁻⁴ Although these two approaches have gone a long way in solving the problem of carbonyl analysis, they have limitations such as poor detection limits, poor reaction kinetics, and time-consuming concentration procedures. As well, analysis of compounds with multiple carbonyl groups using PFBHA

for GC-MS can be a challenge due to a decrease in volatility with each subsequent addition of a bulky derivatizing group.¹⁻⁷

In addition to applications in GC and LC, derivatization with commercially-available reagents like DNPH have also been used to improve detection limits for a range of carbonyl compounds (aldehydes, ketones, carboxylic acids, *etc.*) using fluorescence and electrochemical detectors, as well as mass spectrometry.⁸⁻¹¹ However, though derivatization for the purpose of enhancing detection by MALDI-TOFMS has been undertaken, it is not yet common place.

Volmer *et al.*¹² have coined the term "reactive matrix" to describe rapid derivatization of small molecules with functionalities that assist in ionization and detection by MALDI-MS; in their seminal work they successfully used DNPH to analyze corticosteroids. Lattova and Perreault¹³ used a similar approach for the analysis of saccharides by HPLC-UV, HPLC-MS and MALDI-MS using phenylhydrazine to form the saccharide hydrazone. By exploiting this principle and tailoring derivatizing agents to meet specific criteria, analyses can be made selective and sensitive.

The features of an ideal derivatizing agent for mass spectrometric detection have been delineated by Cartwright *et al.*: it should be easily synthesized, pre-charged or easily protonated, chemically-stable, and should react rapidly and quantitatively with analyte molecule.¹¹ Kempter *et al.*¹⁴⁻¹⁶ advanced the development of what they called "tailor-made" derivatizing agents by combining selective reactive functionality, stability, and good spectroscopic properties in one compound. They synthesized the novel derivatizing agent, 4-dimethylamino-6-(4-methoxy-1-naphthyl)-1,3,5-triazine-2-hydrazine (DMNTH)

for determination of carbonyl compounds by HPLC with detection by UV, fluorescence and MS.

In addition to its desirable spectroscopic properties, the presence of the dimethylamino functionality in DMNTH makes it readily ionizable by positive atmospheric-pressure chemical ionization (APCI).¹⁶ DMNTH has been exploited for the determination of polar carbonyl disinfection by-products (DPBs) by LC-APCI-MS at ng L⁻¹ levels with no preconcentration or extraction.¹⁴⁻¹⁸ Liu *et al.*¹⁷ have also successfully optimized the parameters necessary for capillary electrochromatography in the separation of DMNTH-derivatized carbonyl compounds, which further widens the applicability of this compound. Adding to the many positive features of DMNTH, its reaction with aldehydes and ketones has been found to be rapid (< 30 min), enhancing the efficiency of analyses. Other similar reagents for carbonyl derivatization often require an hour or more before the reaction is sufficiently complete. Based on the experience of others using DNPH as a reactive matrix for MALDI and the integration of a number of key features in DMNTH, we envisioned that DMNTH could be employed as a reactive matrix for analysis of carbonyls by MALDI-MS and it seems this approach could surmount a number of limitations currently facing MALDI-MS for the analysis of small molecules.

Since the initial development of MALDI-MS in 1988 by Karas and Hillenkamp,¹⁹ and Tanaka,²⁰ its soft ionization properties have led to widespread application in the analysis of fragile and non-volatile molecules, especially biomolecules and synthetic polymers. Recently, efforts have been made to extend its strengths (*i.e.* sensitivity, versatility, high-throughput, relatively high tolerance for impurities, and ease of sample preparation) to the analysis of small molecules. The application of MALDI for relatively

small molecules (< 500 Da), however, is impeded by the presence of interfering matrix peaks in the low mass range and irreproducible signal intensities due to non-homogeneous co-crystallization of analyte with the matrix.²¹⁻²⁷

A variety of techniques have been explored in the effort to overcome obstacles that hinder the application of MALDI to small molecule analysis. One tactic involves matrix suppression effects (MSE) through the use of surfactants or by striking a delicate balance of matrix/analyte ratios. In some instances, MSE approaches have been successful but the mechanism of their action is poorly understood and thus difficult to predict and control.^{21,22} Additionally, the use of surfactants for matrix suppression can lead to suppression of analyte ionization as well, negatively impacting the signal-to-noise ratio (S/N).

Another promising approach has been to develop new specialized matrices, usually compounds with inherently low volatility or of high molecular weight that produce fewer peaks in the low mass range than conventional matrices. Conducting polymers, *e.g.* polythiophenes,²³ and carbon nanotubes²⁴ are finding utility in this field, but metallic impurities present in some nanotube samples can be detrimental to the performance of TOFMS. Other matrices being developed include inorganic matrices such as porous silicon powder and silica gel particles.^{25,26} Additionally, the use of selected reaction monitoring (SRM) has been reported as a convenient approach to improve S/N ratio and reduce matrix interference and thus has been demonstrated to be effective for small molecule quantitation.²⁷

On the other hand, the use of analyte derivatization with a high mass, easily ionized reagent (reactive matrix), which selectively tags the analyte of interest, is a

pragmatic solution to matrix interferences. This increases the molecular weight of the ion of interest moving it out of the region that presents the greatest likelihood of interference and, hence, reduces matrix interference that usually limits the sensitivity of analysis. Also, some small molecular weight compounds, which are too volatile under the high vacuum of the mass spectrometer, can be rendered less volatile by derivatization and thus amenable to analysis. Moreover, derivatization introduces a measure of selectivity to the analysis by introducing photoactive moiety only to molecules with the appropriate target functional group. This protocol has been employed successfully in the analysis of a variety of small molecules²⁸⁻³¹ (e.g. small amine molecules, carboxylic acids and neutral oxosteroids) and offers considerable potential in analysis of small molecules by MALDI-MS.

DMNTH has been employed in our work as a derivatizing agent for carbonyls to eliminate the need for a separate matrix in MALDI-MS; it has been noted for its excellent spectroscopic properties such as absorption in the UV region and ease of ionization under acidic conditions. Our research introduces a simple, rapid and sensitive method for the analysis of small carbonyl compounds by DMNTH RM-LDI-TOFMS, with both one-pot and rapid on-plate derivatization approaches yielding good results. The use of this reactive matrix provides a route to better reproducibility for MALDI-MS as the resulting spots are quite homogeneous. This is an advantage over ordinary MALDI, which tends to yield inhomogeneous matrix sample spots due to inconsistent co-crystallization of matrix and sample leading to significant variation in the ion intensities.

6.2 Materials and Methods

Cyanuric chloride, 1-methoxynaphthalene, aluminium chloride, hydrochloric acid, dimethyl amine, potassium carbonate, hydrazine hydrate and analytical grade solvents (acetonitrile, toluene, 1-4 dioxane) were purchased from Sigma Aldrich (Oakville ON, Canada) in analytical grade or higher and used without further purification. Milli-Q-organic free water was used throughout.

DMNTH was synthesized as described by Kempter *et al.*¹⁴, the synthetic scheme is summarized in Figure 6.1. The carbonyl compounds employed in this work include furfural, cyclohexanone, cyclopentanone, methyl-glyoxal, 4-hydroxybenzaldehyde, benzophenone, 4-hydroxyacetophenone, 4-methoxybenzaldehyde, trans-cinnamaldehyde and acetaldehyde all from Sigma Aldrich (Oakville ON, Canada). A Molson Canadian Premium Lager beer was bought locally for use in a study of the effect of real sample matrices on the efficacy of the method.

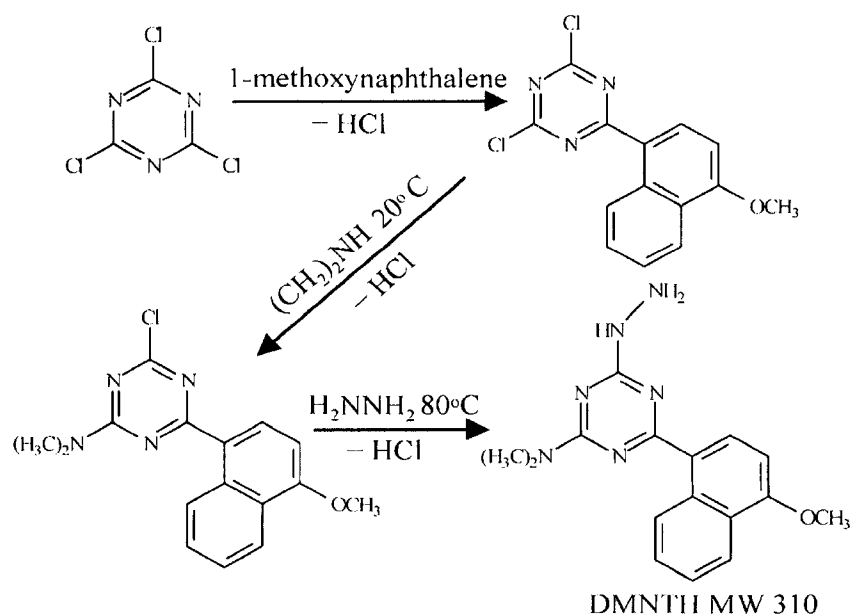


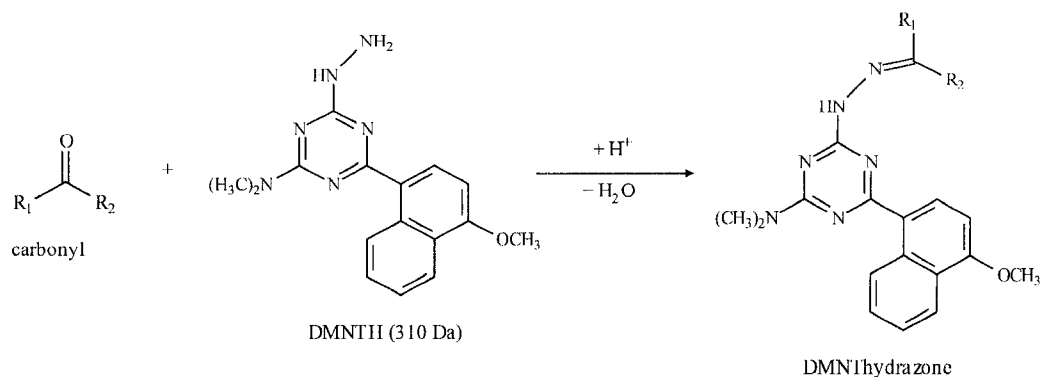
Figure 6.1. Synthesis of DMNTH.¹⁴

6.2.1 Preparation of the DMNTH and Analyte Solutions

A stock solution of 8.05 mmol L^{-1} DMNTH was prepared by dissolving the pure solid in acetonitrile/ water containing 0.1 M hydrochloric acid (4:1, v/v). Various concentrations ($0.1\text{-}100 \text{ }\mu\text{g mL}^{-1}$) of target carbonyl compound solutions were prepared in acetonitrile/water (1:1, v/v).

6.2.2 Derivatization Procedure

Two derivatizing procedures were adopted. In the first method (one-pot derivatization), $100 \text{ }\mu\text{L}$ of the DMNTH solution and $100 \text{ }\mu\text{L}$ of the carbonyl sample solution were combined in a micro-centrifuge vial, mixed by vortex, then allowed to react at room temperature for 30 minutes, the time found to be sufficient for completion of reaction for most carbonyl compounds. A $0.5\text{-}\mu\text{L}$ aliquot of the sample/DMNTH mixture was then deposited on a stainless steel sample stage, dried under ambient conditions, and analyzed using LDI-TOFMS. The second much simplified method involved on-plate derivatization, where $0.5 \text{ }\mu\text{L}$ of the DMNTH solution was spotted on the sample stage, then $0.5 \text{ }\mu\text{L}$ of the sample solution was deposited on the DMNTH spot; with drying allowed after each deposition. The resulting spot was then analyzed by LDI-TOFMS and the performances of the two techniques evaluated. Figure 6.2 shows the structures of the carbonyls studied and delineates the formation of the hydrazones that resulted on derivatization.



Analyte	Analyte structure	R-Substituents in DMNThydrazone	[M+H] ⁺
4-methoxybenzaldehyde		R ₁ = H R ₂ =	429
4-hydroxyacetophenone		R ₁ = CH ₃ R ₂ =	429
4-hydroxybenzaldehyde		R ₁ = H R ₂ =	415
methylglyoxal		R ₁ = CH ₃ , R ₂ = CH ₃ CO	365
acetaldehyde	CH ₃ COH	R ₁ = H R ₂ = CH ₃	337
<i>trans</i> -cinnamaldehyde		R ₁ = H R ₂ =	425
2-furaldehyde		R ₁ = H, R ₂ =	389
cyclopentanone		R ₁ = H R ₂ =	377
benzophenone		R ₁ , R ₂ =	460

Figure 6.2. General scheme for reaction of DMNTII with carbonyl compounds to produce DMNThyrazones.

6.2.3 Synthesis of the Internal Standard

Furfural DMNThydrazone was synthesized for use as an internal standard. Furfural (0.982 mmol) was added to a DMNTH solution (2.142 mmol) in 20 mL of 1:1 acetonitrile and water. The mixture was stirred overnight and then filtered. The product was obtained with satisfactory purity, confirmed by ^1H NMR. Its ionization efficiency was tested by LDI-TOFMS, which showed a “clean” spectrum (Figure 6.3a) of only peaks associated with the protonated furfural DMNThydrazone, with the base peak at m/z 389.

Another approach investigated was to introduce furfural internal standard into the reaction mixture, leaving it to react with DMNTH with the other analytes, hence forming the furfural DMNThydrazone *in-situ*. The reaction of furfural with DMNTH was fast, considered to have gone to completion within 15 min, and the ionizability of the hydrazone was very efficient as seen in Figure 6.3b.

6.2.4 MALDI-MS Instrumentation

An Applied Biosystems DE-RP TOFMS equipped with high performance nitrogen laser (337 nm) and reflectron was used. Spectra from 30 laser shots were acquired in reflectron mode and averaged. The acquisition mass range in positive ion mode was 100-700 Da. Other instrumental parameters included extraction delay time: 200 nsec, grid voltage: 74.4%, accelerating voltage: 20kV, and mirror voltage ratio: 1.12.

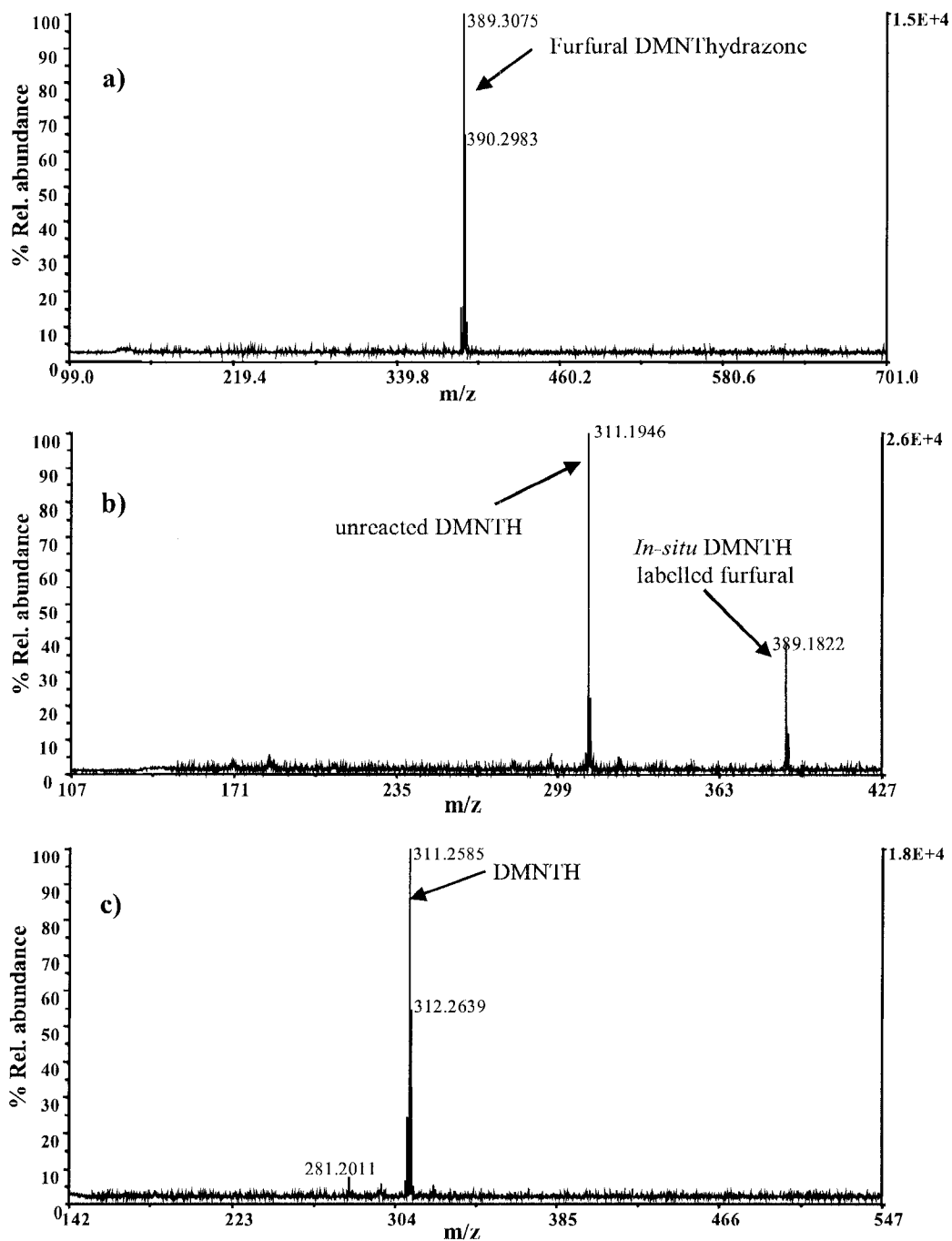


Figure 6.3. RM-LDI-TOFMS spectra of; a) synthesized internal standard, furfural DMNThydrazone, b) Furfural labelled *in-situ*, c) LDI-TOFMS spectrum of 0.161 mM DMNTH.

6.3 Results and Discussion

The appropriate concentration of DMNTH to be employed required optimization since DMNTH had to be in excess to ensure that the analyte would react quantitatively in this acid catalyzed reaction. A range of concentrations (16.1 – 0.0161 mM) were tried, and it was found that for analyte concentrations below the $\mu\text{g mL}^{-1}$ level, 0.161 mM DMNTH in 0.1 M HCl/acetonitrile (1:4, v/v) was most effective for individual analytes. However, for the analysis of carbonyl mixtures, an 8.05 mM DMNTH solution was used to ensure DMNTH was in molar excess.

The LDI-TOF mass spectrum of DMNTH is shown in Figure 6.3c. The DMNTH was found to be sufficiently stable and well ionized by LDI at low laser intensity (~ 2460 arbitrary units) yielding the protonated molecule of the hydrazone. Ionization resulted in very little fragmentation, producing a clean spectrum with the prominent base peak at m/z 311 due to protonated DMNTH. The high ionization efficiency could be attributed to the presence of tertiary amine sites (possessing high proton affinity) in the DMNTH structure. To ascertain the possible ion formation mechanism, DMNTH was analyzed by ESI-MS (spectrum not shown), for which the ionization mechanism is better understood than for MALDI, and a protonated molecule of high intensity resulted. Since ESI works effectively for analytes that are ions in solution, it is presumed that DMNTH ions (under LDI conditions) could be mainly preformed in the condensed phase before desorption. Nonetheless, both condensed and gas phase ion formation might be occurring simultaneously; evidence for gas phase reactions has been reported previously in the analysis of DMNTH derivatives using atmospheric pressure chemical ionization.^{14,16}

As with any derivatization technique, a compromise must be made between using a small derivatizing agent, so that reactions are not inhibited by steric hindrance, and using a high molecular weight (MW) agent that produces a sufficiently high mass product with a good ionization profile.^{28,29} DMNTH is a relatively high MW compound, so the decrease in efficiency of reaction with larger more sterically hindered carbonyls is significant. However, its use offers an important advantage in that it enables a signal to be observed in a higher mass region of the mass spectrum with marked improvement of S/N.

The reaction kinetics for the derivatizations using the one-pot preparation method were found to be dependent on the nature of the carbonyl analyte. A time dependent study of the derivatization of carbonyls with DMNTH was conducted to assess the required time for the reaction to go to completion. The carbonyl compounds were allowed to react at room temperature with molar excess DMNTH, over a range of times (15, 30, 45, 60, 75, 90, 105 min). Aliquots of the mixture from each interval were spotted in duplicate and each spot analyzed in duplicate, giving a total of four data points (peak area) that were averaged. The rate of formation (Figure 6.4) does not significantly increase after 15 minutes and so a thirty minute reaction time was found to be sufficient for analysis. Although, there seems to be a slight decrease in the relative intensity of the hydrazones over time, the decrease may not be statistically significant (RSDs without normalization were around 30%). The apparent decrease may be attributed to possible adsorption of the analyte on the surface of the polycarbonate vial over time.

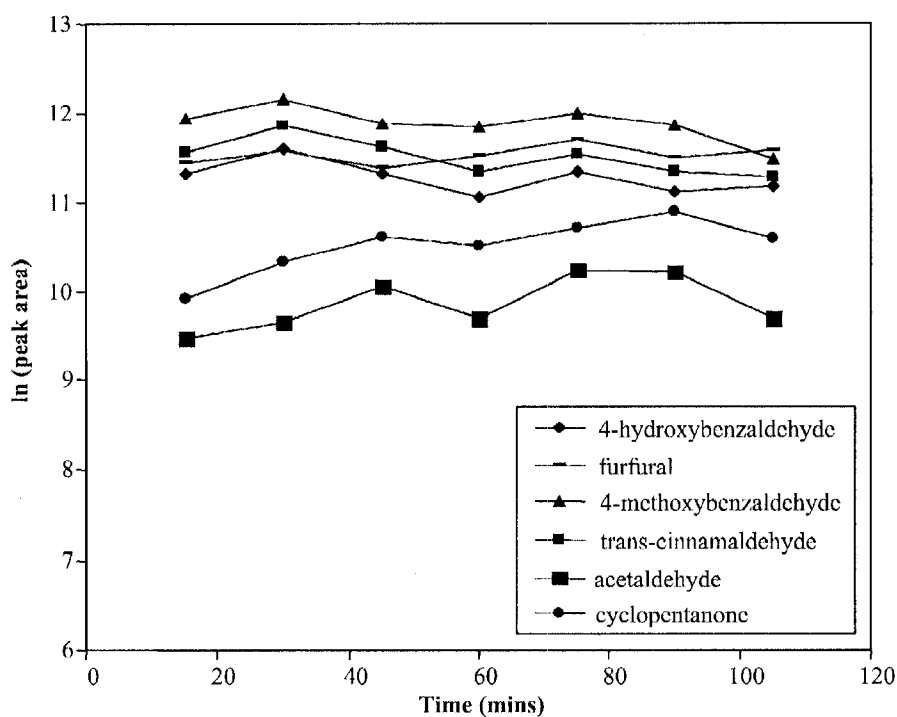


Figure 6.4. Time dependent study of reactions of 8.05 mM DMNTH and 20 $\mu\text{g mL}^{-1}$ carbonyl compounds. Aromatic carbonyls were reacted separately from aliphatic carbonyls.

From the kinetic studies, it was noted that there was an obvious discrepancy in the reactivity of the hydrazones of the different carbonyl compounds. The reactivity of the carbonyl moieties in the aromatic aldehydes (*i.e.* 4-methoxybenzaldehyde, 4-hydroxybenzaldehyde, furfural and *trans*-cinnamaldehyde) was higher compared to the aliphatic carbonyl compounds (acetaldehyde, cyclohexanone, cyclopentanone). This is not surprising since transition state intermediates resulting from aromatic aldehydes and ketones are much more stable than those of the aliphatic analogues (lacking pendant aromatic groups) presumably due to resonance stabilization effect. Reactions with higher

MW aromatic ketone compounds, such as benzophenone, were found to be slower and may not reach completion under ambient conditions, which might be attributed to a larger activation energy borne from greater steric hindrance. Thus, the achievable detection limits (DL) were slightly compromised but were nevertheless satisfactory. It is notable that DMNTH can be utilized for the analysis of small α -dicarbonyls, such as methyl glyoxal (Figure 6.5a), which are normally analyzed following derivatization with ortho-phenylenediamine to form quinoxalines rather than the hydrazones seen here. Due to the differences in ionization efficiency (aromatic hydrazones may be preferentially ionized to aliphatic hydrazones) and reaction kinetics, it is imperative to note that in the analysis of a mixture of aromatic and aliphatic carbonyl compounds, the latter tend to be suppressed making them hard to detect. When the laser intensity is increased to enable detection of aliphatic carbonyls, the aromatic derivatives saturate the detector. It is therefore recommended that for quantitative work, aromatic and aliphatic groups should be analyzed separately; however, for qualitative applications, separation may not be critical. Figure 6.5a and b show the RM-LDI-MS mass spectra of aromatic and aliphatic carbonyl mixtures analyzed separately.

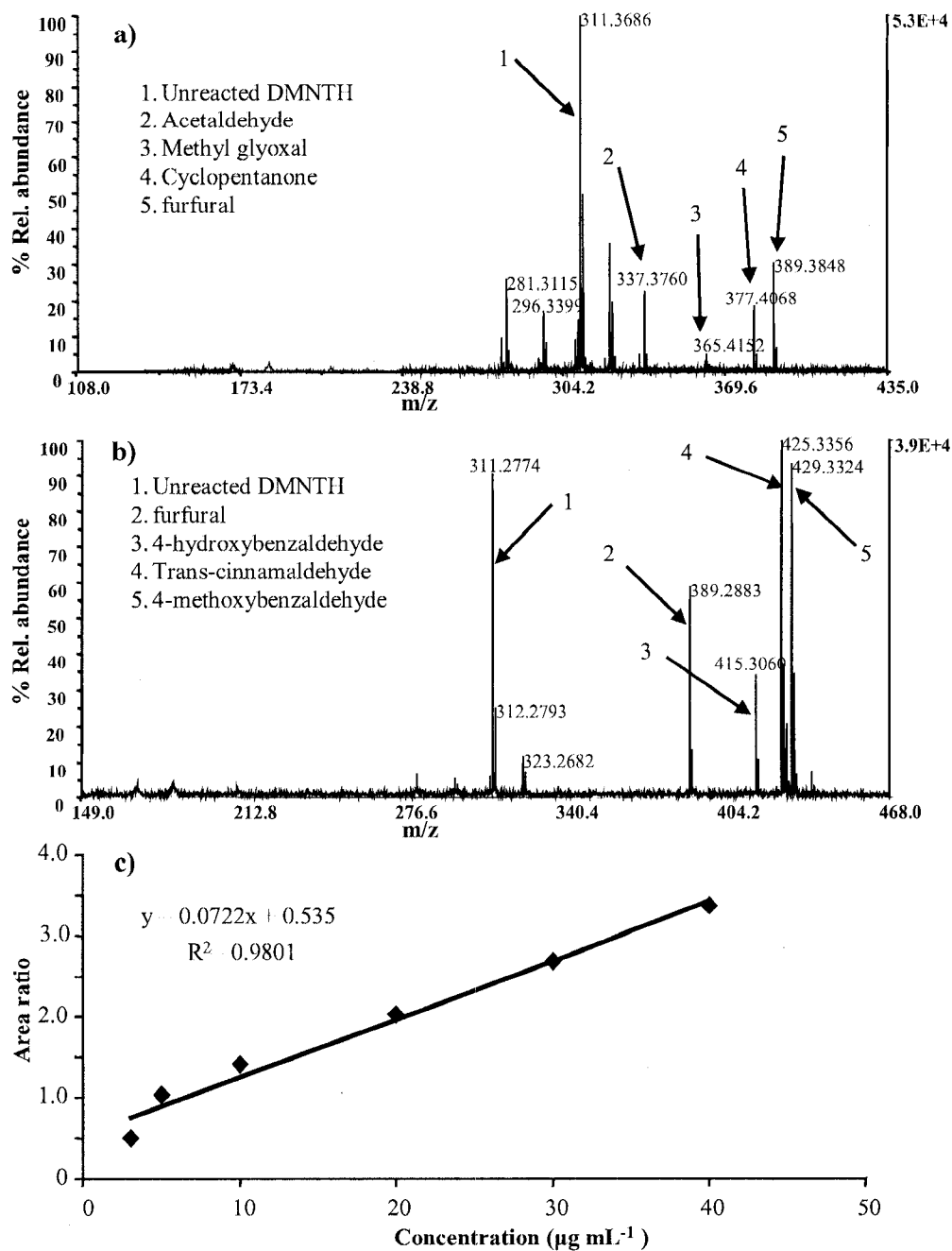


Figure 6.5. RM-LDI-TOFMS spectra of a) $10 \mu\text{g mL}^{-1}$ aliphatic carbonyls, b) $10 \mu\text{g mL}^{-1}$ aromatic carbonyls, c) calibration curve for 4-methoxybenzaldehyde with *in-situ* labelled furfural as an internal standard.

Table 6.1 illustrates the detection limits that were obtained for different carbonyl compounds. The data were acquired from six data points generated from 3 replicate spots with each spot analyzed in duplicate. The sample consisted of a mixture of 25 μL carbonyl ($10 \mu\text{g mL}^{-1}$), 25 μL DMNTH (0.161 mM) and 10 μL pre-labelled furfural DMNThydrazone internal standard ($10 \mu\text{g mL}^{-1}$), with 30 minute reaction time. Generally, precision was significantly improved by normalization of the analyte peak area against that of the internal standard compared to RSDs obtained without normalization, as shown in Table 6.1. Clearly, very low detection limits were achievable using RM-LDI-MS, with aldehydes displaying lower DLs than the ketones. The DLs achieved using this method are comparable to those reported using other techniques, such as DNPH-LC-MS-MS, DMNTH-LC-fluorescence detection and DMNTH-LC-APCI-MS, which were 0.18, 0.088 and 0.88 ng mL^{-1} for acetaldehyde, respectively.^{4,14,16} The detection limit for acetaldehyde using RM-LDI-TOFMS was 0.078 ng mL^{-1} , which is within the range of the most sensitive methods thus reported. Although we do not show great improvements over the best detection limits reported, there is significant improvement over those published previously for MS detection; moreover, the speed, ease of use and applicability to a range of analytes makes the method attractive.

Table 6.1. Detection Limits for DMNThyrazones by RM-LDI-TOFMS

DMNThyrazones	DL [§]	%	Normalized	Normalized
	(ng mL ⁻¹)	RSD	% RSD	%RSD*
4-methoxybenzaldehyde	0.022	23.5	28.9	11
4-hydroxyacetophenone	0.086	36.7	3.7	NA
p-hydroxybenzaldehyde	0.014	27.7	25.7	13
methylglyoxal	11.3	47	7.6	12
acetaldehyde	0.078	61	41.6	7.8
<i>trans</i> -cinnamaldehyde	0.0089	27.7	14.2	11
furfural	0.036	63.9	IS	IS
cyclohexanone	0.36	41.2	40.9	NA
cyclopentanone	0.079	56.1	30.9	15.4
benzophenone	2.8	63.7	29.6	NA
DMNTH	0.081	50.7	36.5	4.8

[§]detection limit = (3 SD of blank)(analyte concentration/net analyte signal intensity).

*Using furfural labelled *in-situ* as the internal standard.

IS - In the case of furfural, it was used as the internal standard in the normalization of the results, thus no %RSD is reported

NA - not available - the reported normalized %RSD*s are for a selection of representative compounds, the remaining compounds have not been assessed.

The utility of using unlabelled furfural as an internal standard instead of the pre-labelled standard (furfuralDMNThyrazone) was also investigated. This approach was found to work very effectively and greatly simplified the analysis since prior synthesis of the internal standard was not required. As is clear from Table 6.1, normalized RSDs

obtained were consistently better when this approach was employed compared to when separately synthesized furfuralDMNThydrazone was used. The improved reproducibility is likely due to the fact that the internal standard is derivatized and analyzed under the same conditions as the analytes. A calibration plot was generated for 4-methoxybenzaldehyde using *in-situ* labelled furfural as an internal standard (Figure 5c) and a good linear regression coefficient ($R^2 = 0.9801$) was observed, indicating that the technique shows good linearity over the range studied. A perfect regression coefficient may have been unachievable due to instrumental limitations; typically TOF-MS methods are not very good for quantitative work. However, it is expected that the use of other MS systems that are better suited to quantitation (such as triple quadrupole mass spectrometers with characteristically high sensitivity, wide linear dynamic range and high ion transmission efficiency assumed to be close to 100%) could greatly improve the linearity.^{27, 32}

On-plate derivatization worked well for both aromatic and aliphatic carbonyls. This method worked particularly well for small aromatic carbonyl molecules such as 4-methoxybenzaldehyde, furfural, 4-hydroxyacetophenone and trans-cinnamaldehyde (mass spectra of three of these are shown in Figure 6.6), but was slightly less sensitive in the analysis of aliphatic compounds and benzophenone; this difference in sensitivity was also observed with the one-pot derivatization approach. A prominent ion of the protonated product molecule can be seen for each derivative, which is often the base peak in the spectrum. Although not shown here, the application of on-plate derivatization to the aromatic and aliphatic carbonyl mixtures also worked effectively, resulting in mass spectra that were very similar to those obtained with one-pot derivatization (Figure 6.5a

and b). It should be noted, however, that the detection limits for on-plate approach were generally one order of magnitude higher than for the one-pot derivatization.

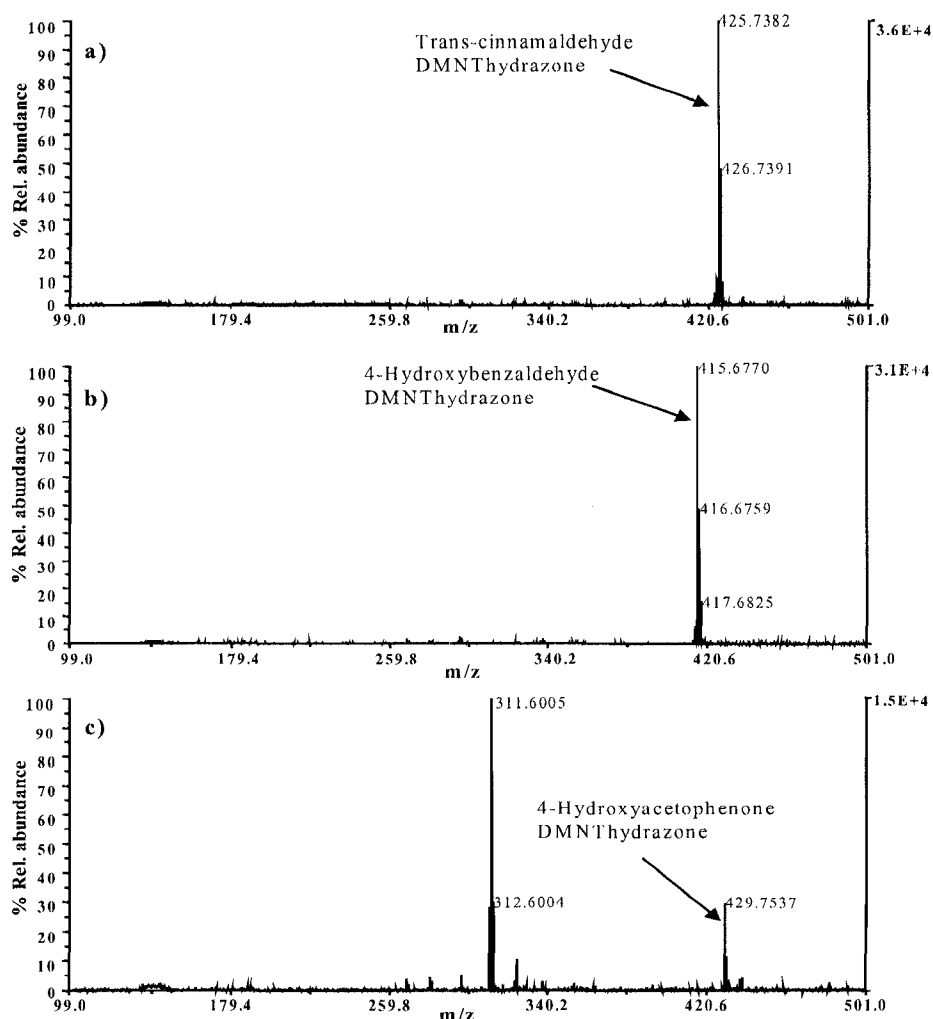


Figure 6.6. Sample RM-LDI-TOFMS spectra for carbonyl compounds that were analyzed by on-plate derivatization with 0.5 μL of 0.161 mM DMNTH. For all carbonyls, 0.5 μL was spotted on-plate at a concentration of 100 $\mu\text{g mL}^{-1}$.

In the analysis of 0.5 ng mL^{-1} of 4-methoxybenzaldehyde, the difference in sensitivity between the one-pot and on-plate methods can be clearly observed, (Figure 6.7). Despite using the same amount of analyte, the 4-methoxybenzaldehyde

DMNThydrazone was more easily detectable with a much better S/N ratio using the one-pot method, Figure 6.7 a, than when prepared on-plate, Figure 6.7 b, a reflection of both a higher signal and a less noisy background for the one-pot method. Because the time allowed for the on-plate derivatization to occur is shorter (roughly the time it takes for the spot to dry ~10 min) and mixing is not possible, the on-plate method is less efficient in producing the desired derivative. As a result, it was necessary to use a higher laser intensity to desorb more material. While this allowed us to achieve an improved detection limit for the on-plate method, it also resulted in more extensive fragmentation, which worsened the signal to noise ratio and still did not result in DLs as good as those seen for the one-pot method. Evidence for the lower reaction efficiency is demonstrated by the presence of a large peak at m/z 311 related to the protonated DMNTH and the decreased intensity of the analyte derivative peak compared to Figure 6.7 a). For detection of carbonyls at low concentrations, it is therefore essential to use the in-vial reaction method; this allows a longer reaction time with greater yields, and better mixing resulting in greater homogeneity of the sample spots. These advantages can be significant when semi-quantitative or quantitative results are desired. In spite of the obvious advantages of using the one-pot method, the on-plate technique offers a rapid and reasonably sensitive (ng range detection) approach for screening various types of samples for carbonyl compounds.

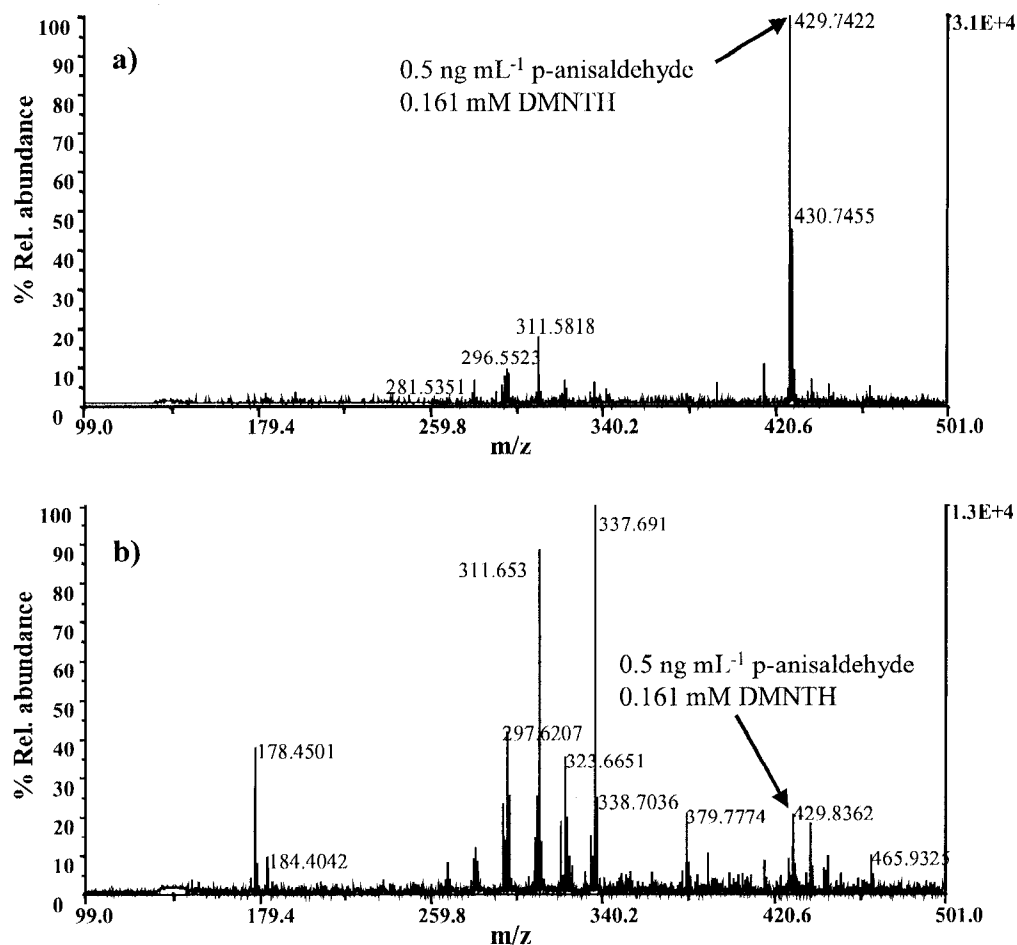


Figure 6.7. RM-LDI-TOFMS spectra of 0.5 ng mL⁻¹ of 4-methoxybenzaldehyde with 0.161 mM DMNTH, a) one-pot derivatization, b) on-plate derivatization. (The identity of the peak at m/z 337 is not clear).

It may be possible to improve the on-plate method by trying to control and slow down the rate of solvent evaporation. Under ambient conditions, the rate of drying and hence reaction was variable due to changes in the room temperature and humidity from day to day; this could be improved by carrying the reaction in a more controlled environment. A slower rate of evaporation allows a longer reaction time and may have the added benefit of facilitating better crystal formation, where quality of crystallization is indicated as a parameter contributing to the success of MALDI-TOFMS. One approach

used to lengthen reaction time and improve derivative product yield was solvent replenishment after the first cycle of spot drying. This was found to significantly improve the reaction yields, but not in a reproducible way.

The use of the DMNTH RM-LDI-TOFMS was also investigated in the analysis of carbonyls in real environmental samples. A beer sample was purchased and a portion degassed by sonication for thirty minutes. A 100- μL aliquot was spiked with furfural to make a final concentration of $5\ \mu\text{g mL}^{-1}$ and a 25- μL aliquot was reacted with 25 μL of DMNTH for thirty minutes, spotted on the MALDI plate, and analyzed. Although the saccharides and other beer matrix components impair the analysis and the furfural DMNTHydrazone is not detected at the laser intensity used with the standards (2460 arbitrary units), by using higher laser intensity (2710 arbitrary units), furfural derivative was clearly identifiable (Figure 6.8). From the mass spectra, the specificity of DMNTH in reacting with carbonyls is clearly evident. Other peaks tentatively identified in the beer sample include, methylglyoxal DMNTHydrazone at m/z 365 and, possibly, propanal DMNTHydrazone at m/z 351.

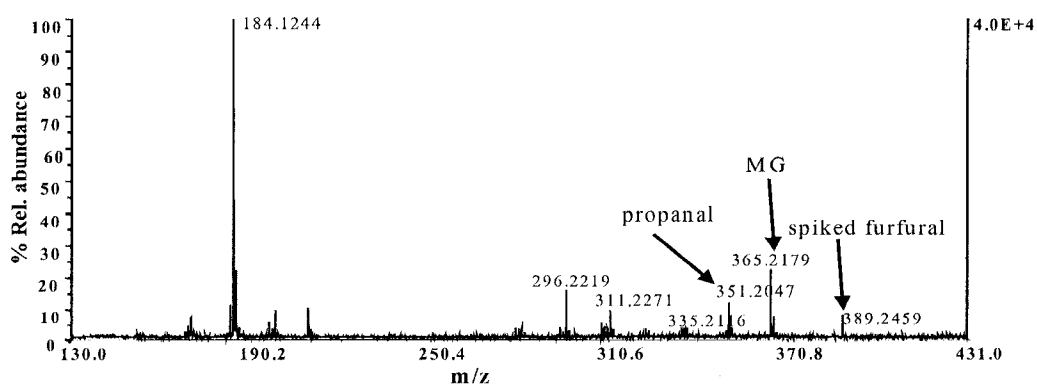


Figure 6.8. RM-LDI-TOFMS spectra of unfiltered beer spiked with $10\ \mu\text{g mL}^{-1}$ furfural and derivatized with 1.61mM DMNTH.

Traditionally, LDI-TOF mass spectrometry and its matrix assisted variant has had a reputation as a poor technique for quantification, primarily due to its poor precision, which is influenced by a number of factors, particularly the level of homogeneity of the sample/matrix spot. The inherent lack of reproducibility that plagues MALDI has also been shown to worsen when matrix ion suppression techniques are used.^{31,34} Though these limitations have hindered the use of MALDI-MS as a quantitative analytical technique, we have found that when RM-LDI-MS is combined with selection of an appropriate internal standard with a response profile similar to the analyte, the method can be useful for semi-quantitative and possibly quantitative work. Furfural was chosen as the internal standard to verify this method for quantitative work as it is a representative compound that reacted readily to form the corresponding DMNTHydrazone and it was found to respond to the laser in the same way as the sample hydrazones. The similarity in response is by design, since the moiety primarily responsible for ionization is introduced through DMNTH derivatization and is, therefore, a consistent feature in all target molecules. The spot-to-spot reproducibility of LDI-TOFMS was determined using the 4-methoxybenzaldehyde hydrazone normalized against the *in-situ* labelled furfural internal standard. Mass spectra were acquired from each of the 35 sample spots, by averaging 30 replicate laser shots per spectrum; the results showed excellent statistical control (Figure 6.9a) with most points falling within $\pm 2\sigma$. The RSD was found to be 15.5 % for the 35 measurements, which is comparable to values reported previously using specialized methods to improve reproducibility such as normalization against an internal standard, as has been used in this work, coumarin fluorescent tags for peptides analysis, and the seed layer sample preparation method.³¹⁻³³ A representative spectrum of those used to derive

the % RSD is shown in Figure 6.9 b). Both peak area and the height of the peaks were used, and peak area was found to produce the best results because it was less sensitive to subtle changes in conditions and gave a better signal to noise ratio in comparison to peak height. This RSD is a considerable improvement over those usually obtained with MALDI, where RSDs can be greater than 40%. Dekker *et al.*³⁴ reported a reproducibility of peak intensities of 30-42% for tryptic digests of cerebrospinal fluid. It is clearly evident from the RSD reported that RM-LDI-MS significantly improves precision.

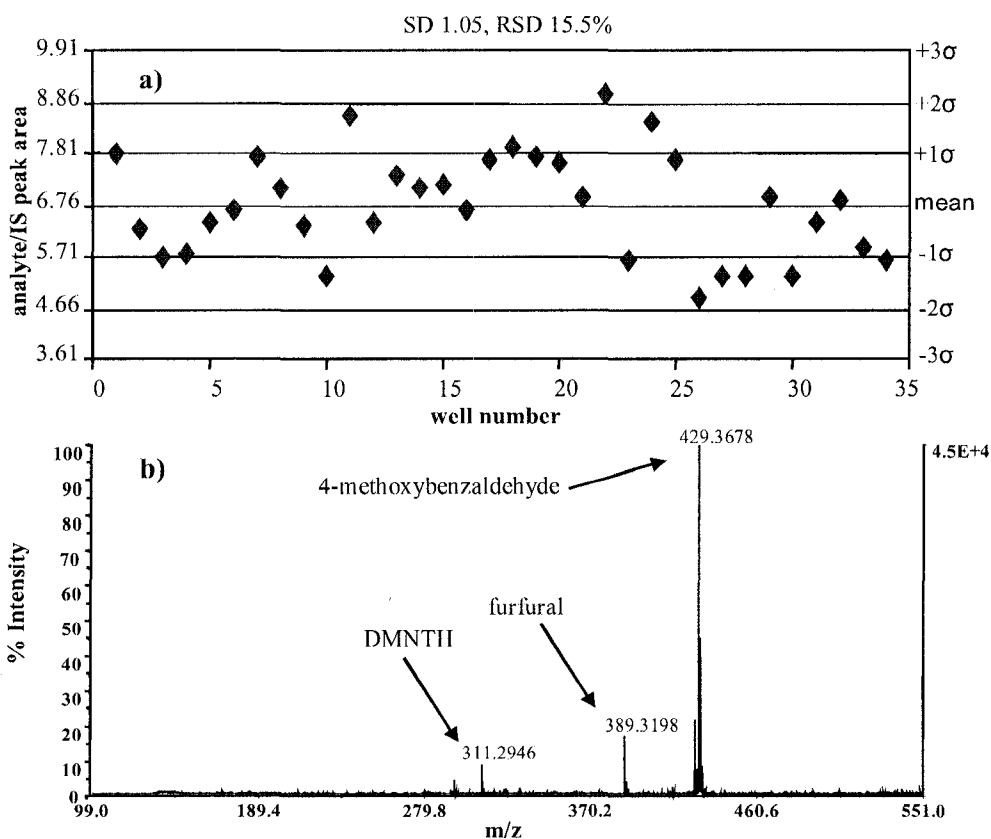


Figure 6.9. a) Spot-spot reproducibility of $5 \mu\text{g mL}^{-1}$ 4-methoxybenzaldehyde derivatized with 1.61mM DMNTH and $5 \mu\text{g mL}^{-1}$ furfural internal standard (IS) using one-pot derivatization method, b) Representative RM-LDI-TOFMS spectrum of resulting hydrazones from which data was drawn in construction of the control chart.

6.4 Conclusions

RM-LDI-TOFMS using DMNTH as the derivatizing agent is a sensitive, economical and rapid method for the analysis of carbonyl compounds. The method can be used quantitatively using very small samples without extensive sample handling. The prime disadvantage of using DMNTH is that it is not commercially available. The on-plate derivatization was found to be effective for concentrations of the carbonyl analyte in the sub- $\mu\text{g mL}^{-1}$ range, useful for qualitative work and high throughput screening. For detection of low concentrations of carbonyls ($<1 \text{ ng mL}^{-1}$), good mixing of DMNTH with carbonyl compound and longer reaction times on the order of 30 minutes are essential; the one-pot derivatization method meets these requirements.

It is certain that DMNTH can be used for analysis of numerous carbonyl containing compounds, which are of importance in environmental and biological systems. In addition, DMNTH is easy to prepare in high yield and purity, very stable and hence could be of practical utility in high throughput labs. The technique opens new frontiers for the analysis of carbonyl compounds using RM-LDI-TOFMS and the application of these derivatization techniques greatly widens the applicability of MALDI-TOFMS instruments. This approach illustrates an extremely efficient procedure for analysis of carbonyl compounds in drinking water, and shows potential for biomedical applications and biomarker research; for example, in the detection of malondialdehyde, a biomarker of oxidative stress, or of formaldehyde in human cancer cells.^{8,9} The technique could be extended for rapid, sensitive analysis of aldehydes in beer, such as acetaldehyde, 2-methylpropanal, methylbutanal, pentanal, hexanal, furfural, methional,

phenylacetaldehyde, and (E)-2-nonenal, which are typically cited as evidence of fouling.^{6,7}

Work is currently underway to synthesize other analyte specific derivatizing agents for RM-LDI-TOFMS of small molecules with different reactive moieties. Further work will involve applying these derivatizing agents to the analysis of real environmental samples.

6.5 References

1. Richardson SD, Caughran TV, Poiger T, Guo Y, Crumley FG. *Ozone Sci. Eng.* 2000; **22**: 653-677.
2. Richardson SD. *Anal. Chem.* 2003; **75**: 2831-2857.
3. Ho, SH, Yu, JZ. *Environ. Sci. Technol.* 2004; **38**: 862-870.
4. Zwicner C, Glauner T, Frimmel FH. *Anal. Bioanal. Chem.* 2002; **372**: 615-621.
5. Jeleń HH, Browska AD, Klensporf D, Nawrocki J, Erwin Wsowicz E. *Chem. Anal. (Warsaw)* 2004; **49**: 869.
6. Liu MM, Zeng ZR, Xiong B. *J. Chromatogr. A* 2005; **1065**: 287-299.
7. Vesely P, Lusk L, Basarova G, Seabrooks J, Ryder D. *J. Agric. Food Chem.* 2003; **51**: 6941-6944.
8. Kato S, Burke PJ, Koch TH, Bierbaum VM. *Anal. Chem.* 2001; **73**: 2992-2997.
9. Nagy K, Pollreisz F, Takats Z, Vekey K. *Rapid Commun. Mass Spectrom.* 2004; **18**: 2473-2478.
10. Brombacher S, Oehme M, Beukes JA. *J. Environ. Monit.* 2001; **3**: 311-316.

11. Cartwright AJ, Jones P, Wolff JC, Evans EH. *Rapid Commun. Mass Spectrom.* 2005; **19**: 1058-1062.
12. Brombacher S, Owen SJ, Volmer DA. *Anal. Bioanal. Chem.* 2003; **376**: 773-779.
13. Lattova E, Perreault H. *J. Chromatogr. B* 2003; **793**: 167-179.
14. Kempter C, Potter W, Binding N, Klaning H, Witting U, Karst U. *Anal. Chim. Acta* 2000; **410**: 47-64.
15. Kempter C, Berkhoudt TW, Tolbol GC, Egmosc KN, Karst U. *Anal. Bioanal. Chem.* 2002; **372**: 639-643.
16. Kempter C, Zurck G, Karst U. *J. Environ. Monit.* 1999; **1**: 307-311.
17. Liu Z, Zou H, Ye M. *Electrophoresis* 2001; **22**: 1298-1304.
18. Richardson SD, Karst U. *Abs. Pap. Am. Chem. Soc.* 2001; **221**: 257-Env.
19. Karas M, Hillenkamp F. *Anal. Chem.* 1988; **60**: 2299-2301.
20. Tanaka K, Waki H, Ido Y, Akiata S, Yoshida Y, Yoshida T. *Rapid Commun. Mass Spectrom.* 1988; **2**: 151-153.
21. McCombie G, Knochenmuss R. *Anal. Chem.* 2004; **76**: 4990-4997.
22. Donegan M, Tomlinson AJ, Nair H, Juhasz P. *Rapid Commun. Mass Spectrom.* 2004; **18**: 1885-1888.
23. Soltzberg LJ, Patel P. *Rapid Commun. Mass Spectrom.* 2004; **18**: 1455-1458.
24. Xu S, Li Y, Zou H, Qiu J, Guo Z, Guo B. *Anal. Chem.* 2003; **75**: 6191-6195.
25. Go E P, Prenni JE, Wei J, Jones A, Hall SC, Witkowska HE, Shen Z, Siuzdak G. *Anal. Chem.* 2003; **75**: 2504-2506.
26. Zhang Q, Zou H, Guo Z, Zhang Q, Chen X, Ni J. *Rapid Commun. Mass Spectrom.* 2001; **15**: 217-223.

27. Hatsis P, Brombacher S, Corr J, Kovarik P, Volmer DA. *Rapid Commun. Mass Spectrom.* 2003; **17**: 2303.
28. Lee PJ, Chen W, Gebler JC. *Anal. Chem.* 2004; **76**: 4888-4893.
29. Griffiths WJ, Liu S, Alvelius G, Sjoval J. *Rapid Commun. Mass Spectrom.* 2003; **17**: 924-935.
30. Tholey A, Wittmann C, Kang M, Bungert D, Hollenmeyer K, Heinzle E; *J. Mass Spectrom.* 2002; **37**: 963-973.
31. Slenc L, Volmer DA. *Rapid Commun. Mass Spectrom.* 2006; **20**: 1517-1524.
32. Pashkova A, Moskovets E, Karger BL. *Anal. Chem.* 2004; **76**: 4550-4557.
33. Önnarfjord P, Ekström S, Bergquist J, Nilsson J, Laurell T, Marko-Varga G. *Rapid Commun. Mass Spectrom.* 1999; **13**: 315-322.
34. Dekker LJ, Dalcbout JC, Siccama I, Jenster G, Smitt PAS, Luijckx TM. *Rapid Commun. Mass Spectrom.* 2005; **19**: 865-870.

CHAPTER 7

Rapid Analysis of Alpha-Dicarbonyl Compounds by MALDI Using 9-(3,4-Diaminophenyl)Acridine (DAA) as a Reactive Matrix.

A version of this chapter will be submitted for publication. Mugo SM, Bottaro CS. Rapid Analysis of Alpha-Dicarbonyl Compounds by MALDI Using 9-(3,4-Diaminophenyl)Acridine (DAA) as a Reactive Matrix.

7.1 Introduction

Alpha-dicarbonyls are an important class of compounds that have attracted the attention of researchers in diverse scientific disciplines such as water quality chemistry, food chemistry, and medical research.¹⁻⁶ Pyruvic aldehyde (methylglyoxal) has been identified as a priority and potentially harmful disinfection by-product in ozonated drinking water.¹ Methylglyoxal and glyoxal are reactive intermediates produced from non-enzymatic glycation (Maillard reaction) and are clinically significant compounds since they are known to react with proteins, basic phospholipids and nucleotides to form advanced glycation end products, which are possible indicators of chronic and age related diseases, such as diabetes mellitus and Alzheimers diseases.²⁻⁴ Diketones are also responsible for the characteristic stale smell in wines and beers and thus act as indicators of aging and deterioration in flavour quality.⁵ Dicarbonyls have also been reported to be present in the cornucopia of toxic compounds present in cigarette smoke and are thus important among environmental toxicologists.⁶

Analysis of these compounds has been traditionally accomplished by reaction of the α -dicarbonyls with o-phenylenediamine to form stable UV- active quinoxalines (with a notable absorbance maximum of 315 nm), which are analyzed by high performance liquid chromatography (HPLC) or capillary electrophoresis (CE) and detected by UV spectrophotometry.²⁻⁶ Current trends in chemical analysis, however, demand high sensitivity and high sample throughput methods, especially with clinical applications where numerous samples must be analyzed in a short period of time. Outstanding performance features such as wide mass range, low sample volume requirements (< 1 μ L),

tolerance to salts and buffers, characteristic ultra low sensitivity and increased throughput have distinguished MALDI-TOFMS from other techniques, making it a leading technology, especially in proteomics. Although MALDI was initially designed for qualitative analysis of relatively high molecular weight biomolecules, there has been burgeoning interest in its utility for the analysis of low molecular weight compounds, particularly those of pharmaceutical importance.⁷ Some of the hurdles, which must be overcome for MALDI to realize its full potential in the analysis of small compounds include solving the pronounced isobaric interferences arising from matrix and matrix cluster ion peaks, which obscure spectra in the low mass region (< 500 Da), poor ionizability of some analytes, inherent inhomogeneity, and problems with high volatility of very small molecules, which are essentially lost in the sample preparation stage and in the vacuum chamber of the mass spectrometer. Different approaches have been implemented for circumventing these problems, such as the use of high molecular weight matrices,⁸ use of matrix suppression effect,⁹ desorption/ionization on silicon (DIOS),¹⁰ application of non-organic matrices such as carbon nanotubes,¹¹ and tandem MS.¹² All these strategies however, have limitations in their effectiveness for small molecule analysis. So small molecules analysis remains an analytical challenge. A potential scientifically pragmatic approach to mitigate some of the small molecules analytical challenges with MALDI could involve the use of easily ionizable reactive matrices, a concept reported by Volmer *et al.*¹³ in his seminal paper, which could be viewed as an extension of derivatization methods used with other analytical techniques.

Chemical derivatization is a routine part of GC and HPLC analysis, particularly used to enhance chromatographic behaviour and detectability of otherwise fragile

analytes. However, recently chemical derivatization has been employed to enhance signal intensities of poorly ionized molecules by converting them into products that can be easily detected by soft ionization methods such as electrospray ionization (ESI) and MALDI.¹⁴ Chemical derivatization in MALDI has become more common particularly for the analysis of peptides and carbohydrates (often referred to as tagging or labelling). A number of very well known, rapid and high yielding chemical reactions such as Schiff's base reactions, guanidation, dehydration of carbonyls with arylhydrazines, and reductive amination with aromatic amines, have been used in MALDI.¹⁵⁻¹⁹ However, despite obvious advantages, derivatization of small molecules for MALDI analysis has only been investigated by a few researchers and within a limited scope.^{13,20-22}

This study demonstrates the application of a specially synthesized and highly ionisable reactive matrix, 9-(3,4-diaminophenyl)acridine (DAA) – originally synthesized by Plater *et al.*²³ as a fluorescent probe for nitric oxide detection – for specific derivatization of α -dicarbonyls to produce relatively high mass and easily ionizable quinoxaline products suitable for analysis by MALDI-TOFMS. The α -dicarbonyls used as test compounds include methylglyoxal, 2,3-butanedione and diphenylglyoxal. Following derivatization of these compounds with DAA, a large increase in sensitivity was obtained and hence low detection limits were achieved.

7.2 Materials and Methods

Chemical supplies such as acridine, o-phenylenediamine, ethanol, ammonia, acetic acid, sodium chloride, sulphur, sulphuric acid, methyl glyoxal, diacetal,

diphenylglyoxal, diethyl ketomalonate, and diethyl oxalate, which were bought from Sigma-Aldrich Canada Ltd, Winston Park Drive, Oakville Ontario. All chemicals were of analytical grade and were used without further purification. A Molson Canadian beer, Premium Lager was bought locally.

7.2.1 Synthesis of 9-(3,4-Diaminophenyl)acridine

9-(3,4-Diaminophenyl)acridine was prepared by the method adopted from Plater *et al.*²³ as summarized schematically in Figure 7.1. Briefly, the synthetic procedure consisted of two steps: first, 9-chloroacridine (pale brown crystals) was synthesized by bubbling anhydrous HCl gas, generated from the reaction of sodium chloride with concentrated sulphuric acid, through an 11 mmol solution of acridine in absolute ethanol. The second step involved a straightforward solventless nucleophilic substitution reaction in which a mixture of 9-chloroacridine (9 mmol), o-phenylenediamine (17 mmol) and sulphur (27 mmol) was heated and stirred for 2 hrs. The resulting product was washed with diethyl ether (2 x 20 mL) and extracted with 10% HCl (150 mL) to give a dark brown solution with a green cast, which was then made alkaline with concentrated aqueous ammonia to pH 9 and a brown solid precipitated. Sample clean up was accomplished by column chromatography and the identity of the product ascertained by ¹H NMR and APCI-MS. The most admirable aspect of this synthesis is the atom economy which was calculated to be > 85% which certainly goes a long way in reducing waste by designing sustainable synthetic schemes.

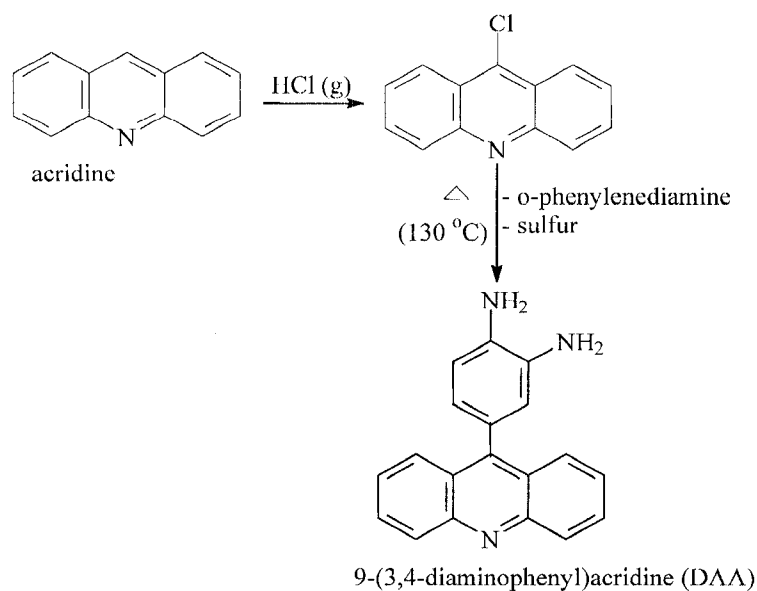


Figure 7.1. Synthetic scheme for derivation of 9-(3,4-Diaminophenyl)acridine.

7.2.2 UV-Vis Spectrophotometry

A UV-Vis spectrum of 0.1 mM DAA in 10mM acetic acid in 8:2 water and acetonitrile was acquired using a Hewlett Packard 8452A diode array spectrophotometer and the data obtained (wavelength range; 190-800 nm) plotted using Minitab.

7.2.3 Sample Preparation

A DAA stock solution (1.0 mM) prepared in water containing 10mM acetic acid and acetonitrile (8:2, v/v) was found ideal for derivatization of dicarbonyls. The pH was 3.39, which is suitable for this acid catalyzed reaction. A 10 μL aliquot of the DAA solution (1mM) was mixed with the same volume of various dicarbonyl solutions (of different concentrations ranging from 1-100 $\mu\text{g mL}^{-1}$), then vortexed and allowed to react at room temperature for 1hr before deposition on a MALDI target. A 0.5 μL aliquot of the

resulting solution was spotted on the MALDI plate and dried at ambient conditions, then analyzed by TOFMS without purification or use of any extraction process. On-plate derivatization was also evaluated where 0.5 μL of the DAA is spotted on the MALDI target and the dicarbonyl solution spotted on the dried spot containing the reactive matrix.

7.2.4 MALDI Mass Spectrometry

A commercial Applied Biosystems DE-RP TOF-MS equipped with high performance nitrogen laser (337 nm emission wavelength) and reflectron was used. Spectra from 30 laser shots were acquired in reflectron mode and averaged. The acquisition mass range was 100-700 Da and the polarity was positive. Other instrumental parameters included, extraction delay time: 200 nscc, grid voltage: 74.4%, accelerating voltage: 20kV, and mirror voltage ratio: 1.12.

7.3 Results and Discussion

UV-Vis spectrum (Figure 7.2) of DAA exhibited a reasonable absorbance at the MALDI nitrogen laser excitation wavelength 337 nm, with two pronounced relative maxima around 258 nm and 356 nm meeting one criterion for use as a reactive matrix in MALDI. Since DAA absorbs more strongly at 355 nm, it would be expected to perform even better as a reactive matrix if a MALDI Nd: YAG laser (not available in our laboratory) emitting at that wavelength is employed. The molar extinction coefficient (ϵ) of DAA in 10mM acetic acid and acetonitrile (8:2, v/v), was calculated to be 37112 L $\text{mole}^{-1}\text{cm}^{-1}$ at 337 nm, which when compared to the commonly used matrix, α -CHCA

(22795) is considerably higher, further showing the capacity of DAA to absorb the energy of the laser. However, it is important to note that the molar absorption coefficient of the resulting quinoxalines (analyte being ablated by the laser) may be different from DAA as the free compound. More importantly, the ionization efficiency of DAA was established to be exemplary at low laser intensity (~ 2496 arbitrary units) producing little to no fragmentation. Figure 7.3 demonstrates the “clean” mass spectrum obtained that is completely free of spectral noise, with the intense peak at m/z 286 representing the protonated molecule, $[\text{DAA}+\text{H}]^+$. Furthermore, the spectrum attests to the excellent photochemical stability of the molecule under laser irradiation. The high ionizability is attributed to the presence of basic sites in the DAA structure, making it particularly prone to protonation. To ascertain the ionization mechanism (MALDI mechanism poorly understood), DAA was analyzed by ESI for which the ionization mechanism is better understood than that of MALDI; DAA was found to be easily protonated under these conditions as well (spectra not shown), suggesting that the DAA ions seen using LDI-TOFMS may be preformed before desorption. Nonetheless, gas phase ion formation cannot be ruled out.

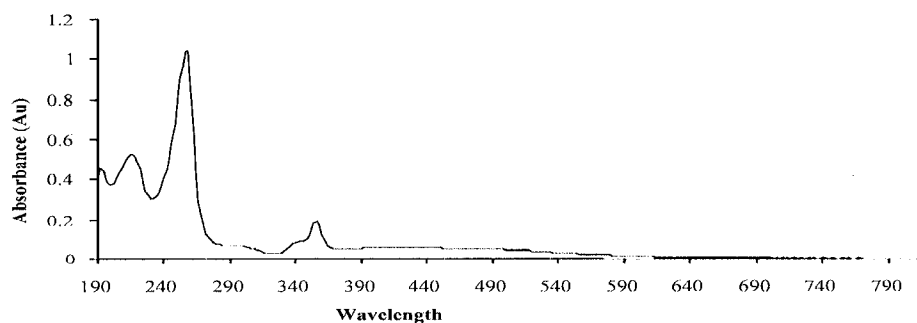


Figure 7.2. UV-Vis absorption spectra of $10 \mu\text{g mL}^{-1}$ DAA in 10mM acetic acid in 8:2, water and acetonitrile.

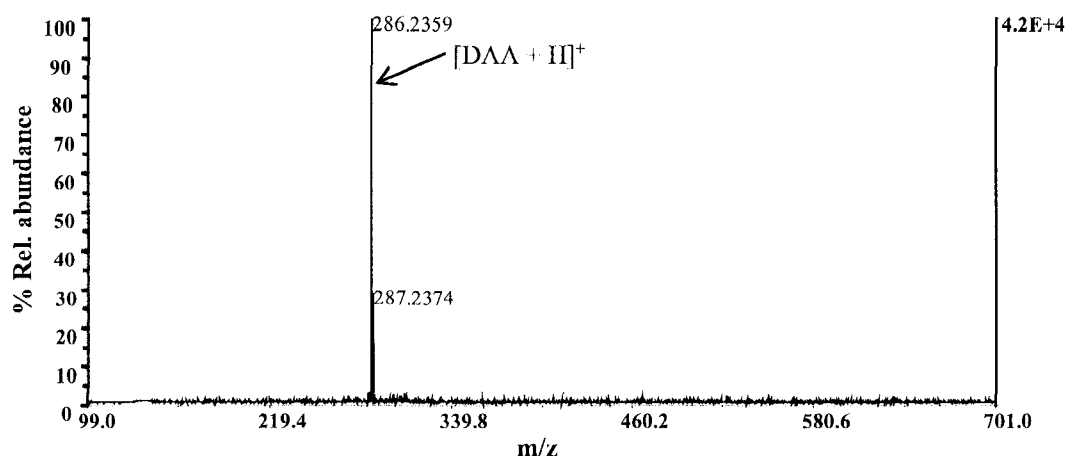


Figure 7.3. LDI-TOFMS spectrum of 10 μ M DAA.

The reaction mechanism between an α -dicarbonyl and DAA (reacting moiety, ortho-diamine) is a straightforward acid catalyzed condensation reaction forming a type of compound called quinoxaline. The derivatization chemistry is illustrated schematically in Figure 7.4. To assess the time required for the reaction to go to completion, an experiment was conducted where the dicarbonyl compounds were allowed to react with DAA at room temperature over a range of times (15, 30, 45, 60, 75, 90, 105 min). Aliquots of the mixture from each time interval were spotted in duplicate on the MALDI plate and each spot analyzed in duplicate, giving a total of four data points (peak area) that were averaged. The time course study is graphically represented in Figure 7.5. The rate of reaction was variable from compound to compound, with small molecules like methyl glyoxal displaying the fastest reaction kinetics compared to diacetal and diphenylglyoxal, attributed to steric accessibility of reacting moieties. However, as is clear from Figure 7.5, a one hour reaction time was established to be sufficient for all the three α -dicarbonyls studied. The reaction kinetics determines the completeness of the

reaction at the time of sampling and consequently influences the limits of detection achievable, as will be evident later.

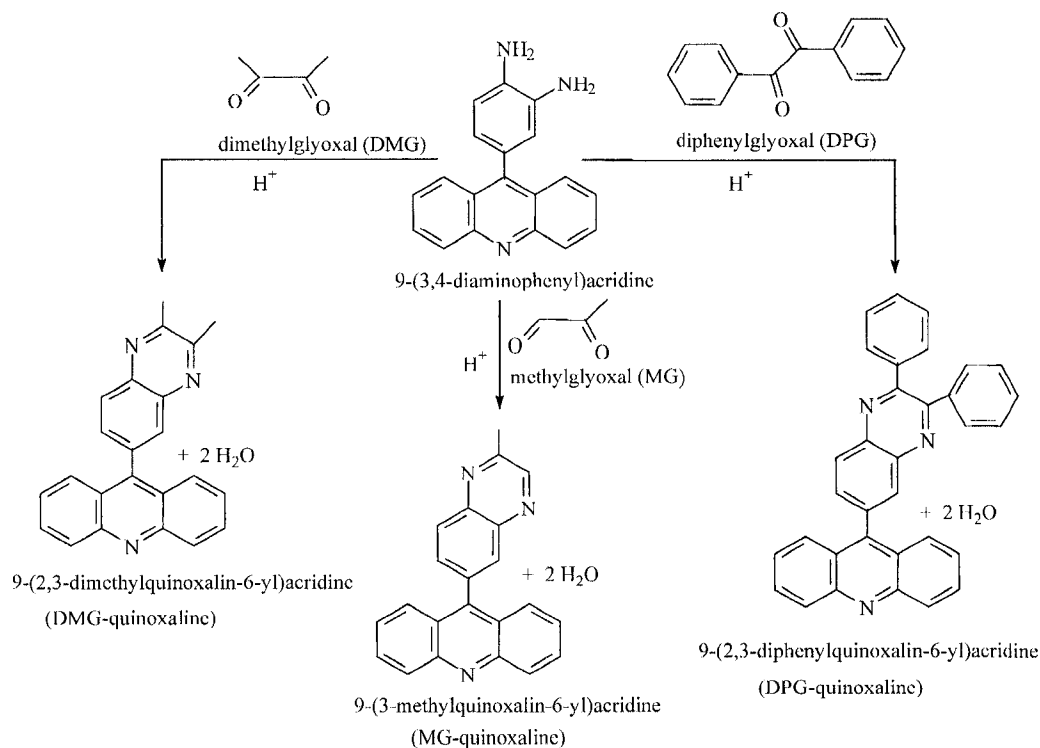


Figure 7.4. Derivatization chemistry. The schematic shows acid catalyzed condensation reaction of DAA and α -dicarbonyl compounds namely; methyl glyoxal, diacetal and diphenylglyoxal to form their respective quinoxalines.

The reaction of DAA and diphenylglyoxal was particularly intriguing because it was very rapid irrespective of the fact that the product and the reactants are quite bulky. This may be attributed to a favourable orientation of dicarbonyl moiety of diphenylglyoxal with respect to the active moiety in DAA. The quinoxaline products reported herein are remarkable compounds to investigate because to our knowledge they have not been previously synthesized or reported, and since quinoxaline derivatives are

known to possess a broad spectrum of biological activity, it is envisioned they could bear interesting chemical and medicinal properties.

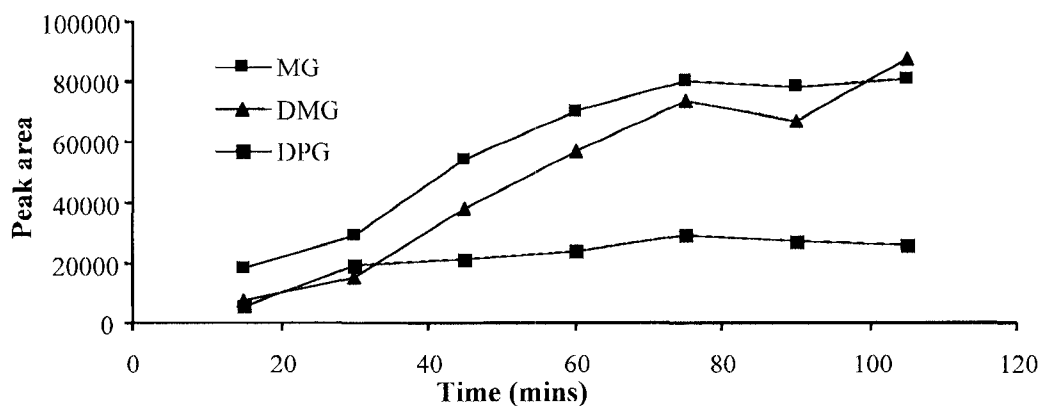


Figure 7.5. A time dependent study of DAA reaction with α -dicarbonyls.

The mass spectra shown in Figure 7.6 confirm that ion peaks of the reaction products (quinoxalines) were observed exclusively along with the unreacted DAA ion peak. The quinoxalines of dicarbonyls, namely 9-(2,3-dimethylquinoxalin-6-yl) acridine, 9-(2,3-diphenylquinoxalin-6-yl) acridine and 9-(2-methylquinoxalin-6-yl) acridine displayed strong protonated molecule peaks at m/z 336, 460 and 322, respectively. Evidently, these quinoxaline products formed were vacuum stable under MALDI conditions, resisting fragmentation on irradiation and ionizing remarkably well, even better than the derivatizing agent, DAA itself. This may be because the derivatives have up to three basic sites available for protonation and therefore the total probability of ionization is higher. It is worth mentioning that the sample spots on the MALDI plate were stable even when stored in the desiccator for over one week and relatively

reproducible mass spectra could be acquired, making it possible to reanalyze the samples if needed.

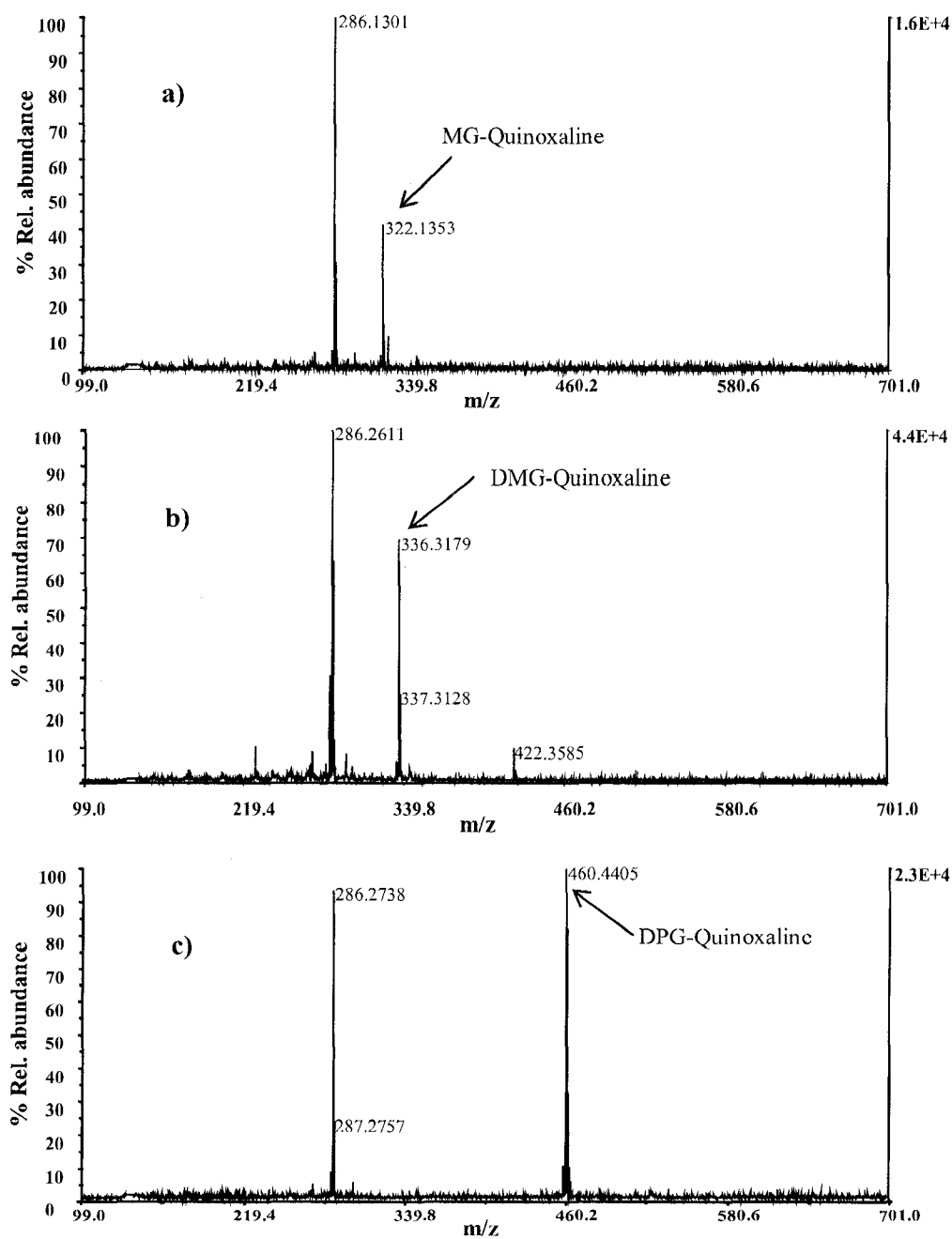


Figure 7.6. RM-LDI TOFMS spectra of alpha-dicarbonyls quinoxalines obtained by one-pot derivatization (1hr reaction time); a) $5 \mu\text{g mL}^{-1}$ methyl glyoxal b) $50 \mu\text{g mL}^{-1}$ 2,3-butanedione c) $50 \mu\text{g mL}^{-1}$ diphenylglyoxal.

Apart from the hour long, one-pot derivatization, a rapid on-plate derivatization, analogous to the on-target trypsinization strategy in proteomics was attempted and a representative mass spectrum is shown in Figure 7.7a. The product ion peaks are much less prominent than with the one-pot derivatization (Figure 7.6), perhaps due to insufficient time for the reaction to occur and the lack of mixing yielding a less than homogeneous reaction mixture. The detection limits achievable are thus compromised as will be illustrated later in this communication; nevertheless, the on-plate derivatization approach is satisfactory for facile screening for relatively high concentrations of α -dicarbonyls and α -ketocarboxylic acids in different sample matrices.

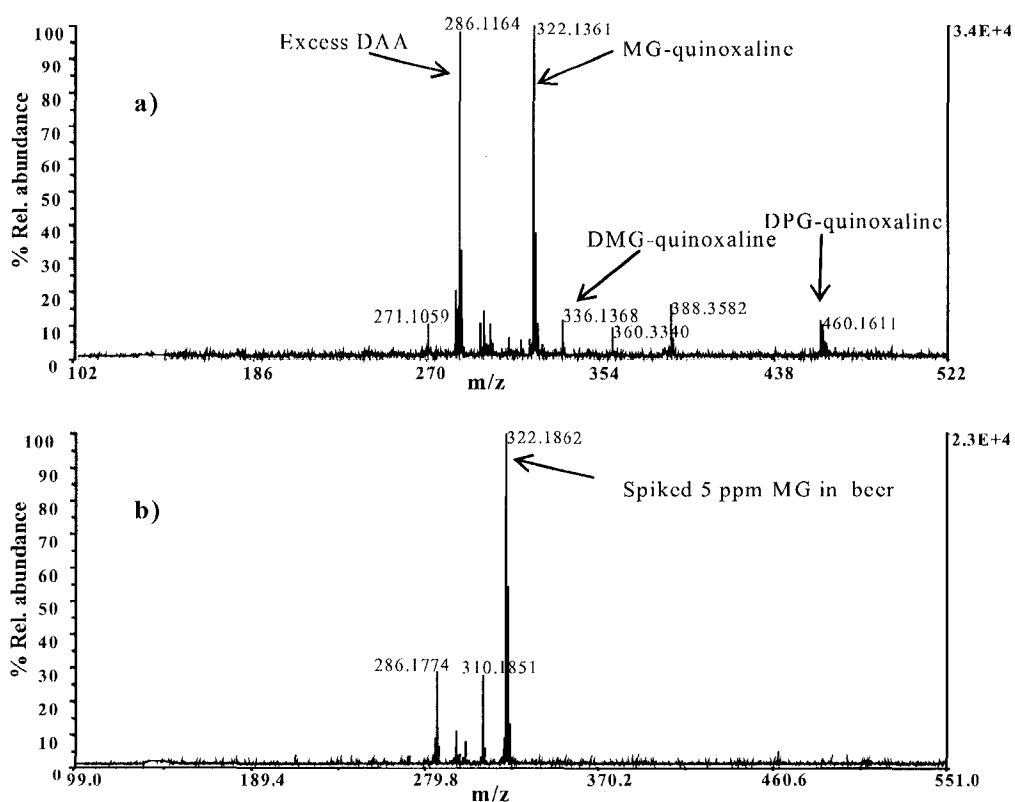


Figure 7.7. a) Representative RM-LDI-TOFMS spectrum obtained by on-plate derivatization of a mixture of $30 \mu\text{g mL}^{-1}$ methyl glyoxal, diphenylglyoxal and diacetal, b) RM-LDI-TOFMS spectrum of beer spiked with $5 \mu\text{g mL}^{-1}$ methyl glyoxal.

To test the applicability of the technique for analysis of real environmental samples, a 100 μL aliquot of beer (degassed for 30 minutes) was spiked with methyl glyoxal to give a final concentration of $5 \mu\text{g mL}^{-1}$. A 25 μL aliquot of spiked beer was reacted with 25 μL DAA solution for one hour and spotted on the MALDI plate for analysis without any prior clean-up or extraction. Figure 7.7b, shows the obtained spectrum, which clearly show the excellent selectivity of DAA to α -dicarbonyl compounds, even in the midst of enormous amount of matrices (saccharides *etc.*). It must be stated that relatively higher laser intensity (2710 arbitrary units) was used in this case because of the possible matrix suppression.

The use of MALDI-TOFMS for quantitative work is generally encumbered by inherent synchronization of desorption/ionization (highly variable) and mass analysis, particularly for conventional axial ion injection mode TOF instruments, which leads to major imprecision. The irreproducibility of mass spectra is exacerbated by the use of matrices, which ideally should cocrystallize with the analyte resulting in heterogeneous sample spots. Hence “sweet spots” have to be searched for during analysis, which is seldom effective for quantitative analysis. Conversely, the reported approach eliminates the use of additional matrix, with DAA acting as its own matrix eliminating one major source of irreproducibility, making it attractive for quantitative work. Accordingly, a calibration plot was constructed to evaluate linearity. The data for the plot was taken from a series of reactions of DAA with methyl glyoxal and dimethyl glyoxal in varying concentrations (ranging, $3\text{-}50 \mu\text{g mL}^{-1}$), with DPG-quinoxaline as the internal standard;

DPG was labelled in situ. The internal standard (ideally should bear structural and physicochemical similarity to analyte, *e.g.* isotopically labelled analogues of analyte) can compensate for variability in composition of the sample spot, which is a source of the irreproducibility typically seen in MALDI. Four replicate mass spectra (representative spectrum, Figure 7.8a) were acquired (from two sample spots, each sampled in duplicate) and the average area of each corresponding quinoxaline calculated. Clearly, as shown in Figure 7.8b, a good linear plot was obtained, qualifying the technique for routine quantitative analysis. The linear range was generally narrow; however, it is envisioned that superior linear dynamic range could be achievable with MALDI coupled to a triple quadrupole mass analyzer (QqQ) in selected reaction monitoring mode (SRM). This technique allows better latitude for quantitation because of its characteristic high sensitivity, wide linear dynamic range, and high ion transmission efficiency, assumed to be close to 100%.²⁴ Further, Figure 7.8a delineates the multi-component analysis of a mixture of all three dicarbonyls without time consuming chromatography, which is a testament to the applicability of the technique for simultaneous determination of various dicarbonyl compounds in a complex sample mixture. Nevertheless, for very complex mixtures, a system in which MALDI is coupled to HPLC, would be attractive.

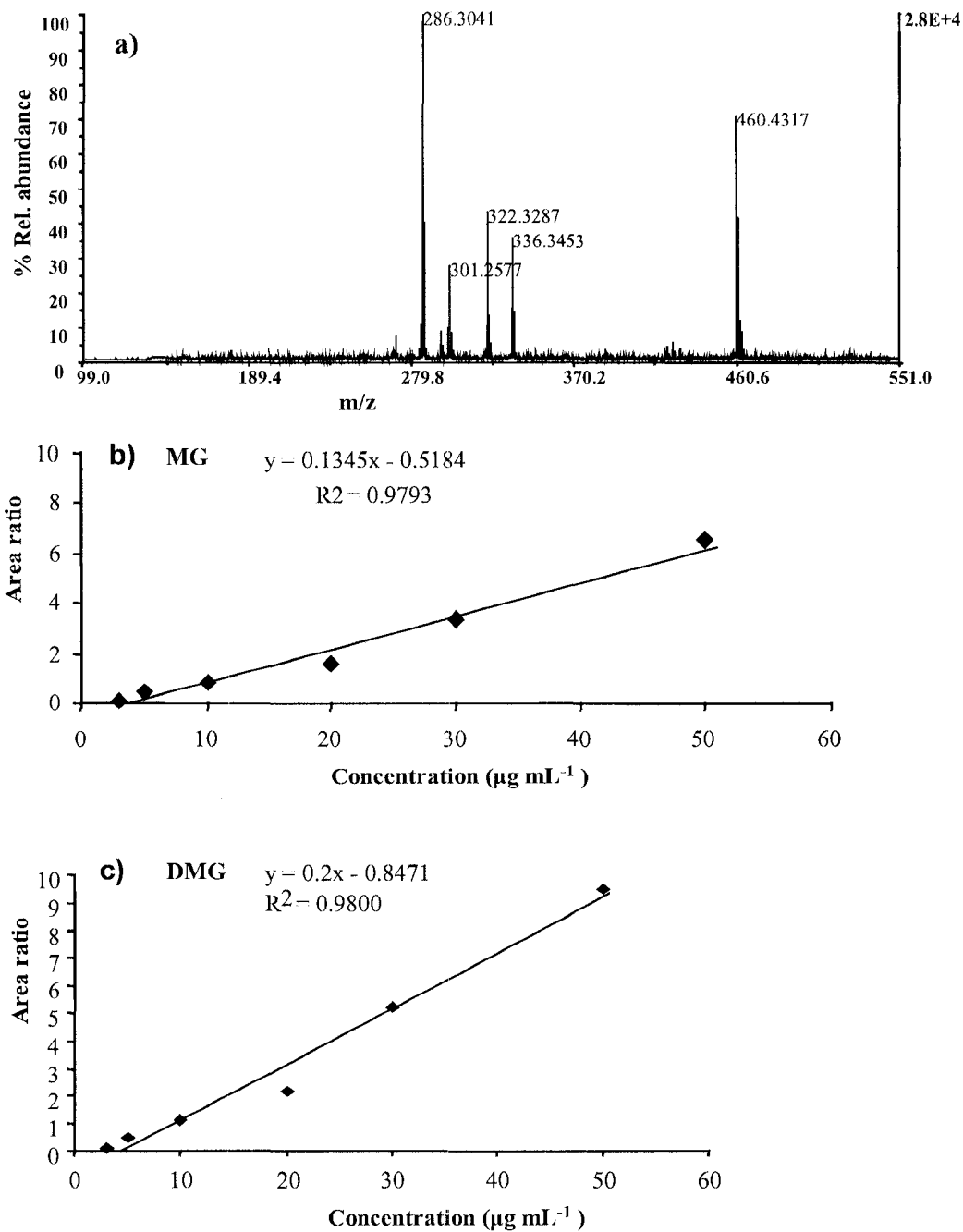


Figure 7.8. a) Representative mass spectra of a mixture of $10 \mu\text{g mL}^{-1}$ methyl glyoxal and diacetal and $20 \mu\text{g mL}^{-1}$ diphenylglyoxal as an *in situ* labelled internal standard, b) Calibration curves for methyl glyoxal and (c) dimethylglyoxal, using $20 \mu\text{g mL}^{-1}$ *in situ* labelled diphenylglyoxal as an internal standard.

Table 7.1 gives the limits of detection (DL) obtained for the dicarbonyl compounds analyzed both by one-pot derivatization and on-plate derivatization, with the sample consisting of $10 \mu\text{g mL}^{-1}$ α -dicarbonyls and $100 \mu\text{g mL}^{-1}$ α -dicarbonyls solution respectively with 1mM DAA. The results were obtained from six data points obtained from 3 different spots, with each spot sampled twice and the mean average of peak area taken. Clearly, the technique described here affords almost a hundred times lower detection limits compared to DL reported ($7.2 \mu\text{g/L}$) by Pedro *et al.*² for methyl glyoxal analysis using capillary electrophoresis with diode array detection. The reproducibility of the technique was found to range from 13.8-25%, with on-plate derivatization giving higher RSDs, obviously due to lower homogeneity of the sample spots compared with one-pot derivatization. Undoubtedly, the RSDs obtained are a great improvement on the non-linear ion response of conventional MALDI, which can be $> 40\%$. This may be primarily due to the inhomogeneity of the analyte distribution in the matrix-analyte cocrystallite.

A specialized hydrophobically coated MALDI target has been designed to reduce the size of the sample spot, and thereby increases sensitivity by enhancing the mass load per unit of area.²⁵ To determine if this new target offered improvement in reproducibility and sensitivity over the standard stainless steel stage, experiments on the determination of detection limits and RSD were repeated. The results are presented in Table 7.2. While there is still significant error in the values reported due to the relative irreproducibility of MALDI-MS in comparison to other techniques, it can be clearly concluded that the hydrophobic plate does not significantly improve the sensitivity or shot-to-shot

reproducibility of this method. Thus, a regular low cost stainless steel MALDI target is sufficient for the analysis. It is crucial to note that the limits of detection reported here for α -dicarbonyls are lower than those obtained by other techniques such as CE with diode array detection, and hence the technique could be a favourable alternative.²⁻⁴

Table 7.1. Summary of limit of detection for quinoxalines of dicarbonyls tested by RM-LDI-TOFMS, at a laser intensity of 2496 (arbitrary units). * denotes data from on-target derivatization.

Quinoxaline derivatives of:	Detection limit in ng mL ⁻¹ (% RSD)	Molecular ions (m/z) [M+H] ⁺
Methyl glyoxal	0.08, (9.0) 0.65* (15.6)	322
Diphenyl glyoxal	0.28, (13.8) 3.2* (24)	460
Dimethyl glyoxal	0.22 (12.4) 2.4* (23.2)	336
DAA	2.8 (18.8)	286

DL= (3SD of blank)(analyte concentration/net analyte signal intensity).

Table 7.2. Figures of merit with hydrophobic MALDI target.

Quinoxaline derivatives of:	Detection limit in ng mL ⁻¹ (% RSD)	Molecular ions (m/z) [M+H] ⁺
Methyl glyoxal	0.11 (18.6) 0.95* (19.8)	322
Diphenyl glyoxal	1.2 (25.6)	460
Dimethyl glyoxal	0.83 (22.6)	336
DAA	2.7 (17.8)	286

7.4 Conclusion

The determination of α -dicarbonyls by chemical modification strategy using 9-(3,4-diaminophenyl)acridine as a reactive matrix with analysis by MALDI-MS has been explicitly demonstrated. The technique is rapid, sensitive and with excellent selectivity for α -dicarbonyls (in principle, α -ketocarboxylic acids), making it suitable for high throughput analysis and sample screening. Additionally, the technique described is particularly efficient as it eliminates the need for sample purification and extraction, which are often time consuming procedures. Likely, it could be employed for analysis of target compounds in whole blood, tissues, urine samples, *etc.* The speed of the on-plate derivatization approach makes it suitable for applications in automated systems, such as those developed with matrix-less targets (like Quickmass™ produced by the Nanohorizons)²⁶ and microfluidic-MALDI systems. The fact that an interpretation of the resulting spectra is also straightforward should arguably captivate the interest of other researchers in the area and be an impetus to investigate other compounds. With the growing interest in coupling HPLC or capillary electrophoresis to MALDI, the use of reactive matrices with MALDI (*viz.* chemical derivatization) is expected to grow.

7.5 References

1. Zwiener C, Glauner T, Frimmel FH. *Water Supply*, 2003; **3**: 321-328.
2. Pedro Miguel AR, Cordeiro CA A, Freire AP, Nogueira JMF. *Electrophoresis* 2005; **26**: 1760-1767.
3. Li R, Kenyon GL. *Anal. Biochem.* 1995; **230**:37-40.

4. Dwyer TJ, Fillo JD. *J. Chem. Educ.* 2006; **83**: 273-276.
5. De Revel G, Pripis-Nicolau L, Barbe JC, Bertrand A. *J. Sci. Food Agric.* 2000; **80**:102-108.
6. Fujioka K, Shibamoto T. *Environ. Toxicol.* 2006; **21**: 47-54.
7. Cohen LH, Gusev AI. *Anal. Bioanal. Chem.* 2002; **373**: 571-586.
8. Soltz LJ, Patel P. *Rapid Commun. Mass Spectrom.* 2004; **18**: 1455-1458.
9. McCombie G, Knochenmuss R. *Anal. Chem.* 2004; **76**: 4990-4997.
10. Kraj A, Dylag T, Gorecka-Drzazga A, Bargiel S, Dziubanand J, Silberring J. *Acta Biochim. Pol.* 2003; **50**: 783-787.
11. Pan C, Xu S, Hu L, Su X, Ou J, Zou H, Guo Z, Zhang Y, Guo B. *J. Am. Soc. Mass Spectrom.* 2005; **16**:883-92.
12. Hatsis P, Brombacher S, Corr J, Kovarik P, Volmer DA. *Rapid Commun. Mass Spectrom.* 2003; **17**: 2303-2309.
13. Brombacher S, Owen S J, Volmer D A. *Anal. Bioanal. Chem.* 2003; **376**: 773-779.
14. Halket JM, Waterman D, Pyzyborowska AM, Patel RK, Fraser PD, Bramley PM. *J. Exp. Bot.* 2004; **56**: 219-244.
15. Saraiva MA, Borger CM, Florencio MH. *J. Mass Spectrom.* 2006; **41**: 216-228.
16. Fenaille F, Tabet JC, Guy PA. *Anal. Chem.* 2004; **76**: 867-873.
17. Lattova E, Perreault H. *J. Chromatogr. B* 2003; **793**: 167-179.
18. Sekiya S, Wada Y, Tanaka K. *Anal. Chem.* 2005; **77**: 4962-4968.
19. Mirzaei H, Regnier F. *Anal. Chem.* 2006; **78**: 4175-4183.
20. Tholey A, Wittmann C, Kang MJ, Bungert D, Hollemeyer K, Heinzle E. *J. Mass Spectrom.* 2002; **37**: 963-973.

21. Barry SJ, Carr RM, Lane SJ, Leavens WJ, Manning CO, Monte S, Waterhouse I. *Rapid Commun. Mass Spectrom.* 2003; **17**: 484-497.
22. Lee P J, Chen W, Gebler JC. *Anal. Chem.* 2004; **76**: 4888-4893.
23. Plater M J, Helfrich M H, Ralston SH. *J. Chem. Soc., Perkin Trans.* 2001; **1**: 2553-2559.
24. Gobcy J, Cole M, Janiszewski J, Covey T, Chau T, Kovarik P, Corr J. *Anal. Chem.* 2005; **77**: 5643-5654.
25. Owen SJ, Meier FS, Brombacher S, Volmer DA. *Rapid Commun. Mass Spectrom.* 2003; **17**: 2439-2449.
26. <http://www.nanohorizons.com/documents/Nano.QuickMass.pdf> (application note).

CHAPTER 8

Summary and Future Work

LDI and MALDI-MS have been used (Chapter 2) to characterize Suwannee River humic substances (HS), obtained from the International Humic Substances Society (IHSS), and Armadale soil fulvic acid (ASFA). Among the MALDI matrices tested for use with HS, 2,5-dihydroxybenzoic acid yielded the best results, exhibiting superior ionization efficiency, low spectral noise, and most importantly producing an abundance of high mass ions, with the largest observed at m/z 1848. A number of sample preparation methods were investigated; the overlay method (analyte/matrix solution spotted on dried matrix spot layer) improved sample-matrix homogeneity and hence shot to shot reproducibility. The choice of the matrix, mass ratio of analyte to matrix, and the sample preparation protocol were found to be the most critical factors governing the quality of the mass spectra. A number of common mass spectral features, particularly specific ions that could not be attributed to the matrices or to contaminants, *e.g.* m/z , 242, 360, 495, 550, 883, 997, 1166, 1280, 1450, *etc.*, were present in all the HS, regardless of origin or operational definition. Additionally, a prominent repeating pattern of peaks separated by 55, 114 and 169 Da was clearly observed in both LDI and MALDI, suggesting that the humic compounds studied here may have quasi-polymeric or oligomeric features. Future work to elucidate structure of the observed HS ions should entail complementary use of MALDI-TOFMS with post source decay (PSD) and ESI instruments with MS-MS capabilities *e.g.*, QqTOFMS as well as FT-ICRMS, which could afford exact assignments of molecular formulae.¹

Thermally assisted hydrolysis and methylation (THM) using TMAH and subsequent analysis by GC-MS (Chapter 3) was also used to study the fundamental structure of HS. Chemolysates containing carboxylic acids were found to be dominant in

Suwannee River natural organic matter (NOM) and its component classes (fulvic and humic acids). To evaluate a possible polysaccharide model for the formation of HS, polymerized 4-oxo-2-butenoic acid was used as a model compound and analyzed by THM-GC-MS. The results were compared with the analysis of Suwannee River NOM standard from the IHSS. This study yielded evidence of structural similarities (presence of chemolysates related to 4-oxo-2-butenoic acid and malic acid) between the two analytes, indicating commonalities in their basic composition and suggesting a clue as to the route of formation for NOM. Further, lignin-type pyrolysates were also found in the analysis the humic acid model, which calls into question the origin of reported lignin-derived moieties in NOM. Based on this finding, it is proposed that some of the associated pyrolysates that have been widely reported to be of unknown origin (*e.g.* butanedioic acid dimethyl esters) are likely derived from HS, which has been formed from polysaccharides. The use of TMAH reagent used in our work to mediate hydrolysis and methylation has been regarded as a relatively harsh reagent that could catalyze other undesirable secondary reactions. It would thus be important to use other methylating reagents such as carbanion and methyl iodide, tetramethyl sulfonium hydroxide *etc.*²

From the MALDI-MS and THM-GC-MS studies, it was evident the dominant structural features of aquatic HS in general and fulvic acid in particular, are the (poly-) carboxylic acids and fewer phenolic constituents, which in principle makes aquatic fulvic acid (AFA) a potential source of acidic protons and suitable for use as a MALDI matrix. In addition, AFA possesses some aromatic and unsaturated aliphatic moieties that make it good at absorbing UV energy, a key requirement for a MALDI matrix. AFA, from the Suwannee River and also locally-extracted (Long Pond, St. John's, Newfoundland), has

been demonstrated to be an effective matrix for MALDI in the analysis of molecular weight compounds ranging between 100-1500 Da (Chapter 4). The efficiency of AFA as a matrix has been shown with a wide range of test compounds, including low molecular weight sugars, cyclodextrins and peptides. The propensity of AFA to enhance protonation of peptides and formation of sodium and potassium adducts of carbohydrates was noted. The applicability of AFA as a MALDI matrix for real environmental samples was evaluated by the analysis of cantaloupe juice and acetaminophen tablets without prior extraction or purification; glucose and acetaminophen could easily be identified as respective components. The suitable concentration of AFA as a matrix solution was found to be 2 mg mL⁻¹. When lower concentrations of fulvic acid were used in the presence of sugars, a reversal of roles was observed, in which the sugars instead aided in the ionization of the fulvic acid components. This interesting discovery could be utilized in the structural determination of fulvic acid, an ongoing area of interest for humic substances researchers. Further work will involve the use of AFA immobilized on MALDI stage for surface enhanced neat desorption technology.³ It is additionally envisioned that AFA-iron (III) or Al (III) complex could be immobilized on MALDI stage and used as an immobilized metal-ion affinity chromatography substrate for analysis of analytes such as phosphopeptides.⁴⁻⁶

HS have also been studied by degradation using oxidative agents such as chlorine and chloramines typically used as disinfectants during water treatment (Chapter 5). This work has served two functions; it has revealed information about the structural makeup of HS as well as generating possible disinfection byproducts (DBPs) for study. In our study, chlorination and chloramination of different classes of NOM were carried out, with

subsequent adsorption on macroporous XAD resins, elution with ethyl acetate followed by analysis by GC-MS. Possible new DBPs were tentatively identified based on mass spectra library searches and mass spectral interpretation. It should be noted that among samples (NOM, FA, HA), most of the resultant DBPs were quite similar, demonstrating commonality in the structures of humic and fulvic acids. Highly substituted haloketones were found to be an important class of chlorine and chloramine by-products. To model haloketones DBPs formation, selected model compounds, chrysin, quercetin, quercetrin and chlorogenic acid were used. On chlorination, haloketones formed from HS were also observed, but only for flavanoids containing *meta*-substituted hydroxy phenol substituents. From this work, precursors of haloketones, which are high-priority DBPs, have been tentatively identified. Further studies on more rigorous mechanistic procedures are, however, essential.

Many DBPs observed in this work contained carbonyl and dicarbonyl moieties, which make them difficult to be analyzed by GC-MS due to their high polarity. This directed our focus to the development of two tailor-made derivatizing agents for use in laser desorption ionization mass spectrometry, namely, dimethylamino-6-(4-methoxy-1-naphthyl)-1,3,5-triazine-2-hydrazine (DMNTH) and 9-(3,4-diaminophenyl)acridine (DAA), which could react quantitatively, selectively and rapidly with carbonyl (Chapter 6) and α -dicarbonyl (Chapter 7) compounds respectively. The products formed (hydrazones and quinoxalines respectively) were very stable and demonstrated high ionization efficiency. They could be detected expediently by LDI-TOFMS, thus eliminating the need for the matrix assisted variant (MALDI) and the associated issue of

matrix optimization. As such, it greatly simplifies the analysis. Both one-pot and rapid on-plate chemical modification approaches were developed, with the latter in particular found to be ideal for high-throughput analysis. It has been demonstrated that a wide range of carbonyl and α -dicarbonyl compounds, even in complex matrices (*e.g.* beer), can be conveniently analyzed by these techniques; christened in our work as “reactive matrix LDI-TOFMS (RM-LDI-TOFMS)”. These technique offers very low detection limits, typically in the sub parts per billion range (especially using the one-pot derivatization), improved precision and relatively wide linear dynamic range especially with the use of *in-situ* labelled internal standards. These attributes qualify the technique as suitable for quantitative analysis. Further research is underway to synthesize new reactive matrices for analysis of other environmentally important contaminants such as nitrosamines and other polar pollutants. In addition, extensive application of the aforementioned synthesized reactive matrices to real world samples is also being conducted with capillary electrophoresis and reversed phase chromatography being used for separation. In addition, other separation strategies such as hydrophilic interaction chromatography (HILIC), suited for resolving highly polar analytes, could be an attractive method to use for analysis of the polar DBPs extract fraction, especially when coupled to ESI-MS-MS.⁷ The demonstrated on-plate derivatization is also believed to be easily applicable as an analytical screening system for integrated microfluidics systems with on-line MALDI-MS.⁸

8.1 References

1. Rccmtsa T, These A, Springer A, Linscheid M. *Environ. Sci. Technol.* 2006; **40**: 5839-5845.
2. Ikeya K, Ishida Y, Ohtani H, Watanabe A. *J. Anal. Appl. Pyrolysis.* 2006; **75**: 174-180.
3. Merchant M, Weinberger SR. *Electrophoresis* 2000; **21**: 1164-1167.
4. Ueda EKM, Gout PW, Morganti L. *J. Chromatogr A* 2003; **988**: 1-23.
5. Klavins M, Eglite L. *Colloids and Surfaces A: Physicochemical and Engineering Aspects*, 2002; **203**: 47-54.
6. Klavis M, Eglite L, Zicmanis A. *Chemosphere*, 2006; **62**: 1500-1506.
7. Dixon AM, Delinsky DC, Bruckner JV, Fisher JW, Bartlett MG. *J. Liq. Chromatogr. Relat. Technol.* 2004; **27**: 2343-2355.
8. Brivio M, Fokkens RH, Verboom W, Reinhoudt DN. *Anal. Chem.* 2002; **74**:3972-3976.

